uOttawa

L'Université canadienne
Canada's university

FACULTÉ DES ÉTUDES SUPÉRIEURES ET POSTOCTORALES

uOttawa

L'Université canadienne
Canada's university

FACULTY OF GRADUATE AND POSDOCTORAL STUDIES

Nelson F. Eng
AUTEUR DE LA THÈSE / AUTHOR OF THESIS

Ph.D. (Microbiology and Immunology)
GRADE / DEGREE

Department of Microbiology and Immunology
FACULTÉ, ÉCOLE, DÉPARTEMENT / FACULTY, SCHOOL, DEPARTMENT

Functional characterization of the cell division protein MinE from the Gram-negative coccus *Neisseria gonorrhoeae*

TITRE DE LA THÈSE / TITLE OF THESIS

Jo-Anne R. Dillon
DIRECTEUR (DIRECTRICE) DE LA THÈSE / THESIS SUPERVISOR

CO-DIRECTEUR (CO-DIRECTRICE) DE LA THÈSE / THESIS CO-SUPERVISOR

EXAMINATEURS (EXAMINATRICES) DE LA THÈSE / THESIS EXAMINERS

Piet de Boer

Craig Lee

Guy Drouin

Kathryn Wright

Gary W. Slater
Le Doyen de la Faculté des études supérieures et postdoctorales / Dean of the Faculty of Graduate and Postdoctoral Studies

Functional characterization of the cell division protein MinE from the Gram-negative coccus *Neisseria gonorrhoeae*

By

Nelson F. Eng

Thesis Submitted to the
Faculty of Graduate and Postdoctoral Studies
In partial fulfillment of the requirements
For the degree of Doctor of Philosophy in Microbiology and Immunology

Department of Biochemistry, Microbiology, and Immunology
Faculty of Medicine
University of Ottawa

Your file Votre référence
ISBN: 978-0-494-49343-4
Our file Notre référence
ISBN: 978-0-494-49343-4

ABSTRACT

The Min system, comprising MinC, MinD, and MinE, is found in many Gram-negative bacterial species, including the bacillus *Escherichia coli* (Ec), and the coccus *Neisseria gonorrhoeae* (Ng). The Min proteins are important to properly initiate cell division in bacteria at the midcell. Previously, it had been considered that Min proteins were implicated in midcell site selection in only rod-shaped bacteria. Our laboratory previously identified and examined MinC and MinD from *N. gonorrhoeae* and discovered that these proteins were involved in cell division in *N. gonorrhoeae*. Since our laboratory also identified *minE* in *N. gonorrhoeae*, a coccal organism, I speculated that MinE also played a role in the cell division of round-shaped bacteria.

Inactivating $minE_{Ng}$ by gene disruption failed to produce a mutant *N. gonorrhoeae* knockout, suggesting that $minE_{Ng}$ is an essential gene. Growth curves of *N. gonorrhoeae* cells overexpressing $MinE_{Ng}$ showed increased log phase growth, followed by an abrupt death phase compared to wild-type *N. gonorrhoeae*. While overexpression of $MinE_{Ng}$ also delayed chromosome condensation and ultimately, cell division in *N. gonorrhoeae*, it did not affect cell morphology or division in alternating perpendicular planes typical of *N. gonorrhoeae*.

Our laboratory previously established that *E. coli* was a useful model organism to study $MinE_{Ng}$ function. Using this model, I determined that two $MinE_{Ng}$ domains (aa 12-26 and aa 57-72) were responsible for $MinD_{Ng}$ interaction. Furthermore, by mutating five conserved $MinE_{Ng}$ residues (A18, L22, R30, K53 and E67), I discovered that the N-terminus of $MinE_{Ng}$ (aa 1-30) was essential for $MinD_{Ng}$ binding and recruitment to the coiled subcellular architecture formed by Min proteins in *E. coli*. With an intact N-terminus, $MinD_{Ng}$ localized to the coiled array and could oscillate irrespective of ATPase stimulation

by $MinE_{Ng}$. Differences in $MinD_{Ng}$ binding to the C-terminus of $MinE_{Ng}$ (aa 31-87) were associated with differences in their ability to stimulate the ATPase activity of $MinD_{Ng}$. Thus, ATPase stimulation by $MinE_{Ng}$ is dependent on the amount of interaction between $MinD_{Ng}$ and $MinE_{Ng}$. This property of $MinE_{Ng}$ is likely required to ensure that $MinD_{Ng}$ oscillation is $MinE_{Ng}$-specific so that proper midcell site selection for cytokinesis can occur. Interestingly, I discovered that $MinE_{Ng}$-GFP ring/coil formation did not occur unless the fusion protein was highly expressed relative to $MinE_{Ec}$-GFP; in addition, the $MinE_{Ng}$-GFP superstructures do not oscillate.

The domains of $MinE_{Ng}$ self-interaction included a predicted C-terminal α-helix (aa 39-54) and β-sheet (aa 74-78). These domains were also important for $MinD_{Ng}$ interaction. Disrupting $MinE_{Ng}$/$MinE_{Ng}$ interaction caused GFP-$MinD_{Ng}$ to primarily localize to the cell membrane and few cells showed proper $MinD_{Ng}$ localization (i.e. rapid $MinD_{Ng}$ oscillation). In those cells, the $MinD_{Ng}$ periodicity cycle was increased approximately 10-fold. Loss of $MinE_{Ng}$ self-interaction also caused some cells to filament. These results implied that proper $MinD_{Ng}$ function was dependent on $MinE_{Ng}$ self-interaction. Therefore, it is likely that $MinD_{Ng}$ interacts with dimerized $MinE_{Ng}$.

This is the first study that critically analyzes MinE from naturally round bacteria and its function in *N. gonorrhoeae* and *E. coli*. These studies not only enhanced the current knowledge of MinE functionality, but also provide insight into unique $MinE_{Ng}$ behaviour.

ACKNOWLEDGEMENTS

First and foremost, I would like to thank Dr. Jo-Anne Dillon, for giving me the opportunity to work in her laboratory, both at the University of Ottawa and at the Vaccine and Infectious Disease Organization (VIDO) at the University of Saskatchewan, on this project. Despite her hectic schedule, I particularly thank her for making time for me when I needed it most.

To my advisory committee, Dr. Earl Brown, Dr. Martin Holcik and Dr. Natalie Goto. I wish to express my gratitude for your guidance in helping me strengthen my project. I would also like to thank Dr. Gustavo Di Lallo, Università via della Ricerca Scientifica, for providing *E. coli* strain R721 and plasmids p434FtsZ and p22MinC which were important in completing my studies.

A big thank you to the past and present lab crew in Saskatoon and in Ottawa. During my time at VIDO, special gratitude goes to Mingmin, the only other Dillon lab member from Ottawa to come with me to Saskatoon. He made my transition to the prairies easy and effortless. To Kelli, the first to enter the new Dillon lab at VIDO, thank you for your friendship and showing me what Saskatoon has to offer to this long-time Ontario resident. Thank you to Monique and Cherise, who were also fellow Dragonboat paddlers – it was a lot of fun in and out of the lab. Monica, Yan, Debu, Yang, Shanna and Wenkai, thanks for being great lab members. To everyone else at VIDO, particularly Shakiba, Jason K., Peter, Ryan, and Patrick, thank you. Of course, I have not forgotten Ottawa. To Jason S. and Sandra, I am not sure what I would have done without the two of you in the lab. You made me feel very welcomed when I joined the lab. Your friendship, patience and help with my project were invaluable. To the rest of the Ottawa crew, Dan, Valerie, Marc, Sudeep, Pat, and Susan,

thanks for all the good times in the lab. I will always remember them. To Lauren, my first apprentice, I can only hope that I was able to live up to your expectations. To the many other former Dillon members, graduate students and BMI department staff at Ottawa, all of you contributed something special to my experience as a graduate student: Neil, Tamyo, Sheila, Pierre, Holly, Paulina, Karine, Julia, Julian, Tanya, Hui, Andre, Cathy, Lisa, Nicole, and Carol Ann. Special thanks to all of the Toronto-Ottawa weekend duffers for inviting me to hit the links – to relieve lab stress.

I am very grateful to the Natural Sciences and Engineering Research Council of Canada (NSERC), the Canadian Institutes of Health Research (CIHR), and the University of Ottawa for financially supporting my graduate program. It is the investment in future graduate students that drives research excellence.

At last, a special, huge, thank you to my family. My Mom and Dad, they are the emotional anchors in my life. Even though they did not understand a single word of my research, I still love them. I will not forget all the care packages and how well I ate whenever I had a chance to visit home. To my sister and brother, thank you for being there... and keeping my "big brother" ego alive.

Best wishes to all,

Nelson

TABLE OF CONTENTS

LIST OF TABLES

Appendices

LIST OF FIGURES

Chapter 1

Chapter 2

Chapter 3

LIST OF COMMONLY USED ABBREVIATIONS

aa	amino acids
AD	activating domain
Amp	ampicillin
ATP	adenosine 5' triphosphate
BD	binding domain
Bs	*Bacillus subtilis*
BSA	bovine serum albumin
Cm	chloramphenicol
CT	C-terminal truncation
dcw	division cell wall cluster
DIC	differential interference contrast
DNA	deoxyribonucleic acid
dNTP	deoxynucleoside triphosphate
Ec	*Escherichia coli*
GFP	green fluorescent protein
IPCR	inverse polymerase chain reaction
IPTG	isopropyl-β-D-thiogalactopyranoside
Kan	kanamycin
kb	kilobase
kDa	kilodalton
Min	minicell
Ng	*Neisseria gonorrhoeae*

NT	N-terminal truncation
OD	optical density
ONPG	o-nitro-phenyl-D-galactopyranoside
PBS	phosphate buffered saline
PCR	polymerase chain reaction
PG	phosphatidylglycerol
rpm	rotations per minute
s	seconds
SDS-PAGE	sodium dodecyl sulphate polyacrylamide gel electrophoresis
X-gal	5-bromo-4-chloro-3-indolyl-β-D-galactopyranoside

CHAPTER 1

Introduction, hypothesis, and objectives

INTRODUCTION

The continuity of life relies on being able to duplicate and maintain its genetic code. DNA must first replicate and be able to segregate so that genetic information and other cellular components are distributed faithfully and efficiently into two daughter cells. This process is known as cell division or cytokinesis. However, cell division is not a straightforward event. It is a complicated process that involves a variety of proteins with unique and specific functions that work together towards complete cytokinesis. One of the most important events that must take place in a cell is to determine where division occurs. In bacteria, this generally means the middle of the cell. How the cell selects the midsite requires synchronized spatial and temporal timing as the bacterium replicates and partitions duplicated genetic complement (Donachie, 1993).

Within the last two decades, knowledge concerning bacterial cell division has increased greatly. Early research on midcell site selection in prokaryotes focused on rod-shaped bacteria like *Escherichia coli* (Ec) and *Bacillus subtilis* (Bs), where after one round of division, there are typically two equally sized daughter cells. In *E. coli*, there are two mechanisms that facilitate the determination of a cell division site, the Min system (de Boer and Crossley, 1989) and nucleoid occlusion (Woldringh *et al.*, 1990). The Min system, MinC, MinD, and MinE, must function in concert through dynamic localization to ensure that cell division machinery is recruited to the middle of the cell. Nucleoid occlusion ensures that division does not occur over duplicated nucleoids. Unfortunately, such strategies are not conserved among bacteria. Bacterial cytokinesis is, in fact, not confined to simple symmetrical binary fission in parallel planes, similar to *E. coli* (Chen *et al.*, 1999). Bacteria may also divide in alternating perpendicular planes, like the coccus *Neisseria gonorrhoeae* (Ng) (Westling-Haggstrom *et al.*, 1977) or divide asymmetrically, such as *Caulobacter*

crescentus (Jensen and Shapiro, 1999). In addition, some bacteria do not possess a Min system at all (e.g. *Enterococcus faecalis*); as a result, other unique strategies must have evolved to deal with cell division site selection in such cases. This research examines and characterizes the cell division protein MinE from *N. gonorrhoeae*, a Gram-negative coccus – the first study of its kind.

Here, the current state of knowledge on cell division in bacteria is reviewed as it applies to this project. An overview ranging from the cell division machinery in various bacteria to chromosome segregation will be explained, with particular emphasis on *E. coli*. Another section will describe the process of division site selection, especially in *E. coli*, and finally, cell division in *N. gonorrhoeae* will be examined.

1.1 Bacterial cell division and segregation

1.1.1. The division cell wall (*dcw*) cluster

Most of our current knowledge of bacterial cell division has been derived from studies of the Gram-negative rod *E. coli*. A group of 16 essential genes encode not only cell division proteins, but also proteins for peptidoglycan synthesis in *E. coli* (Ayala *et al.*, 1994): *mraZ*, *mraW*, *ftsL*, *ftsI*, *murE*, *murF*, *mraY*, *murD*, *ftsW*, *murG*, *murC*, *ddlB*, *ftsQ*, *ftsA*, *ftsZ*, and *envA* (Fig. 1.1). This group of highly conserved genes is known as the division cell wall (*dcw*) cluster. Within the *dcw* cluster of *E. coli*, all of the genes are transcribed in the same direction. There is an initial transcriptional promoter, *mraZ1p*, upstream of *mraZ* (Mengin-Lecreulx *et al.*, 1998), and a terminator downstream of *envA* (Vicente *et al.*, 1998). While there are no internal terminators within the *dcw* cluster of *E. coli*, there are many other internal promoters, suggesting the presence of partial transcripts (Mengin-Lecreulx *et al.*, 1998). Indeed, DNA microarrays have shown that there are three regions of differing mRNA levels (Selinger *et al.*, 2003).

The *dcw* cluster has been identified in most other organisms as well, including *N. gonorrhoeae* (Francis *et al.*, 2000), *B. subtilis* (Daniel *et al.*, 1996;Henriques *et al.*, 1992) *Staphylococcus aureus* (Pucci *et al.*, 1997), and *Haemophilus influenzae* (Fleischmann *et al.*, 1995). Figure 1.1 shows the *dcw* clusters of *E. coli*, *N. gonorrhoeae*, and *B. subtilis*. While the *dcw* genes themselves are highly conserved, it has been proposed that the gene arrangement may be a factor in determining cell shape based on phylogenetic tree comparisons between the *dcw* genes and FtsZ (Tamames *et al.*, 2001). As such, the term "genomic channelling" is used to describe how the order of the *dcw* cluster may be linked to grouped protein assembly that can affect how a cell elongates and septates (Mingorance *et al.*, 2004). Generally, *dcw* gene order is highly conserved among rod-shaped bacteria.

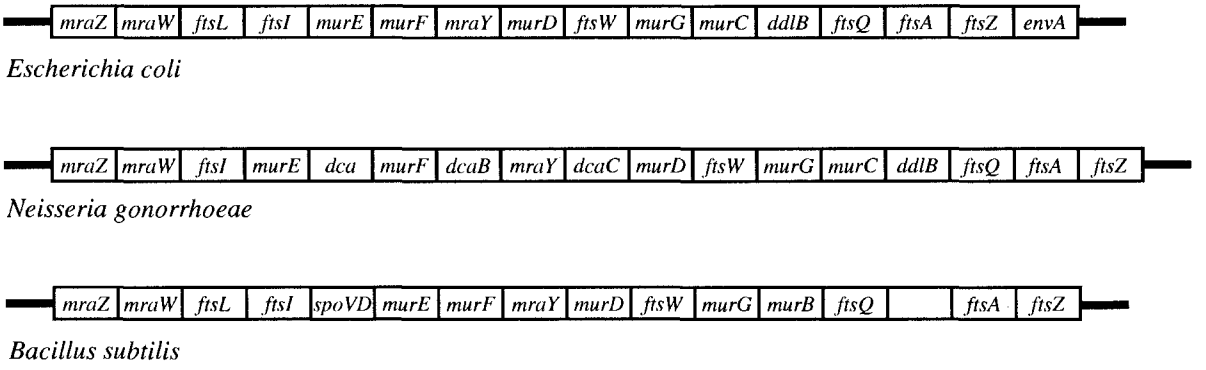

Figure 1.1. Schematic representation of the *dcw* clusters from *E. coli*, *N. gonorrhoeae*, and *B. subtilis*. Generally, the *dcw* clusters are very similar across species in terms of gene composition. However, Mingorance *et al.*, 2004, proposed that "genomic channeling" related to gene arrangement may differentiate how rod- and round-shaped bacteria divide.

The "genomic channelling" model suggests that a specific gene order is needed to coordinate elongation and septation. In contrast, the *dcw* arrangement in round bacteria is predicted to be less conserved relative to rod-shaped bacteria, since elongation is not necessary (Mingorance *et al.*, 2004). However, there are examples that disagree with this idea; the bacillus *E. coli* and the coccus *N. gonorrhoeae* instead have very similar *dcw* cluster arrangements (Mingorance *et al.*, 2004). Many of the proteins involved in the cell division machinery are encoded in the *dcw* cluster. These and others not encoded by the *dcw* cluster are briefly described in the following sections with respect to *E. coli*.

1.1.2. FtsZ and cell division initiation

Before cell division occurs, a division complex or divisome, must form at the site where cell division and ultimately, septation will begin. The first protein to localize to this site that allows for the recruitment of other cell division proteins is the highly conserved GTPase FtsZ (filamenting temperature sensitive mutant protein Z), which closely resembles the eukaryotic tubulin protein (Bi and Lutkenhaus, 1991;Mukherjee *et al.*, 1993;RayChaudhuri and Park, 1992). FtsZ from *E. coli* (Fig. 1.2 A) and *N. gonorrhoeae* (Fig. 1.2 B) can assemble into a ring-like structure in an *E. coli* background as evidenced by recent enhancements in immunofluorescence techniques and green fluorescent protein (GFP) fusion to FtsZ, which can then be visualized *in vivo* (Addinall and Holland, 2002;Ma *et al.*, 1996;Salimnia *et al.*, 2000). FtsZ is found in nearly all major groups of bacteria, save for some species in the Planctomycetes, Chlamydiae and Verrucomicrobia groups (Margolin, 2005). The GTPase can also be found in chloroplasts and mitochondria (Miyagishima *et al.*, 2004;Osteryoung and Nunnari, 2003).

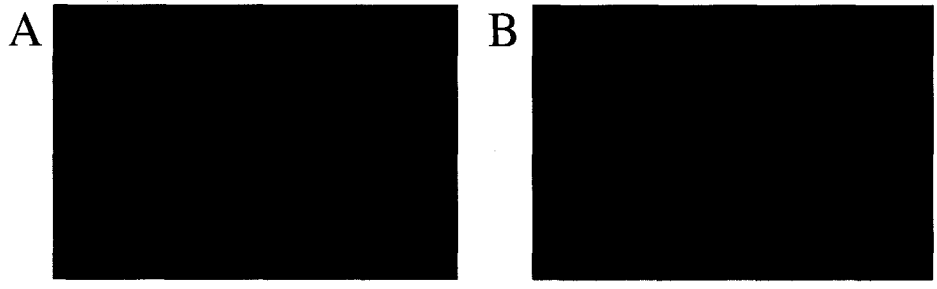

Figure 1.2. FtsZ localization in *E. coli* and *N. gonorrhoeae* (A) *E. coli* stained with anti-FtsZ antisera show FtsZ localization at the middle of each cell. [Reprinted with permission from Elsevier (Addinall and Holland, 2002)]. (B) Expression of GFP-fusion to *N. gonorrhoeae* FtsZ protein in *E. coli* also results in midcell localization of fluorescent fusion protein (Salminia *et al.*, 2000).

While FtsZ is mostly known as a cell division protein, recent studies have shown that it may have other functions. For example, when FtsZ and specific penicillin-binding proteins are inactivated, *E. coli* cells become helical at the poles or even branches off, suggesting that FtsZ, not associated with a ring, may be involved in cell shape (Varma and Young, 2004). In many *Bacillus* spp., FtsZ may also have a role in plasmid duplication, as a weak homologue of FtsZ is encoded by a plasmid (Margolin, 2005). In *Bacillus anthracis*, a FtsZ variant could contribute to its virulence (Margolin, 2005).

There are four main domains of FtsZ, based on the crystal structure of FtsZ from *Thermotoga maritima* (Lowe and Amos, 1998). A highly conserved core region of FtsZ contains two independently folded segments which are responsible for GTPase activity and FtsZ assembly, and a motif that makes this protein structurally similar to the eukaryotic protein tubulin (Oliva *et al.*, 2004). The extreme C-terminal end of FtsZ, although not essential in ring assembly, is, however, needed for the recruitment of downstream proteins such as FtsA and ZipA (Pichoff and Lutkenhaus, 2002). FtsZ can exhibit cross species functionality, since FtsZ from *N. gonorrhoeae* can localize to the midcell of *E. coli* (Fig. 1.2 B) (Salimnia *et al.*, 2000); however, many FtsZs from other species are unable to replace $FtsZ_{Ec}$, likely due to the specialized role of the C-terminal end (Redick *et al.*, 2005).

In the presence of GTP, FtsZ ring assembly occurs in the form of protofilaments assembled from the highly conserved core region (Oliva *et al.*, 2004). Several FtsZ protofilaments then laterally form bundles and sheets in the presence of such factors as Ca^{2+} (Yu and Margolin, 1997) and other proteins that promote bundling like ZipA (RayChaudhuri, 1999). In the recruitment of cell division proteins, the FtsZ ring needs to be maintained from the time it is formed until the rest of the divisome can be established, which can take up nearly 80% of the time in a typical cell cycle (Den Blaauwen *et al.*, 1999).

However, the FtsZ ring is not a fixed structure. Fluorescence recovery after photobleaching (FRAP) experiments have showed that ring-associated FtsZ is constantly being exchanged with cytoplasmic FtsZ at a high turnover rate (Anderson *et al.*, 2004). Since GTP-bound FtsZ readily hydrolyses (Anderson *et al.*, 2004), the question of why the FtsZ ring needs so much energy throughout the cell cycle is raised. One suggestion is that the existence of the FtsZ ring may also act as a signal for the initiation of peptidoglycan elongation and septation, which is dependent on where FtsZ is localized; both events could take some time to prepare (Vicente *et al.*, 2006).

After the FtsZ ring is formed, details on how the ring constricts are not clear. First, in *E. coli*, constriction is postponed for a significant period of time after ring formation for reasons not well understood, although the switch from cell wall elongation to septal formation may account for this delay (Margolin, 2005). As the ring contracts, evidence has shown that polymers of FtsZ-GFP remain in a helical pattern that rapidly move throughout the cell (Thanedar and Margolin, 2004). However, it is unknown if FtsZ itself forms the helical patterns or if a pre-existing structure acts as a scaffold for FtsZ trafficking.

After FtsZ ring assembly, the other downstream proteins are recruited from the cytoplasm towards the outer membrane. Generally, it was previously accepted that the temporal recruitment of the cell division proteins is linear and each protein depends on the previous one for proper localization to the FtsZ ring (Fig. 1.3 A): FtsA/ZipA, FtsE/FtsX, FtsK, FtsQ, FtsB/FtsL, FtsW, FtsI, FtsN, AmiC, and EnvC (Buddelmeijer and Beckwith, 2002;Chen and Beckwith, 2001;Vicente and Rico, 2006). The *dcw* cluster encodes only some of these proteins (FtsL, FtsI, FtsW, FtsQ, FtsA, and FtsZ). Recent studies suggest that divisome formation in *E. coli* occurs in early and late/FtsA-independent assembly stages.

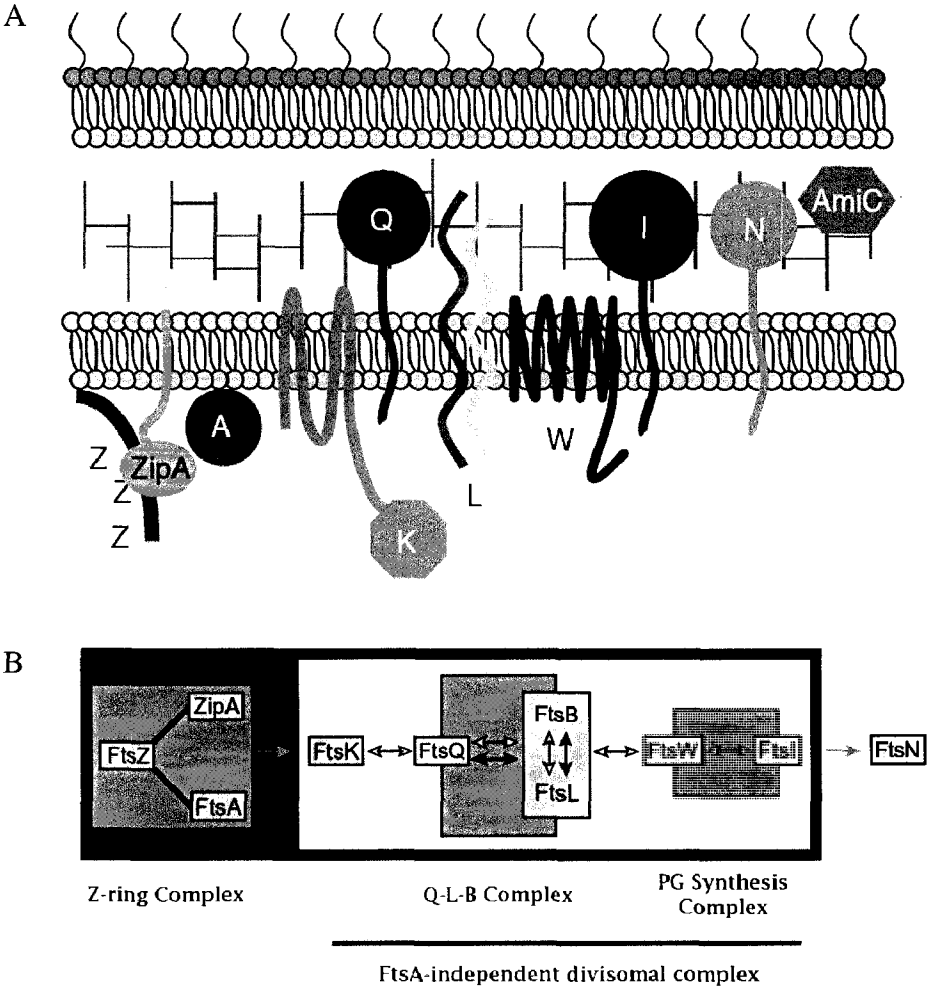

Figure 1.3. Assembly of divisome proteins at the *E. coli* cell division site. (A) A linear model of divisome assembly. FtsZ (Z) initiates polymerization at the division site and may be stabilized by FtsA (A) and ZipA. ZipA may act as a membrane anchor for FtsZ. Proteins subsequently recruited to the septal FtsZ-ring include FtsK (K), FtsQ (Q), FtsL (L), FtsW (W), FtsI (I), FtsN (N) and AmiC [Reprinted with permission from Elsevier (Goehring and Beckwith, 2005)]. (B) A recent proposal by Goehring *et al.*, (2006) suggests that assembly is done in pre-formed complexes. First, the stability of the Z-ring complex requires ZipA and FtsA. However, the remaining divisome proteins can form complexes independently of FtsA. A periplasmic connector consisting FtsQ, FtsB, and FtsL form together, while a murein synthesis complex of FtsW and FtsI is formed simultaneously. It is believed that FtsK interconnects the Z-ring with the connector and the synthesis complex. Once assembled, FtsN is then recruited to the divisome to possibly regulate the initiation of FtsZ ring constriction. [Reprinted with permission from Wiley-Blackwell (Goehring *et al.*, 2006)].

FtsZ, FtsA, and ZipA are believed to be recruited at the same time early on. Once FtsK is recruited, FtsQ, FtsB, and FtsL (periplasmic connector) simultaneously recruit (Buddelmeijer and Beckwith, 2004) other divisome proteins (i.e. FtsW, FtsI, and FtsN) involved with peptidoglycan production (Fig. 1.3 B) (Goehring *et al.*, 2006).

1.1.3. Z-ring stabilizers: FtsA and ZipA

While the FtsZ ring is responsible for recruiting other cell division proteins, FtsZ cannot form a ring alone, as evidenced by a *ftsA zipA* double mutant (Pichoff and Lutkenhaus, 2002). At least one of FtsA or ZipA must be present to stabilize the Z ring. Regardless, FtsZ can still localize into spaces between replicated chromosomes in the *ftsA zipA* double mutant, indicating that the FtsZ site selection function is retained (Pichoff and Lutkenhaus, 2002). Subsequent recruitment of FtsA and ZipA into the divisome is dependent on the localized FtsZ ring and are not dependent on each other or the rest of the downstream proteins (Hale and de Boer, 1999). As a result, it is believed that FtsZ, FtsA and ZipA form at the same time, with FtsA or ZipA providing the tether necessary for membrane binding (Aarsman *et al.*, 2005).

FtsA is a member of the actin/Hsp70/sugar kinase superfamily (Feucht *et al.*, 2001;Sanchez *et al.*, 1994). Although FtsA has been found to bind ATP, only FtsA from *B. subtilis* has been shown to display ATPase activity (Feucht *et al.*, 2001); FtsA homologues from *E. coli*, *S. pneumoniae* and *Thermotoga maritima* do not exhibit any ATPase activity (Lara *et al.*, 2005). Deletions of key domains of *E. coli* FtsA, using the crystal structure of FtsA from *T. maritima*, revealed two significant regions (aa 84-161 and aa 274-290) that are involved with FtsA self-interaction and divisome localization, respectively (Rico *et al.*, 2004). $FtsA_{Ec}$ can also interact with FtsQ, FtsI and FtsN (Di Lallo *et al.*, 2003;Karimova *et*

al., 2005). Once bound to FtsZ, a C-terminal amphipathic helix of FtsA acts as a membrane targeting sequence that facilitate the indirect binding of FtsZ to the cell membrane (Pichoff and Lutkenhaus, 2005).

While $FtsA_{Ec}$ can interact with downstream Fts proteins, $ZipA_{Ec}$ can only interact with FtsZ and itself as determined by bacterial two-hybrid studies (Di Lallo *et al.*, 2003). Interestingly, ZipA is absent from many bacteria, including *N. gonorrhoeae*, as it is only present in γ-proteobacteria (Vicente *et al.*, 2006). However, under normal conditions, $ZipA_{Ec}$ is involved in localizing other Fts proteins, possibly suggesting that recruitment of downstream proteins by ZipA requires another unknown interaction, or that ZipA functions only in conjunction with the Z-ring (Vicente *et al.*, 2006). Like FtsA, ZipA can also associate with the membrane through its N-terminal transmembrane domain (Hale and de Boer, 1997). However, studies have shown that ZipA function can be bypassed (Geissler *et al.*, 2003), suggesting that ZipA function may be redundant and that FtsA is the major factor in downstream recruitment. Another positive regulator, ZapA, found in *E. coli* (Small *et al.*, 2007), has also been found to promote FtsZ bundling (Gueiros and Losick, 2002); however, ZapA is not essential, unless coupled with other deficiencies (Gueiros and Losick, 2002;Johnson *et al.*, 2004), suggesting possible redundancy.

As FtsA and ZipA stabilize the FtsZ ring, there are negative regulators that inhibit FtsZ polymerization. MinC, a member of the Min system in *E. coli* (de Boer and Crossley, 1989), is a general cell division inhibitor that interacts with FtsZ and prevents the completion of FtsZ ring formation. Overexpression of MinC leads to elongated filamentous phenotype, establishing its role in cell division inhibition (de Boer *et al.*, 1992). Further discussion of the Min system will be described later in this introduction. Other factors that

promote FtsZ ring inhibition include EzrA (Haeusser *et al.*, 2004;Levin *et al.*, 1999) from Gram-positive bacteria, ClpX (Weart *et al.*, 2005) from *B. subtilis*, and SulA from *E. coli* (Bi and Lutkenhaus, 1993). EzrA binds directly to FtsZ and thus acts on FtsZ assembly at the membrane (Haeusser *et al.*, 2004). Deletion of EzrA was found to lower the critical concentration of FtsZ that is needed for ring assembly (Levin *et al.*, 1999), implying the role of EzrA in FtsZ inhibition. ClpX inhibits FtsZ assembly at the protofilament level since GTP hydrolysis was not affected (Weart *et al.*, 2005). SulA is only expressed under DNA damage conditions by binding to FtsZ to avert protofilament formation (Cordell *et al.*, 2003), thereby delaying cell division until DNA is repaired. The combination of the positive and negative regulators may account for some of the constant and rapid turnover of FtsZ between ring formation and the cytoplasm (Gueiros and Losick, 2002;Stricker *et al.*, 2002).

1.1.4. The completion of the divisome assembly and progeny separation

Following FtsA and ZipA association to FtsZ, FtsE and FtsX are next in the assembly sequence (Buddelmeijer and Beckwith, 2002). Both FtsE and FtsX are related to the ABC transporter family (Schmidt *et al.*, 2004). Recently, studies have shown that *E. coli* FtsE and FtsX are essential environmental regulators, but only are key in cell division in low salt conditions and are redundant in high osmolar strength (Reddy, 2007). As a result, many models exclude FtsE and FtsX in divisome formation. Interestingly, a recent study by Corbin and others (2007) demonstrated the interaction between FtsZ and FtsE without the need for FtsA by FLAG-fusion pulldown experiments. However, it is not clear how this interaction affects divisome formation under normal conditions.

FtsK recruitment to the divisome acts as a septum formation checkpoint. This protein is key to preventing septum formation in emergency cases where the duplicated

chromosomes have yet to fully segregate before the rest of the divisome is completed (Aussel *et al.*, 2002). Once bound to the divisome, FtsK can align the terminus of replication of the duplicated chromosomes, which contain FtsK oriented polar sequences (KOPS), to the septum, allowing the XerCD system to resolve unsegregated DNA into the respective daughter cells (Aussel *et al.*, 2002). As a result, FtsK is multifunctional as it contains an N-terminal transmembrane domain that is needed for septum localization, a linker region that also has a role in cell division, and a C-terminal domain that is responsible for recognizing KOPS and providing translocase activity that is dependent on ATP (Begg *et al.*, 1995;Bigot *et al.*, 2004).

Next, FtsQ, FtsB, and FtsL assemble together before incorporation into the divisome (Buddelmeijer and Beckwith, 2004), although recent studies have shown that FtsQ is not required for FtsB and FtsL to interact together before ring assembly (Goehring *et al.*, 2006). The FtsQBL complex serves as a connector protein that links the peptidoglycan producers (FtsW, FtsI, and FtsN) to the divisome through the use of a polypeptide transport-associated (POTRA) domain that facilitates the interaction of the downstream proteins (Sanchez-Pulido *et al.*, 2003).

Next in the assembly process is FtsW and FtsI. Both proteins are believed to function together in peptidoglycan production to form the septum that will physically divide the daughter cells (Ikeda *et al.*, 1989). FtsW is a member of a polytopic family of multi-transmembrane-spanning proteins (Henriques *et al.*, 1998) involved with shape, elongation, and division and is a putative precursor transporter. Since such members are usually associated with a penicillin-binding protein (PBP), it is not surprising that it interacts with FtsI (PBP3) (Datta *et al.*, 2006;Di Lallo *et al.*, 2003). FtsI itself is a transpeptidase which, in the presence of FtsW, is recruited to the future division site through its N-terminus

transmembrane domain (Weiss *et al.*, 1997). The larger C-terminal domain that contains catalytic motifs characteristic of other PBPs is believed to incorporate new murein by integrating three cross-linked glycan strands underneath a single strand of glycan at the division site ("three-for-one" model), which will then serve as the basis for divisome constriction (Holtje, 1998). As a result, the addition of more murein triplets drives constriction towards two separated daughter cells (Holtje, 1998).

FtsN is the last Fts protein to be recruited to the divisome complex. It carries a short N-terminal cytoplasmic domain, a single transmembrane region, and a large periplasmic domain that is responsible for targeting to the septal ring (Addinall *et al.*, 1997). FtsN can bind to murein; as the divisome constricts, this ability may play a role in degrading the cell wall that is necessary during the constriction process (Errington *et al.*, 2003).

After all the Fts proteins are recruited, hydrolysis of the new septum is required to completely separate the two daughter cells by way of murein hydrolases. The last two known proteins to recruit to the ring complex in *E. coli* have been discovered to facilitate this process: AmiC and EnvC. AmiC is an amidase that is released to the periplasm by the twin-arginine protein transport (Tat) pathway and is recruited to the septal ring in the presence of FtsN. The amidase specifically targets the cleavage of the glycan backbone and peptide side-chain. Not surprisingly, Tat mutants show a phenotype of chained cells that are unable to fully separate (Bernhardt and de Boer, 2003). More recently, the murein hydrolase EnvC has been discovered to localize to the septum; although its function is not clear, it is believed that it cleaves peptide cross-links (Bernhardt and de Boer, 2004).

1.1.5. Chromosome segregation

DNA replication in bacteria, in most cases, is initiated at a single site on the chromosome, the replication origin *oriC* (Draper and Gober, 2002). DnaA initiates this process (Messer, 2002) when a critical mass/volume is reached in the cell (Donachie, 2001). Several mechanisms exist to limit replication events to only once per divisional event (Bartosik and Jagura-Burdzy, 2005). In bacteria that have circular chromosomes, like *E. coli* or *B. subtilis*, replication then proceeds bi-directionally from *oriC* towards the nearly opposite terminus (*ter*) (Draper and Gober, 2002). Once there, a terminator complex causes the replication machinery to dissociate from DNA and stop replication. However, physical separation of the newly replicated chromosomes is not complete, as they are catenated. As such, they need to be unlinked to prevent the guillotining of any chromosome in the path of septation. Topoisomerase IV resolves these issues by causing decatenation, ensuring complete separation and proper cytokinesis (Aussel *et al.*, 2002).

Recent immunofluorescence studies have led to two models of chromosome segregation that conflict with each other. The current views are the factory model (Lemon and Grossman, 1998) and the sister cohesion model (Sunako *et al.*, 2001). Such studies have also discovered that replisomes, in fact, are stationary at the cell centre, while DNA moves through them, which contradicts previous beliefs of a moving replisome (Lemon and Grossman, 1998).

In the factory or extrusion-capture model, the replication process causes the concomitant movement of DNA and segregation. In this model, newly synthesized DNA is pushed, directed, condensed, held, and separated (Fig. 1.4) before cytokinesis is completed (Sawitzke and Austin, 2001). As replication proceeds, new DNA at the stationary *oriC* is *pushed* outwards to the poles in opposite directions by the replication machinery as it feeds

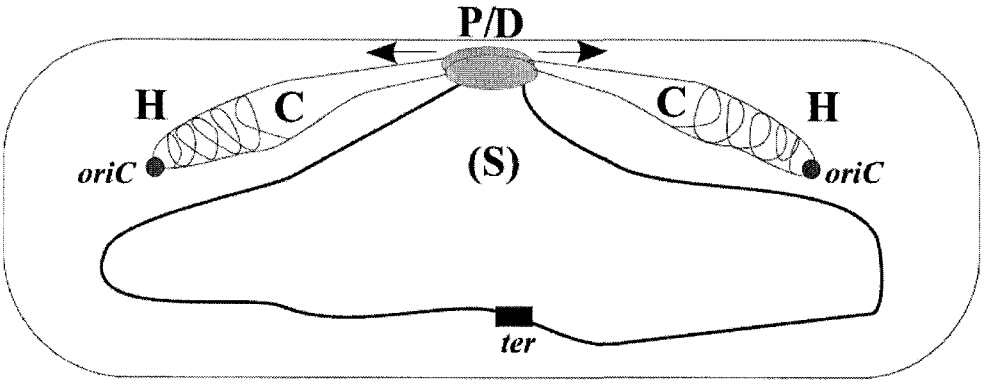

Figure 1.4. Factory or extrusion-capture model of chromosome segregation. Newly synthesized DNA at *oriC* is pushed (P) to the cell poles in opposite directions by the replication complex (grey oval). Eventually, *oriC* becomes stationary at the cell poles, allowing the remainder of replicated DNA to be directed (D) there. Many proteins condense (C) and hold (H) the replicated DNA to prevent the DNA from randomly moving back to the midcell. Finally, the DNA is separated (S) by proteins (e.g. FtsK) to ensure complete dissociation of the nascent chromosomes at the terminus (*ter*). Figure from Bartosik and Jagura-Burdzy (2005).

the chromosome through the replisome (Lemon and Grossman, 2001). Replication forks and information near or at the *oriC* itself may also facilitate the movement of new DNA to the cell poles, since *oriC* is replicated first. The new origins quickly migrate to the polar ends (Gordon *et al.*, 1997), where various systems such as ParAB (Moller-Jensen *et al.*, 2002) and MinCDE (Shih *et al.*, 2003) facilitate the conclusion of chromosome segregation. Once oriC arrives at the opposite ends, it is fixed, leading to the remainder of DNA synthesis to be *directed* there by such proteins like *E. coli* SeqA (Sawitzke and Austin, 2001). The newly replicated DNA needs to be *condensed* in order to provide sufficient room for septation; this process is performed by many proteins such as structural maintenance of chromosome (SMC) proteins from *B. subtilis* and *C. crescentus* (Draper and Gober, 2002) and MukB from *E. coli* (Niki *et al.*, 1991). Proteins such as Spo0J from *B. subtilis* (Lin and Grossman, 1998), MreB/SetB from *E. coli* (Espeli *et al.*, 2003) and ParB from *C. crescentus* and *Pseudomonas aeruginosa* (Moller-Jensen *et al.*, 2002) facilitate replicated DNA being *held* at each pole to prevent spontaneous drifting to midcell. Finally, replicated DNA is *separated* where FtsK is required to divide the ends of the sister chromosomes that often stay together (Aussel *et al.*, 2002).

While the extrusion-capture model implies that new DNA is moving as it is being replicated, the sister cohesion model is quite the opposite; using fluorescence *in situ* hybridization, studies have shown that duplicated chromosomes remain cohesive to one another (Sunako *et al.*, 2001) until late in replication, where the sister chromosomes move quickly to the opposite cell poles (Hiraga *et al.*, 2000). This model dismisses the motive force that the replication machinery provides in the factory model.

1.2. Cell division site selection in the Gram-negative rod *Escherichia coli*

Before cell division can even be initiated, bacteria must identify the site where future division will occur. As most cytokinetic events usually take place at midcell, the question of how the division complex is localized there initially is an important issue to address. Two major mechanisms are proposed to explain how bacteria select division sites properly: nucleoid occlusion (Woldringh *et al.*, 1990) and the Min system (de Boer and Crossley, 1989). Special emphasis will be placed on the Min system as it pertains to this research.

1.2.1. Nucleoid occlusion

Nucleoid occlusion (NO) is defined as the prevention of septum formation over nucleoids (Woldringh *et al.*, 1990). Such a mechanism became evident when division complexes (i.e. FtsZ rings) were observed not to form over nucleoids when replication or segregation was blocked (Fig. 1.5) (Sun and Margolin, 2001;Woldringh *et al.*, 1991;Yu and Margolin, 1999). One recent hypothesis proposed that the combined effects of translation, transcription, and translocation (known as transertion) of proteins prevented divisome assembly over the nucleoid (i.e. the crowding of proteins through transertion around the nucleoid prevented FtsZ assembly) (Woldringh, 2002). While a significant amount of chromosome decondensation alone can abolish NO (Sun and Margolin, 2004), recent studies have directly shown that there are at least two such proteins that act as checkpoints in preventing nucleoids from being guillotined, Noc (YyaA) in *B. subtilis* (Wu and Errington, 2004), and SlmA (Ttk) in *E. coli* (Bernhardt and de Boer, 2005), which better explains the prevention of FtsZ assembly over nucleoids. Interestingly, both Noc and SlmA are major factors in preventing FtsZ ring formation over nucleoids only where Min is not present. As such, Min appears to be the dominant mechanism in the correct

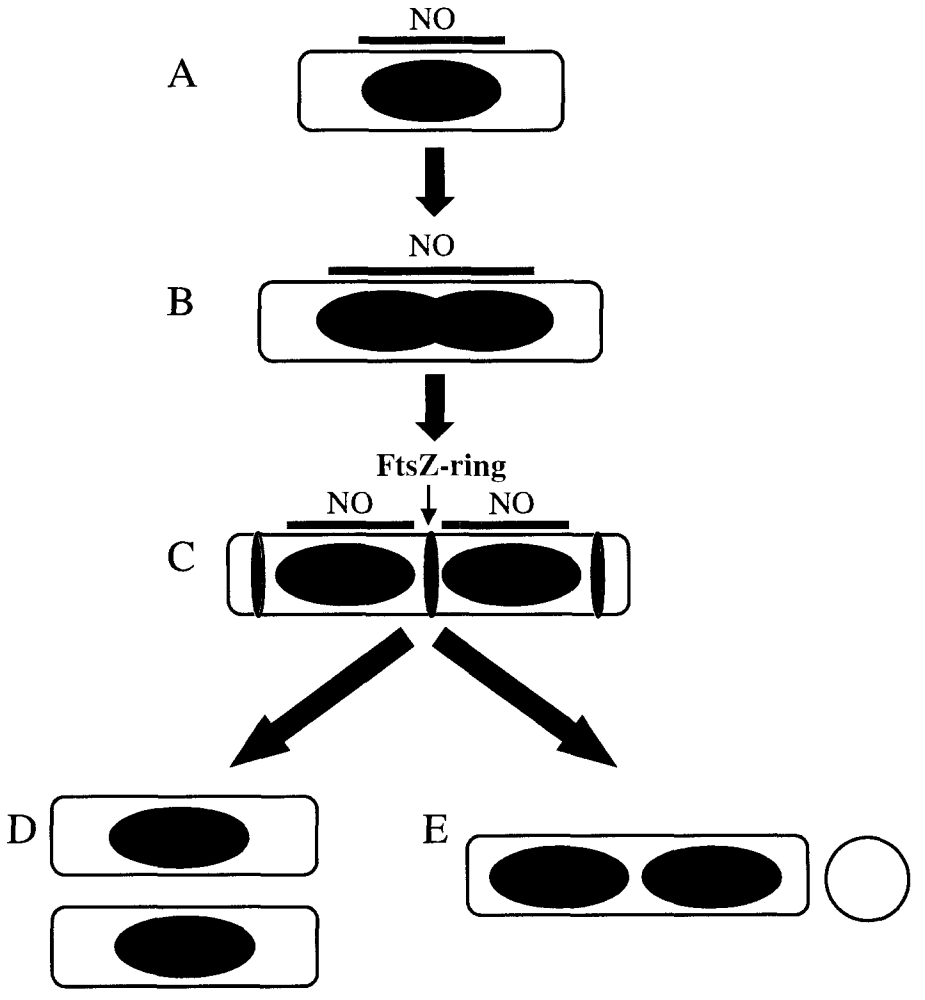

Figure 1.5. Nucleoid occlusion (NO). In the predivisional cell (A-B), the nucleoid (black oval) prevents FtsZ ring formation throughout the central areas of the cell (red bar). In a Δ*min* cell, as DNA replication terminates, a nucleoid-free zone is established between the newly replicated chromosomes. However, if NO was the only mechanism that regulates cell division site selection, then the poles also provide nucleoid-free zones, allowing FtsZ rings to form at midcell or at the cell poles (C), giving rise to population of cells that include normal equally-divided progeny (D) and minicells (E).

positioning of the divisome. Regardless, these two proteins, despite their unrelatedness in terms of sequence similarity and being from bacteria that are far removed from each other genetically, show amazing coherence when it comes to preventing the fragmentation of the chromosome during cell division.

In the absence of Noc, FtsZ ring formation occurs over the nucleoid in non-replicating *B. subtilis* cells (Wu and Errington, 2004). In particular, FtsZ non-discriminately forms many rings over replicated nucleoids throughout filamenting cells as a helical superstructure (Wu and Errington, 2004), providing initial evidence that Noc is a factor in nucleoid occlusion. The possibility of Noc affecting cell division at the transcriptional level was dismissed as 1) microarray studies revealed no changes to gene expression in the absence of Noc, 2) Noc is constitutively expressed regardless of cell cycle or DNA damage, and 3) Noc clearly has an effect on FtsZ localization (Wu and Errington, 2004), despite direct interaction with FtsZ has yet to be determined. As such, Noc is deemed to function directly at the protein level as a site-specific inhibitor of cell division.

In an attempt to find a NO-related protein in *E. coli*, Bernhardt and de Boer (2005) identified SlmA as another protein that localizes to the nucleoid. A putative member of the TetR family of DNA binding proteins, SlmA is not related to Noc (ParB DNA-binding member) and shares no amino acid sequence similarity. Both Noc and SlmA localize uniformly over the nucleoid and have also been found to provide partial cytokinetic inhibition when overexpressed (Bernhardt and de Boer, 2005;Wu and Errington, 2004), leading to a filamentous phenotype; most likely, excess protein takes up any DNA-binding sites in the nucleoid, allowing free Noc or SlmA to inhibit cell division elsewhere. Interestingly, SlmA also directly interacts with FtsZ (Bernhardt and de Boer, 2005). Thus, this interaction might imply FtsZ sequestering to the nucleoid by SlmA to prevent Z ring

formation and interfering with cell division; however, there have been no studies that have shown the localization of large quantities of FtsZ on the nucleoid (Addinall *et al.*, 1996;Ma *et al.*, 1996). As a result, it is not known how Noc or SlmA alter FtsZ polymerization; perhaps identifying the specific DNA sequences that these proteins bind to may provide insight into how this is done.

1.2.2. The Min system of site-specific cytokinesis

One of the models that best describes how the Min proteins function is the Gram-negative bacillus, *E. coli*. Numerous studies have shown that the Min system has a dominant effect over nucleoid occlusion in division site selection (Bernhardt and de Boer, 2005;Wu and Errington, 2004). Located in the *minB* operon, *minC*, *minD*, and *minE* were identified (Davie *et al.*, 1984;de Boer *et al.*, 1988) after further study of a phenomenon in which an *E. coli* mutant was found to have a *mini*cell phenotype. Adler and co-workers (1967) discovered that septation was occurring at the cell poles, giving rise to a small spherical cell (minicell) that lacked any nuclear content, and a short filamentous cell. Despite the fact that the anucleoid minicell could not replicate (and thus divide), the population was maintained from division of the short *E. coli* filamentous cells that still contained chromosomal DNA (Margolin, 2001). In *E. coli*, MinC, MinD, and MinE must work in concert to prevent septation events from occurring anywhere in the cell but in the middle. However, not all bacteria use the Min system to selectively identify a future division site. Some organisms like *B. subtilis*, possess MinC and MinD, but DivIVA replaces MinE in determining site selection (Marston *et al.*, 1998). The Gram-positive coccus *Enterococcus faecalis* and Gram-negative *Caulobacter crescentus* do not have any Min proteins at all and must use a completely different system to divide. Sections 1.2.3. to 1.2.5. provide details of the

structure/function relationships of each of the three Min proteins as they relate to *E. coli*. Details of the Min system in other bacteria follow.

1.2.3. MinC

E. coli MinC ($MinC_{Ec}$) is the general cell division inhibitor that prevents FtsZ ring assembly (de Boer and Crossley, 1989;Hu *et al.*, 2003). Approximately 25 kDa in size, and consisting of 231 amino acids (aa), overexpression of $MinC_{Ec}$ in wild-type cells causes a filamentous phenotype, producing cells that are very long, since an excess of $MinC_{Ec}$ would encompass all potential division sites and therefore block cell division altogether. Conversely, the absence of $MinC_{Ec}$ leads to a minicell phenotype as FtsZ rings can form at the cell poles in addition to midcell (de Boer and Crossley, 1989). In strains of *E. coli* which are devoid of any endogenous *min* (Δ*min*) genes, cells are also filamentous when $MinC_{Ec}$ and $MinD_{Ec}$ are overexpressed, suggesting that the two proteins may complex to form a division inhibitor that acts throughout the cell (de Boer and Crossley, 1989). Interestingly, a greater than 25-fold overexpression of $MinC_{Ec}$ alone can also inhibit cell division completely (de Boer *et al.*, 1992). Since such an increase of $MinC_{Ec}$ overexpression is needed, it was speculated that $MinD_{Ec}$ must play a role in coordinating the function of $MinC_{Ec}$ more efficiently (de Boer *et al.*, 1992).

MinC from *Thermotoga maritima* (Tm) was the first MinC protein to be resolved as a crystal structure (Cordell *et al.*, 2001). $MinC_{Tm}$ consists of 4 $MinC_{Tm}$ molecules organized as two dimers, where each monomer also contains two domains (Cordell *et al.*, 2001). The N-terminus comprises two α-helices and five β-strands, while the C-terminus is a helical structure comprising β-sheets that consists of three surfaces (A, B, and C) that wind as a

triangular barrel-like structure, where the A face was proposed to be the $MinC_{Tm}$ dimerization interface (Cordell *et al.*, 2001)

There are three main regions of *E. coli* MinC: an N-terminus (aa 1-99), a linker region (aa 100-124), and a C-terminus (aa 125-231) (Hu and Lutkenhaus, 2000). The N-terminus of $MinC_{Ec}$ is involved with the inhibition of FtsZ assembly (Hu and Lutkenhaus, 2000); this was shown by overexpression of a MalE-$MinC_{Ec}$ fusion encoding only the first 115 residues of *E. coli* $MinC_{Ec}$ (Hu and Lutkenhaus, 2000). While the C-terminus predominantly comprises β-sheet characteristics as determined by far-UV circular dichroism (Szeto *et al.*, 2001b), the C-terminus of $MinC_{Ec}$ is involved in the interaction with itself and with $MinD_{Ec}$ (Hu and Lutkenhaus, 2000;Szeto *et al.*, 2001b). Upon further analysis of the C-terminus of $MinC_{Ec}$, Zhou and Lutkenhaus (2005) identified R133 and S134 as key residues involved in MinC/MinD interaction using the junction of the B and C surfaces of $MinC_{Tm}$ as a model. Recently, it has also been shown that, while in the presence of $MinD_{Ec}$, the C-terminus of $MinC_{Ec}$ also contributes to the inhibition of FtsZ ring assembly (Shiomi and Margolin, 2007). This may not have been observed in previous experiments due to the fusion of $MinC_{Ec}$ to GFP, which could have caused structural changes that would affect interaction with $MinD_{Ec}$ (Shiomi and Margolin, 2007).

1.2.4. MinD

Aside from FtsZ, MinD is the most conserved bacterial protein associated with cell division site selection (Sakai *et al.*, 2001). There are many structural MinD models that include crystal structures of MinD homologues from *Pyrococcus* species and *Archaeoglobus fuldigus* (Cordell and Lowe, 2001;Hayashi *et al.*, 2001;Sakai *et al.*, 2001). Generally, the

crystal structures of MinD from these Archael species comprise a β-sheet of seven parallel strands and one antiparallel β-strand. The β-sheet is also surrounded by 11 α-helices (Cordell and Lowe, 2001;Hayashi *et al.*, 2001;Sakai *et al.*, 2001). Interestingly, these solved MinD structures bear a resemblance to the nitrogenase iron protein NifH (Schindelin *et al.*, 1997). The key features of NifH include an ATP-binding site and the ability to dimerize which apparently facilitates efficient ATP hydrolysis (Schindelin *et al.*, 1997).

E. coli MinD ($MinD_{Ec}$) is a 270 aa, 30 kDa, membrane-binding protein that also has a conserved ATP-binding motif and is a member of the ParA family involved in chromosome segregation (de Boer *et al.*, 1991;Lutkenhaus and Sundaramoorthy, 2003). This ATP-binding site (aa 10-17) is a "deviant" Walker A motif which typically has a X**K**GGXXK[T/S] sequence (X is any amino acid) which includes a characteristic lysine (bold) (Koonin, 1993;Lutkenhaus and Sundaramoorthy, 2003). Like NifH, $MinD_{Ec}$ also dimerizes in the presence of ATP by binding to the nucleotide (de Boer *et al.*, 1991;Hu *et al.*, 2003). Using a dimeric model of MinD based on NifH, it is believed that the dimerization of $MinD_{Ec}$ may also be needed for MinD ATPase activity (Lutkenhaus and Sundaramoorthy, 2003). Independently, $MinD_{Ec}$ exhibits basal and weak ATPase activity, while mutating the Walker A motif (e.g. K16Q) abolishes ATP hydrolysis altogether (de Boer *et al.*, 1991).

The biological function of $MinD_{Ec}$ does resemble that of the DNA segregation function of ParA family proteins in indirectly ensuring proper nucleoid partitioning. Like MinD, ParA can also associate with the membrane and is an ATPase (Lin and Mallavia, 1998); also, as ParA assists in complete segregation of DNA, proper functioning of MinD ensures that FtsZ rings do not form over replicated nucleoids. Many experiments show that $MinD_{Ec}$ is an activator of $MinC_{Ec}$ (de Boer *et al.*, 1992) which primes cell division and

eventual DNA segregation. Studies have shown that dimerized $MinD_{Ec}$ recruits dimerized $MinC_{Ec}$ to the membrane, implying that MinC dimerization may be needed to inhibit FtsZ polymerization (Szeto *et al.*, 2001b). As previously stated (section 1.2.3.), the amount of $MinC_{Ec}$ needed to cause cells to filament is dramatically reduced with the presence of $MinD_{Ec}$ (de Boer *et al.*, 1992). However, since $MinD_{Ec}$ overexpression does not cause filamentation to occur in cells devoid of $MinC_{Ec}$, $MinD_{Ec}$ alone cannot induce cell division inhibition. In the absence of $MinD_{Ec}$, a minicell phenotype is also observed in wild-type *E. coli* cells (de Boer *et al.*, 1988). Finally, $MinD_{Ec}$ was shown to localize to the cell membrane using immunoelectron microscopy, suggesting cell division is blocked when $MinD_{Ec}$ recruits $MinC_{Ec}$ to the membrane (de Boer *et al.*, 1991;de Boer and Crossley, 1989). Therefore, $MinD_{Ec}$ provides directionality to $MinC_{Ec}$; without the latter, a significantly higher amount of $MinC_{Ec}$ is required to act on FtsZ ring assembly (de Boer *et al.*, 1992). Indeed, a short C-terminal membrane targeting sequence (MTS) was found to be responsible for membrane localization in MinD (Hu and Lutkenhaus, 2003;Szeto *et al.*, 2002). Of interest, ParA does not possess a MTS motif.

Size-exclusion chromatography showed that in the presence of ATP, $MinD_{Ec}$ interacts with a MalE-$MinC_{Ec}$ fusion (Hu *et al.*, 2003). Recent studies have shown that multiple domains of $MinD_{Ec}$ may be involved with $MinC_{Ec}$ interaction. Yeast two-hybrid data indicated that residues E146 and D152 within the α-7 helix of $MinD_{Ec}$ were involved with $MinC_{Ec}$ interaction, while switch I (residues G42 and R44) and II (residue I125) domains of $MinD_{Ec}$, implicated in nucleotide-induced conformational changes (Vale, 1996), were also implicated in $MinC_{Ec}$ association (Zhou and Lutkenhaus, 2004).

1.2.5. MinE

Unlike $MinC_{Ec}$ and $MinD_{Ec}$, overexpression of *E. coli* MinE ($MinE_{Ec}$) does not lead to cell filamentation; instead minicell formation is observed (de Boer and Crossley, 1989). This phenotype is also seen when all three Min proteins are overexpressed, suggesting that among the Min proteins, $MinE_{Ec}$ plays the dominant role in site selection (de Boer and Crossley, 1989). $MinE_{Ec}$ is the smallest of the Min proteins (88 aa, 10 kDa) and is structurally unique. Using a variety of biochemical methods, $MinE_{Ec}$ was shown to interact with $MinD_{Ec}$ and to disrupt $MinC_{Ec}/MinD_{Ec}$ complexes, as well as interacting with itself (Huang *et al.*, 1996;King *et al.*, 2000). These studies suggest that $MinE_{Ec}$ counters the inhibitory effects of $MinC_{Ec}/MinD_{Ec}$ complexes by providing topological specificity to the localization of MinCD complexes to the cell poles (de Boer and Crossley, 1989;Pichoff *et al.*, 1995;Zhao *et al.*, 1995).

From the generation of deletional mutants, two predominant domains were found to contribute to the proper functioning of $MinE_{Ec}$. Amino acids 1-22 of *E. coli* MinE is an anti-MinCD domain that is responsible for MinD interaction (Zhao *et al.*, 1995). The rest of $MinE_{Ec}$ is responsible for preventing MinCD complexes from inhibiting FtsZ ring assembly at midcell and not at the cell poles to ensure proper cell division; this function has been termed "topological specificity" (King *et al.*, 2000;Pichoff *et al.*, 1995;Zhao *et al.*, 1995). Nuclear magnetic resonance (NMR) studies revealed that the N-terminus of $MinE_{Ec}$ interchangeably switches between α-helical or random coil formations (King *et al.*, 1999). When in the α-helical conformation, studies have suggested that one face of the helix does interact with another helix of $MinD_{Ec}$ (Ma *et al.*, 2003).

Several studies have shown that $MinE_{Ec}$ can also self-interact. Pichoff and co-workers (1995) showed that residues 36-62 are involved with $MinE_{Ec}$ self-association using yeast two-hybrid analysis and size-exclusion chromatography. The resolution of a dimeric structure of $MinE_{Ec}$ using NMR (encompassing residues 31-88 of $MinE_{Ec}$) confirmed this self-interaction (King *et al.*, 2000;King *et al.*, 1999) (Fig. 1.6). This peptide comprises an α-helix (aa 39-53 of *E. coli* MinE) that apparently interacts with another monomer in forming an anti-parallel coiled-coil, while two β-strands form a four stranded hydrophobic sandwich with the coiled-coil region (King *et al.*, 2000).

Previous studies have shown that mutations in the α-helix did not disrupt self-interaction. While alanine substitution of two $MinE_{Ec}$ residues of the α-helix, D45 and V49, reduced the propensity of $MinE_{Ec}$ ring formation, the mutations did not disrupt $MinE_{Ec}$ dimerization (King *et al.*, 2000;Shih *et al.*, 2002). As such, whether $MinE_{Ec}$ self-interaction is linked to biological function has yet to be addressed.

1.2.6. Dynamism of the Min proteins in *E. coli*

Advancement in microscopic techniques in live bacterial cell imaging using fluorescent fusion tags such as the green fluorescent protein (GFP) have provided critical details in how cell division site selection occurs in bacteria. One of the most surprising findings in these studies is that all three Min_{Ec} proteins are in a constant state of dynamic movement from pole-to-pole in negatively regulating FtsZ assembly to the midcell of bacteria (Fu *et al.*, 2001;Hale *et al.*, 2001;Hu and Lutkenhaus, 1999;Raskin and de Boer, 1999a;Raskin and de Boer, 1999b).

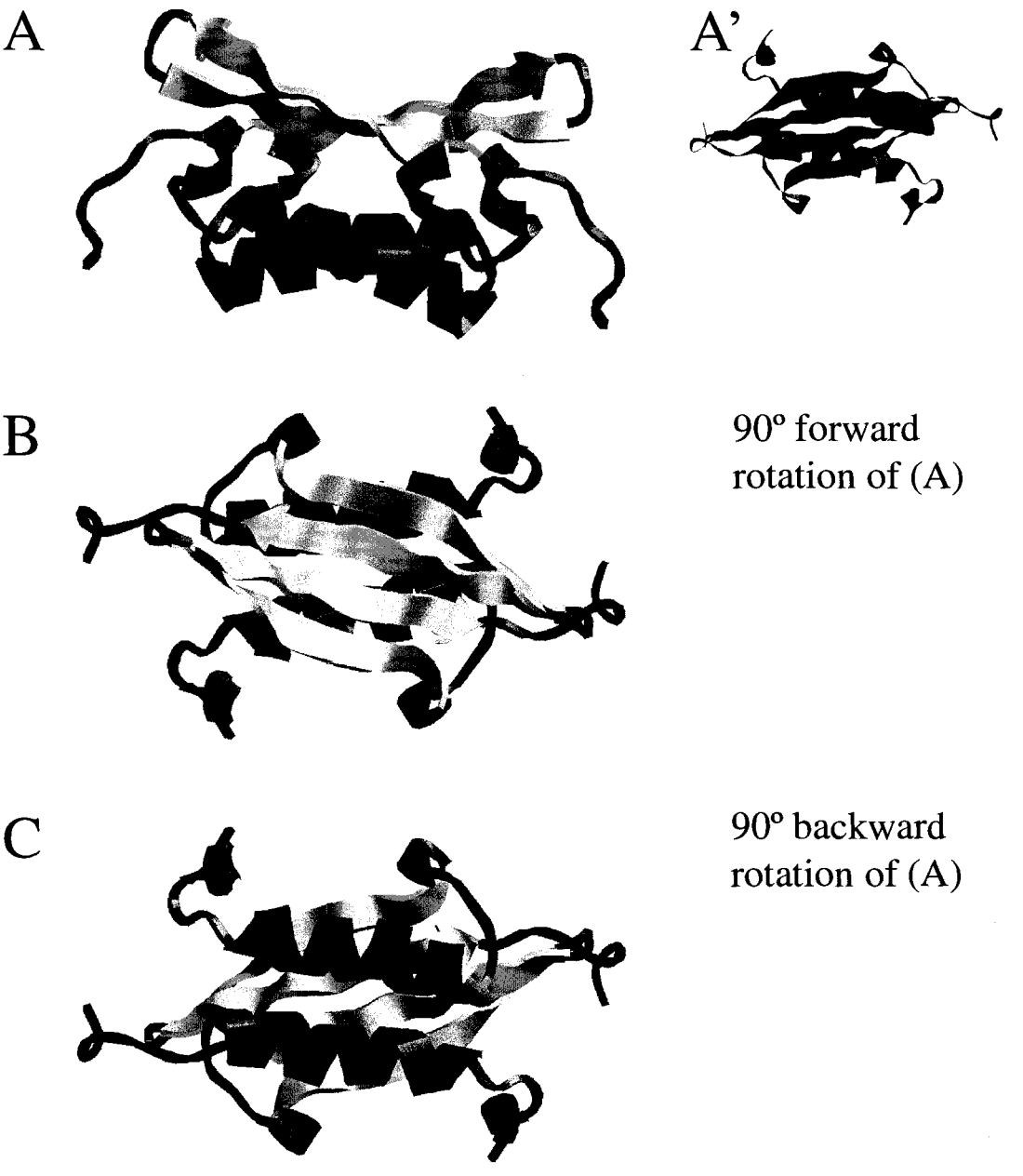

Figure 1.6. Nuclear magnetic resonance (NMR) structure of *E. coli* MinE (King et al., 2000). (A, B, and C) show differing views of a dimeric (A' shows two monomers in blue and green colours) structure of the C-terminus of *E. coli* MinE (aa 31-88), which comprises two parallel β-sheets (B, yellow) and two anti-parallel α-helices that face each other (C, red).

Several studies have shown that GFP-$MinD_{Ec}$ oscillates from pole-to-pole in the presence of $MinE_{Ec}$ in *E. coli* (Raskin and de Boer, 1999b;Rowland *et al.*, 2000). A growing zone of GFP-$MinD_{Ec}$ molecules develops from the pole to the midcell along the membrane, forming a tube-like structure; there, the fluorescent signal persists (~10 seconds) after which the zone recedes and a new zone starts to form at the opposite pole concurrently (Raskin and de Boer, 1999b;Rowland *et al.*, 2000). GFP-$MinD_{Ec}$ continues to oscillate in this manner in 40 second cycles/periods (Fig. 1.7 A shows the time it takes for $MinD_{Ec}$ to move from one pole to the other and back). However, $MinE_{Ec}$ is essential to this oscillation. Without $MinE_{Ec}$, GFP-$MinD_{Ec}$ localizes along the cell membrane with no detectable oscillation (Raskin and de Boer, 1999b;Rowland *et al.*, 2000). GFP-$MinD_{Ec}$ oscillation can be varied by increasing or decreasing the ratio of GFP-$MinD_{Ec}$/$MinE_{Ec}$; increasing the ratio led to increased periodicity of GFP-$MinD_{Ec}$ (Raskin and de Boer, 1999b). However, the formation of minicells was visualized with the increased periods, suggesting that a threshold frequency of oscillation is required to maintain proper division site selection in *E. coli* (Raskin and de Boer, 1999b).

Oscillation was also observed in GFP-$MinC_{Ec}$ fusions; however, the presence of $MinD_{Ec}$ and $MinE_{Ec}$ were required (Hu and Lutkenhaus, 1999;Raskin and de Boer, 1999a). In the absence of $MinE_{Ec}$, GFP-$MinC_{Ec}$ also localized to the cell membrane, as long as $MinD_{Ec}$ was present as well; if $MinD_{Ec}$ was not present, GFP-$MinC_{Ec}$ fluorescence was completely cytoplasmic (Hu and Lutkenhaus, 1999;Raskin and de Boer, 1999a).

Finally, $MinE_{Ec}$-GFP was also reported to display oscillatory properties (Fu *et al.*, 2001;Hale *et al.*, 2001). At first, $MinE_{Ec}$-GFP was thought to only form a ring at midcell that regulates the size of $MinD_{Ec}$ zones (Raskin and de Boer, 1997). However, further analysis

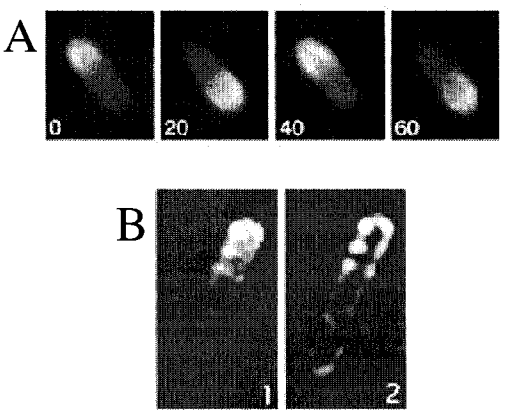

Figure 1.7. Localization of GFP-MinD$_{Ec}$ in *E. coli*. (A) GFP-MinD$_{Ec}$ exhibits pole-to-pole movement in rod-shaped *E. coli* in 40 s cycles. Timepoints are indicated in seconds in each panel (image from Raskin and de Boer, 1999a). (B) Image deconvolution shows GFP-MinD$_{Ec}$ localizing as a coiled-structure in *E. coli*. Note the majority of fluorescent signal at one half of the cell and a residual coiled array at the other. Image 1 is raw image, image 2 shows deconvolution of image 1 (image from Shih *et al.*, 2003).

showed that $MinE_{Ec}$-GFP localization was observed in a tube-like arrangement that seem to colocalize to the $MinD_{Ec}$ zones (Hale *et al.*, 2001). With the ring and tube-like formation of $MinE_{Ec}$-GFP, it is believed that the ring causes the leading edge of $MinD_{Ec}$ zones to disperse as it proceeds to the cell pole, while the tube of $MinE_{Ec}$-GFP fluorescence is believed to prime the $MinD_{Ec}$ molecules to disassemble (Shih *et al.*, 2002). Effectively, once $MinD_{Ec}$ localizes to the opposite pole, the $MinE_{Ec}$ ring and zone follow suit, thereby establishing an oscillation pattern. The time it takes for $MinE_{Ec}$ to oscillate from pole-to-pole is also similar to that required for $MinC_{Ec}$ and $MinD_{Ec}$ oscillation (Hale *et al.*, 2001).

Recently, using deconvolution and three-dimensional imaging, Shih and co-workers (2003) observed that the zones or tubes of GFP-tagged Min fluorescence localized to a single coiled array that winds internally along the cell membrane, suggesting that a subcellular cytoskeletal architecture of Min proteins could exist (Fig. 1.7 B shows MinD coiled array). As long as $MinE_{Ec}$ was present, $MinC_{Ec}$ and $MinD_{Ec}$ both localize to the coiled array (Shih *et al.*, 2003). This same study also showed that the $MinE_{Ec}$ ring actually comprises one or two tight loops of the array (Shih *et al.*, 2003). It is currently unknown if the Min proteins comprise the coiled array; alternatively, the array may be a pre-existing structure.

1.2.7. Biochemical basis of Min function in *E. coli*

Based on observations of how GFP-tagged Min proteins behave in *E. coli*, many questions have been posed concerning how the Min proteins are able to coordinate their dynamic activities. How does $MinD_{Ec}$ bind to the cell membrane? Why is $MinE_{Ec}$ necessary for oscillation? To answer these, a plethora of studies were conducted in order to explore the biochemical basis for Min function.

In vitro studies using electron microscopy have showed that purified $MinD_{Ec}$ protein can bundle in the presence of ATP (Suefuji *et al.*, 2002). The bundles, in turn, disassembled when purified $MinE_{Ec}$ was added (Hu *et al.*, 2002;Suefuji *et al.*, 2002). However, when $MinE_{Ec}$ and $MinD_{Ec}$ were equally present, there was additional $MinD_{Ec}$ bundling. This finding is significant since there are approximately 2000 and 1400 molecules of $MinD_{Ec}$ and $MinE_{Ec}$ in an *E. coli* cell (Shih *et al.*, 2002). Thus, the ability of $MinE_{Ec}$ to disassemble and assemble $MinD_{Ec}$ protein bundles could explain why $MinE_{Ec}$ can exist as a ring and as a zone which disassembles $MinD_{Ec}$ polymers (Hale *et al.*, 2001).

To imitate physiological conditions *in vitro*, the role of *E. coli* phospholipid vesicles, which enhanced the bundling and lengthening of $MinD_{Ec}$ filaments, was investigated (Suefuji *et al.*, 2002). Further studies into the role of phospholipids in $MinD_{Ec}$ behaviour showed that ATP was critical in binding $MinD_{Ec}$ to phospholipids (Hu *et al.*, 2002). As such, $MinD_{Ec}$-ATP was able to recruit $MinC_{Ec}$ to the phospholipid vesicles (Fig. 1.8) (Hu *et al.*, 2003;Lackner *et al.*, 2003). When ADP or a $MinD_{Ec}$ mutant that could not bind ATP (e.g. K16Q) were used in the lipid binding assays, no protein binding to the vesicles was observed (Hu *et al.*, 2002). In the presence of phospholipids and $MinE_{Ec}$, the ATPase activity of $MinD_{Ec}$ increased 10 fold (Hu and Lutkenhaus, 2001); subsequent release of $MinD_{Ec}$ from the vesicles was associated with the increased hydrolytic activity (Hu *et al.*, 2002). If $MinE_{Ec}$ was less able to bind to $MinD_{Ec}$, (e.g. N-terminal anti-MinCD domain mutation), ATPase activity was supressed greatly or non-existent altogether (Hu and Lutkenhaus, 2001). Hu and co-workers (2002) proposed that when $MinD_{Ec}$ binds to ATP, the protein undergoes a favourable conformation change in its structure that permitted membrane binding. At this point, the inherently weak ATPase activity of ATP-bound $MinD_{Ec}$ (de Boer *et al.*, 1991), is not stimulated until it interacted with $MinE_{Ec}$. Subsequently, $MinD_{Ec}$-ADP favours

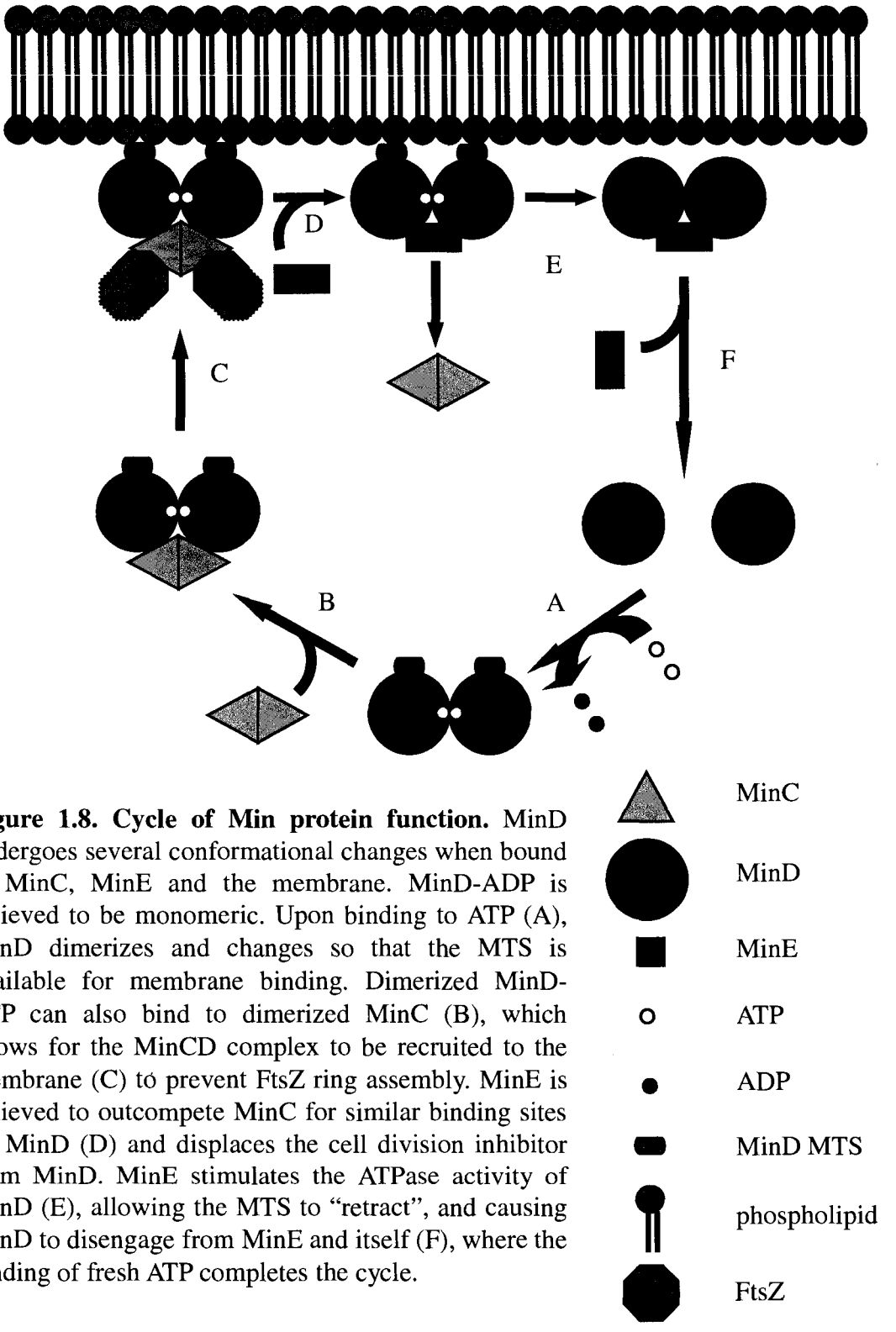

Figure 1.8. Cycle of Min protein function. MinD undergoes several conformational changes when bound to MinC, MinE and the membrane. MinD-ADP is believed to be monomeric. Upon binding to ATP (A), MinD dimerizes and changes so that the MTS is available for membrane binding. Dimerized MinD-ATP can also bind to dimerized MinC (B), which allows for the MinCD complex to be recruited to the membrane (C) to prevent FtsZ ring assembly. MinE is believed to outcompete MinC for similar binding sites on MinD (D) and displaces the cell division inhibitor from MinD. MinE stimulates the ATPase activity of MinD (E), allowing the MTS to "retract", and causing MinD to disengage from MinE and itself (F), where the binding of fresh ATP completes the cycle.

dissociation (along with $MinC_{Ec}$) from the cell membrane (Fig. 1.8) (Hu *et al.*, 2002;Hu *et al.*, 2003;Lackner *et al.*, 2003). Interestingly, $MinC_{Ec}$ and $MinE_{Ec}$ seem to compete for the same $MinD_{Ec}$ binding site at D152 (Ma *et al.*, 2004). Previous studies showed that $MinE_{Ec}$ could displace $MinC_{Ec}$ from vesicles, while retaining $MinD_{Ec}$ at the membrane (Hu *et al.*, 2003;Lackner *et al.*, 2003). Recent studies using a yeast three-hybrid system showed that *in trans* expression of $MinE_{Ec}$ disrupts $MinC_{Ec}$-$MinD_{Ec}$ interaction; however, these same studies suggested that $MinC_{Ec}$ also interferes with $MinD_{Ec}$-$MinE_{Ec}$ binding (Ma *et al.*, 2004). Phospholipid assays argue against the latter finding, since $MinC_{Ec}$ did not displace $MinD_{Ec}$-$MinE_{Ec}$ complexes from the vesicles, or affect the stimulation of $MinD_{Ec}$ ATPase activity by $MinE_{Ec}$ (Hu *et al.*, 2003). Based on these observations, although it is possible that $MinC_{Ec}$ and $MinE_{Ec}$ may share similar or overlapping $MinD_{Ec}$ binding sites, at least in the presence of phospholipids, $MinE_{Ec}$ may have a greater affinity for $MinD_{Ec}$ than $MinC_{Ec}$.

The extreme C-terminus (aa 261-268) of $MinD_{Ec}$ contains an amphipathic helix that is required for membrane localization to the cell membrane (Hu and Lutkenhaus, 2003;Szeto *et al.*, 2002). Deletion of this membrane targeting sequence (MTS) from *E. coli* and *B. subtilis* MinD caused GFP fusions of each of those proteins to remain completely cytoplasmic, unable to localize to the cell membrane of *E. coli* (Hu and Lutkenhaus, 2003;Szeto *et al.*, 2002). Loss of the MTS also affected MinC-dependent cell division inhibition (Hu and Lutkenhaus, 2003). This phenomenon was also observed if mutations that altered the helicity or amphipathicity of the MTS were introduced to $MinD_{Ec}$ (Szeto *et al.*, 2002). The highly conserved MTS is also transplantable since fusing the MTS to normally cytosolic proteins caused them to translocate to the cell membrane (Szeto *et al.*, 2003). In the presence of phospholipids, the MTS domain changes from a random coil into an α-helical

conformation that is positively charged (Szeto *et al.*, 2003). Since phospholipids are negatively-charged, the MTS should bind to them, a fact confirmed by Mileykovskaya and others (2003). Interestingly, the ability of MTS to associate with the membrane can vary; a single $MinD_{Bs}$ MTS is sufficient for membrane binding in *E. coli*, while two $MinD_{Ec}$ MTSs are required to accomplish the same goal (Szeto *et al.*, 2003). One possible explanation for this is that Min proteins do not oscillate in *B. subtilis*; thus, $MinD_{Bs}$ can remain membrane-bound, while the lower affinity of $MinD_{Ec}$ MTS for the membrane allows for easier disengagement from the cell membrane so that it can oscillate (Szeto *et al.*, 2003).

The above studies gave rise to two possible models that describe how $MinD_{Ec}$ binds to the membrane. In the "dimer-trigger" model, $MinD_{Ec}$ dimerizes upon ATP binding, which causes a conformational change that allows the MTS to bind to the membrane (Hu and Lutkenhaus, 2003). This model helps explain the finding that two $MinD_{Ec}$ MTS are needed for membrane binding (Szeto *et al.*, 2003) (Fig. 1.8). In the "zipper" model, binding of ATP and phospholipids are believed to promote the cooperative assembly of $MinD_{Ec}$ molecules (Lackner *et al.*, 2003;Szeto *et al.*, 2003); the model is not dependent on dimers, rather the presence of ATP-bound $MinD_{Ec}$ increases the affinity of MTS to bind to the cell membrane (Szeto *et al.*, 2003).

1.2.8. Model of cell division site selection in *E. coli*

Studies that examined the localization of the Min proteins and how they behave at the molecular level culminate into a working model describing Min-dependent cell division site selection in *E. coli* (Hu *et al.*, 2003;Lackner *et al.*, 2003;Shih *et al.*, 2003). $MinC_{Ec}$ may be recruited to the cell membrane/helical array in the presence of $MinD_{Ec}$ (Fig. 1.9, Shih *et*

Figure 1.9. Current model of cell division site selection of *E. coli* Min proteins. (A) In the cytosol, dimeric $MinD_{Ec}$ bind to ATP and recruits $MinC_{Ec}$ the membrane and/or a permanent $MinCDE_{Ec}$ coiled array. (B) $MinE_{Ec}$ binds to $MinD_{Ec}$-ATP, and localizes near the cell center as 1-2 loops of the coiled structure. $MinE_{Ec}$ causes $MinC_{Ec}$ to dissociate and stimulates $MinD_{Ec}$ ATPase activity, inducing $MinD_{Ec}$-ADP to dissociate as well, traveling to the other cell pole. (C) Cytoplasmic $MinD_{Ec}$ diffuses towards the other cell pole, binds ATP again, and associates with the coiled array at the opposite cell pole. (D) The $MinE_{Ec}$-dependent oscillation of $MinD_{Ec}$ and $MinC_{Ec}$, allows Z-ring assembly at midcell since time-averaged concentration of $MinC_{Ec}$ is lowest at midcell. (Adapted from Szeto Ph.D. thesis, 2004)

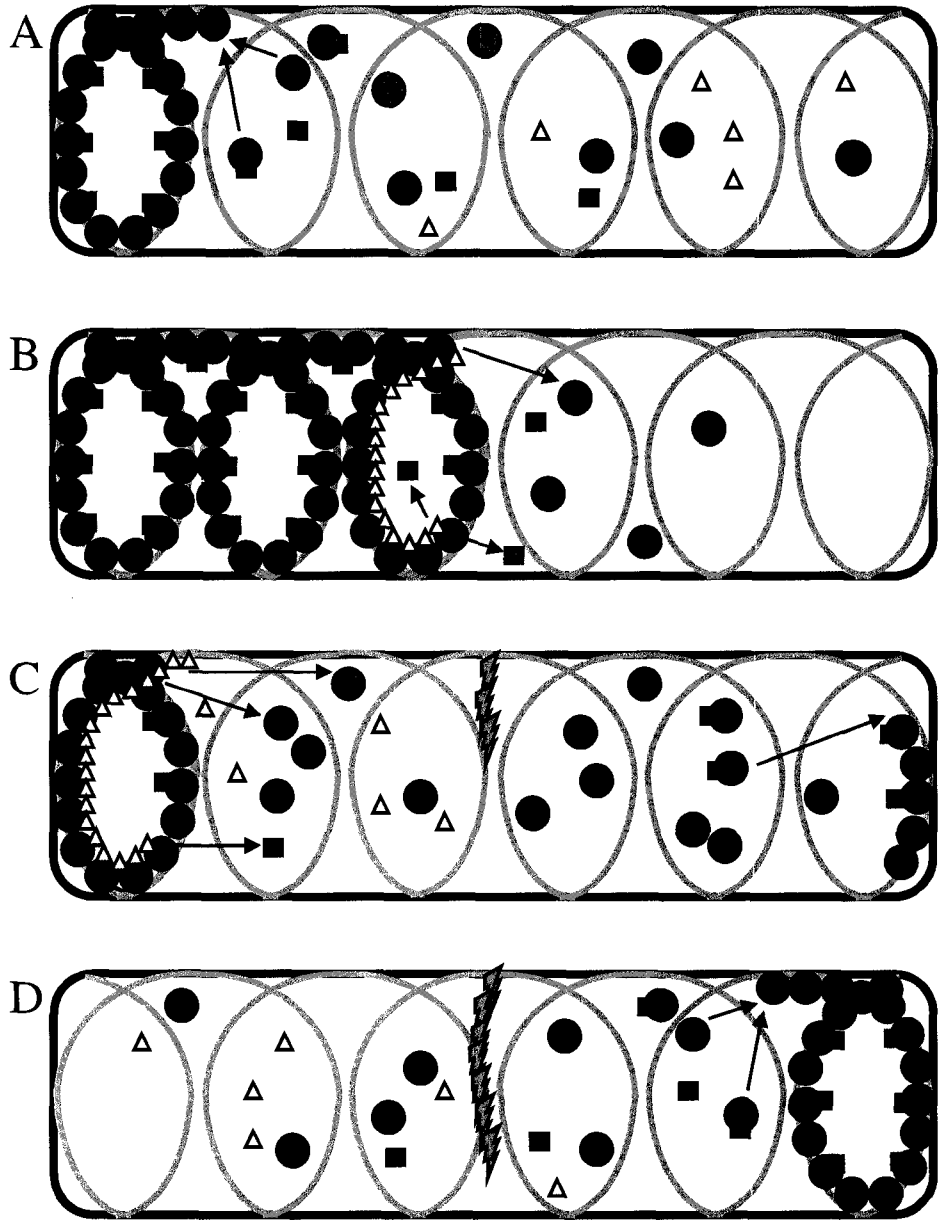
A
B
C
D
MinD$_{Ec}$-ATP
MinD$_{Ec}$-ADP
MinC$_{Ec}$
MinE$_{Ec}$
coiled array
FtsZ

al., 2003). While it is not clear if the recruitment happens in the cytoplasm or at the membrane, studies showed that $MinC_{Ec}$ can interact with mutant $MinD_{Ec}$ that cannot bind to phospholipids (Zhou and Lutkenhaus, 2004); however, phospholipids can enhance $MinC_{Ec}$ recruitment by $MinD_{Ec}$ (Hu *et al.*, 2003). Based on GFP localization experiments, both $MinC_{Ec}$ and $MinD_{Ec}$ localize to concomitant zones (Hu *et al.*, 1999;Raskin and de Boer, 1999a) in one half of the cell where any cell division is inhibited due to MinC preventing FtsZ ring assembly (Hu and Lutkenhaus, 2000).

In order for $MinD_{Ec}$ to localize to the cell membrane, $MinD_{Ec}$ must bind ATP before dimerization (Fig. 1.8). Membrane binding occurs via the C-terminal amphipathic MTS domain (Fig. 1.8) (Hu and Lutkenhaus, 2003;Szeto *et al.*, 2003), while the α-7 helix of $MinD_{Ec}$ interacts with the junction of the B and C surfaces of the C-terminus of $MinC_{Ec}$ (Zhou *et al.*, 2005;Zhou and Lutkenhaus, 2005). The N-terminus of $MinC_{Ec}$ primarily acts on FtsZ to hinder ring assembly in its presence (Hu and Lutkenhaus, 2000).

Without $MinE_{Ec}$, $MinC_{Ec}$ and $MinD_{Ec}$ remain statically colocalized at the cell membrane (Hu and Lutkenhaus, 1999;Raskin and de Boer, 1999a). A ring-like structure of $MinE_{Ec}$, comprising 1-2 loops of the helical array (Shih *et al.*, 2003) forms near midcell at the leading edge of the $MinD_{Ec}$ zone to limit the $MinCD_{Ec}$ zones from developing past the middle (Fig. 1.9) (Shih *et al.*, 2002). The $MinE_{Ec}$ ring interacts with $MinD_{Ec}$ and stimulates the ATPase activity of the latter, causing $MinD_{Ec}$-ATP to turn into $MinD_{Ec}$-ADP (Fig. 1.8 and 1.9). The conformational change in $MinD_{Ec}$ associated with ATP hydrolysis no longer favours membrane binding and $MinD_{Ec}$ dimerization, and $MinC_{Ec}$ and $MinD_{Ec}$ dissociate from the membrane into the cytosol (Hu *et al.*, 2003). As the $MinD_{Ec}$ lattice disassembles, the $MinE_{Ec}$ ring progresses towards the cell pole along the coiled array until all $MinD_{Ec}$ is

completely removed from the membrane at one pole (Fig. 1.9) (Shih *et al.*, 2003). During this time, cytoplasmic $MinD_{Ec}$ binds to ATP again (Fig. 1.8), and possibly due to a concentration gradient, nascent $MinD_{Ec}$-ATP reestablishes the zones of cell division inhibition at the other end of the cell, while the $MinE_{Ec}$ ring continues to disassembly the original $MinD_{Ec}$ zone (Fig. 1.9). Once completed, the $MinE_{Ec}$ ring subsequently reforms to the other cell half, where it an act on the nascent $MinD_{Ec}$ (and $MinC_{Ec}$) zone, thus inducing the oscillation patterns observed (Fig. 1.9) (Lackner *et al.*, 2003).

Therefore, the nucleoid occlusion model alone cannot account for the selection of cell division at midcell. While the presence of the nucleoid prevents FtsZ ring assembly, it allows for site selection to occur at midcell AND at the cell poles. As such, Δ*min E. coli* strains exhibit a minicell phenotype to show that division can occur at the cell poles in addition to the midcell (de Boer *et al.*, 1988;Sun and Margolin, 2001). Hence, the Min system is the dominant mechanism in directing cell division machinery to localize at midcell through pole-to-pole oscillation of the Min proteins along the coiled array (Fig. 1.9); the oscillation of Min causes the time-averaged concentration of $MinC_{Ec}$ to be lowest at midcell; thereby allowing FtsZ ring and eventually, divisome formation to occur (Fig. 1.9) (Raskin and de Boer, 1999a).

Many studies have used computer models to simulate MinD and MinE oscillation in a closed system, since MinC is not required for oscillation (Howard *et al.*, 2001;Kruse, 2002;Meinhardt and de Boer, 2001). However, with the finding of the helical coiled arrays (Shih *et al.*, 2003), more recent models have been able to explain most of the dynamic behaviour of Min proteins (Drew *et al.*, 2005;Tostevin and Howard, 2006).

1.3. Cell division site selection in other bacteria

1.3.1. Min proteins in the Gram-positive rod *Bacillus subtilis*

While *E. coli* Min proteins have been thoroughly examined, Min from the Gram-positive rod *B. subtilis* (Bs) have also been studied in significant detail. One major difference between *B. subtilis* and *E. coli* is that the former lacks a MinE homologue (Varley and Stewart, 1992). $MinC_{Bs}$ and $MinD_{Bs}$ behave similarly to their *E. coli* equivalents (Marston and Errington, 1999): 1) both proteins interact with each other; 2) $MinC_{Bs}$ depends on $MinD_{Ec}$ in order to be recruited to the cell membrane; 3) as in *E. coli*, overexpression of both proteins lead to filamentation as a result of cell division inhibition in *B. subtilis*. Inactivation of either gene induces a minicell phenotype (Varley and Stewart, 1992). Studies of GFP-$MinD_{Bs}$ showed that MinD is localized at the cell poles and at the midcell between completely segregated replicated nucleoids; suggesting that it can bind to future and past divisional sites (Marston *et al.*, 1998).

There are no observable oscillation patterns of $MinC_{Bs}$ and $MinD_{Bs}$ in *B. subtilis* cells, which contrasts to their *E. coli* counterparts. Instead, DivIVA (~19 kDa) participates in the topological regulation of the $MinCD_{Bs}$ inhibitor complex (Cha and Stewart, 1997;Edwards and Errington, 1997). GFP-tagged $DivIVA_{Bs}$ localizes to the cell poles and at nascent division sites just before septum completion (Edwards and Errington, 1997;Marston *et al.*, 1998). Without $DivIVA_{Bs}$, $MinD_{Bs}$ is distributed throughout *B. subtilis* cells in diffuse regions along the membrane, inducing cells to become filamentous (Edwards and Errington, 1997;Marston *et al.*, 1998).

These findings led to a "polar piloting" model to explain how $DivIVA_{Bs}$ keeps the $MinCD_{Bs}$ complex at the poles (Fig. 1.10) (Marston *et al.*, 1998). It is believed that once the chromosome has replicated, $FtsZ_{Bs}$ ring assembly begins. Once the FtsZ ring is completed,

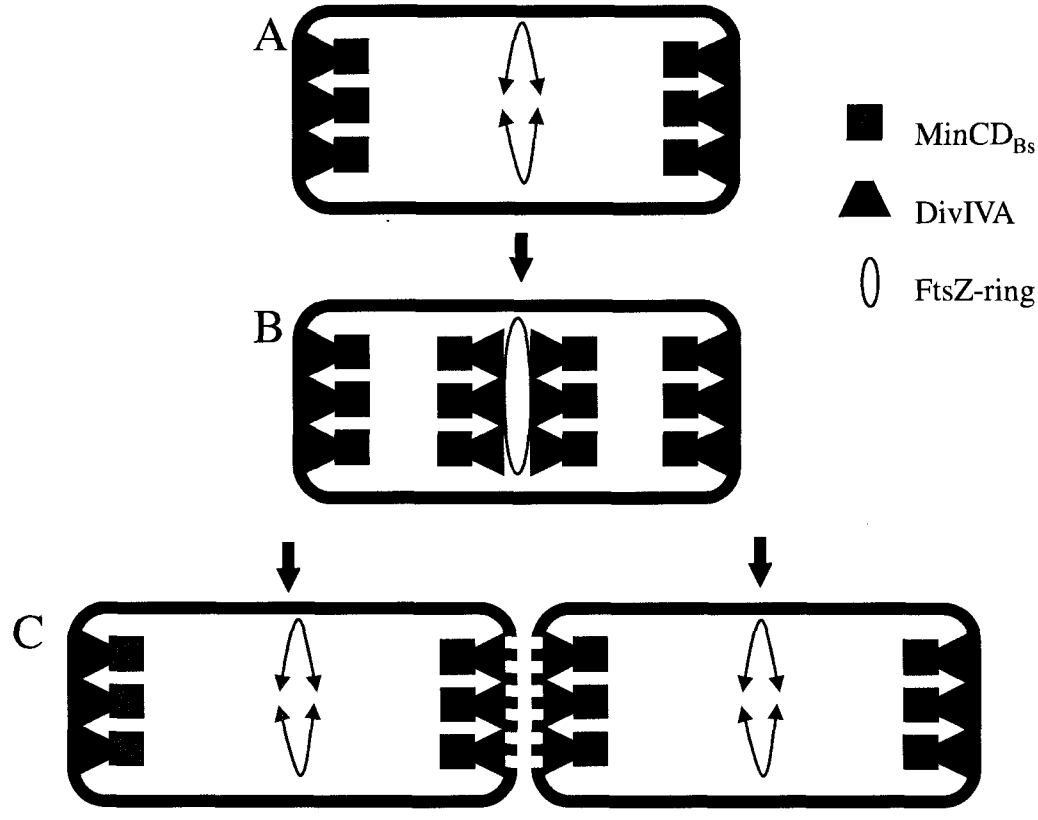

Figure 1.10. Cell division site selection in *B. subtilis* (adapted from Marston *et al.*, 1998). (A) In the 'polar piloting' model, *B. subtilis* cells have DivIVA localized at both poles, which sequesters both $MinC_{Bs}$ and $MinD_{Bs}$ to these regions as well, leading to division inhibition at the cell ends. (B) Once DNA replication nears completion, Z-ring assembly is complete and stabilized, allowing for the recruitment of other cell division proteins at midcell. DivIVA, $MinD_{Bs}$, and $MinC_{Bs}$ can assemble at midcell division sites before Z-ring constriction begins. Presumably, the Z-ring has assembled to a point where it will be resistant to the effects of $MinCD_{Bs}$. (C) Upon completion of cell division, the DivIVA-$MinCD_{Bs}$ complex remains associated with nascent (dotted line) and old cell poles in each daughter cell; thus, both cells have $MinCD_{Bs}$ retained at either ends to control future cytokinetic events.

$MinC_{Bs}$, $MinD_{Bs}$ and $DivIVA_{Bs}$ assemble at midcell as well before the FtsZ ring constricts (Harry and Lewis, 2003;Perry and Edwards, 2004), where presumably, $MinC_{Bs}$ cannot alter the completed Z ring. After septation is complete, $DivIVA_{Bs}$ and the $MinCD_{Bs}$ complexes are at the current and new cell poles, so as to be ready for subsequent division (Marston *et al.*, 1998). Interestingly, DivIVA is also found at the midcell and cell poles of the rod-shaped yeast *Schizosaccharomyces pombe* (Aldridge *et al.*, 2005), raising the possibility of a relationship between bacterial and yeast divisional components.

During sporulation, $DivIVA_{Bs}$ has another role. Even though levels of $DivIVA_{Bs}$ fall during the cell cycle of *B. subtilis*, the protein is still required for the attachment of the chromosomes to the cell pole (Thomaides *et al.*, 2001). This event is facilitated by $DivIVA_{Bs}$ recruiting a complex comprising the chromosomal origin and the DNA-binding RacA (Ben Yehuda *et al.*, 2002). In the absence of RacA, a second system takes over, involving the Spo0J and Soj proteins to make sure that the origins are directed to the cell poles (Wu and Errington, 2003).

Site-directed mutagenesis of $DivIVA_{Bs}$ revealed that the highly conserved R18 and G19 residues are responsible for targeting $DivIVA_{Bs}$ to the cell poles (Perry and Edwards, 2004). A R18C mutant was unable to target $DivIVA_{Bs}$ to the cell poles; however, vegetative growth and sporulation remained permissive, suggesting that $DivIVA_{Bs}$ pole targeting is not critical to the viability of *B. subtilis* (Perry and Edwards, 2004). In fact, this $DivIVA_{Bs}$ mutant could still localize to the midcell and be viable, despite minicell formation, suggesting that viability of *B. subtilis* minimally requires midcell localization of $DivIVA_{Bs}$ (Perry and Edwards, 2004).

Other studies of DivIVA from other bacteria usually led to abnormal cell division when a null mutant was generated, such as the Gram-positive cocci *E. faecalis* (Ramirez-

Arcos *et al.*, 2005), *Streptococcus pneumoniae* (Fadda *et al.*, 2007) and the bacillus *Brevibacterium lactofermentum* (Ramos *et al.*, 2003). Interestingly, a *divIVA* mutant in *Staphylococcus aureus* did not impair cell growth, chromosome segregation or morphology (Pinho and Errington, 2004).

1.3.2. Cell division site selection in *Caulobacter crescentus*

Recent studies on Min proteins from other bacteria revealed that phenotypes can differ from the minicell and filamentous phenotypes seen in *E. coli* and *B. subtilis*. For example, *Sinorhizobium meliloti*, a Gram-negative rod that induces nitrogen fixation, possesses all three of the Min proteins. However, upon deletion of the *min* genes, mutant cells were not distinguishable from wild-type cells (Cheng *et al.*, 2007). Furthermore, overexpression of MinC and MinD from this nitrogen fixator displayed a phenotype comprising large, swollen, and branched morphologies (Cheng *et al.*, 2007). A *Synechocystis* spp. Δ*min* mutant displayed spiral and heart-shaped cells (Mazouni *et al.*, 2004). This suggests that the Min system in these bacteria may have alternate functions.

There are very few prokaryotes that contain MinC, MinD, MinE and DivIVA – *Clostridium* species seem to be the one of the select few (Errington *et al.*, 2003). However, many other species do not have Min proteins at all, including *C. crescentus*, *Haemophilus influenzae*, *S. aureus*, *S. pneumoniae*, and *E. faecalis* (Fadda *et al.*, 2007;Jensen, 2006;Margolin, 2001;Massidda *et al.*, 1998;Ramirez-Arcos *et al.*, 2005). As such, other mechanisms must regulate cell division site selection in these prokaryotes.

Cell division and DNA replication in *C. crescentus* is asymmetrical; cells have a stalk at one pole for surface attachment, while a flagellum is present at the other pole for

motility after division (Brun *et al.*, 1994). Not only are Min proteins absent in this organism, but also a nucleoid occlusion system (Jensen, 2006). A recent study by Thanbichler and Shapiro (2006) discovered a new protein, MipZ, whose function combines the roles involved with both the nucleoid occlusion and MinCD inhibitory complexes. Like MinD, MipZ is an ATPase ParA family member; MipZ also remains statically localized to the cell poles; similar to $MinD_{Bs}$. Overexpression of MipZ induced a filamentous phenotype, which mimicked the MinCD inhibitor complexes; deletion of MipZ affected cell viability and also displayed filaments and minicells (Thanbichler and Shapiro, 2006).

Since MipZ binds to ParB, which in turn, binds to DNA sequences near *oriC* (Figge *et al.*, 2003), it was not surprising to see MipZ pattern its localization to the duplication event of *oriC* (Thanbichler and Shapiro, 2006) from the stalked pole to the flagellated pole (Jensen *et al.*, 2002). If MipZ is localized to the poles in this manner, how does it topologically regulate FtsZ ring formation? Purified MipZ stimulated the GTPase activity of FtsZ, causing FtsZ protofilaments to shorten and curve, thereby destabilizing the FtsZ ring, a characteristic of GDP-bound FtsZ (Thanbichler and Shapiro, 2006). Non-ring FtsZ was localized at the flagellated pole. When one of the duplicated *oriC*, bound with MipZ, rapidly moves to the flagellated pole, the bound MipZ causes FtsZ there to destabilize, leaving FtsZ to form the Z-ring only at the cell center where division eventually takes place (Fig. 1.11).

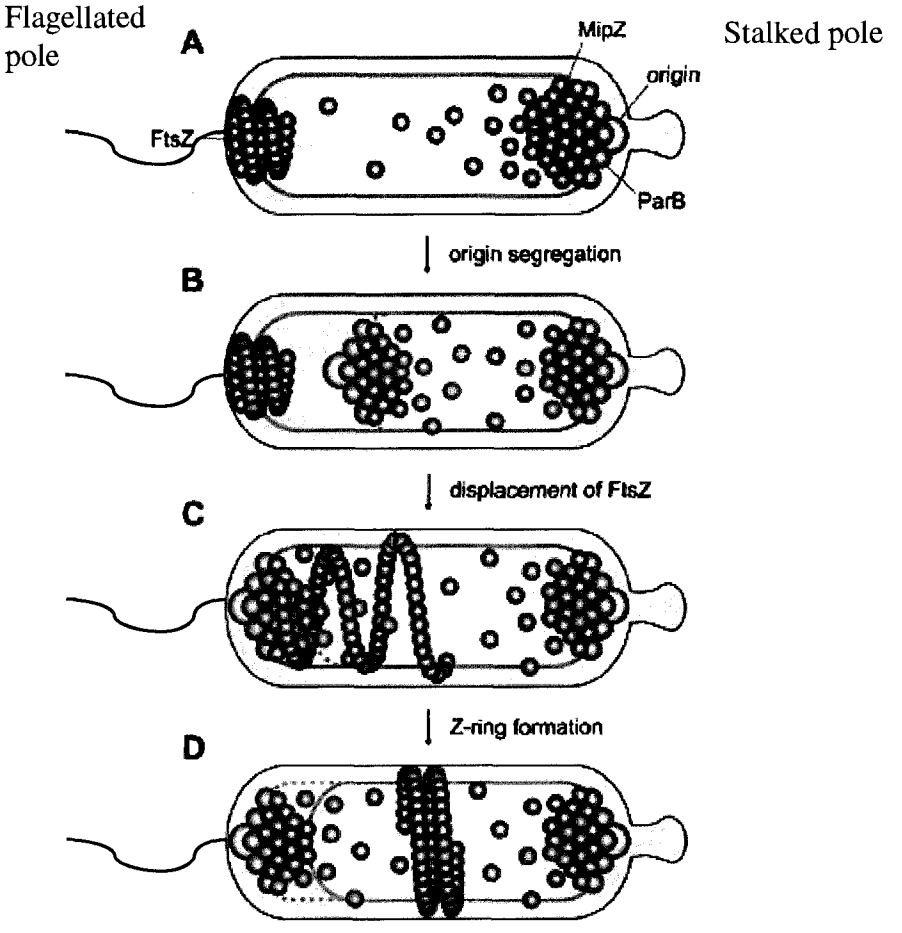

Figure 1.11. Cell division site selection in *C. crescentus*. (A) Non-ring FtsZ is localizaed at the flagellated pole while MipZ/ParB binds to DNA near *oriC* (origin) at the stalked pole. (B) As DNA replicates, *oriC* moves towards the flagellated pole, MipZ causes FtsZ to destabilize (C). When MipZ is at both poles, Z-ring formation can only occur at midcell (D). [Reprinted with permission from Elsevier (Thanbichler and Shapiro, 2006)].

1.4. Current state of knowledge of cell division in *Neisseria gonorrhoeae*

1.4.1. The Gram-negative *N. gonorrhoeae*: medical importance and etiology

One of the oldest recorded diseases in man, dating back to biblical times (Lev. 15:1-15:19), the Gram-negative diplococcus *N. gonorrhoeae*, or the gonococcus, is the etiological agent of the sexually transmitted disease (STD) gonorrhea. The disease is still a global health problem with more than sixty million cases per year (Gerbase *et al.*, 1998). Unfortunately, this number is likely to be even higher since females are often asymptomatic (Sparling, 1999). Subsequent primary infection causes spreading to the upper genital tract, which left untreated, can cause pelvic inflammatory disease (PID). In turn, PID may produce scarring and blockage of the fallopian tube, leading to persistent pain, possible infertilities and ectopic pregnancies (Sparling, 1999). Males afflicted with *N. gonorrhoeae* often experience painful discharge from the urethra, where Gram-negative diplococci are often found in polymorphonuclear neutrophils (Sparling, 1999). *N. gonorrhoeae* is an exclusive human pathogen that mainly infects the urogenital epithelia, although cases of infection of the conjuctiva, pharynx, and rectal mucosa are reported as well, along with rare systemic infections such as arthritis, endocarditis, and meningitis (Sparling, 1999). Often associated with a co-infection of *Chlamydia trachomatis*, the lesions and loss of mucosal integrity caused by *N. gonorrhoeae* lead to increased susceptibility to the human immunodeficiency virus (HIV) type 1 (Chen *et al.*, 2003).

N. gonorrhoeae adheres to and invades epithelial mucosal surfaces (Merz and So, 2000), where infection takes place (Apicella *et al.*, 1996). Once internalized after attachment to cells by gonococcal type IV pili and other adhesins (Merz and So, 2000), a repertoire of virulence factors allows this diplococcus to adapt to many environmental conditions and to escape detection by the immune system. Various surface molecules may undergo

phase/antigenic variation including the pilus, opacity-associated (Opa) outer membrane proteins, and lipooligosaccharide (LOS) (Merz and So, 2000). While the highly variable porins are immunogenic and stable for a given gonococcal strain (Snapper *et al.*, 1997), they are often associated with the reduction-modifiable protein (Rmp) and with LOS. Blocking antibodies to Rmp and LOS impair an appropriate immune response against porin (Elkins *et al.*, 1992). Thus, both antigenic variation and lack of antigenic exposure ensure that the immune system cannot be effectively stimulated by *N. gonorrhoeae*. This explains why no effective vaccine against *N. gonorrhoeae* has been developed to date.

1.4.2. Morphology of dividing *N. gonorrhoeae*

Under a microscope, the coccal *N. gonorrhoeae* cells are seen as a single, pair or a tetrad of cells. Clinically, they often appear as diplococci. Unlike rod-shaped *E. coli* cells which divide along a single plane, resulting in two daughter cells (Nanninga, 1998), gonococci divide in two planes that are perpendicular to each other (Ramirez-Arcos *et al.*, 2001b;Westling-Haggstrom *et al.*, 1977). The first round of division, is followed by a second divisional event, in which the division plane is perpendicular to the septum, giving rise to tetrad formation (Westling-Haggstrom *et al.*, 1977) (Fig. 1.12, Eng *et al.*, unpublished data).

One of the first observable events in gonococcal cell division is the presence of a slight invagination on one side of the cell, indicating early septum formation (Fitz-James, 1964;Westling-Haggstrom *et al.*, 1977). As the septum continues to form, no portion of the duplicated nucleoid appear to interfere with septum formation; thus, this initial constriction acts as a marker for cell division (Fitz-James, 1964). Once division is completed, there is a slight delay in the completion of the cell wall that would physically separate the progeny;

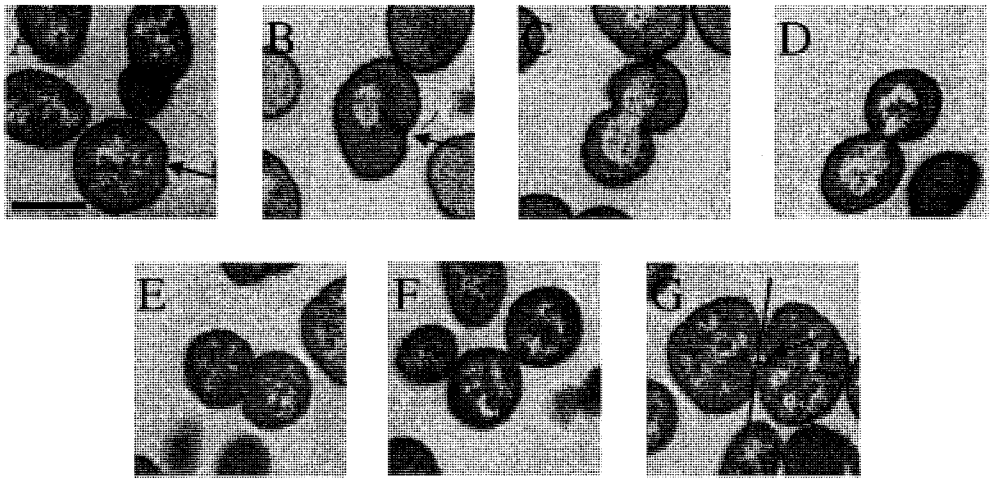

Figure 1.12. Transmission electron microscopy of *N. gonorrhoeae* F62. As a single invagination point (arrows) signals the start of cell division (A), the nucleoid condenses as the peptidoglycan is being assembled at the invagination point (B). As this occurs, the nucleoid is replicated and starts to migrate in opposite directions into the future daughter cells (C). Another invagination occurs at the other side of the initial invagination (C, D) and when the septum is nearly completely formed, the condensed chromosomes revert back to the uncondensed nucleoid (E, F). When the daughter cells grow to sufficient size, a second divisional event (solid line) perpendicular to the first plane (dotted line) occurs (G) with new invagination points at the junction of the diplococcal daughter cells and a tetrad will form. Scale bar is 500 nm. Images are unpublished data from Dillon laboratory.

as a result, the daughter cells remain attached to each other and are thus presented as diplococci, as frequently seen in diagnostic specimens of *N. gonorrhoeae* (Fitz-James, 1964). At the junction of the diplococci, subsequent division also reveals a single invagination point of cell wall synthesis in each daughter cell on a plane perpendicular to the existing septum (Westling-Haggstrom *et al.*, 1977). This second divisional event therefore permits two-by-two tetrad formation. However, tetrads need to physically separate in order to divide again, since single and diplococcal morphologies are often seen. Fussenegger and co-workers (1996) discovered that when the tetrapac (*tpc*) gene was disrupted, electron microscopy showed that over 95% of *N. gonorrhoeae* cells were present as tetrads that were connected by two layers of peptidoglycan. Thus, *tpc* may encode a murein hydrolase that would separate the nascent cell wall peptidoglycan between divided gonococcal cells (Fussenegger *et al.*, 1996).

1.4.3. The *dcw* cluster of *N. gonorrhoeae* and FtsZ

The division cell wall cluster of *N. gonorrhoeae* contains 17 known and putative genes (Fig. 1.1). While similar to the *E. coli dcw* cluster, there are also some differences between the two organisms. There are three hypothetical genes in the *dcw* cluster of *N. gonorrhoeae*, *hyp1*, *hyp2*, and *hyp3*, which are similar to *ybiP*, *yebT*, and *yieG*, found outside of the *dcw* cluster in *E. coli* (Francis *et al.*, 2000). While *envA* was not found within the *dcw* cluster of *N. gonorrhoeae* (Francis *et al.*, 2000), there are conflicting reports as to whether *ftsL* is (Snyder *et al.*, 2001) or is not (Francis *et al.*, 2000) part of the *N. gonorrhoeae dcw* cluster since there is only 22% amino acid similarity to *E. coli ftsL*. The gene order of the *dcw* cluster of *N. gonorrhoeae* CH811 was previously identified by Francis and co-workers (2000) using the raw data of the *N. gonorrhoeae* FA1090 genome project (Roe *et al.*, 2000)

as: *mraZ*, *mraW*, *ftsI*, *murE*, *hyp1*, *murF*, *mraY*, *hyp2*, *murD*, *ftsW*, *murG*, *murC*, *ddl*, *ftsQ*, *ftsA*, *ftsZ*, and *hyp3*. Unlike *E. coli*, where there are no internal transcriptional terminators, the gonococcal *dcw* cluster contains four transcriptional terminators (Francis *et al.*, 2000). Three of them (between *mraY-hyp2*, *murD-ftsW*, and *murG-murC*) are inverted repeats of the gonococcal uptake sequence (5'-GCCGTCTGAA-3'), which is required for *N. gonorrhoeae* both to be transformed with DNA and to terminate transcription (Francis *et al.*, 2000;Goodman and Scocca, 1988). Studies showed that a repeat sequence known as the Correia element is also a terminator between *murF* and *mraY* (Francis *et al.*, 2000); however, additional studies of the *dcw* cluster of *N. gonorrhoeae* and *N. meningitidis* suggest that this may not the case (Snyder *et al.*, 2003).

FtsZ from *N. gonorrhoeae* ($FtsZ_{Ng}$) is a 41.5 kDa, 392 aa protein that is 67% and 65% similar to $FtsZ_{Ec}$ and $FtsZ_{Bs}$, respectively (Salimnia *et al.*, 2000). $FtsZ_{Ng}$ is an essential protein for survival that can also localize to the midcell and exhibit cross-functionality in *E. coli* cells (Fig. 2B) (Salimnia *et al.*, 2000). Furthermore, overexpression of $FtsZ_{Ng}$-GFP can form a helical array or display a banding pattern, depending on the *E. coli* strain used (Salimnia *et al.*, 2000). Overexpression of $FtsZ_{Ng}$-GFP in *N. gonorrhoeae* F62 cells caused cell shape abnormalities, resulting from the many cell division planes that were observed (Salimnia *et al.*, 2000). $FtsZ_{Ng}$-GFP was also found only in insoluble fractions, suggesting the presence of inclusion bodies; this may explain the dispersed and grainy fluorescence that was observed in *N. gonorrhoeae* F62 cells (Salimnia *et al.*, 2000).

$FtsZ_{Ng}$ expression can be regulated depending on the environmental conditions. There are three promoters that are upstream of $ftsZ_{Ng}$ (Ramirez-Arcos *et al.*, 2001a). This promoter region is significantly active under anaerobic conditions. The P_Z1 promoter, that is closest to $ftsZ_{Ng}$, is particularly active (Francis *et al.*, 2000;Ramirez-Arcos *et al.*, 2001a).

Under anaerobiosis, there was also increased expression of $FtsE_{Ng}$ and $MinD_{Ng}$ (Ramirez-Arcos *et al.*, 2001a). Interestingly, $FtsZ_{Ng}$ expression was decreased in the presence of urea (Ramirez-Arcos *et al.*, 2001a). Since $FtsZ_{Ng}$ and other cell division proteins are partly regulated by environmental conditions, these findings provide a possible explanation as to how *N. gonorrhoeae* adapts to the environmental stress that the organism faces when invading the human genitourinary tract.

While *E. coli* FtsE and FtsX play a role in cell division in low salt conditions (Reddy, 2007), the role of these two proteins in the gonococcus is not clear. Disrupting $ftsE_{Ng}$ and $ftsX_{Ng}$ by insertional mutagenesis did not alter the viability of mutant *N. gonorrhoeae* cells, suggesting that these genes are not essential to the gonococcus (Bernatchez *et al.*, 2000). However, transmission electron microscopy indicated that these mutants displayed aberrant gonococcal morphologies, indicating defective divisional patterns (Bernatchez *et al.*, 2000), in contrast to the alternating perpendicular planes usually associated with gonococcal division. Furthermore, the $ftsE_{Ng}$ mutants caused chromosomal condensation, thereby preventing normal DNA segregation (Bernatchez *et al.*, 2000).

1.4.4. Identification of gonococcal *min* genes

Gonococcal *minC*, *minD*, and *minE* homologues were first identified by Ramirez-Arcos *et al.* (2001b) by a BLAST analysis of the raw sequence data from the *N. gonorrhoeae* FA1090 genome project (Roe *et al.*, 2000). The three gonococcal *min* genes, $minC_{Ng}$, $minD_{Ng}$, and $minE_{Ng}$ (GenBank accession number AF345908), were sequenced from *N. gonorrhoeae* CH811, and found to be 97% identical to meningococcal *min* genes (Ramirez-Arcos *et al.*, 2001b). They are part of a 17 kb cluster of genes, flanked by gonococcal uptake sequences, that includes *rpoA* (α subunit of RNA polymerase), *secY* (secretion protein), IF1

(initiation factor) upstream of the *minB* locus and *oxyR* (oxidative stress transcriptional regulator) downstream, which are all transcribed in the same direction (Ramirez-Arcos *et al.*, 2001b). Interestingly, the *min* genes in *E. coli* and *B. subtilis* are contained within a 1.7 kb and 5 kb gene cluster, respectively (Fig. 1.13) (Ramirez-Arcos *et al.*, 2001b). Gonococcal *minC* and *minD* are separated by 28 bp, while *minD* and *minE* are only separated by 3 bp. Promoter regions have been identified for $minC_{Ng}$ (between *rplQ* and $minC_{Ng}$), $minD_{Ng}$ (at the 3' end of $minC_{Ng}$) and $minE_{Ng}$ (at the 3' end of $minD_{Ng}$); there is also increased expression of $MinC_{Ng}$ and $MinD_{Ng}$ under anaerobiosis (Ramirez-Arcos *et al.*, 2001a).

1.4.5. Gonococcal MinC ($MinC_{Ng}$)

MinC from *N. gonorrhoeae* ($MinC_{Ng}$) is a 237 aa, 26.3 kDa protein that is required for correct cell division; deletion of $minC_{Ng}$ generated uncontrolled cell division along many planes, resulting in the formation of abnormal clusters of cells of differing size and shape with occasional incomplete septa (Ramirez-Arcos *et al.*, 2001b). There were also many cells that had lysed or lacked any internal components, termed "ghost cells" (Fig. 1.14) (Ramirez-Arcos *et al.*, 2001b). These mutations likely contributed to the decreased cell viability of *N. gonorrhoeae* in the absence of $minC_{Ng}$ (Ramirez-Arcos *et al.*, 2001b). In *E. coli*, $MinC_{Ng}$ complemented an *E. coli minC* knockout by restoring the ability to divide at midcell, suggesting that $MinC_{Ng}$ is functional across species; this was further evident when overexpression of $MinC_{Ng}$ in an *E. coli* background led to the formation of long filamentous cells (Ramirez-Arcos *et al.*, 2001b).

Even though $MinC_{Ng}$ is 36% and 22% identical to MinC from *E. coli* and *B. subtilis*, respectively, there are only five residues that are perfectly conserved between all MinC sequences; they correspond to R136, G138, G157, G164, and G174 of $MinC_{Ng}$

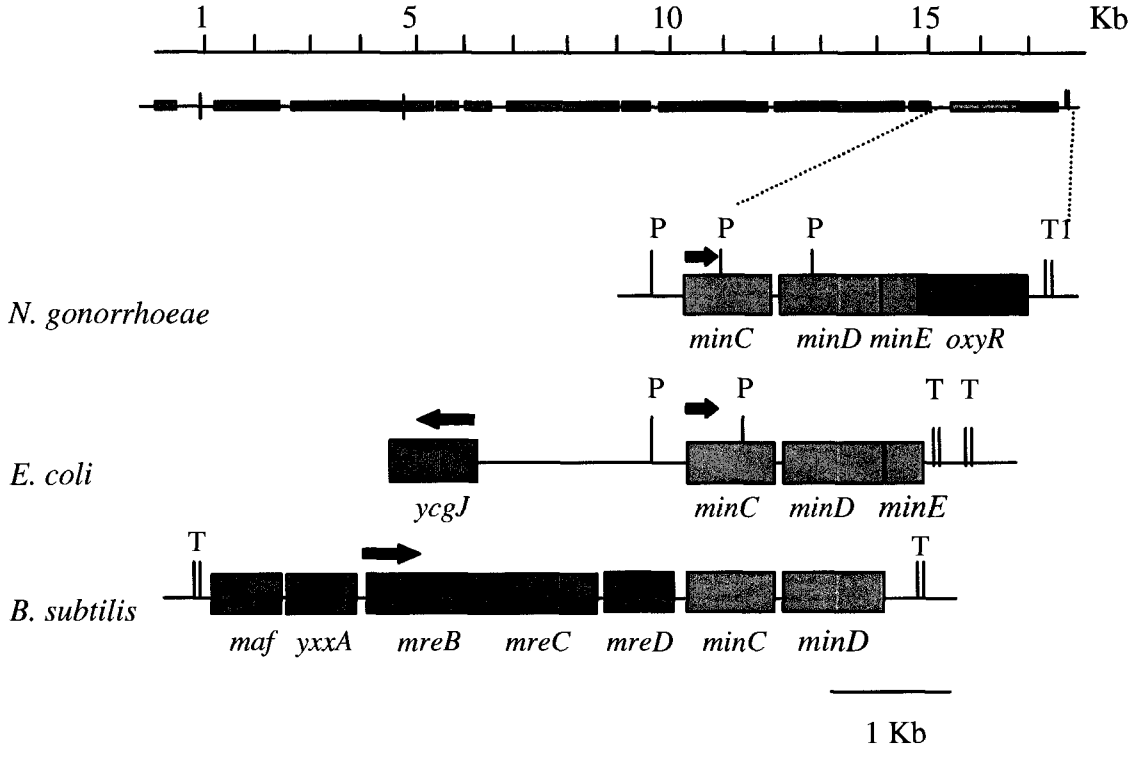

Figure 1.13. Comparison of *min* gene clusters from *N. gonorrhoeae*, *E. coli*, and *B. subtilis*. Transcriptional terminators at T1 are gonococcal uptake sequences, which flank the 17 kb gonococcal gene cluster that encompass the *minC*, *minD*, and *minE* genes. The *min* genes from *E. coli* are part of a smaller 1.7 kb cluster, while *B. subtilis minC* and *minD* are part of a 5 kb gene cluster and does not possess *minE*. Direction of translation is indicated by the arrows (Figure from Ramirez-Arcos *et al.*, 2001). P indicates the promoter sites, while T shows non-gonococcal terminator sites.

Figure 1.14. Morphology of *N. gonorrhoeae* cells in the absence of *minC*$_{Ng}$. Deleting functional *minC*$_{Ng}$ induced uncontrolled cell division along many planes, giving rise to abnormal clusters of cells, where many have lysed to give the appearance of "ghost" cells [Reprinted with permission from Society for General Microbiology (Ramirez-Arcos *et al.* 2001b)].

(Ramirez-Arcos *et al.*, 2001b). Mutating each of the four conserved glycine residues in $MinC_{Ng}$ resulted in the failure to inhibit cell division in an *E. coli* background as indicated by the failure to produce filaments upon overexpression (Ramirez-Arcos *et al.*, 2004). When these glycine residues from $MinC_{Ng}$ were mapped onto MinC from *T. maritima*, G138, G157, and G174 were located at or near the B/C surface junction of $MinC_{Tm}$; molecular modeling showed that the B/C junction may interact with the α-7 helix of archael MinD (Ramirez-Arcos *et al.*, 2004). Indeed, when these glycine residues were mutated in the corresponding $MinC_{Ec}$ residues, yeast two-hybrid assays showed that G135, G154, and G171 of $MinC_{Ec}$ are involved in MinD interaction (Ramirez-Arcos *et al.*, 2004). G164 of $MinC_{Ng}$ was located within the A surface of $MinC_{Tm}$ believed to be involved with dimerization (Cordell *et al.*, 2001;Ramirez-Arcos *et al.*, 2004); the corresponding mutation in $MinC_{Ec}$ showed disrupted MinC self-interaction, suggesting that molecular modeling was correct in predicting the surface interaction between MinC and MinD (Ramirez-Arcos *et al.*, 2004).

Recent studies showed that the thirteenth amino acid at the N-terminus of gonococcal MinC may be required to inhibit cell division as overexpression of a mutant deficient in the first 13 residues of $MinC_{Ng}$ failed to induce a filamentous phenotype in *E. coli* (Greco-Stewart *et al.*, 2007). In addition, there may be conserved structural motifs in the N-terminus of $MinC_{Ng}$ that are important for functionality, despite the lack of conservation at the amino acid level; for example, two α-helices in the N-terminus of $MinC_{Ng}$ are believed to be required for interaction with $FtsZ_{Ng}$ since division inhibition was impaired in mutants where each of the helices was disrupted with the introduction of a proline residue (Kini and Evans, 1995). These mutants were unable to induce filamentation when overexpressed in *E. coli* (Greco-Stewart *et al.*, 2007).

1.4.6. Gonococcal MinD ($MinD_{Ng}$)

$MinD_{Ng}$ is a 271 aa, 29.6 kDa protein that is 73% and 39% identical to MinD from *E. coli* and *B. subtilis*, respectively (Ramirez-Arcos *et al.*, 2001b). A gonococcal mutant of *minD*$_{Ng}$ that was insertionally inactivated displayed aberrant cell division, morphology, and altered cell viability (Szeto *et al.*, 2001a). Overexpression of both $MinC_{Ng}$ and $MinD_{Ng}$ in a gonococcal background showed significant cell enlargement, which is typical of cell division inhibition (Szeto *et al.*, 2001a). Combined, these results show that gonococcal MinD is needed for proper cell division and growth in *N. gonorrhoeae*. $MinD_{Ng}$ is also functional across species; its overexpression was able to complement an inactivated *E. coli minD* mutant and restore wild-type *E. coli* phenotype, while overexpression in an *E. coli* background produced cell filamentation (Szeto *et al.*, 2001a). Gonococcal MinD also localized to a coiled array in *E. coli* (Fig. 1.15) (Szeto, 2004), as observed with *E. coli* MinD (Shih *et al.*, 2003) Yeast two-hybrid assays and size-exclusion chromatography studies showed that $MinD_{Ng}$ interacts with itself and with *E. coli* MinD, the first study to demonstrate self-interaction of MinD (Szeto *et al.*, 2001a). Since *E. coli* MinD also self-interacts (Hu and Lutkenhaus, 2003), MinD localization is likely important in maintaining proper cell division site selection.

In *E. coli*, ATP hydrolysis by $MinD_{Ec}$ was stimulated upon interaction with $MinE_{Ec}$ (Hu and Lutkenhaus, 2001); recent studies showed that gonococcal MinD also possesses ATPase activity (Szeto *et al.*, 2004;Szeto *et al.*, 2005). Further characterization of $MinD_{Ng}$ showed that a conserved polar region (aa 92-94) is needed for relaying the stimulatory effects of MinE-induced oscillation (Szeto *et al.*, 2005). Mutation of these conserved residues ($MinD_{Ng\text{-}loop}$) did not abolish $MinD_{Ng}$ interaction with itself, $MinC_{Ng}$ or $MinE_{Ng}$;

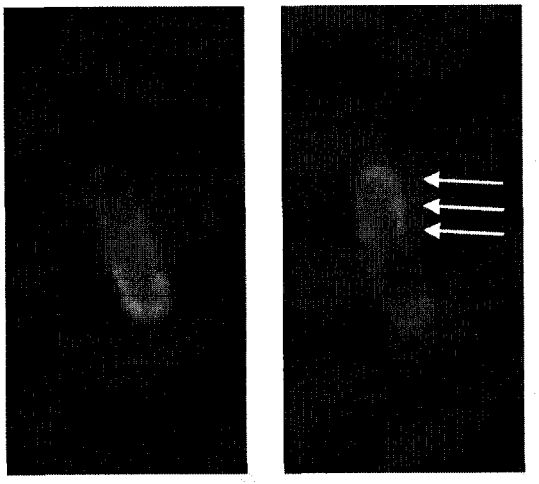

Figure 1.15. GFP-MinD$_{Ng}$ is recruited to the coiled array in the presence of MinE$_{Ng}$. Coexpression of GFP-MinD$_{Ng}$ and MinE$_{Ng}$ induced oscillation from one pole to the other and back in ~ 30 seconds. Also, GFP-MinD$_{Ng}$ localizes the coiled array (arrows). Figure from Szeto *et al.*, 2005.

furthermore, mutating this region in either $MinD_{Ng}$ or $MinD_{Ec}$ did not alter their abilities to localize to the coiled arrays (Szeto *et al.*, 2005). However, $MinE_{Ng}$ did not stimulate the ATPase activity of the $MinD_{Ng\text{-}loop}$ mutant and caused GFP-$MinD_{Ng\text{-}loop}$ to be uniformly distributed along the coiled array instead of inducing GFP-$MinD_{Ng}$ pole-to-pole oscillation (Szeto *et al.*, 2005). Interestingly, yeast two-hybrid assays showed that interaction of $MinD_{Ng\text{-}loop}$ to $MinE_{Ng}$ was stronger than wild-type $MinD_{Ng}$; thus it is possible that the stronger $MinD_{Ng\text{-}loop}$/$MinE_{Ng}$ interaction may have prevented the normal dissociation of GFP-$MinD_{Ng\text{-}loop}$ subunits from the coiled array and any subsequent oscillation (Szeto *et al.*, 2005). $MinD_{Ng\text{-}loop}$ self-association was also stronger than wild-type $MinD_{Ng}$; this observation could also prevent normal dissociation from the coiled array (Szeto *et al.*, 2005). Protein modelling suggests that residues 92-94 is predicted to be involved with ATP binding between MinD monomers (Szeto *et al.*, 2005). As a result, it is believed that the apparent loop structure of residues 92-94, as seen in *A. fulgidus* MinD (Cordell and Lowe, 2001) changes conformation in $MinD_{Ng\text{-}loop}$, so that this mutant could no longer transduce the effects of $MinE_{Ng}$ binding to $MinD_{Ng}$ (Szeto *et al.*, 2005). Therefore, this conserved polar region in $MinD_{Ng}$ is required for relaying the effects of $MinE_{Ng}$.

Further characterization of gonococcal MinD revealed that the extreme N-terminus of $MinD_{Ng}$ contains determinants that are implicated in regulating its ATPase activity and dynamic localization (Szeto *et al.*, 2004). Truncation or substitution of the first five amino acids of $MinD_{Ng}$ disrupted $MinD_{Ng}$ interaction with itself and with $MinE_{Ng}$; this was accompanied by faster GFP-$MinD_{Ng}$ oscillation cycles and increased cytoplasmic localization. Protein modelling using *A. fulgidus* MinD showed that the extreme N-terminus of MinD may form part of a buried β-strand the connects directly to the Walker A motif (P

loop) found at the opposite side of the protein (Szeto *et al.*, 2004). It is possible that some of the effects of ATP binding are relayed from the ATP-binding face, through the N-terminal residues, to other regions of MinD involved with ATP hydrolysis; thus, mutation of the extreme N-terminus may cause MinD to become more sensitive to the effects of ATP binding, independent of $MinE_{Ng}$ (Szeto *et al.*, 2004). The absence of the N-terminus would cause $MinD_{Ng}$ to become intrinsically more active than normal, which could explain the positive correlation between the amount of each GFP-$MinD_{Ng}$ variant found in the cytosol and its rate of protein oscillation (Szeto *et al.*, 2004). Thus, in a MinE-independent manner, more severe alterations to the extreme N-terminus are predicted to induce higher ATPase activity and more cytosolic localization of $MinD_{Ng}$; deletion of the first three residues and an I5E substitution mutant led to increased $MinD_{Ng}$ ATPase activities and virtually complete cytoplasmic localization of $MinD_{Ng}$ (Szeto *et al.*, 2004). A four amino acid deletion of $MinD_{Ng}$ also abrogated membrane localization and oscillation of GFP-$MinD_{Ng}$ (Ramirez-Arcos *et al.*, 2002). Thus, these findings suggest a new function of the extreme N-terminus of $MinD_{Ng}$; it is a domain that serves as a "buffer" that attenuates the effects of ATP binding by the Walker A motif. This "buffer" is required to avoid autonomous MinD ATPase activity that disrupts normal cell division site selection. As such, the extreme N-terminus is needed to ensure that only $MinE_{Ng}$ can stimulate $MinD_{Ng}$ ATPase activity.

Recent studies of the kinetics of $MinD_{Ng}$ showed that $MinE_{Ng}$ binding increases the maximal activity, but not the substrate concentration at half maximal activity (Acharya M.Sc. thesis, 2006). This finding may have an impact into the global knowledge of MinD. Since MinD forms filaments that can change in the presence of ATP and MinE, it is possible that these changes themselves contribute to increased MinD cooperativity. The longer filaments of MinD may be able to hydrolyse ATP more effectively and encourage

disassociation from the cell membrane; this suggests that the length of cooperativity of MinD filaments can be regulated by MinE.

1.4.7. Gonococcal MinE ($MinE_{Ng}$)

Gonococcal MinE is a small 10 kDa protein that spans 87 residues. It is primarily found in Gram-negative bacteria. Early studies have shown that $MinE_{Ng}$ exhibits functionality across species as a cell division protein that promotes oscillation of MinD from both *E. coli* and *N. gonorrhoeae* in a Δ*min E. coli* background (Ramirez-Arcos *et al.*, 2002). Interaction between $MinE_{Ng}$ and $MinD_{Ng}$ also was observed using yeast two-hybrid assays (Szeto *et al.*, 2004;Szeto *et al.*, 2005). Discussion of the characterization of $MinE_{Ng}$ and its biological function is the focus of this study.

1.5. Rationale and hypothesis of this study

While the mechanisms of cell division in rod-shaped bacteria like *E. coli* and *B. subtilis* are becoming well understood, only through recent studies in round-shaped bacteria in the Dillon laboratory have some of the subtle similarities and differences in how cytokinesis progresses in cocci been observed. Since cocci lack an obvious "middle", unlike bacilli, this adds to the mystique of how cell division is achieved in round bacteria. Our laboratory is using *N. gonorrhoeae* as a model organism to study cell division site selection by examining the three Min proteins, MinC, MinD, and MinE. Since *N. gonorrhoeae* is also one of the most clinically significant and prevalent infectious diseases, one of our long-term goals is to target cell division proteins for possible antimicrobial development.

Since all three *min* genes exist in *N. gonorrhoeae* and *E. coli*, our laboratory has performed many studies of the gonococcal Min proteins using *E. coli* as an effective model system (Ramirez-Arcos *et al.*, 2001b;Szeto *et al.*, 2001a). Gonococcal MinC and MinD can complement *minC* and *minD* mutant strains of *E. coli* (Ramirez-Arcos *et al.*, 2001b;Szeto *et al.*, 2001a). As a result, I also used *E. coli* as a model organism to study gonococcal MinE functionality.

With the discovery of gonococcal Min homologues, it was proposed that these proteins would play a role in cell division (Ramirez-Arcos *et al.*, 2001b). Both $MinC_{Ng}$ and $MinD_{Ng}$ have been previously studied; their absence in *N. gonorrhoeae* disrupts normal cell division patterns, indicating their role in determining the site for proper cell division (Ramirez-Arcos *et al.*, 2001b;Szeto *et al.*, 2001a). Since the role of MinE has been primarily elucidated in the rod-shaped *E. coli*, investigation of the structure/function relationship of gonococcal MinE would provide insight into cytokinesis in coccal bacteria.

There are still many important questions that need to be answered in order to fully understand the function of the MinE protein. Does $MinE_{Ng}$ participate in gonococcal cell division? Are there other functions of $MinE_{Ng}$ that have yet to be discovered? Even though $MinE_{Ng}$ exhibited cross-functionality in *E. coli* (Ramirez-Arcos *et al.*, 2002), $MinE_{Ng}$ is only 42% identical to $MinE_{Ec}$. Thus, it would be interesting to determine if $MinE_{Ng}$ function is conserved based on structure or amino acid sequence. It is also not clear how the C-terminus of MinE confers topological specificity to MinC and MinD at the molecular level. Under what conditions do subcellular architectures form in the presence of Min proteins? Finally, although MinE is known to dimerize (King *et al.*, 1999), the importance of dimeric MinE in biological function has not be determined. Finding answers to these questions will provide important information that will expand the current knowledge of MinE behaviour.

Therefore, **I hypothesized that $MinE_{Ng}$ is required for coccal cell division in *N. gonorrhoeae*. Its biological function is reliant on its ability to interact with itself and with $MinD_{Ng}$. Anomalies in cell division site selection will develop without these critical interactions.**

As the gonococcus continues to become more resistant to a broad spectrum of antibiotics, it is reasonable that targeting the ability of this pathogen to divide is a plausible strategy in developing novel antimicrobials. The studies will also provide important insight into the cell division mechanisms of other medically important round bacteria, such as *S. aureus*, *E. faecalis*, and *N. meningitidis*, leading to the development of novel antimicrobial therapies for treating bacterial and clinical infections.

1.6. Objectives

This research was designed to determine if MinE from *N. gonorrhoeae* is involved in cell division site selection in its native organism and if it the function is homologous (i.e. function in *E. coli*). My following objectives were:

1. To characterize the function of $MinE_{Ng}$ in its native organism, *N. gonorrhoeae*. This was achieved by overexpressing $MinE_{Ng}$ in the gonococcus and disrupting the $minE_{Ng}$ gene by homologous recombination. After, growth studies and electron microscopy provided insight into the role of $MinE_{Ng}$.

2. To study the structure/function relationship of the interaction between $MinE_{Ng}$ and $MinD_{Ng}$. The effects of $MinE_{Ng}$ mutants that did not interact with $MinD_{Ng}$ were monitored by ATPase assays, protein localization, and heterologous expression studies, using *E. coli* as an indicator strain for $MinE_{Ng}$ functionality.

3. To study the relationship of $MinE_{Ng}$ self-interaction and biological function. The ability of $MinE_{Ng}$ mutants to self-interact was tested by bacterial two-hybrid assays and function of the $MinE_{Ng}$ mutants was examined by their abilities to induce $MinD_{Ng}$ oscillation.

CHAPTER 2

Materials and Methods

Portions of this chapter were published in:

[**Eng, N.F.**, Szeto, J., Acharya, S., Tessier, D., and Dillon, J.R. (2006) The C-terminus of MinE from *Neisseria gonorrhoeae* acts as a topological specificity factor by modulating MinD activity in bacterial cell division. Res Microbiol. 157, 333-344.]

2.1. Gonococcal *minE* gene sequence and protein sequence alignment of MinE homologues

N. gonorrhoeae CH811 *minE* was first identified and sequenced by Ramirez-Arcos and others (2001b). The nucleotide and amino acid sequences were made available at the National Centre for Biotechnology Information (http://www.ncbi.nlm.nih.gov/entrez/viewer.fcgi?db=nucleotide&val=13560599), Genbank accession number AAK30127. Homologues of $MinE_{Ng}$ from other organisms were obtained from The Institute for Genomic Research (TIGR) website (http://www.tigr.org). Alignment of over 30 MinE homologues was performed using ClustalW Version 1.8 software (http://dot.imgen.bcm.tmc.edu:9331/multi-align/multi-align.html). The alignment was converted for visualization using BOXSHADE Version 3.21 (http://www.ch.embnet.org/software/BOX_form.html).

2.2. Strains and growth conditions

The strains and their respective genotypes are listed in Table 1. *E. coli* DH5α (Gibco, Burlington, ON) and XL1-Blue (Stratagene, La Jolla, CA) were host strains used to clone wild-type and mutant $minE_{Ng}$ (Table 1). Chromosomal DNA from *N. gonorrhoeae* CH811 was used as a template for gonococcal *min* gene amplification. *N. gonorrhoeae* F62 and NE1 were used for determining growth curves and electron microscopy. Morphological studies of wild-type and mutant $MinE_{Ng}$ overexpression was performed using *E. coli* PB103, while *E. coli* PB114 (Δ*minCDE*) was used to study the dynamics of GFP-$MinD_{Ng}$ and $MinE_{Ec}$/$MinE_{Ng}$-GFP localization (Table 1). *E. coli* C41 (DE3) was used to overexpress proteins for purification of His-tagged $MinD_{Ng}$ and $MinE_{Ng}$, while *E. coli* R721 was used in

Table 1. Strains used in this study.

Strains	Relevant Genotype	Source/Reference
E. coli DH5α	*supE44 ? lacU169 (80lacZ? M15) hsdR17 endA1 gyrA96 thi-1 relA1*	Gibco
E. coli XL1 Blue	*recA1 endA1 gyrA96 thi-1 hsdR17 supE44 relA1 lac* [F' *proAB* $lacI^q$ *Z? M15* Tn*10* (Tet^r)]	Stratagene
N. gonorrhoeae CH811	Auxotype (A)/serotype (S)/plasmid content class (P): non-requiring/IB-2/plasmid free, Sm^r	(Picard and Dillon, 1989)
N. gonorrhoeae F62	A/S/P class: proline/IB-7/2.6	(West and Clark, 1989)
N. gonorrhoeae NE1	A/S/P class: proline/IB-7/2.6/pNE13 (*N. gonorrhoeae* F62 derivative)	This study
E. coli PB103	*dadR1 trpE61 trpA62 tna-5 purB*$^+$	(de Boer *et al.*, 1988)
E. coli PB114	*dadR1 trpE61 trpA62 tna-5 purB*$^+$ *?* *? minCDE aph* (Kan^r)	(de Boer *et al.*, 1988)
E. coli C41 (DE3)	*F' ompT hsdSB* (r^-_B m^-_B) *gal dcmD(srl-recA)* 306::Tn10 (Tet^r) *(DE3)*	(Miroux and Walker, 1996)
E. coli R721	*supE thy* D(*lac-proAB*) F' [*proAB*$^+$ $lacI^q$ *lacZ*DM15] *glpT*::O-$P_{434/P22}$*lacZ*	(Di Lallo *et al.*, 2001)
S. cerevisiae SFY526	*trp 1-901 leu2-3 112 can*^{r} *gal4-542 gal80-538 URA3::GAL1*$_{UAS}$*-GAL1*$_{TATA}$*-lacZ*	Clontech

the bacterial two-hybrid assays (Table 1). *Saccharomyces cerevisiae* SFY526 (Clontech, Palo Alto, CA) was used for yeast two-hybrid assays (Table 1).

E. coli DH5α, XL1, PB103, C41 (DE3), and R721 were grown at 37 °C in Luria-Bertani (LB) medium, while *E. coli* PB114 was grown at 30 °C in LB medium (Szeto *et al.*, 2001a). Any liquid cultures of the above were incubated with orbital shaking at 200 rpm. *N. gonorrhoeae* CH811, F62, and NE1 were grown on GC medium agar base (Difco, Oakville, ON) supplemented with Kellogg's defined supplement (GCMBK, 40 g D-glucose, 1 g glutamine, 10 ml of 0.5% ferric nitrate and 1 ml of 20% cocarboxylase) and incubated at 35 °C, with 5 % CO_2, in a humid environment, for 18-24 hours (Kellogg *et al.*, 1963;Pagotto *et al.*, 2000). Cultures of *N. gonorrhoeae* were grown in liquid GCMBK supplemented with 0.04% $NaHCO_3$ with 5% CO_2 and shaking at 200 rpm at 35°C. *E. coli* and *N. gonorrhoeae* stock cultures were prepared in 2 ml polypropylene microtubes (Sarstedt, Montreal, QC) in brain heart infusion (BHI) broth (Difco) containing 20% glycerol and were stored at –80 °C (Revco, Asheville, NC).

S. cerevisiae cells were grown at 30 °C on yeast extract-peptone-adenine-dextrose (YPAD) media (Clontech) or on suitable synthetic dropout (SD) media, as described in the Clontech Yeast Two-Hybrid Protocols Manual (Clontech). Yeast cells to be frozen at –80 °C were stored in YPAD with 20% glycerol as stated in the Clontech Yeast Manual.

Antibiotics were used, when required, at the following concentrations: kanamycin (Kan, Sigma, Oakville, ON), 50 μg/ml and ampicillin (Amp, Sigma), 100 μg/ml for general bacterial selection. The bacterial two-hybrid assays required the following concentrations: Kan, 30 μg/ml; Amp, and chloramphenicol (Cm, Sigma), 50 μg/ml. Kan 75 μg/ml was used to select for *N. gonorrhoeae* NE1.

2.3. Primer oligonucleotide construction and polymerase chain reactions (PCR)

Oligonucleotide primers used for PCR and inverse PCR (IPCR) amplification were designed using Primer Designer Software (Scientific and Education Software, Cary, NC, Table 2). Primers were purchased from the Core DNA Sequencing and Synthesis Facility, University of Ottawa and from Invitrogen (Burlington, ON). DNA for amplifying chromosomal $minE_{Ng}$ was derived from overnight whole cell suspensions of *N. gonorrhoeae* CH811 that were previously adjusted to 0.5 McFarland Equivalence Turbidity Standards (Remel, Lenexa, KS) using deionized distilled water (ddH_2O). DNA for constructing some of the mutant $minE_{Ng}$ plasmids was derived from previously generated vectors that contained the appropriate cloned mutant $minE_{Ng}$ gene. The plasmid DNA concentration used for PCR amplifications was 0.01 μg/ml.

PCR reactions were performed using a Perkin Elmer Gene Amp PCR System 9600 Thermocycler (Perkin Elmer, Waltham, MA) with the following protocol: 3 minutes at 94°C; denaturing for 30 cycles of 30 seconds at 94°C, annealing for 30 seconds at temperatures dependent on the primers used, extension/polymerization at 72°C for an amount of time dependent on the desired size of amplicon using 1 kb/minute as a guide (Sambrook and Russell D.W., 2001), and finally, a 5 minute polishing step at 72°C. A typical 100 μl PCR reaction comprised 1X PCR buffer (Fermentas, Burlington, ON or New England Biolabs, Pickering, ON), 1.5 mM $MgCl_2$, 0.2 mM deoxynucleoside triphosphates (dNTPs, Fermentas), 0.2 μg of each primer, 2.5 U of *Taq* DNA polymerase (Fermentas or New England Biolabs) and appropriate template. Some PCR reactions instead required 2.5 U *Pfu* DNA polymerase (Fermentas) with *Pfu*-specific 1X PCR buffer since this polymerase has 3'-5' exonuclease activity for high fidelity and prevents the addition of 3' adenine

Table 2. Primer sequences used for PCR and inverse PCR.

Primer	Sequence (5'- 3'; restriction sites underlined)	Encoded mutation	Restriction Site
minD2	GCGCGGATCCACCTTATCCTCCGAACAGA		BamHI
minE6	GCGCGAATTCGTTTCATTAGACAATATCC	$MinE_{Ng-54aaNT}$	EcoRI
NgMinCSphI	GCGCGCATGCATGATGGTTTATATAAT		SphI
JSC2	GCGCCTGCAGCAAACAATTACTCTGAG[a]		PstI
NgMinESphI	GCGCGCATGCATGTCATTGATCGAACTT		SphI
JSE2	GCGCCTGCAGCATGTCCTATACCTTTTTC[a]		PstI
ESminE1	GCGCCATATGTCATTGATCGAACTT		NdeI
ESminE2	GCGCCTCGAGTACCTTTTTCTGTTC[a]		XhoI
A18D-1	GCAACCGTTGATCGCGACC	$MinE_{Ng-A18D}$	MboI
A18D-2	CGTTTTCTGCTTTCTACCG[a]		
L22D-1	CGCGATCAAATCATCATTGC	$MinE_{Ng-L22D}$	MboI
L22D-2	GTCGCGGGCAACGGTTGCCG[a]		
R30D-1	GAGGACGCCCAAGAAGGTCAG	$MinE_{Ng-R30D}$	HgaI
R30D-2	TTGGGCAATGATGATTTGAAG[a]		
K53A-1	GAAGTCCTGTCCGCATATGTG	$MinE_{Ng-K53A}$	NdeI
K53A-2	CATCAACTCTTTACGTAAAGT[a]		
E67L-1	CCAGCTAAAGCAGGATGGTATG	$MinE_{Ng-E67L}$	AluI
E67L-2	GAAATACGGATATTGTCTAATG[a]		
minEdel39_54F	GTGAATGTTTCATTAGAC	$MinE_{Ng(\Delta 39-54)}$	
minEdel39_54R	ATCCGGAGTCTGACCTTC[a]		

minEdel74_78F	ATTACTTTGCCGGAACAG	$MinE_{Ng(\Delta 74-78)}$	
minEdel74_78R	ATCCATACCATCCTGCTT[a]		
minE46_50_54P	CGTAAACCGTTGATGGAACCCCTGTCCAAACCTGTGAAT	$MinE_{Ng-E46P,V50P,Y54P}$	
minE45R	TAAAGTCGGCAGGTAATCCGGAGTCTGACC[a]		
JSminE7	GCGCGAATTCCTTTTATTCGGTAGAAAGC	$MinE_{Ng-5aaNT}$	EcoRI
minE2	GCGCGGATCCCATGTCCTATACCTTTTTC[a]		BamHI
JSminE8	GCGCGAATTCCAGAAAACGGCAACCGTTG	$MinE_{Ng-11aaNT}$	EcoRI
minE5	GCGCGAATTCGAGCGCGCCCAAGAAGGTC	$MinE_{Ng-26aaNT}$	EcoRI
minE1	GCGCGAATTCATGTCATTGATCGAACTTT		EcoRI
JSminE9	GCGCGGATCCTTCCGGCAAAGTAATGTTC[a]	$MinE_{Ng-4aaCT}$	BamHI
JSminE10	GCGCGGATCCCATACCATCCTGCTTTTCT[a]	$MinE_{Ng-15aaCT}$	BamHI
minE3	GCGCGGATCCCTTGGGCAATGATGATTTG[a]	$MinE_{Ng-30aaCT}$	BamHI
minE4	GCGCGGATCCGAAACATTCACATATTTGG[a]	$MinE_{Ng-59aaCT}$	BamHI
DNminE1	GCGCGAATTCCATGTCATTGATCGAAC		EcoRI
WTminEBTM	GCGCGTCGACTATGTCATTGATCGAACTTTTA		SalI
minE3M	CGTAAAGCGTTGATGGAAGATCTGTCCAAAGCTGTGAAT	$MinE_{Ng-E46A,V50D,Y54A}$	BglII

[a] Denotes primer annealing to complementary strand.

overhangs to produce blunt-end amplicons.

To efficiently screen for *E. coli* transformed with plasmids with mutant $minE_{Ng}$ by PCR amplification, PCR reactions were performed by resuspending *E. coli* cells in ddH_2O to match a 0.5 McFarland standard turbidity and using approximately 2.5 µl of the dilution as template for an adjusted 25 µl PCR reaction.

2.4. DNA purification, high-yield plasmid purification, and agarose gel electrophoresis

PCR amplicons and plasmid DNA that was chemically modified (i.e. restriction endonuclease digestion, phosphorylation) were purified using the PCR Purification Kit (Qiagen, Mississauga, ON) in order to remove nucleotides and salts. Plasmids isolated from *E. coli* DH5α and XL1 were purified using the Miniprep Kit (Qiagen) as per the manufacturer's instructions. Plasmid DNA and plasmids digested by restriction endonucleases were resolved on 1-3% agarose gels containing 1 mg/ml ethidium bromide using Tris-acetate EDTA (TAE) buffer (40 mM Tris-acetate, 1 mM EDTA) at various voltages and times, as required. DNA in agarose gels was visualized using an ultraviolet illuminator and photographed with the MultiImage Light Cabinet using Alpha Imager 1220 (Alpha Innotech, San Leandro, CA). Sizes of DNA fragments were approximated using 1 kb plus DNA ladder and supercoiled DNA ladder (Invitrogen).

2.5. Transformation of *E. coli*, bacterial lysis to verify plasmid construction, and DNA sequencing

Plasmids were transformed into *E. coli* DH5α, XL1, R721, PB103, PB114 and C41 (DE3) using the calcium chloride method (Sambrook and Russell D.W., 2001). In cases

where a DNA fragment was cloned into a vector, transformed *E. coli* colonies that may have the DNA insert cloned into the original vector were verified by lysing bacteria to release the plasmid (Sambrook and Russell D.W., 2001) and then compared to the size of the original vector on a 1% agarose gel that was electrophoresed at 100 V for 1-1.5 hours. To lyse bacteria, about 25 µl of resuspended bacteria that was adjusted to match a 0.5 McFarland standard was added to 25 µl of cell lysis solution (50 mM EDTA, 100 mM NaOH, 1% SDS, 0.05% bromophenol blue, 0.1% glycerol). After 15 minutes, the cell lysates were centrifuged at 12000 rpm, and 25 µl of supernatant was loaded and visualized on a 1% agarose gel.

All plasmid constructs were confirmed by DNA sequencing (Core DNA Sequencing and Synthesis Facility, University of Ottawa, Ottawa, Ontario, and Plant Biotechnology Institute, National Research Council of Canada, Saskatoon, Saskatchewan).

2.6. Insertional disruption of chromosomal *minE* in *N. gonorrhoeae* CH811

To disrupt expression of chromosomal *minE* from *N. gonorrhoeae* CH811, a suicide vector, derived from pBluescript KS II (+) (Stratagene), was generated using pJS6cat (Table 3) (Szeto *et al.*, 2001a) as a template. pJS6cat contains $minC_{Ng}$, $minD_{Ng}$, $minE_{Ng}$, a chloramphenicol acetyl transferase (*cat*) cassette, *oxyR*, and consecutive gonococcal uptake sequences, which are needed for *N. gonorrhoeae* to uptake DNA (Goodman and Scocca, 1988). Primers minD2 and minE6 were used to amplify most of the vector by deleting the first 168 bp of $minE_{Ng}$, leaving 96 bp of the C-terminus of $minE_{Ng}$ intact, flanked by $minC_{Ng}$ and $minD_{Ng}$ at the 5' end and a *cat* cassette and *oxyR* at the 3' end of $minE_{Ng}$. The amplicon was religated to form pCNEE1 (Table 3). The flanking regions allow for homologous recombination to occur in *N. gonorrhoeae.* This plasmid is a suicide vector because

Table 3. Plasmids used in this study.

Plasmids	Relevant genotype	Source/reference
Gonococcus studies		
pBluescript KS II (+)	Cloning vector (Amp^R)	Stratagene
pJS6cat	P_{lac}::*minC*$_{Ng}$, *minD*$_{Ng}$, *minE*$_{Ng}$::*cat*, *oxyR* ($Amp^R Cm^R$)	(Szeto, 2004)
pCNEE1	P_{lac}::*minC*$_{Ng}$, *minD*$_{Ng}$, *minE*$_{Ng}$ (deletion of N-terminal 56 aa)::*cat*, *oxyR* ($Amp^R Cm^R$)	This study
pFP20	Kan^R oriJRD5	(Pagotto *et al.*, 2000)
pVG14	$Kan^R P_{lac}$::*minDE*$_{Ng}$-*gfp* ori JRD5	(Greco, 2004)
pNE2	$Kan^R P_{lac}$ oriJRD5	This study
pNE11	$Kan^R P_{lac}$::*minC*$_{Ng}$ oriJRD5	This study
pNE13	$Kan^R P_{lac}$::*minE*$_{Ng}$ oriJRD5	This study
Protein Purification		
pET30a	$Kan^R P_{T7}$::6XHis	Novagen
pEC1	$Kan^R P_{T7}$::*minE*$_{Ng}$-6XHis	(Ramirez-Arcos *et al.*, 2002)
pSC9	$Kan^R P_{T7}$::*minD*$_{Ng}$-6XHis	(Szeto *et al.*, 2005)
pSC10	$Kan^R P_{T7}$::*minD*$_{Ng\text{-}K16Q}$-6XHis	(Szeto *et al.*, 2005)
pEA18D	$Kan^R P_{T7}$::*minE*$_{Ng\text{-}A18D}$-6XHis	(Eng *et al.*, 2006)
pEL22D	$Kan^R P_{T7}$::*minE*$_{Ng\text{-}L22D}$-6XHis	(Eng *et al.*, 2006)
pER30D	$Kan^R P_{T7}$::*minE*$_{Ng\text{-}R30D}$-6XHis	(Eng *et al.*, 2006)
pEK53A	$Kan^R P_{T7}$::*minE*$_{Ng\text{-}K53A}$-6XHis	(Eng *et al.*, 2006)
pEE67L	$Kan^R P_{T7}$::*minE*$_{Ng\text{-}E67L}$-6XHis	(Eng *et al.*, 2006)

pECa	Kan^R P_{T7}::*minE*$_{Ng(\Delta 39\text{-}54)}$-6XHis	This study
pECb	Kan^R P_{T7}::*minE*$_{Ng(\Delta 74\text{-}78)}$-6XHis	This study
pECp	Kan^R P_{T7}::*minE*$_{Ng\text{-}E46P,V50P,Y54P}$-6XHis	This study
pEC3	Kan^R P_{T7}::*minE*$_{Ng\text{-}E46A,V50D,Y54A}$-6XHis	This study
pEC2	Kan^R P_{T7}::*minE*$_{Ng\text{-}E46A,V50D}$-6XHis	This study
Yeast Two-Hybrid Assays		
pGAD424	Amp^R P_{ADH1}::*gal4*(AD)[a]	Clontech
pGBT9	Amp^R P_{ADH1}::*gal4*(BD)[b]	Clontech
pGADminD	Amp^R P_{ADH1}::*gal4*(AD)-*minD*$_{Ng}$	(Szeto *et al.*, 2001a)
pGBT9minE	Amp^R P_{ADH1}::*gal4*(BD)-*minE*$_{Ng}$	(Ramirez-Arcos *et al.*, 2002)
pJminE5	Amp^R P_{ADH1}::*gal4*(BD)-*minE*$_{Ng\text{-}5aaNT}$[c]	(Eng *et al.*, 2006)
pJminE6	Amp^R P_{ADH1}::*gal4*(BD)-*minE*$_{Ng\text{-}11aaNT}$	(Eng *et al.*, 2006)
pJminE3	Amp^R P_{ADH1}::*gal4*(BD)-*minE*$_{Ng\text{-}26aaNT}$	(Eng *et al.*, 2006)
pJminE4	Amp^R P_{ADH1}::*gal4*(BD)-*minE*$_{Ng\text{-}54aaNT}$	(Eng *et al.*, 2006)
pJminE7	Amp^R P_{ADH1}::*gal4*(BD)-*minE*$_{Ng\text{-}4aaCT}$[d]	(Eng *et al.*, 2006)
pJminE8	Amp^R P_{ADH1}::*gal4*(BD)-*minE*$_{Ng\text{-}15aaCT}$	(Eng *et al.*, 2006)
pJminE2	Amp^R P_{ADH1}::*gal4*(BD)-*minE*$_{Ng\text{-}30aaCT}$	(Eng *et al.*, 2006)
pJminE1	Amp^R P_{ADH1}::*gal4*(BD)-*minE*$_{Ng\text{-}59aaCT}$	(Eng *et al.*, 2006)
pEGBT1	Amp^R P_{ADH1}::*gal4*(BD)-*minE*$_{Ng\text{-}A18D}$	(Eng *et al.*, 2006)
pEGBT2	Amp^R P_{ADH1}::*gal4*(BD)-*minE*$_{Ng\text{-}L22D}$	(Eng *et al.*, 2006)
pSRBDER30D	Amp^R P_{ADH1}::*gal4*(BD)-*minE*$_{Ng\text{-}R30D}$	(Eng *et al.*, 2006)
pEGBT3	Amp^R P_{ADH1}::*gal4*(BD)-*minE*$_{Ng\text{-}K53A}$	(Eng *et al.*, 2006)

pEGBT4	Amp^R P_{ADH1}::*gal4*(BD)-$minE_{Ng\text{-}E67L}$	(Eng *et al.*, 2006)
Morphological studies		
pUC18	Amp^R P_{lac}	Amersham
pEUC1	Amp^R P_{lac}::$minE_{Ng}$	(Eng *et al.*, 2006)
pEUC18	Amp^R P_{lac}::$minE_{Ng\text{-}A18D}$	(Eng *et al.*, 2006)
pEUC22	Amp^R P_{lac}::$minE_{Ng\text{-}L22D}$	(Eng *et al.*, 2006)
pEUC30	Amp^R P_{lac}::$minE_{Ng\text{-}R30D}$	(Eng *et al.*, 2006)
pEUC53	Amp^R P_{lac}::$minE_{Ng\text{-}K53A}$	(Eng *et al.*, 2006)
pEUC67	Amp^R P_{lac}::$minE_{Ng\text{-}E67L}$	(Eng *et al.*, 2006)
Localization Studies		
pSR15	Amp^R P_{trc}::*gfp-minD*$_{Ng}$, $minE_{Ng}$	(Ramirez-Arcos *et al.*, 2002)
pSRDT18	Amp^R P_{trc}::*gfp-minD*$_{Ng}$, $minE_{Ng\text{-}A18D}$	(Eng *et al.*, 2006)
pSRDT22	Amp^R P_{trc}::*gfp-minD*$_{Ng}$, $minE_{Ng\text{-}L22D}$	(Eng *et al.*, 2006)
pSR15ER30D	Amp^R P_{trc}::*gfp-minD*$_{Ng}$, $minE_{Ng\text{-}R30D}$	(Ramirez-Arcos *et al.*, 2002)
pSRDT53	Amp^R P_{trc}::*gfp-minD*$_{Ng}$, $minE_{Ng\text{-}K53A}$	(Eng *et al.*, 2006)
pSRDT67	Amp^R P_{trc}::*gfp-minD*$_{Ng}$, $minE_{Ng\text{-}E67L}$	(Eng *et al.*, 2006)
pSRNE1	Amp^R P_{trc}::*gfp-minD*$_{Ng}$, $minE_{Ng(\Delta 39\text{-}54)}$	This study
pSRNE2	Amp^R P_{trc}::*gfp-minD*$_{Ng}$, $minE_{Ng\text{-}E46A,V50D}$	This study
pWM1079-H	Cm^R P_{ara}::*minC*'$_{Ec}$, $minD_{Ec}$, $minE_{Ec}$-*gfp*	Ramirez-Arcos et al., 2002
pSRE-GFP	Cm^R P_{ara}::*minC*'$_{Ng}$ (last 100bp), $minD_{Ng}$, $minE_{Ng}$-*gfp*	Ramirez-Arcos et al., 2002

Bacterial two-hybrid plasmids

p434FtsZ	Kan^R 15A ori, P_{lac}::N-terminus of 434 repressor-*ftsZ*$_{Ec}$	(Di Lallo *et al.*, 2001)
p22MinC	Amp^R ColE1 ori, P_{lac}::N-terminus of P22 repressor-*minC*$_{Ec}$	(Di Lallo *et al.*, 2001)
p434minE	Kan^R 15A ori, P_{lac}::N-terminus of 434 repressor-*minE*$_{Ng}$	This study
p22minE	Amp^R ColE1 ori, P_{lac}::N-terminus of P22 repressor-*minE*$_{Ng}$	This study
p434EA18D	Kan^R 15A ori, P_{lac}::N-terminus of 434 repressor-*minE*$_{Ng\text{-}A18D}$	This study
p22EA18D	Amp^R ColE1 ori, P_{lac}::N-terminus of P22 repressor-*minE*$_{Ng\text{-}A18D}$	This study
p434EL22D	Kan^R 15A ori, P_{lac}::N-terminus of 434 repressor-*minE*$_{Ng\text{-}L22D}$	This study
p22EL22D	Amp^R ColE1 ori, P_{lac}::N-terminus of P22 repressor-*minE*$_{Ng\text{-}L22D}$	This study
p434ER30D	Kan^R 15A ori, P_{lac}::N-terminus of 434 repressor-*minE*$_{Ng\text{-}R30D}$	This study
p22ER30D	Amp^R ColE1 ori, P_{lac}::N-terminus of P22 repressor-*minE*$_{Ng\text{-}R30D}$	This study
p434EK53A	Kan^R 15A ori, P_{lac}::N-terminus of 434 repressor-*minE*$_{Ng\text{-}K53A}$	This study
p22EK53A	Amp^R ColE1 ori, P_{lac}::N-terminus of P22 repressor-*minE*$_{Ng\text{-}K53A}$	This study
p434EE67L	Kan^R 15A ori, P_{lac}::N-terminus of 434 repressor-*minE*$_{Ng\text{-}E67L}$	This study
p22EE67L	Amp^R ColE1 ori, P_{lac}::N-terminus of P22 repressor-*minE*$_{Ng\text{-}E67L}$	This study

p434a	Kan^R 15A ori, P_{lac}::N-terminus of 434 repressor-*minE*$_{Ng(\Delta 39\text{-}54)}$	This study
p22a	Amp^R ColE1 ori, P_{lac}::N-terminus of P22 repressor-*minE*$_{Ng(\Delta 39\text{-}54)}$	This study
p434b	Kan^R 15A ori, P_{lac}::N-terminus of 434 repressor-*minE*$_{Ng(\Delta 74\text{-}78)}$	This study
p22b	Amp^R ColE1 ori, P_{lac}::N-terminus of P22 repressor-*minE*$_{Ng(\Delta 74\text{-}78)}$	This study
p434p	Kan^R 15A ori, P_{lac}::N-terminus of 434 repressor-*minE*$_{Ng\text{-}E46P,V50P,Y54P}$	This study
p22p	Amp^R ColE1 ori, P_{lac}::N-terminus of P22 repressor-*minE*$_{Ng\text{-}E46P,V50P,Y54P}$	This study

[a] GAL4 activation domain
[b] GAL4 DNA binding domain
[c] NT – N-terminal $MinE_{Ng}$ truncation
[d] CT – C-terminal $MinE_{Ng}$ truncation

the parent plasmid, pJS6cat is unable to replicate in *N. gonorrhoeae*. PCR analysis and DNA sequencing of pCNEE1 showed that the first 168 bp of $minE_{Ng}$ were deleted (data not shown).

2.7. Construction of shuttle vector expressing $MinE_{Ng}$

The availability of genetic tools to study *N. gonorrhoeae* is limited; the Dillon laboratory previously constructed a unique shuttle vector, pFP10, that can replicate in *N. gonorrhoeae*, *E. coli*, and *Haemophilus* species (Pagotto *et al.*, 2000). An improved shuttle vector, pFP20, also generated by Pagotto and co-workers (2000), contained more restriction sites for cloning purposes, additional gonococcal uptake sequences to increase gonococcal transformation efficiency, and a kanamycin resistance gene for selection. Subsequently, the *lac* promoter, $minD_{Ng}$, $minE_{Ng}$, and *gfp* were cloned into pFP20 to give rise to pVG14 (Table 3) (Greco, 2004). The latter three genes were then removed from pVG14 by restriction endonuclease digestion. The resulting DNA was religated to form pNE2 (Table 3), which only contained the *lac* promoter, as determined by agarose gel electrophoresis and DNA sequencing. Gonococcal *minC* and *minE* were amplified from *N. gonorrhoeae* CH811 using primers NgMinCSphI/JSC2 and NgMinESphI/JSE2, which contain sites for SphI and PstI, respectively. The amplicons and pNE2 were digested with SphI and PstI sites and ligated to form pNE11 and pNE13, respectively (Table 3).

2.8. Transforming suicide and shuttle vectors into *N. gonorrhoeae*

To transform *N. gonorrhoeae* F62 and CH811, frozen stocks of each strain were streaked onto fresh GCMBK agar plates and grown for 18 hours. Type II (or T2) cells, which are known to be piliated, were identified (Juni and Heym, 1977;Kellogg *et al.*, 1963).

T2 cells were then subcultured once more on GCMBK agar plates to increase their numbers. Approximately 1 μg of the suicide and shuttle vectors were spotted onto fresh streaked plates of *N. gonorrhoeae* CH811 and F62 for 6 hours at 35 °C. After, the gonococcal cells were transferred, using a sterile cotton swab, and streaked onto fresh GCMBK agar plates with appropriate antibiotics. Plates were then incubated for 24-48 hours until isolated colonies were visible. The presence of plasmids in *N. gonorrhoeae* CH811 or F62 was screened by bacterial cell lysis as described earlier.

2.9. Growth studies

The effect of $MinE_{Ng}$ overexpression in *N. gonorrhoeae* F62 was monitored by growth and viability studies. This gonococcal strain was used since the parent pFP20 shuttle vector was not taken up by *N. gonorrhoeae* CH811 (unpublished results), the strain typically used to study cell division in our laboratory. Standardizing the inoculum for growth studies as follows ensured equivalent numbers of *N. gonorrhoeae* F62 and NE1 cells. Gonococcal cells were subcultured twice on GCMBK agar plates. To determine the number of colony-forming units (cfu)/ml of *N. gonorrhoeae* F62 and NE1 ($MinE_{Ng}$ overexpression) cells, each strain was diluted 25-fold from overnight liquid GCMBK cultures to obtain an OD_{550} of 0.05. Ten-fold serial dilutions were performed to determine the numbers of cfu/ml that were present in each culture.

Growth curves were performed in duplicate on two separate occasions. Overnight cultures were adjusted with GCMBK broth to match the 0.5 McFarland turbidity standard, where OD at 550 nm of the inoculum was approximately 0.05 or 1 x 10^8 cfu. An inoculum of 250 μl was placed in 24.75 ml of GCMBK (1:100 dilution) broth to produce an

approximate starting concentration of 1 x 10^6 cfu. For growth curves, a total of 9 timepoints, 0, 2, 4, 6, 8, 10, 12, 16, and 20 hours, was sampled. At each timepoint, 1 ml of *N. gonorrhoeae* cells was removed; approximately 0.3 ml of each sample was further diluted 1:100 to 3 ml. With this volume for each sample, serial dilutions were completed by serially diluting 100 µl of cells in 900 µl of GCMBK broth (1:10 serial dilutions) up to a final dilution of 10^{-8}. The 10^{-3} to 10^{-8} serial dilutions were plated on appropriate GCMBK plates by spotting 25 µl twice, allowing for 12 dilution spots per GCMBK plate. The plates were incubated for 24 hours prior to counting colonies per spot in cases where colonies were easily distinguishable. The average count was calculated per dilution. During the course of sample collection, another 1 ml of cells was removed at 8, 12 and 16 hours for transmission electron microscopy (see below).

2.10. Transmission electron microscopy

Transmission electron microscopy was performed on *N. gonorrhoeae* F62 and NE1 at the Laboratory Pathology facilities, Ottawa Hospital, Civic Campus, Ottawa, ON. Cells were fixed in 1.6% glutaraldehyde in 0.1 M sodium cacodylate buffer pH 7.2. Subsequent to washing in 0.1 M sodium cacodylate buffer pH 7.2, the cells were resuspended in 15% BSA and pelleted by centrifugation at 9000 rpm for 5 minutes. Using established protocols at the Ottawa Hospital, the resulting pellets were cut into 1 mm pieces, postfixed in 1% osmium tetroxide, stained en-bloc with 3% uranyl acetate, dehydrated in ethanol and acetone and embedded in Spurr epoxy resin. Ultrathin sections were stained with Reynold's lead citrate and electron micrographs were imaged using a Jeol 1230 electron microscope using AMT software.

The diameters of twenty *N. gonorrhoeae* F62 and NE1 cells were measured from electron micrographs taken at the same magnification and average diameters at their widest points were calculated for both samples. Statistical analysis using the unpaired Student's *t*-test was applied to the averages, and differences were considered significant for p values <0.001.

2.11. Construction of plasmids used for protein purification

Plasmids are listed in Table 3; primers are listed in Table 2. The vector pET30a (Novagen, Table 3) encodes for a His-tag that was used for bacterial protein expression and nickel affinity purification. A cell suspension of *N. gonorrhoeae* CH811 was used to amplify wild-type $minE_{Ng}$ using primers ESMinE1 and ESMinE2 (Table 2). Amplicons were cloned into pET30a at the NdeI and XhoI restriction sites to generate pEC1. This allows for *E. coli* expression of a fusion of $MinE_{Ng}$ to a C-terminal 6XHis tag (Ramirez-Arcos *et al.*, 2002). Constructs expressing $MinD_{Ng}$-6XHis (pSC9) and $MinD_{Ng\text{-}K16Q}$-6XHis (pSC10) were generated previously (Szeto *et al.*, 2005). The K16Q $MinD_{Ng}$ mutant was unable to bind to ATP (Szeto *et al.*, 2005), and thus served as a control in ATPase assays (see below). Plasmid pEC1 was used to generate the following $MinE_{Ng}$ mutant substitutions of conserved residues by site-directed mutagenesis: A18D, L22D, R30D, K53A, and E67L. These residues were selected based on their conservation in MinE across species (amino acid sequences from www.tigr.org) identified by an amino acid sequence alignment using BCM Search Launcher (http://searchlauncher.bcm.tmc.edu/multi-align/multi-align.html). Table 3 lists the plasmids generated by this process: pEA18D (primers A18D-1, A18D-2), pEL22D (primers L22D-1, L22D-2), pER30D (primers R30D-1, R30D-2), pEK53A (primers K53A-1, K53A-2), and pEE67L (primers E67L-1, E67L-2).

In order to investigate the effects of disrupting MinE self-interaction, aa 39-54 and aa 74-78 were mutated. These residues were selected based on previous work studying $MinE_{Ec}$ ring disruption and self-interaction (King *et al.*, 2000). The corresponding amino acids in $MinE_{Ng}$ were identified by amino acid sequence alignment using BCM Search Launcher as indicated above. Using this information, three mutations were introduced to pEC1 using IPCR and site-directed mutagenesis methods: 1) deletion of aa 39-54, 2) deletion of aa 74-78, and 3) mutating E46, Y50 and Y54 to proline. This process generated pECa (primers minEdel39_54F, minEdel39_54R), pECb (primers minEdel74_78F, minEdel74_78R), and pECp (primers minE46_50_54P, minE45R) respectively (Table 3). In case the above mutations were harsh, two additional $MinE_{Ng}$ mutations were introduced to pEC1. Primers minE3M and minE45R (Table 2) were used to construct pEC3 (Table 3) that encoded a triple E46A, V50D, and Y54A mutation. Another mutation, a double E46A and V50D mutation was encoded on pEC2 using minE3M and minE45R as well; however, upon DNA sequencing, it was revealed that only E46 and V50 were mutated.

2.12. Protein purification

Wild-type $MinD_{Ng}$ and $MinD_{Ng\text{-}K16Q}$ were purified as previously described (Szeto *et al.*, 2004;Szeto *et al.*, 2005). To purify wild-type and mutant $MinE_{Ng}$, plasmids encoding wild-type or mutant $MinE_{Ng}$ derived from pET30a (Novagen, San Diego, CA) were transformed into *E. coli* C41 (DE3) using methods described earlier (Szeto *et al.*, 2001a). Exponential phase cultures of 350 ml were induced with a final concentration of 0.4 mM isopropyl-β-D-thiogalactopyranoside (IPTG) for 2-3 hours with orbital shaking at 250 rpm and incubation at 37 °C. *E. coli* cells were pelleted by centrifugation at 6000 rpm for 10

minutes (Sorvall RC 50, Asheville, NC) and stored at -20°C. Pellets were resuspended in 25 ml of binding buffer (5 mM imidazole). The resuspension was sonicated 5 times for 30 seconds with one minute intervals on ice (Fisher Scientific 60 Sonic Dismembrator, Ottawa, ON). Lysed cells were then centrifuged at 25000 rpm for 25 minutes at 4°C (Beckman Coulter Optima L-100 XP, Mississauga, ON). Soluble fractions were collected and applied to 3 ml of His-bind resin (Novagen) column, which was washed with 5 mM, 60 mM, and 100 mM imidazole. Wild-type and mutant $MinE_{Ng}$ were eluted with 250 mM imidazole. Eluted protein was then dialyzed in buffer A (50 mM Tris, 20 mM NaCl, 1 mM EDTA, pH 7.4). Biomax-5 centrifugal filter columns with a 5 kDa molecular cutoff (Millipore, Billerica, MA) were used to concentrate wild-type and mutant $MinE_{Ng}$ proteins.

In cases where protein was not soluble using the purification protocol described above, a more rigourous method was alternately used. Insoluble fractions from centrifuged samples of sonicated *E. coli* C41 cells were resuspended in suspension buffer (20 mM Tris-HCl, pH 7.8, 500 mM NaCl, 5 mM imidazole, 8 M urea). Solubilization was allowed to proceed for one hour at room temperature with gentle agitation. After, the reaction was spun at 12000 rpm for 15 minutes at room temperature. The supernatant was then removed and transferred to a His-charged binding resin column that had been previously equilibriated in the suspension buffer. The column was incubated for another hour at room temperature and then allowed to settle. The suspension buffer was eluted slowly and then six resin volumes of wash buffer (20 mM Tris-HCl, pH 7.8, 500 mM NaCl, 20 mM imidazole, 8 M urea) was added carefully. Six volumes of renaturation buffer (suspension buffer without urea) was added in the column. Finally, three volumes of elution buffer (20 mM Tris-HCl, pH 7.8, 500 mM NaCl, 300 mM imidazole) eluted the renatured protein.

2.13. Mass spectrometry analysis

Purified His-tagged $MinE_{Ng}$ was analyzed by SDS-PAGE (see 2.28) using 15% polyacrylamide gels and stained with Coomassie brilliant blue (Sambrook *et al.*, 1989). Bands of $MinE_{Ng}$ were excised from the gel using a sterile scalpel following destaining so that multiple mass spectrometry analyses could be performed. The molecular mass of $MinE_{Ng}$ and its pI was determined using predicting software (http://ca.expasy.org/cgi-bin/pi_tool). The identity of gonococcal MinE was confirmed by using Q-TOF mass spectrometry analysis at the Institute of Biological Sciences, National Research Council of Canada (NRC-IBS), Ottawa, ON.

2.14. Construction of plasmids for yeast two-hybrid assay

Yeast plasmids (Table 3) encoding $minD_{Ng}$ and $minE_{Ng}$ were previously cloned into pGAD424 (Clontech) and pGBT9 (Clontech) to generate pGADminD (Szeto *et al.*, 2001a), and pGBT9minE (Ramirez-Arcos *et al.*, 2002) respectively. Truncations to $minE_{Ng}$ were generated by PCR and amplicons were cloned into pGBT9. Deletions to the 5' end of $minE_{Ng}$ (N-terminal truncation, NT) were made by using primers JSminE7/minE2, JSminE8/minE2, minE5/minE2, and minE6/minE2 (Table 2). Once cloned into pGBT9, the plasmids generated were named pJminE5 ($MinE_{Ng\text{-}5aaNT}$), pJminE6 ($MinE_{Ng\text{-}11aaNT}$), pJminE3 ($MinE_{Ng\text{-}26aaNT}$), and pJminE4 ($MinE_{Ng\text{-}54aaNT}$), respectively. C-terminal (CT) truncations (deletions to the 3' end of $minE_{Ng}$) were made using primers minE1/JSminE9, minE1/JSminE10, minE1/minE3, and minE1/minE4 (Table 2). The amplicons were cloned into pGBT9 and generated plasmids pJminE7 ($MinE_{Ng\text{-}4aaCT}$), pJminE8 ($MinE_{Ng\text{-}15aaCT}$), pJminE2 ($MinE_{Ng\text{-}30aaCT}$), and pJminE1 ($MinE_{Ng\text{-}59aaCT}$), respectively (Table 3). Primers minE1 and minE2 (Table 2), which included the EcoRI and BamHI restriction sites,

respectively, were used to amplify wild-type and mutant *minE*$_{Ng}$ from pET30a-derived plasmids and the resulting amplicons were cloned into respective sites in pGBT9 (Clontech). These constructs, in Table 3, were called pEGBT1 (*minE*$_{Ng\text{-}A18D}$), pEGBT2 (*minE*$_{Ng\text{-}L22D}$), pSRBDER30D (*minE*$_{Ng\text{-}R30D}$), pEGBT3 (*minE*$_{Ng\text{-}K53A}$) and pEGBT4 (*minE*$_{Ng\text{-}E67L}$). Fusions of AD-MinD$_{Ng}$ (GAL4 activating domain fused to MinD$_{Ng}$) and BD-MinE$_{Ng}$ (GAL4 DNA-binding domain fused to MinE$_{Ng}$) were generated for these experiments. AD-MinE$_{Ng}$ and BD-MinD$_{Ng}$ fusions were unable to associate with each other using this system, because of the possibility of occasional unstable yeast fusion proteins as indicated by the manufacturer.

2.15. Yeast two-hybrid assays

The MATCHMAKER yeast two-hybrid system from Clontech was used to assess protein-protein interactions. Initially, each yeast two-hybrid plasmid was individually transformed into the reporter strain *S. cerevisiae* SFY526 by the lithium acetate method (Clontech Yeast Two-Hybrid Manual) to ensure that the GAL4 fusions did not activate the β-galactosidase reporter gene. SD-Leu media (Clontech) was used to plate yeast transformants that carried only pGAD424-derived vectors. SD-Trp media (Clontech) was used to plate yeast cells that only possessed pGBT9-derived vectors. Yeast, co-transformed with both pGAD424 and pGBT9 derivatives, was plated on SD-Leu/-Trp media (Clontech). Using sterile filters, colony lift assays were performed by lifting yeast colonies off of the plates. These filters were immediately frozen with liquid nitrogen and then thawed to lyse the yeast cells. By adding completed Z-buffer (60 mM Na_2HPO_4, 40 mM $NaH_2PO_4{\cdot}H_2O$, 2 mM KCl, 1 mM $MgSO_47{\cdot}H_2O$, 0.28% β-mercaptoethanol) and X-gal substrate overnight, colonies turned blue, indicating a protein-protein interaction. Interaction was quantified

using liquid β-galactosidase assays when o-nitro-phenyl-D-galactopyranoside (ONPG) was used as a substrate (Clontech Yeast Two-Hybrid Manual). Using a formula to calculate the β-galactosidase units (Miller, 1972), the relative average strength of each interaction was determined ± 1 standard deviation. All assays were performed in duplicate.

2.16. Construction of plasmids for morphological studies

Wild-type and mutant *minE*$_{Ng}$ from the pEC1, pEA18D, pEL22D, pER30D, pEK53A, and pEE67L (Table 3) were amplified using primers DNminE1 and minE2 (Table 2) that contained EcoRI and BamHI restriction sites, respectively, and the amplicons were cloned into respective sites in pUC18 (Amersham) to generate wild-type and mutant *minE*$_{Ng}$ plasmids for morphological studies. Plasmids (Table 3) generated were named pEUC1 (*minE*$_{Ng}$), pEUC18 (*minE*$_{Ng\text{-}A18D}$), pEUC22 (*minE*$_{Ng\text{-}L22D}$), pEUC30 (*minE*$_{Ng\text{-}R30D}$), pEUC53 (*minE*$_{Ng\text{-}K53A}$), and pEUC67 (*minE*$_{Ng\text{-}E67L}$).

2.17. Construction of plasmids for fluorescence microscopy

The same mutagenic primers used to generate the A18D, L22D, R30D, K53A, and E67L MinE$_{Ng}$ mutants in constructing protein purification plasmids were also used to mutate *minE*$_{Ng}$ from pSR15, which encoded for GFP-MinD$_{Ng}$ and MinE$_{Ng}$ (Ramirez-Arcos *et al.*, 2002) to generate pSRDT18 (*minE*$_{Ng\text{-}A18D}$), pSRDT22 (*minE*$_{Ng\text{-}L22D}$), pSR15ER30D (*minE*$_{Ng\text{-}R30D}$), pSRDT53 (*minE*$_{Ng\text{-}K53A}$), and pSRDT67 (*minE*$_{Ng\text{-}E67L}$) (Table 3). Using pSR15 (Ramirez-Arcos *et al.*, 2002) as a template, primers minEdel39_54F and minEdel39_54R were used to introduce the deletion of aa 39-54 of MinE$_{Ng}$, via IPCR, giving rise to pSRNE1. Primers minEdel74_78F and minEdel74_78R were used to delete aa 74-78 of MinE$_{Ng}$ from

pSR15, generating pSRNE2 (Table 3). pWM1079-H and pSRE-GFP (Table 3) were previously constructed (Ramirez-Arcos *et al.*, 2002).

2.18. Microscopy

Morphological differences observed in *E. coli* PB103 overexpressing wild-type and mutant $minE_{Ng}$ were examined using an Olympus BX61 microscope equipped with a Photometrics CoolSnap ES camera, ImagePro Version 5 software (Media Cybernetics, Bethesda, MD) and InVitro 3 (Media Cybernetics) software with differential interference contrast (DIC) and fluorescence microscopy capabilities. Phase contrast microscopy was also used to examine various *E. coli* cells using a Zeiss Axioskop microscope (Toronto, ON) under a 100X oil immersion lens, while images were captured using Northern Eclipse Version 5.0 software (Mississauga, ON). Competent *E. coli* PB114 cells were transformed with pSR15 and its derivatives (Table 3) in order to co-express GFP-$MinD_{Ng}$ and wild-type or mutant $MinE_{Ng}$ *in cis*. Differences in the localization patterns of GFP-$MinD_{Ng}$ were observed using ultraviolet illumination using the Olympus BX61 microscope. The average periodicity/cycle of GFP-$MinD_{Ng}$ oscillation was determined in *E. coli* by measuring the time it takes for the GFP signal to translocate from one pole to the other and back. In addition, cells examined were of a consistent length (2-3 μm) as a control to measure the oscillation cycles. *E. coli* PB114 cells were induced with 40 μM IPTG to co-express GFP-$MinD_{Ng}$ and $MinE_{Ng}$ and immobilized with 2 % LB low-melting agarose. *E. coli* PB114 cells transformed with pWM1079-H and pSRE-GFP (Table 3) were induced with 0.005 – 0.2 % arabinose. Images were captured every 5 seconds using an exposure time of 500 ms. Enhancement of raw images was performed by using contrast and display range

enhancement available with ImagePro. Further enhancement of intracellular substructures was performed using Gauss filtering using a 3 X 3 kernal size with four passes at strength 10. Average periodicity (i.e. time it takes for GFP-$MinD_{Ng}$ to move from one pole to the other and back) was calculated using cells of similar lengths within the same sample with ± 1 standard deviation. The unpaired Student's *t*-test was used to determine whether average oscillation cycles differed from one another, with $p < 0.001$ considered significantly different.

2.19. ATPase assays

The concentration of His-tagged purified $MinD_{Ng}$, $MinD_{Ng\text{-}K16Q}$, wild-type and mutant $MinE_{Ng}$ was determined using the Bradford assay (BioRad) and equalized in appropriate dialysis buffers. $MinD_{Ng\text{-}K16Q}$, a variant that has a mutation in its ATP binding domain, rendering it unable to bind and hydrolyse ATP (Szeto *et al.*, 2005), served as a control in these studies. A typical 100 µl reaction comprised, in the following order, reaction buffer RB (25 mM Tris-Cl, 50 mM KCl, pH 7.5), His-tagged $MinD_{Ng}$ or $MinD_{Ng\text{-}K16Q}$ (0.012 mg/ml), ATP (1 mM), phosphotidylglycerol (PG) vesicles (0.5 mg/ml), and $MgCl_2$ (1 mM). Briefly, phosphatidylglycerol (PG) vesicles were created by drying 0.1 ml of PG (10 mg/ml in chloroform, Avanti Polar Lipids, Alabaster, AL) with a stream of filtered air. PG was then resuspended in RB buffer to give a 5 mg/ml stock concentration of PG vesicles. The lipid vesicles were visualized by phase-contrast microscopy to ensure the presence of vesicles (Fig. 2.1). PG vesicles were used because of higher affinity for MinD molecules (Mileykovskaya *et al.*, 2003). Reactions proceeded for five minutes at room temperature and, when required, wild-type and mutant His-tagged $MinE_{Ng}$ (0.012 mg/ml) was added and

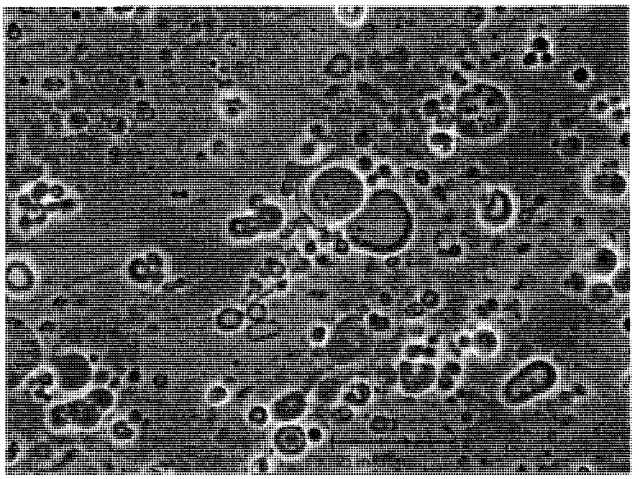

Figure 2.1. Phosphatidylglycerol vesicle formation. Anionic phospholipids, immersed in chloroform, were dehydrated, and Resuspended in RB buffer to a 5 mg/ml stock concentration of vesicles. Phase-contrast microscopy was used to examine vesicle integrity.

the reaction was allowed to continue for another five minutes. ATP assays were completed as previously described (Harder *et al.*, 1994;Szeto *et al.*, 2004;Szeto *et al.*, 2005), except where detection of free phosphates was measured at 5, 10, 25, 40, and 60 minutes. The rate of ATPase activity was measured by the slope of phosphate release as a function of time. We previously showed that the attachment of C-terminal His residues to $MinD_{Ng}$ and $MinE_{Ng}$ did not alter their respective cell division functions in *E. coli* (Szeto *et al.*, 2005). The amount of inorganic phosphate released was determined by comparing absorbance readings with those obtained from inorganic phosphate standards prepared from dilutions of KH_2PO_4 in a blank buffer. These experiments were done in duplicates with the average amount of phosphates released expressed in pmol ± 1 standard deviation.

2.20. Lipid binding assays

A sedimentation assay to demonstrate binding of $MinD_{Ng}$ to artificial phospholipid vesicles was established using protocols previously discussed (Szeto *et al.*, 2004). Purified His-tagged $MinD_{Ng}$ and $MinE_{Ng}$ were obtained using methods previously described.

In each experiment, the concentration of His-$MinD_{Ng}$ and $MinE_{Ng}$-His were standardized using the Bio-rad protein assay. Necessary dilutions were done with the same dialyzed buffer used to purify both proteins. A typical 50 µl reaction comprised 0.2 mg/ml $MinD_{Ng}$-His, 1 mM ATP, 0.5 mg/ml PG vesicles, and 1 mM $MgCl_2$, all in RB buffer. Reactions were allowed to incubate at room temperature for five minutes, and when necessary, various concentrations of $MinE_{Ng}$-His were added. An additional five minutes of incubation passed. The reactions were then centrifuged at 14000 rpm for one minute. The supernatant was removed and the pellet (containing the PG vesicles) was resuspended in RB

buffer. Both fractions were analyzed by 15% SDS-PAGE. Experiments were done in duplicate. Previous studies showed that phosphatidylethanolamine (PE) vesicle could also be used in these assays (Szeto, 2004); however, there was little association between $MinD_{Ng}$ and the PE vesicles.

2.21. Construction of plasmids used for bacterial two-hybrid assays

Bacterial two-hybrid plasmids p434FtsZ and p22MinC (Table 3) and the *E. coli* strain R721 (Table 1) (Di Lallo *et al.*, 2001) were donated by Gustavo Di Lallo (Università via della Ricerca Scientifica). *ftsZ* and *minC* were removed by restriction endonuclease digestion using the unique SalI and BamHI sites on these plasmids. *minE* was amplified from *N. gonorrhoeae* CH811 using primers WTminEBTM and minE2 (Table 2) and digested with the same enzymes as above. The resulting *minE* amplicons were cloned into both linearized p434 and p22 vectors to generate p434minE and p22minE (Table 3).

Mutations to *minE* were generated by the following strategies. To incorporate the A18D, L22D, R30D, K53A, and E67L $minE_{Ng}$ mutations, each mutant $minE_{Ng}$ was amplified from their respective pEC1-derived vectors (Table 3) using primers WTminEBTM and minE2 (Table 2). The amplicons were digested with SalI and BamHI and cloned into linearized p434 and p22 to generate the A18D (plasmids p434EA18D and p22EA18D), L22D (plasmids p434EL22D and p22EL22D), R30D (plasmids p434ER30D and p22ER30D), K53A (plasmids p434EK53A and p22EK53A), and E67L (plasmids p434EE67L and p22EE67L) $minE_{Ng}$ mutations in these recombinant vectors (Table 3). Deletion of amino acids 39-54 of $MinE_{Ng}$ was performed using IPCR on p434minE and p22minE using primers minEdel39_54F and minEdel39_54R (Table 2) in order to generate p434a and p22a. IPCR was also used to delete residues 74-78 from p434minE and p22minE

(primers minEdel74_78F and minEdel74_78R, Table 2) to generate p434b and p22b. p434p and p22p were generated using site-directed mutagenesis (primers minE46_50_54P / minE45R; and minE3M / minE45R, respectively, Table 2). All plasmids are listed in Table 3.

2.22. Bacterial two-hybrid assays

Each bacterial two-hybrid plasmid was separately transformed into *E. coli* R721 to ensure that the inhibition of the β-galactosidase reporter gene was not entirely caused by a homodimer (Di Lallo *et al.*, 2001). Both plasmids were then co-transformed into *E. coli* R721. Since both plasmids contained different origins of replications, the two plasmids were able to co-exist in *E. coli* and express the fusion proteins. Following confirmation of both plasmids in *E. coli* by cell lysis (Section 2.4), each strain was subcultured into LB medium for 14-16 hours at 37 °C with the required antibiotics. Cells were then diluted 1:100 into fresh LB medium and grown to mid-log phase (OD600 ~ 0.4) at 37 °C at which time, they were placed on ice for 20 minutes. Approximately 1.5 ml of this culture was centrifuged at 6000 rpm for 10 minutes, the supernatant was removed, and the subsequent pellet was resuspended with the same volume of pre-chilled Z-buffer (60 mM Na_2HPO_4, 40 mM $NaH_2PO_4 \cdot H_2O$, 2 mM KCl, 1 mM $MgSO_4 \cdot 7H_2O$, 0.28% β-mercaptoethanol, pH 7) and OD_{600} was again measured. Resuspended cells were further diluted 1:10 in Z-buffer. To permeabilize the cells, 0.1 ml of chloroform and 0.05 ml of 0.1% SDS were added. Cells were vortexed and incubated for 5 minutes at 28 °C. 0.2 ml of 4 mg/ml solution (in 0.1 M phosphate buffer, pH 7) of ONPG was added to the cells and allowed to continue to incubate at 28 °C until a sufficient yellow colour appeared, at which time 0.5 ml of 1 M Na_2CO_3 was

added to stop the reaction. Time (in minutes) was recorded from the time of ONPG addition to the addition of Na_2CO_3. Cells were centrifuged for 5 minutes at 12000 rpm and the OD_{420} and OD_{550} of the supernatant were recorded. The average activity of β-galactosidase (in Miller units) was calculated as seen in Miller (1972) ± 1 standard deviation. Experiments were done in triplicate. Unlike yeast two-hybrid assays, lower β-galactosidase activities in these experiments indicated protein-protein interactions, as the *lacZ* reporter gene is repressed when a heterodimeric repressor is formed between interacting p22- and 434-fusion repressors. As such, the addition of ONPG substrate will not lead to colour development in the presence of protein-protein interaction.

2.23. Antiserum production against gonococcal MinE

Antiserum against $MinE_{Ng}$ was produced as follows. A 5:1 mixture of purified $MinE_{Ng}$-His and Gerbu adjuvant (GERBU Biotechnik) was injected into female New Zealand white rabbits. Two additional boosters were administered over three week intervals (University of Ottawa Animal Care). Serum was collected from rabbit blood using established procedures (Sambrook and Russell D.W., 2001). Antisera specific for $MinE_{Ng}$ was obtained by using a modified affinity purification on nitrocellulose membranes as described (Pringle *et al.*, 1991).

In addition, two other methods were conducted. A second approach also involved NZW female rabbits, as conducted by Animal Care Unit at Western College of Veterinary Medicine (University of Saskatchewan, protocol ID 19940212). Differences include the use of TiterMax as the adjuvant, a 1:1 mixture of protein and adjuvant, 1st booster injection after

4 weeks, followed by 3 subsequent boosters each additional week. Antiserum was purified by affinity purification or IgG bead purification (Amersham).

The third approach used was to raise antisera against a specific peptide of $MinE_{Ng}$ by Genemed Synthesis Inc. Peptides constructed were $MinE_{Ng-1}$ (aa 2-21, SLIELLFGRKQKTATVARDR) and $MinE_{Ng-2}$ (aa 28-46, QERAQEGQTPDYLPTLRKE). These peptide sequences were chosen because they were to be most immunogenic, theoretically, as suggested by the company. Keyhole limpet hemocyanin (KLH) was conjugated to both peptides to increase immunogenicity, followed by rabbit immunization and blood collection by Genemed Synthesis Inc. Antisera was purified as described above. Western blotting (described in 2.25) revealed that the two latter methods were not able to detect $MinE_{Ng}$ from *N. gonorrhoeae* extracts (data not shown). As such, the first method of antibody production described in this section was used to detect purified $MinE_{Ng}$ and overexpression in an *E. coli* background.

2.24. Antibody purification

Affinity purification was carried out by spotting approximately 8 μg of purified $MinE_{Ng}$ protein on nitrocellulose paper (Amersham, Piscataway, NJ). The membrane was allowed to air dry, followed by membrane blocking with 5% skim milk in phosphate-buffer saline (PBS) at room temperature for one hour with shaking at 100 rpm. After, three washes of PBS were performed, and a 1:5 dilution of antisera in PBS was added overnight at 4°C. The PBS washes were repeated three times once more and $MinE_{Ng}$-specific antiserum was eluted with 0.1 M glycine buffer, pH 2, followed by neutralization with 1 M Tris-HCl to bring the pH of the antiserum to 7.

For IgG purification, Protein G sepharose beads (Amersham) was packed in a column and equilibriated with PBS. A 1:2 dilution of rabbit antiserum in PBS was added to the column and collected by gravity flow. The column was washed with PBS and IgG was eluted with 0.1 M glycine pH 2.8 into tubes that contained 1.5 M Tris-HCl pH 8.8. Antisera was dialyzed in PBS overnight and collected and checked on 12% SDS-PAGE for the presence of the heavy (55 kDa) and light (25 kDa) chains.

Polyclonal affinity-purified anti-$MinD_{Ng}$ was prepared in the laboratory as previously described (Szeto *et al.*, 2001a).

2.25. SDS-PAGE and western blotting

Protein samples resolved by sodium dodecyl sulphate polyacrylamide gel electrophoresis (SDS-PAGE) were either whole cell extracts or purified protein. Whole cell extracts from *E. coli* or *N. gonorrhoeae* were prepared by resuspending pelleted log-phase cells in PBS, pH 7.4. Resuspended cells, after the addition of 5X SDS-PAGE loading buffer (15% β-mercaptoethanol, 15% SDS, 1.5% bromophenol blue, 50% glycerol), were boiled for 10 minutes, centrifuged for 10 minutes at 12000 rpm (Sorvall MC 12V Microfuge), and the supernatant fraction was collected. The supernatant was resolved on a 15% polyacrylamide gel (5% stacking phase and 15% resolving phase) as described by Sambrook *et al.* (1989), using the Mini-PROTEAN II Electrophoresis Cell (Bio-Rad, Mississauga, ON). Coomassie blue staining for one hour, followed by the addition of a destaining solution (50% ddH_2O, 40% methanol, 10% acetic acid) was performed to visualize the purity of gonococcal MinD/MinE or to standardize the whole cell extracts for western blotting. Densitometric analysis, available on Alpha imager 1220 v5.04 software (AlphaEase™

version 5.00, Alpha Innotech Corp.) was used to compare and standardize the intensities of common protein bands in each whole cell extract. From this analysis, the amounts of whole cell extract to load for Western blotting was adjusted for equal loading on another resolved polyacrylamide gel.

Resolved gels were incubated in transfer buffer (25 mM Tris, 192 mM glycine, 20% methanol, pH 8.3) to remove residual salts. The gel was then transferred on Immobilon-P^{SQ} membranes (Millipore) that had previously been rinsed in methanol, ddH_2O, and transfer buffer as per the manufacturer's instructions (Millipore), using the Mini Trans-Blot Electrophoretic Transfer Cell (BioRad) at 100 V for one hour. After transfer, membranes were blocked with 3% skim milk for one hour at room temperature, followed by 3 washes of TTBS (50 mM Tris, 1.25 M NaCl, 0.5% Tween-20, pH 7.5). Membranes were then exposed to a 1:800 dilution of anti-$MinD_{Ng}$ or a 1:100 dilution of anti-$MinE_{Ng}$, overnight, at 4 °C. Blots were then washed 3 X 10 minutes in TTBS, followed by incubation of 1:3000 dilution of goat anti-rabbit secondary antibody conjugated with alkaline phosphatase (BioRad). After another TTBS washing, the membranes were developed using AttoPhos Plus kit (Promega, Nepean, ON) as the substrate for alkaline phosphatase and photographed using the Alpha imager 1220 software.

2.26. Analytical ultracentrifugation

Sedimentation equilibrium experiments were conducted on wild-type $MinE_{Ng}$-6XHis and on five mutations discussed in 2.11, namely the A18D, L22D, R30D, K53A, and E67L $MinE_{Ng}$ mutants which all have a His-tag fused to the C-terminal end of $MinE_{Ng}$. The experiments were performed at 4°C in a Beckman XL-I analytical ultracentrifuge using absorbance optics as described (Laue and Stafford, 1999) by Emmanuel Guigard and Dr.

Cyril Kay (University of Alberta). Approximately 110 µl of 4 mg/ml concentration of wild-type and mutant $MinE_{Ng}$ protein (all dialyzed in buffer A, section 2.12) were aliquotted and loaded into six sector CFE (Charcoal-filled Epon) sample cells, allowing three concentrations to be run simultaneously. Runs were performed at a minimum of three different speeds and each speed was maintained until there was no significant difference in $r^2/2$ versus absorbance scans taken 2 h apart to ensure that equilibrium was achieved. Sedimentation equilibrium data were evaluated using the NONLIN program, which employs a nonlinear least squares curve-fitting algorithm as described (Johnson *et al.*, 1981). The program allows for analysis of both single and multiple data files and can be fit to models containing up to four associating species, depending upon which parameters are permitted to vary during the fitting routine. The protein's partial specific volume and the solvent density were estimated using the Sednterp program (Laue *et al.*, 1991).

2.27. Size-exclusion chromatography

Gel filtration analysis was carried out on two separate occasions, by Protein Chemistry at the Vaccine and Infectious Disease Organization (VIDO, University of Saskatchewan) using an XK26/87 column packed manually with approximately 460 mL of Superdex-200 resin prep grade (Amersham) as per the manufacturer's instructions and equilibrated with MinE buffer (50 mM Tris, 20 mM NaCl, 1 mM EDTA, pH 7.52). Flow rate was maintained at 0.5 mL/min with a column pressure limit of 0.5 MPa. Approximately 1 ml of a 3 mg/ml solution of protein was injected onto the column and fractions collected using a Pharmacia Frac-3000 fraction collector. Elution volumes were collected in 8 ml intervals.

Following sample collection, the protein elution profile was constructed using Unicorn 4.0 (Amersham). The elution profile for each sample was compared to the elution profile of standards purchased from Amersham Biosciences to determine the molecular mass of the protein complex. Retention time and volume of each sample was compared to the retention time and volume of each standard in order to determine the molecular weight. The calculated protein complex mass was determined and then divided by the bioinformatically determined monomer mass to determine the number of $MinE_{Ng}$ monomers present in the complex.

CHAPTER 3

Results

Portions of this chapter were published in:

[**Eng, N.F.**, Szeto, J., Acharya, S., Tessier, D., and Dillon, J.R. (2006) The C-terminus of MinE from *Neisseria gonorrhoeae* acts as a topological specificity factor by modulating MinD activity in bacterial cell division. Res Microbiol. 157, 333-344.]

[Szeto, J., **Eng, N.F.**, Acharya, S., Rigden, M.D., and Dillon, J.R. (2004) A conserved polar region in the cell division site determinant MinD is required for responding to MinE-induced oscillation, but not for localization within coiled arrays, Res Microbiol. 156, 17-29.]

and

[Ramos, D., Ducat, T., Cheng, J., **Eng, N. F.**, Dillon, J. A. R., and Goto, N. K. (2006) Conformation of the cell division regulator MinE: Evidence for interactions between the topological specificity and anti-minCD domains. Biochem. 45, 4593-4601]

3.1. Identification of gonococcal MinE

Since many experiments in this research required purified $MinE_{Ng}$, mass spectrometry was performed to confirm the identity of $MinE_{Ng}$. Purified $MinE_{Ng}$-His protein expressed from pEC1 (Table 3) was run on 15% SDS-PAGE. Four independent experiments by Q-TOF mass spectrometry of excised $MinE_{Ng}$ protein bands revealed that the *minE* gene from *N. gonorrhoeae* does encode for the predicted $MinE_{Ng}$ protein (Table 4). Every peptide sequence generated in each trial by Q-TOF mass spectrometry was blasted against NCBI protein sequences and each trial led to the conclusion that the protein of interest was $MinE_{Ng}$ (GI number 14285581). The predicted molecular mass of $MinE_{Ng}$ was 10.03 kDa, with a pI of 6.26.

3.2. MinE proteins have domains of high conservation

From amino acid sequence alignments, bacteria that encoded MinE could be grouped into three main classes: Gram-negative cocci (Fig. 3.1, green bars), Gram-negative bacilli (Fig. 3.1, red bars), and Gram-positive bacteria (Fig. 3.1, blue bars). As seen in Figure 3.1, the majority of bacteria that possessed *minE* were from Gram-negative bacteria. MinE from *N. gonorrhoeae* ($MinE_{Ng}$; 87 aa) is 42% identical and 61% similar to *E. coli* MinE ($MinE_{Ec}$), and is 25% identical and 49% similar to MinE from *Clostridium perfringens* based on the amino acid sequence alignment from Figure 3.1. Notable Gram-negative bacilli expressing MinE were selected from the alignment, while all Gram-negative cocci and Gram-positive bacteria encoding MinE were included.

The nucleotide sequences of *minE* from *N. gonorrhoeae* FA1090, F62, and CH811 strains were identical (data not shown). The alignment of MinE from the *N. gonorrhoeae* FA1090 genome sequencing project (Roe *et al.*, 2000), with the sequences of 30 other MinE

Table 4. Identification of gonococcal MinE using Q-Tof mass spectrometry

Sample ID	Protein candidate	Mass (kDa) / pI	Peptide sequences (m/z)	Mascot Score
Ng 1	1 - cell division topological specificity factor (14285581 – NCBI)	10.03 / 6.26	-ELMEVLSK -ELMEVLSK + Ox. of M -LQIIIAQER -KELMEVLSK + Ox. of M -YVNVSLDNIR -MSLIELLFGR + Ox. of M -AQEGQTPDYLPTLR -AQEGQTPDYLPTLRK	373
Ng 2	1 - cell division topological specificity factor (14285581 – NCBI)	10.03 / 6.26	-ELMEVLSK -ELMEVLSK + Ox. of M -SLIELLFGR -KELMEVLSK -LQIIIAQER -KELMEVLSK + Ox. of M -SLIELLFGRK -YVNVSLDNIR -MSLIELLFGR + Ox. of M -MSLIELLFGRK + Ox. of M -DRLQIIIAQER -AQEGQTPDYLPTLR -AQEGQTPDYLPTLRK	531
Ng 3	1 - cell division topological specificity factor (14285581 – NCBI)	10.03 / 6.26	-ELMEVLSK -ELMEVLSK + Ox. of M -LQIIIAQER -KELMEVLSK + Ox. of M -YVNVSLDNIR -MSLIELLFGR + Ox. of M -AQEGQTPDYLPTLR -AQEGQTPDYLPTLRK	312
Ng 4	1 - cell division topological specificity factor (14285581 – NCBI)	10.03 / 6.26	-ELMEVLSK -ELMEVLSK + Ox. of M -LQIIIAQER -SLIELLFGRK -YVNVSLDNIR -MSLIELLFGR + Ox. of M -MSLIELLFGRK + Ox. of M -AQEGQTPDYLPTLR -AQEGQTPDYLPTLRK	372

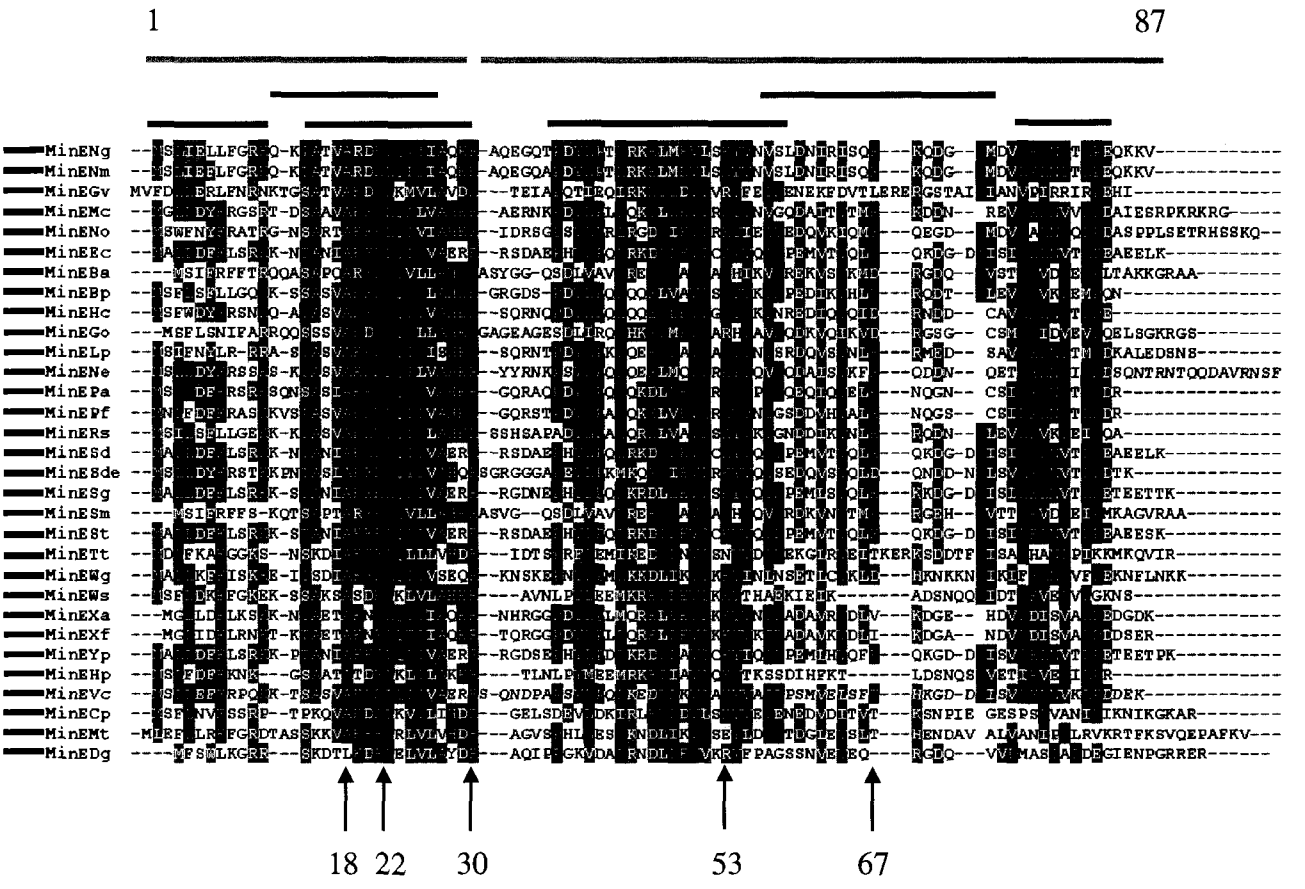

Figure 3.1. Sequence alignment of MinE proteins from various bacterial species. Abbreviations used: *Neisseria gonorrhoeae* (Ng), *Neisseria meningitidis* (Nm), *Gloeobacter violaceus* (Gv), *Methylococcus capsulatus* (Mc), *Nitrosococcus oceani* (No), *Escherichia coli* (Ec), *Brucella abortus* (Ba), *Bordetella pertussis* (Bp), *Hahella chejuensis* (Hc), *Gluconobacter oxydans* (Go), *Legionella pneumophila* (Lp), *Nitrosomonas europea* (Ne), *Pseudomonas aeruginosa* (Pa), *Pseudomonas fluorescens* (Pf), *Ralstonia solanacearum* (Rs), *Shigella dysenteriae* (Sd), *Shewanella denitrificans* (Sde), *Sodalis glossinidius* (Sg), *Sinorhizobium meliloti* (Sm), *Salmonella enterica* serovar Typhi (St), *Thermoanaerobacter tengcongensis* (Tt), *Wigglesworthia glossinidia* (Wg), *Wolinella succinogenes* (Ws), *Xanthomonas axonopodis* (Xa), *Xylella fastidosa* (Xf), *Yersinia pestis* (Yp), *Helicobacter pylori* (Hp), *Vibrio cholerae* (Vc), *Clostridium perfringens* (Cp), *Moorella thermoacetica* (Mt), *Deinococcus geothermalis* (Dg). Short coloured bars adjacent to the organism names show their general classifications: green = Gram-negative cocci, red = Gram-negative bacilli, blue = Gram-positive bacteria. Black bars show regions of conservation between MinE sequences. Grey bars indicate the N-terminus (aa 1-30) and the C-terminus (aa 31-87) of $MinE_{Ng}$. Purple bars indicate aa 12-26 and aa 57-72 as $MinD_{Ng}$ binding domains (D1 and D2, respectively, Eng *et al.*, 2006). Numbers and arrows refer to amino acids using $MinE_{Ng}$ as a reference, as outlined in 3.7.

homologues from different bacteria showed four regions of high conservation (using gonococcal MinE as a reference) throughout the protein, from amino acids 1-11, 14-30, 37-58, and 75-82 (Fig. 3.1, black bars), while domains between the second and third conserved regions and after the fourth region were not conserved at all (aa 31-36 and aa 83-87).

3.3. The *minE*$_{Ng}$ gene may code for an essential protein for the viability of *N. gonorrhoeae*

When the suicide vector carrying the disrupted *minE*$_{Ng}$ gene, pCNEE1 (deletion of first 168 nucleotides of *minE*$_{Ng}$, Table 3), was transformed into *N. gonorrhoeae* CH811 or F62, no viable colonies were observed, indicating that *minE*$_{Ng}$ may be an essential gene. The same result was achieved after an additional six attempts for two strains of *N. gonorrhoeae*, CH811 and F62 strains.

3.4. Morphological analysis of gonococcal Min overexpression from shuttle vectors in an *E. coli* background

The shuttle vector with only the *lac* promoter (pNE2) and the shuttle vectors overexpressing MinC$_{Ng}$ (pNE11) and MinE$_{Ng}$ (pNE13, Table 3) were individually transformed into *E. coli* PB103 to observe the effects of Min$_{Ng}$ protein overexpression in *E. coli* by observing the cell morphologies of each transformant by phase contrast or differential interference contrast microscopy. *E. coli* cells transformed with pNE2 showed wild-type *E. coli* phenotype, indicating that this construct (devoid of *min*) did not alter the morphology of *E. coli* (Fig. 3.2 A and C). When pNE11 was transformed into *E. coli*, overexpression of MinC$_{Ng}$ led to severe cell filamentation, resulting in elongated cells (Fig. 3.2 B). When pNE13 was transformed into *E. coli* PB103, the presence of minicells

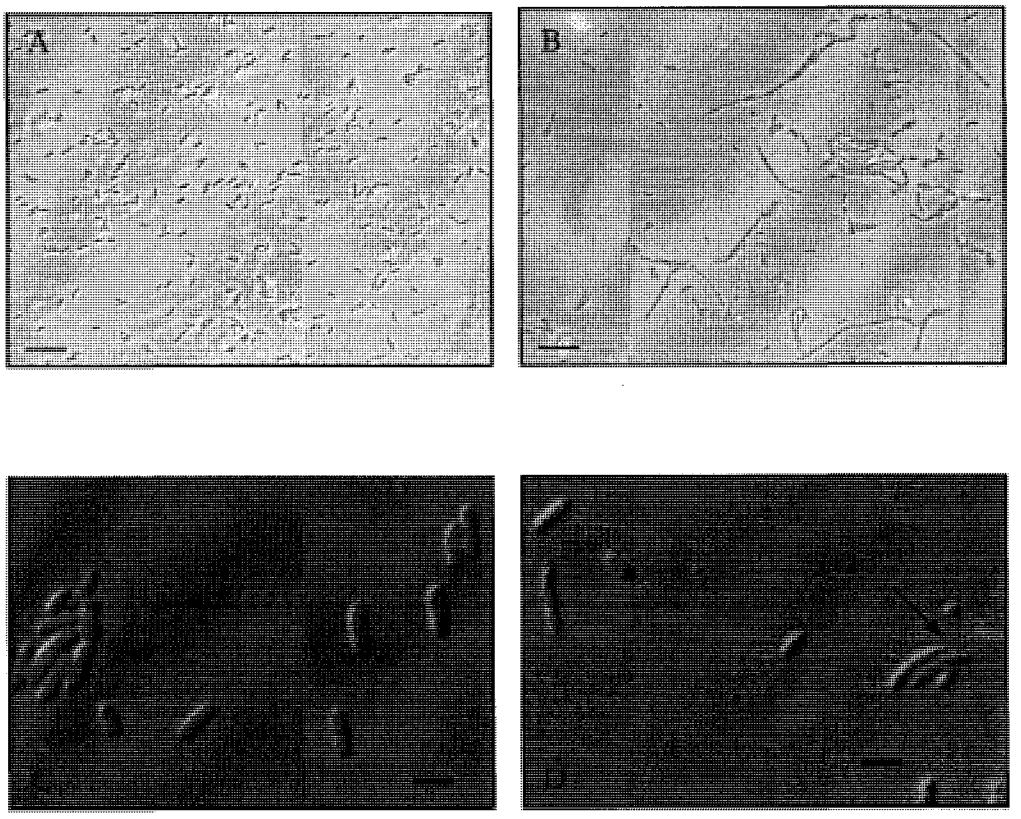

Figure 3.2. Expression of gonococcal MinC and MinE from a gonococcal shuttle vector in *E. coli* PB103. Microscopy showed the effects of Min_{Ng} protein overexpression from the shuttle vectors on *E. coli* phenotype by overexpressing $MinC_{Ng}$ and $MinE_{Ng}$ respectively. Transformation of pNE2 into *E. coli* did not alter *E. coli* phenotype (A and C), while $MinC_{Ng}$ overexpression from pNE11 (B) induced severe filamentation. Overexpression of $MinE_{Ng}$ from pNE13 (D) caused minicell formation (arrow). Images (A) and (B) were captured using phase-contrast microscopy. Scale bar for (A) and (B) is 10 μm to emphasize filamentation. Scale bar for (C) and (D) is 1 μm. Images (C) and (D) were captured using DIC microscopy to show the presence of minicells (arrows). These studies were done in duplicates.

and short filaments suggested that excess $MinE_{Ng}$ was able to counteract division inhibition at the cell poles, giving rise to minicell formation (Fig. 3.2 D). This indicated that the shuttle vectors were overexpressing $MinC_{Ng}$ (pNE11) and $MinE_{Ng}$ (pNE13).

3.5. Overexpression of $MinE_{Ng}$ affects growth rates of *N. gonorrhoeae* F62

Since previous growth studies in our laboratory normally involved *N. gonorrhoeae* CH811 (Ramirez-Arcos *et al.*, 2001b;Szeto *et al.*, 2001a), I used this strain initially to examine how the overexpression of $MinE_{Ng}$ might affect the growth of *N. gonorrhoeae*. I was unable to transform *N. gonorrhoeae* CH811 with pNE13 (encodes wild-type $MinE_{Ng}$) after multiple attempts (data not shown), while transformation of pNE13 into *N. gonorrhoeae* F62 was successful, generating a new strain called NE1 (Table 1). It was not known if this phenomenon was related to the fact that the F62 strain naturally carries a 4.2 kb cryptic plasmid (Roberts *et al.*, 1979), while CH811 is plasmid-free.

When growth curves were performed with *N. gonorrhoeae* F62 and NE1, in duplicate on two different occasions, the lag and exponential phases were similar; however, differences could be observed during the stationary and death phases (Fig. 3.3). From 10 hours to 12 hours, there was continued log phase growth of *N. gonorrhoeae* NE1 cells, while F62 cells maintained a steady-state after 10 hours for approximately 6 hours (Fig. 3.3). By 12 hours, there was a log factor difference in viable cells between the two strains (Fig. 3.3). Interestingly, the sharp increase in the number of viable *N. gonorrhoeae* NE1 cells was accompanied by a sudden death phase 4 hours earlier than *N. gonorrhoeae* F62 cells so that by 16 hours, the difference between the number of viable cells was nearly a log factor of 1.5 (Fig. 3.3).

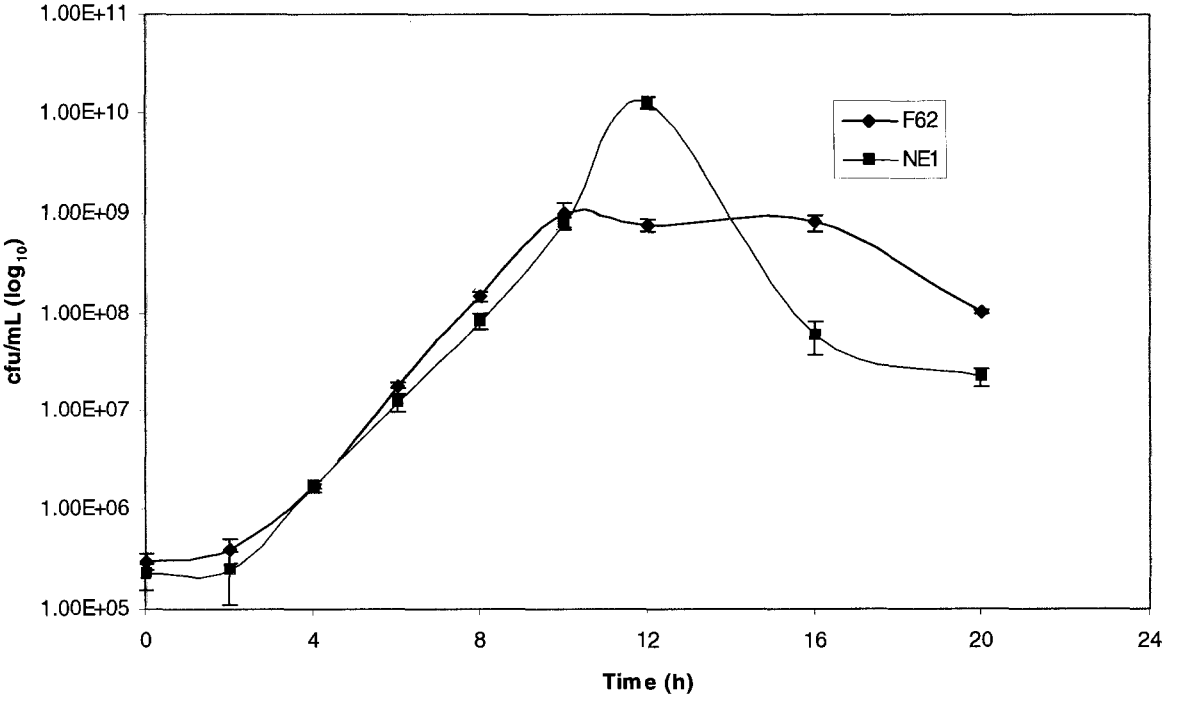

Figure 3.3. Growth curve of *N. gonorrhoeae* F62 and NE1. Up to 10 h, both strains grow similarly. At 12 h, wild-type F62 cells (blue line) entered a stationary phase until 16 h, while the number of viable *N. gonorrhoeae* NE1 cells (red line) continue to increase by about one log order at 12 h, followed by a sharp death phase 4 hours later. Lines connecting the data points were drawn to guide the eye. Error bars indicate ± 1 standard deviation. Growth curves were done in duplicate on two different occasions.

3.6. Overexpression of $MinE_{Ng}$ affects chromosome condensation

Gross morphological changes in *N. gonorrhoeae* due to overexpression of $MinE_{Ng}$ were initially examined by DIC microscopy. However, I was unable to discern any morphological or size differences between *N. gonorrhoeae* F62 and NE1 (data not shown) using this approach. Instead, transmission electron microscopy (TEM) of gonococcal F62 and NE1, showed that the size of the cells did not vary significantly at 12 hours ($p < 0.001$). At that time, wild-type *N. gonorrhoeae* F62 cells showed healthy wild-type morphology with many cells showing condensed nucleoids undergoing segregation and division (Fig. 3.4 A). At 16 hours, however, many of the wild-type cells appeared to be enlarged, dying, having lysed (Fig. 3.4 B), leaving many "ghost cells". In *N. gonorrhoeae* NE1, many cells appeared normal, but most of the cells did not display nucleoid condensation at 12 hours (Fig. 3.4 C). At 16 hours, these same cells remained healthy, but at this point, nucleoids were finally condensing (Fig. 3.4 D). At 16 hours, *N. gonorrhoeae* NE1 cells looked like *N. gonorrhoeae* F62 cells at 12 hours, suggesting that chromosome condensation was delayed by $MinE_{Ng}$ overexpression. The average diameter of *N. gonorrhoeae* NE1 cells at 16 hours was calculated to be ~29% greater than that of wild-type F62 cells. Statistical analysis confirmed that this difference was significant ($p<0.001$). Cells at 12 hours from either strain did not significantly vary in size. Western blotting did not detect MinE expression from *N. gonorrhoeae* F62 and NE1 (data not shown).

3.7. Gonococcal MinE contains two sites that are involved with $MinD_{Ng}$ interaction

The yeast two-hybrid system was used, in duplicate, to study the interaction between gonococcal MinE and gonococcal MinD. To efficiently pinpoint the sites of $MinE_{Ng}$ that are involved with $MinD_{Ng}$ interaction, a series of N-terminal (NT) and C-terminal (CT)

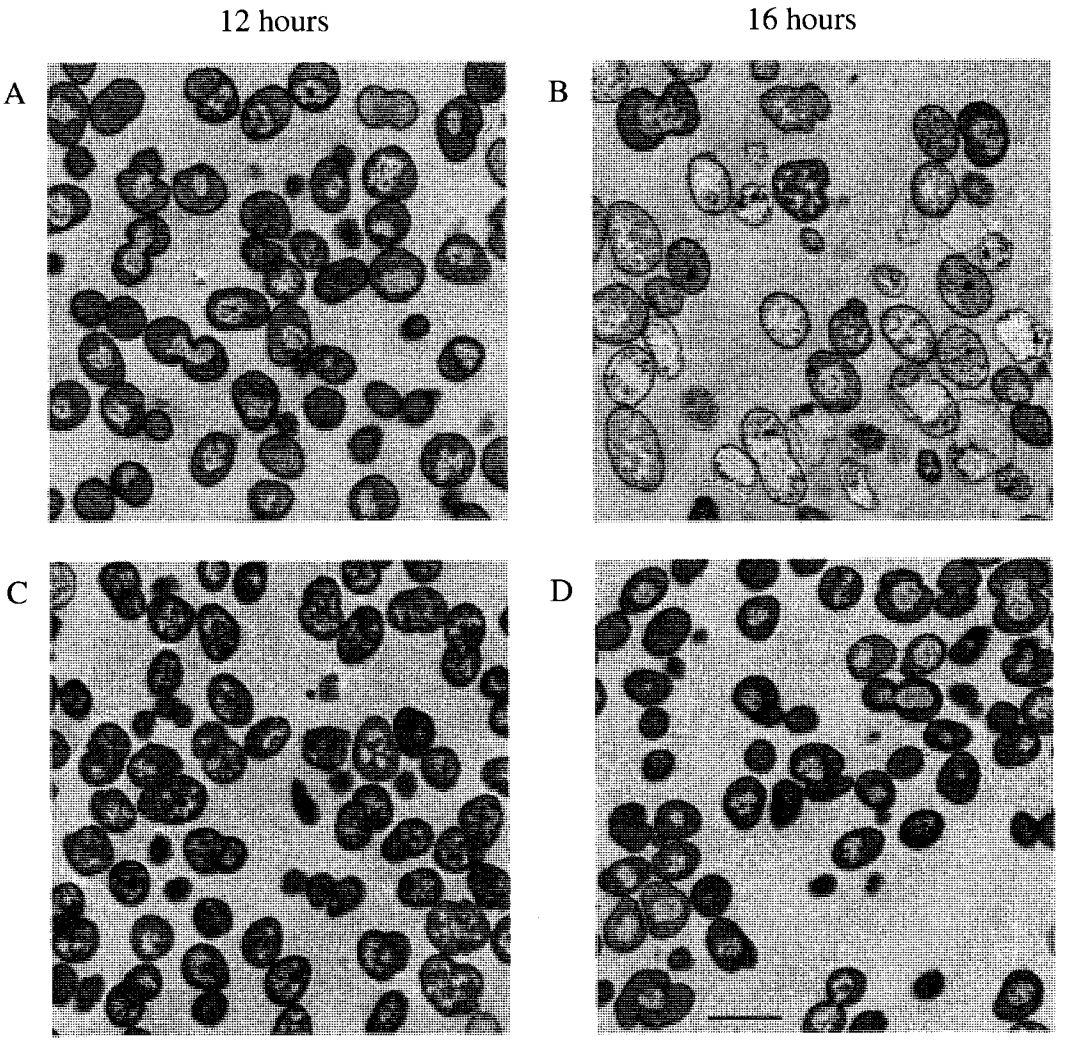

Figure 3.4. Transmission electron microscopy of *N. gonorrhoeae* F62 and NE1. Samples of wild-type gonococcal F62 (A and B) and NE1 cells (C and D) were taken at 12 h (A and C) and 16 h (B and D), sectioned and examined to discern any morphological changes. Wild-type *N. gonorrhoeae* F62 cells appeared healthy at 12 h (A). However, 4 hours later, most of the cells were unhealthy, enlarged and dying ($n = 20$, $p < 0.001$) (B). *N. gonorrhoeae* NE1 cells also appeared healthy at 12 h (C) and at 16 h (D). However, nucleoid condensation seemed to be delayed in *N. gonorrhoeae* NE1 cells by 4 hours, as cells in (D) were similar to those seen in (A). Size of cells in A, C, and D, were not statistically significant. Scale bar is 1 μm.

truncations to the 87 amino acid, 10 kDa protein were generated. The N-terminus (aa 1-30) and the C-terminus (aa 31-87) of $MinE_{Ng}$ (Fig. 3.1, grey bars) were defined based on previous studies of *E. coli* MinE (Ma *et al.*, 2003) which examined $MinE_{Ec}$ from residues 1-31 as a peptide, while I only considered this domain in $MinE_{Ng}$ up to and including R30, since aa 31-36 were highly variable among other homologous MinE sequences. First, $minE_{Ng}$ and $minD_{Ng}$ were individually cloned into both the pGAD424 and pGBT9 yeast vectors, so that each gene was fused to a GAL4 activation domain and a GAL4 DNA binding domain, respectively, to give rise to pGADminD, pGADminE, pGBT9minD, and pGBT9minE (Table 3). Each plasmid was singly transformed into *S. cerevisiase* SFY526; the yeast two-hybrid assays indicated that no interaction was detected, as expected with such controls (Table 5). When pGADminD and pGBT9minE were co-transformed into yeast, a positive interaction was observed by the presence of blue yeast colonies from the colony lift assays and a strong yellow colour that developed quickly after adding ONPG in β-galactosidase liquid assays (data not shown). However, no interaction was observed when pGADminE and pGBT9minD were co-transformed into *S. cerevisiase* (data not shown).

Using inverse PCR strategies, and pGBT9minE as a template, four N-terminal (NT) truncations were introduced in $minE_{Ng}$. Deleting the first 15, 33, 78 and 162 bp of $minE_{Ng}$ produced the following $MinE_{Ng}$ mutant constructs fused to the GAL4 DNA binding domain: $MinE_{Ng\text{-}5aaNT}$, $MinE_{Ng\text{-}11aaNT}$, $MinE_{Ng\text{-}26aaNT}$, and $MinE_{Ng\text{-}54aaNT}$ (Table 3). Using similar procedures to delete 12, 45, 90, and 177 bp from the 3' end of $minE_{Ng}$ generated $MinE_{Ng\text{-}4aaCT}$, $MinE_{Ng\text{-}15aaCT}$, $MinE_{Ng\text{-}30aaCT}$, and $MinE_{Ng\text{-}59aaCT}$ fusions (Table 3). Each of the eight plasmids was co-transformed with pGADminD into yeast. Colony lift assays indicated that formation of blue colonies was observed when $MinE_{Ng\text{-}5aaNT}$, $MinE_{Ng\text{-}11aaNT}$, $MinE_{Ng\text{-}4aaCT}$,

Table 5. Interaction assessment between $MinD_{Ng}$ and wild-type/mutant $MinE_{Ng}$ using the yeast two-hybrid system.

Fusion to GAL4 activating domain	Fusion to GAL4 DNA binding domain	Interaction detected[a]	β-Galactosidase activity (Miller units)
$MinD_{Ng}$	-	NO	ND[b]
-	$MinD_{Ng}$	NO	ND
$MinE_{Ng}$	-	NO	ND
-	$MinE_{Ng}$	NO	ND
$MinD_{Ng}$	$MinE_{Ng}$	YES	20.74 ± 1.30
$MinE_{Ng}$	$MinD_{Ng}$	NO	ND
$MinD_{Ng}$	$MinE_{Ng\text{-}5aaNT}$[c]	YES	ND
$MinD_{Ng}$	$MinE_{Ng\text{-}11aaNT}$	YES	ND
$MinD_{Ng}$	$MinE_{Ng\text{-}26aaNT}$	NO	ND
$MinD_{Ng}$	$MinE_{Ng\text{-}54aaNT}$	NO	ND
$MinD_{Ng}$	$MinE_{Ng\text{-}4aaCT}$[d]	YES	ND
$MinD_{Ng}$	$MinE_{Ng\text{-}15aaCT}$	YES	ND
$MinD_{Ng}$	$MinE_{Ng\text{-}30aaCT}$	NO	ND
$MinD_{Ng}$	$MinE_{Ng\text{-}59aaCT}$	NO	ND
$MinD_{Ng}$	$MinE_{Ng\text{-}A18D}$	NO	0.01 ± 0.02
$MinD_{Ng}$	$MinE_{Ng\text{-}L22D}$	NO	0.02 ± 0.04
$MinD_{Ng}$	$MinE_{Ng\text{-}R30D}$	YES	17.00 ± 2.84
$MinD_{Ng}$	$MinE_{Ng\text{-}K53A}$	YES	5.06 ± 0.58
$MinD_{Ng}$	$MinE_{Ng\text{-}E67L}$	YES	2.42 ± 0.28

[a] Colony-lift assay performed
[b] ND = not determined
[c] NT = N-terminal $MinE_{Ng}$ truncation
[d] CT = C-terminal $MinE_{Ng}$ truncation

and $MinE_{Ng\text{-}15aaCT}$ fusions were expressed, while colourless colonies were seen when $MinE_{Ng\text{-}26aaNT}$, $MinE_{Ng\text{-}54aaNT}$, $MinE_{Ng\text{-}30aaCT}$, and $MinE_{Ng\text{-}59aaCT}$ fusions were expressed (Fig. 3.5). These results suggested that interaction with $MinD_{Ng}$ was lost when the first 26 and last 30 residues of $MinE_{Ng}$ were deleted ($MinE_{Ng\text{-}26aaNT}$ and $MinE_{Ng\text{-}30aaCT}$, respectively), while $MinE_{Ng\text{-}11aaNT}$ and $MinE_{Ng\text{-}15aaCT}$ yeast fusions yielded interaction with $MinD_{Ng}$. As a result, gonococcal MinE possesses two sites that are involved with $MinD_{Ng}$ interaction; the two regions spanned from residues 12-26 (D1) and 57-72 (D2) (Fig. 3.1, purple bars).

With regions of $MinE_{Ng}$ that may interact with $MinD_{Ng}$ elucidated, five conserved $MinE_{Ng}$ residues were singly substituted using site-directed mutagenesis to further investigate the significance of these sites identified from the amino acid sequence alignment in Figure 3.1. Three residues within the N-terminus of $MinE_{Ng}$ were chosen; within domain D1, alanine 18 and leucine 22 were mutated to aspartate. As a control, another conserved amino acid was selected external to D1, arginine 30, to illustrate that not any mutation will alter $MinE_{Ng}/MinD_{Ng}$ interaction. This amino acid was mutated to aspartate as well. In the C-terminus of $MinE_{Ng}$, lysine 53, which is outside of D2, was mutated to alanine, while glutamate 67, conserved in terms of having negatively-charged side chains, was chosen within D2, and substituted with leucine. These residues have been previously studied in the *E. coli* MinE equivalent (Hu and Lutkenhaus, 2001;King *et al.*, 2000;Ma *et al.*, 2003); however, this study provides a more comprehensive examination of each mutation in a variety of experiments (protein-protein interactions, morphology, ATPase assays, protein localization) which was not completely performed with each $MinE_{Ec}$ mutant. In addition, the selection of these amino acids allowed for a comparison of MinE protein function between round (*N. gonorrhoeae*) and rod-shaped (*E. coli*) Gram-negative bacteria.

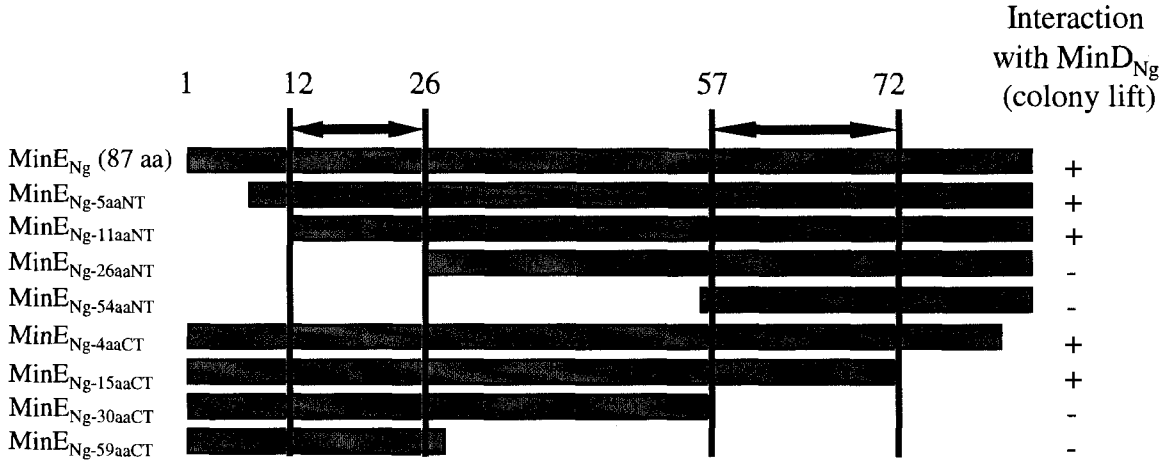

Figure 3.5. Yeast two-hybrid assays reveal the presence of two MinE$_{Ng}$ sites that are associated with MinD$_{Ng}$ interaction . Various MinE$_{Ng}$ truncations were used in the yeast two-hybrid system to determine if MinD$_{Ng}$ interaction is retained (gray bars are visual representation of the truncations). This suggests two possible MinD$_{Ng}$ binding domains (between aa 12-26 and aa 57-72) on MinE$_{Ng}$. Positive colony-life assays are indicated by +, indicating interaction between MinD$_{Ng}$ and MinE$_{Ng}$, while a negative result is indicated by -. These studies were done in duplicate.

The five point mutations of $MinE_{Ng}$ were separately introduced into pGBT9minE. Each plasmid was then co-transformed with pGADminD into yeast to determine the ability of the mutant $MinE_{Ng}$ fusions to interact with $MinD_{Ng}$. Colony lift assays revealed that, in addition to wild-type $MinE_{Ng}$, expression of $MinE_{Ng\text{-}R30D}$, and the C-terminal $MinE_{Ng\text{-}K53A}$ and $MinE_{Ng\text{-}E67L}$ mutants led to the formation of blue yeast colonies (Fig. 3.6), while the N-terminal $MinE_{Ng\text{-}A18D}$ and $MinE_{Ng\text{-}L22D}$ mutants did not. These results were verified by β-galactosidase liquid activity assays (Table 5). Interaction was measured in Miller units and showed that the $MinE_{Ng}$ mutants showed varying degrees of interaction with $MinD_{Ng}$. Wild-type $MinE_{Ng}$ and $MinE_{Ng\text{-}R30D}$ interacted the strongest with $MinD_{Ng}$ similarly (20.74 ± 1.30 and 17.00 ± 2.84 Miller units, respectively, Table 5), followed by the C-terminal mutants $MinE_{Ng\text{-}K53A}$ and $MinE_{Ng\text{-}E67L}$ (5.06 ± 0.58 and 2.42 ± 0.28 Miller units, respectively, Table 5). Despite the ability of the C-terminal $MinE_{Ng}$ mutants to maintain interaction with $MinD_{Ng}$, the decreased interaction suggests that the C-terminus of $MinE_{Ng}$ plays a role in $MinD_{Ng}$ interaction. Liquid assays were unable to measure any interaction between $MinD_{Ng}$ and the N-terminal $MinE_{Ng\text{-}A18D}$ and $MinE_{Ng\text{-}L22D}$ mutants, indicating that $MinD_{Ng}$ interaction was completely abolished. These studies showed that both the N- and C-termini of $MinE_{Ng}$ are involved with $MinD_{Ng}$ interaction.

3.8. *E. coli* minicell formation as an indicator for $MinE_{Ng}$ functionality

Our laboratory has previously used *E. coli* as a model organism to determine the functionality of $MinC_{Ng}$ (Ramirez-Arcos *et al.*, 2001b), $MinD_{Ng}$ (Szeto *et al.*, 2001a), and $MinE_{Ng}$ (Ramirez-Arcos *et al.*, 2002). Thus, one of the more effective models in determining $MinE_{Ng}$ function would be to overexpress the protein in *E. coli* PB103 (+*min*, Table 1), a

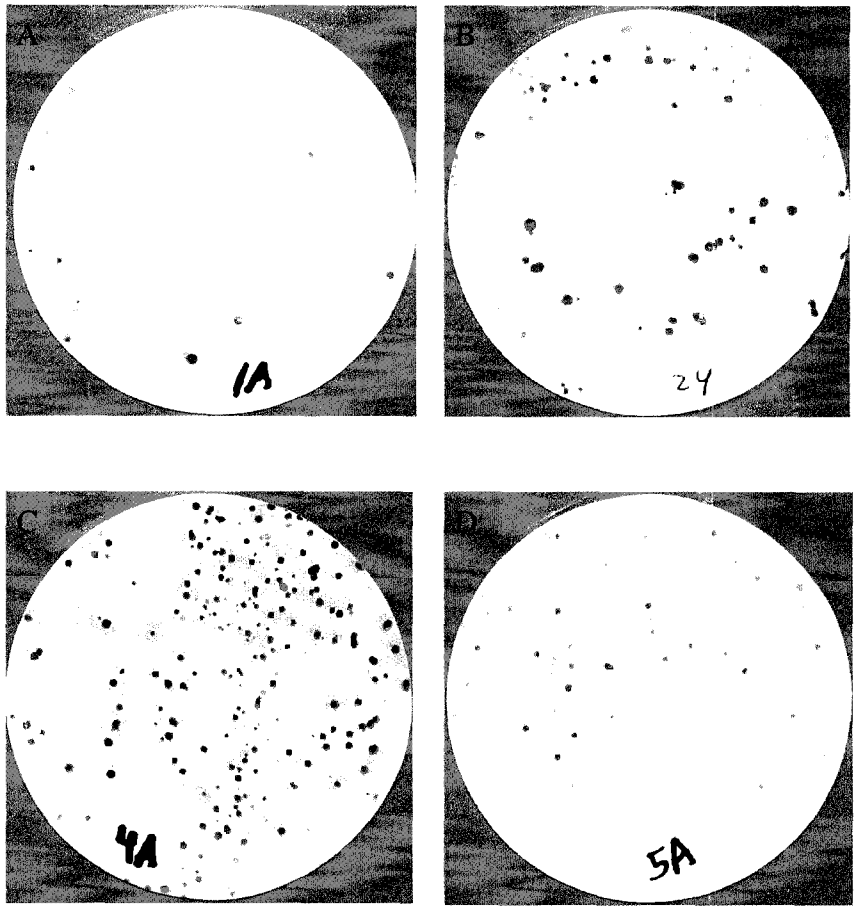

Figure 3.6. Colony lift assays to determine the ability of $MinE_{Ng}$ mutants to interact with $MinD_{Ng}$. When $MinE_{Ng}$ and $MinD_{Ng}$ interact, blue colonies appear, indicating that lacZ is able to process the X-gal substrate. In duplicate, blue colonies were observed with wild-type $MinE_{Ng}$ (A), $MinE_{Ng\text{-}R30D}$ (B), $MinE_{Ng\text{-}K53A}$ (C), and $MinE_{Ng\text{-}E67L}$ (D) were expressed, indicating interaction. $MinE_{Ng\text{-}A18D}$ and $MinE_{Ng\text{-}L22D}$ expression did not reveal any blue colonies.

common approach used to study Min phenotypes (de Boer *et al.*, 1988). In this system, functional $MinE_{Ng}$ should be characterized by the ability to induce a minicell (round, nucleoid-free cells) phenotype when overexpressed. Based on current models of Min function (Fig. 1.9), an excess of $MinE_{Ng}$ should prevent $MinC_{Ec}$ and $MinD_{Ec}$ from binding to the membrane, thereby allowing cell division to initiate at midcell and at the cell poles. Examination of cells by differential interference contrast (DIC) microscopy indicated that wild-type $MinE_{Ng}$ overexpression from pEUC1 (pUC18 + $minE_{Ng}$) in *E. coli* PB103 induced a minicell phenotype, indicating $MinE_{Ng}$ functionality (Fig. 3.7 A, minicells indicated by arrows). A similar morphology was seen when $MinE_{Ng\text{-}R30D}$ was overexpressed from pEUC30 (pUC18 + $minE_{Ng\text{-}R30D}$) (Fig. 3.7 D, arrows). However, overexpression of the N-terminal $MinE_{Ng\text{-}A18D}$ (expressed from pEUC18) and $MinE_{Ng\text{-}L22D}$ (expressed from pEUC22) mutants did not induce minicell formation, and the presence of wild-type *E. coli* phenotype was observed (Fig. 3.7 B, C). A similar effect was also observed in *E. coli* cells overexpressing $MinE_{Ng\text{-}E67L}$ (Fig. 3.7 F). In contrast, $MinE_{Ng\text{-}K53A}$ (expressed from pEUC53) overexpression in *E. coli* PB103 induced a minicell phenotype (Fig. 3.7 E). Western blotting indicated that wild-type and mutant $MinE_{Ng}$ were expressed at similar levels in *E. coli* (Fig. 3.7 G). These studies showed that heterologous expression of wild-type $MinE_{Ng}$ in an *E. coli* background induced a minicell phenotype; in addition, the inability of the A18D, L22D, and E67L $MinE_{Ng}$ mutants to cause minicell formation upon overexpression suggested that these mutants were not functional. Thus, *E. coli* can be used as an effective biological model to study *N. gonorrhoeae* MinE function.

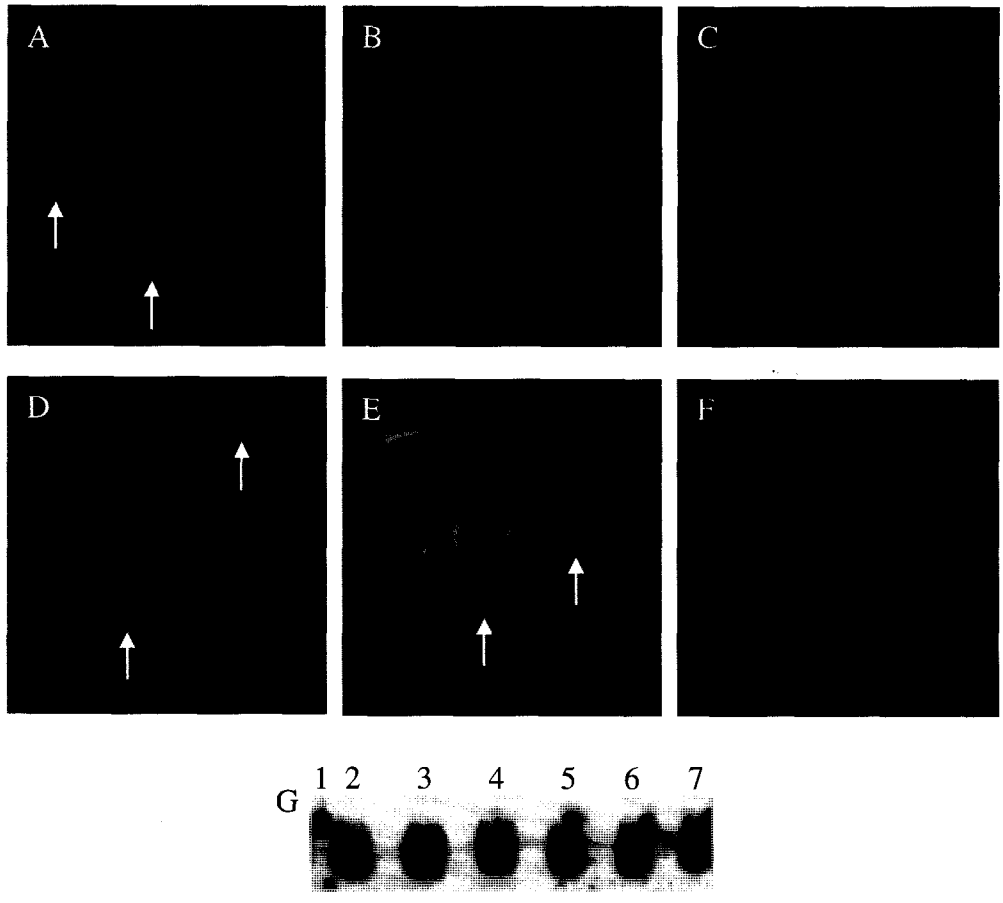

Figure 3.7. Overexpression of mutant $MinE_{Ng}$ in *E. coli* PB103. Functional $MinE_{Ng}$ causes a minicell phenotype when overexpressed in *E. coli* PB103. Overexpression of functional $MinE_{Ng}$ is characterized by the formation of minicells (A, D, E, arrows). Wild-type $MinE_{Ng}$ overexpressed from pEUC1 is able to induce minicell phenotype (A), as $MinE_{Ng\text{-}R30D}$ overexpression (from pEUC30, D) and $MinE_{Ng\text{-}K53A}$ (from pEUC53, E). N-terminal $MinE_{Ng}$ mutants did not disturb the normal division patterns in *E. coli* upon overexpression and only equally sized *E. coli* daughter cells are produced (B and C show $MinE_{Ng\text{-}A18D}$ and $MinE_{Ng\text{-}L22D}$ overexpression, from pEUC18 and pEUC22, respectively). C-terminal $MinE_{Ng}$ mutants caused differing *E. coli* morphologies. $MinE_{Ng\text{-}K53A}$ caused a minicell phenotype (E, arrows), while $MinE_{Ng\text{-}E67L}$ resulted in normal *E. coli* phenotype (expressed from pEUC67, F). G) Western blotting using anti-$MinE_{Ng}$ antisera showed relatively equal amounts of $MinE_{Ng}$ overexpression in *E. coli* PB103. Lane 1: purified $MinE_{Ng}$-His; lane 2: wild-type $MinE_{Ng}$; lane 3: $MinE_{Ng\text{-}A18D}$; lane 4, $MinE_{Ng\text{-}L22D}$; lane 5, $MinE_{Ng\text{-}R30D}$; lane 6, $MinE_{Ng\text{-}K53A}$; lane 7, $MinE_{Ng\text{-}E67L}$. Scale bar represents 1 μm. These studies were done on two different occasions.

3.9. $MinE_{Ng}$-$MinD_{Ng}$ interaction is a prerequisite for $MinD_{Ng}$ oscillation

Using fluorescence microscopy, oscillation of $MinD_{Ng}$ in *E. coli* can be visualized by co-expressing $MinE_{Ng}$ and GFP-$MinD_{Ng}$ *in cis* (Ramirez-Arcos *et al.*, 2002). Site-directed mutagenesis was used to introduce A18D, L22D, R30D, K53A, and E67L mutations in pSR15, a plasmid which encodes *gfp-minD*$_{Ng}$ and *minE*$_{Ng}$ *in cis*, which had been used in previous studies to observe GFP-$MinD_{Ng}$ oscillations (Ramirez-Arcos *et al.*, 2002;Szeto *et al.*, 2005;Szeto *et al.*, 2004). Each plasmid encoding mutant *minE*$_{Ng}$ was then transformed into *E. coli* PB114, a strain genetically modified by inserting a kanamycin cassette into the *minCDE*$_{Ec}$ locus, thereby disrupting its expression (de Boer *et al.*, 1988). This prevented the interference of endogenous *E. coli* Min proteins on GFP-$MinD_{Ng}$ oscillation patterns. As with previous studies (Szeto *et al.*, 2004;Szeto *et al.*, 2005), the period of time for GFP-$MinD_{Ng}$ to cycle (from one pole to the other and back) in *E. coli* PB114 in the presence of $MinE_{Ng}$ was about 29.1 ± 7.3 seconds (n = 10, Fig. 3.8 A-C). Similarly, in the presence of $MinE_{Ng\text{-}R30D}$, the period of GFP-$MinD_{Ng}$ trafficking was (33.6 ± 7.7 s, n = 10, Fig 3.8 F-H). The N-terminal $MinE_{Ng\text{-}A18D}$ and $MinE_{Ng\text{-}L22D}$ mutants did not induce GFP-$MinD_{Ng}$ movement; instead fluorescence was completely localized along the entire membrane periphery (Fig. 3.8 D and E respectively). The C-terminal $MinE_{Ng}$ mutants were also able to initiate pole-to-pole movement of GFP-$MinD_{Ng}$, although periods were significantly slower that those induced by wild-type $MinE_{Ng}$. Oscillation cycles induced by $MinE_{Ng\text{-}K53A}$ took 51.8 ± 3.8 s (n = 10, Fig. 3.8 I-K) to complete, while on average, $MinE_{Ng\text{-}E67L}$ caused GFP-$MinD_{Ng}$ to translocate from one end of the cell to the other in 66.0 ± 8.8 seconds (n = 10, Fig. 3.8 L-P). The unpaired Student's t-test determined that these differences were statistically significant with $p<0.001$. Protein levels of GFP-$MinD_{Ng}$ and wild-type/mutant $MinE_{Ng}$ were similar as determined by Western blotting (Fig. 3.8 Q). Among the $MinE_{Ng}$

Figure 3.8. Oscillation of GFP-$MinD_{Ng}$ requires interaction with $MinE_{Ng}$. Wild-type expression of $MinE_{Ng}$ caused GFP-$MinD_{Ng}$ to oscillate in ~30s complete cycles (A-C). Oscillation is abrogated and becomes entirely localized to the membrane when N-terminal mutants, $MinE_{Ng\text{-}A18D}$ and $MinE_{Ng\text{-}L22D}$, were coexpressed with $MinD_{Ng}$ (D, E, respectively). The presence of $MinE_{Ng\text{-}R30D}$ also induced $MinD_{Ng}$ oscillation periods similar to wild-type $MinE_{Ng}$ (F-H). Expression of C-terminal $MinE_{Ng}$ mutants, such as $MinE_{Ng\text{-}K53A}$, induced slower periods of oscillation (I-K, ~50s cycles), while $MinE_{Ng\text{-}E67L}$ slowed $MinD_{Ng}$ cycling from pole to pole to ~60s cycles (L-P). Q) Western blotting showed that GFP-$MinD_{Ng}$ expression was detected using anti-$MinD_{Ng}$ antisera at 1:800 dilution. $MinE_{Ng}$ was detected using rabbit-derived anti-$MinE_{Ng}$ antisera at 1:100 dilution. Lane 1 denotes expression from untransformed *E. coli* PB114; lane 2, shows coexpression of wild-type GFP-$MinD_{Ng}$ and $MinE_{Ng}$ from pSR15; lane 3, pSRDT18; lane 4, pSRDT22; lane 5, pSRDT30; lane 6, pSRDT53; lane 7, pSRDT67. The asterisk represents purified $MinE_{Ng}$ protein. All oscillation periods were statistically significant ($p<0.001$). Ten cells were counted for each sample to determine the average oscillation periods in seconds ± 1 standard deviation. Scale bars represent 2 μm.

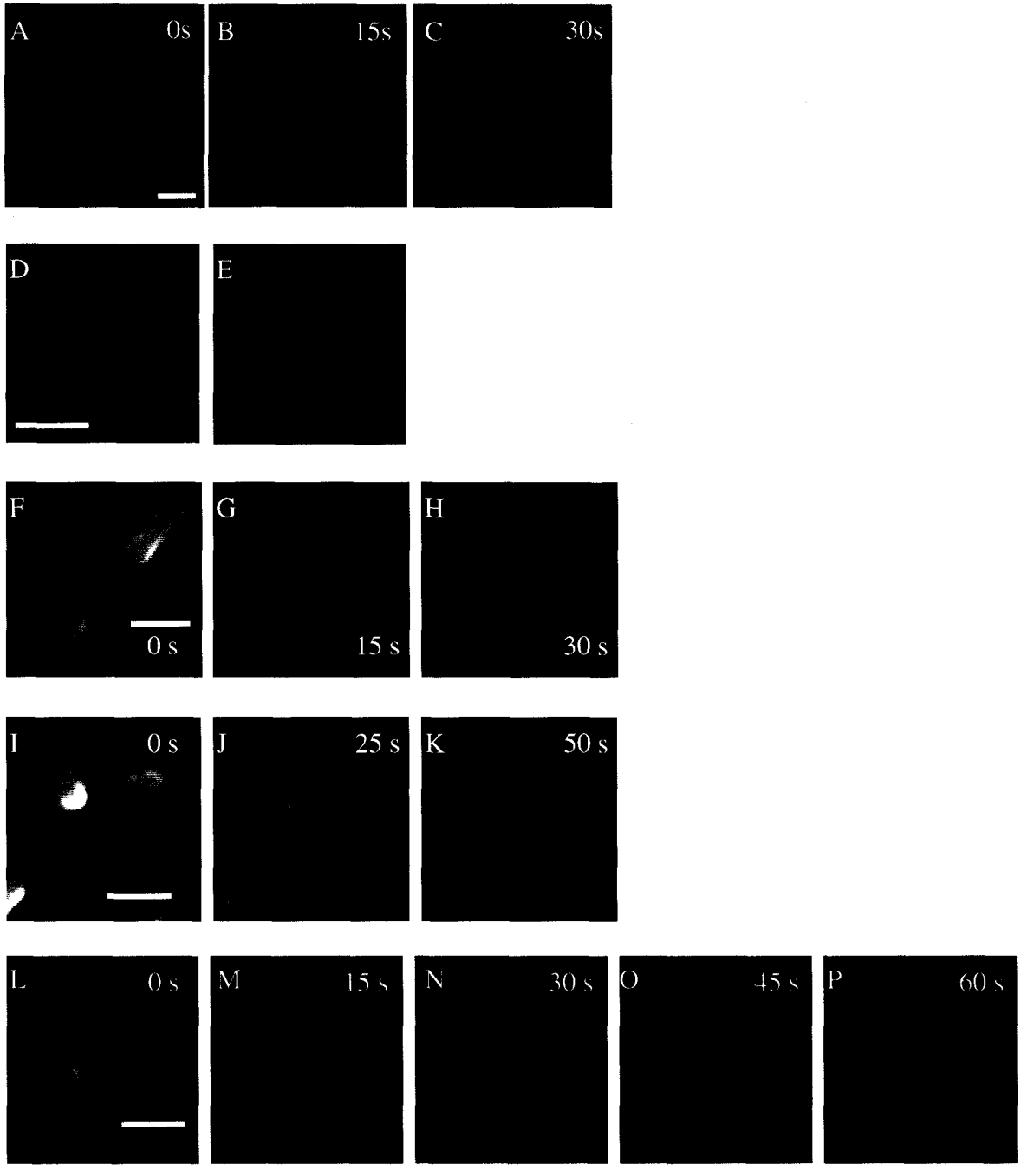
A
0s
B
15s
C
30s
D
E
F
0 s
G
15 s
H
30 s
I
0 s
J
25 s
K
50 s
L
0 s
M
15 s
N
30 s
O
45 s
P
60 s
Q
1 2 3 4 5 6 7
GFP-MinD$_{Ng}$
MinE$_{Ng}$
*

mutants that retained the ability to interact with $MinD_{Ng}$ (e.g. R30D, K53A, and E67L $MinE_{Ng}$ mutants), their co-expression with GFP-$MinD_{Ng}$, permitted $MinD_{Ng}$ oscillation from pole-to-pole, regardless of the degree of interaction between the two proteins (Table 5). The absence of this association, such as the A18D and L22D $MinE_{Ng}$ mutants, therefore, does not permit $MinD_{Ng}$ to move from pole-to-pole at all, sequestering the ATPase protein to the cell membrane. Therefore, $MinE_{Ng}$ must interact with $MinD_{Ng}$ in order to induce dynamic oscillation.

3.10. The coiled array is correlated with $MinD_{Ng}$ oscillation

Studies of *E. coli* Min proteins showed that $MinD_{Ec}$ and $MinE_{Ec}$ were recruited to coiled structures associated with the cell membrane (Shih *et al.*, 2003). Our laboratory has also reported the presence of these coiled subcellular architectures in *E. coli* in the presence of gonococcal MinD and MinE (Szeto *et al.*, 2004;Szeto *et al.*, 2005). I examined the nature of $MinD_{Ng}$ localization to the coiled array using fluorescence microscopy. $MinD_{Ng}$ recruitment to the coiled array was observed in the presence of wild-type $MinE_{Ng}$ (Fig. 3.9 A, arrows). The subcellular structures, showing a banding pattern of GFP-$MinD_{Ng}$ fluorescence, were also visualized in the presence of $MinE_{Ng\text{-}R30D}$ (data not shown), $MinE_{Ng\text{-}K53A}$, and $MinE_{Ng\text{-}E67L}$ (Fig. 3.9 C and D respectively). In contrast, the N-terminal $MinE_{Ng\text{-}A18D}$ and $MinE_{Ng\text{-}L22D}$ mutants did not cause $MinD_{Ng}$ to be localized to the array, but peripherally at the cell membrane (Fig. 3.9 B showed $MinD_{Ng}$ localization in the presence of $MinE_{Ng\text{-}A18D}$). $MinD_{Ng}$ recruitment to the coiled array was only observed in the presence of $MinE_{Ng}$ mutants that induced $MinD_{Ng}$ oscillation, suggesting that the oscillation of Min_{Ng} and the coiled array were linked. In addition, oscillation and the subcellular architectures

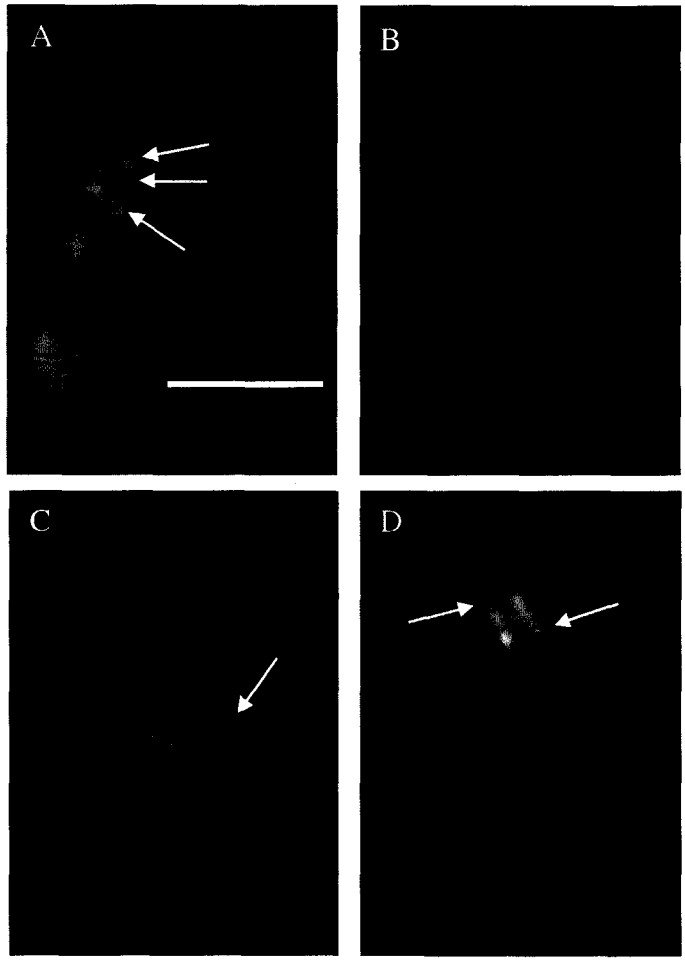

Figure 3.9. Interaction between $MinD_{Ng}$ and $MinE_{Ng}$ permits $MinD_{Ng}$ recruitment to the polymeric/coiled array. When GFP-$MinD_{Ng}$ and wild-type $MinE_{Ng}$ are coexpressed in *E. coli* PB114, GFP-$MinD_{Ng}$ is localized to a coiled protein array (A, arrows). This same phenomenon is also seen when $MinD_{Ng\text{-}R30D}$ (C, arrows) and $MinE_{Ng\text{-}E67L}$ are coexpressed (D, arrows). When interaction with $MinE_{Ng}$ is abolished, GFP-$MinD_{Ng}$ remained membrane-localized with no recruitment of the GFP fusion to the polymeric array (e.g. $MinE_{Ng\text{-}A18D}$, B). Scale bar represents 2 μm.

corresponded with $MinE_{Ng}$ mutants that can interact with $MinD_{Ng}$, indicating that this association was necessary for $MinD_{Ng}$ recruitment to the coiled array and subsequently, $MinD_{Ng}$ oscillation.

3.11. Stimulation of $MinD_{Ng}$ ATPase activity is linked to the strength of $MinE_{Ng}$-$MinD_{Ng}$ interaction

In *E. coli*, the stimulation of MinD ATPase activity required the presence of MinE; in turn, stimulation of ATPase activity was also required for $MinD_{Ec}$ oscillation (Hu *et al.*, 2002;Hu and Lutkenhaus, 2001;Lackner *et al.*, 2003). Recent studies showed that gonococcal $MinD_{Ng}$ ATPase activity was also stimulated in the presence of $MinE_{Ng}$ (Szeto *et al.*, 2004;Szeto *et al.*, 2005). Assuming that interaction between $MinE_{Ng}$ and $MinD_{Ng}$ was required, I predicted that non-MinD-interacting $MinE_{Ng}$ mutants would be unable to stimulate ATP hydrolysis by $MinD_{Ng}$, while $MinD_{Ng}$ ATPase activity should be linked to how strong $MinD_{Ng}$ and $MinE_{Ng}$ interacted. As such, I evaluated the ability of the N- and C-terminal $MinE_{Ng}$ mutants to stimulate the ATPase activity of $MinD_{Ng}$. An assay to measure the amount of inorganic phosphates released by the hydrolysis of ATP was performed to determine if the $MinE_{Ng}$ mutants were able to increase basal $MinD_{Ng}$ ATP hydrolytic activity. Using a phosphate curve to correlate optical density with the amount of inorganic phosphate released (Fig. 3.10), I determined that wild-type $MinE_{Ng}$ and $MinE_{Ng\text{-}R30D}$ stimulated high rates (amount of inorganic phosphate released as a function of time) of $MinD_{Ng}$ ATPase activity relative to unstimulated $MinD_{Ng}$ (i.e. basal $MinD_{Ng}$ ATPase activity in the absence of $MinE_{Ng}$, Fig. 3.11) over the course of 60 minutes. The N-terminal mutants $MinE_{Ng\text{-}A18D}$ and $MinE_{Ng\text{-}L22D}$ did not stimulate $MinD_{Ng}$ ATPase activity (Fig. 3.11). The C-terminal $MinE_{Ng}$ mutants, K53A and E67L, behaved differentially like in the morphology

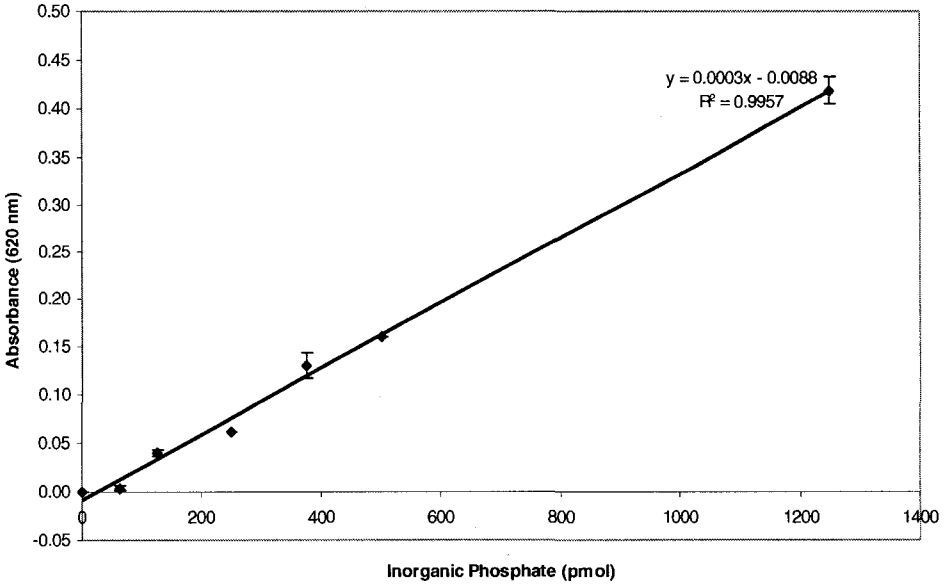

Figure 3.10. Standard curve of inorganic phosphates released. The amount of inorganic phosphate released was determined by comparing absorbance readings with those obtained from inorganic phosphate standards prepared from dilutions of KH_2PO_4 in a blank buffer. Error bars indicate ± 1 standard deviation.

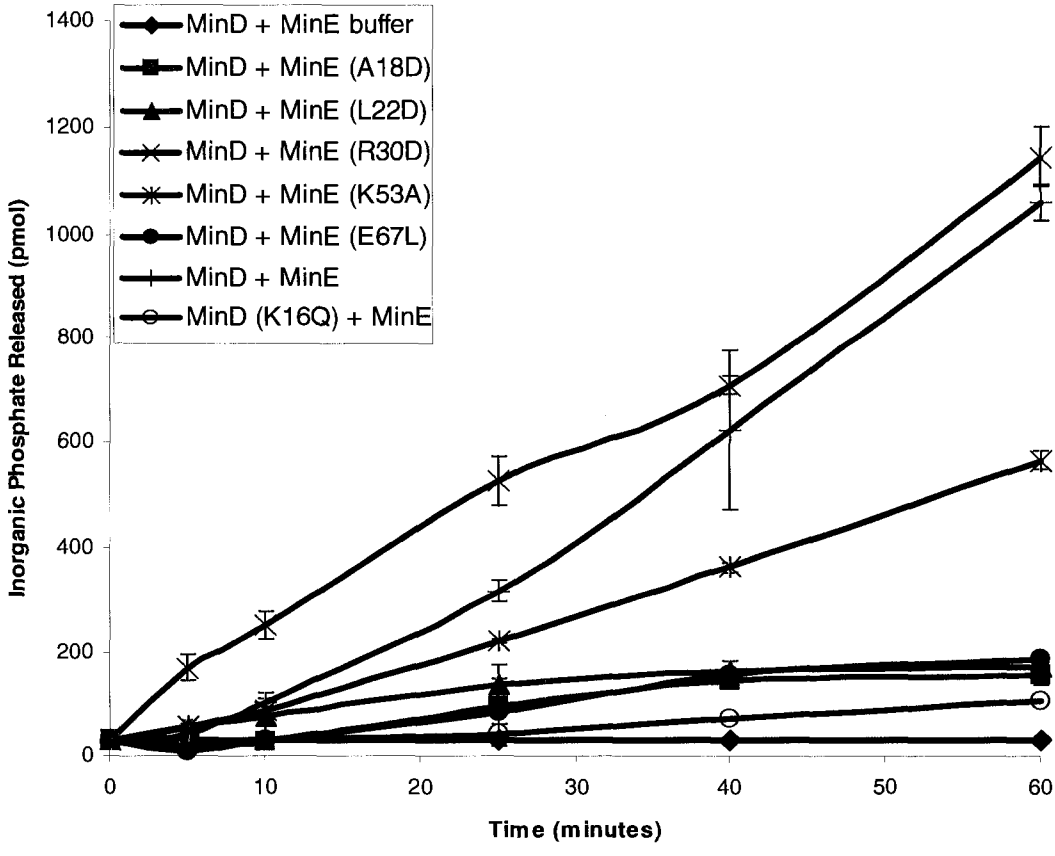

Figure 3.11. Comparing $MinD_{Ng}$ ATPase activities in the presence of $MinE_{Ng}$ mutants. Over 60 minutes, both wild-type $MinE_{Ng}$ and $MinE_{Ng\text{-}R30D}$ stimulated high $MinD_{Ng}$ ATPase activities. In contrast, the presence of N-terminal mutants ($MinE_{Ng\text{-}A18D}$ and $MinE_{Ng\text{-}L22D}$) did not induce ATPase activity. In the presence of wild-type $MinE_{Ng}$, $MinD_{Ng\text{-}K16Q}$, a non-functional $MinD_{Ng}$ mutant, displayed basal activity as well. Among the C-terminal mutants, $MinE_{Ng\text{-}K53A}$ stimulated moderate levels of hydrolytic activity relative to wild-type $MinE_{Ng}$ stimulation, while $MinE_{Ng\text{-}E67L}$ was unable to stimulate basal $MinD_{Ng}$ ATPase activity. Parentheses indicate $MinE_{Ng}$ mutation. Error bars indicate ± 1 standard deviation. Assays were performed in duplicates.

studies (i.e. $MinE_{Ng\text{-}K53A}$ overexpression induced minicell phenotype, $MinE_{Ng\text{-}E67L}$ overexpression did not alter wild-type *E. coli* morphology); the malachite green assay determined that the $MinE_{Ng\text{-}K53A}$ mutant was able to cause $MinD_{Ng}$ to induce a moderate amount of ATP activity, while $MinE_{Ng\text{-}E67L}$ stimulated very little $MinD_{Ng}$ ATPase activity (Fig. 3.11). A control study of wild-type $MinE_{Ng}$ and $MinD_{Ng\text{-}K16Q}$ (expressed from pSC10, Table 3) revealed that $MinD_{Ng}$ was not stimulated as previously shown (Szeto *et al.*, 2005). This control experiment was performed to show the requirement of ATP for hydrolysis since $MinD_{Ng\text{-}K16Q}$ was unable to bind to ATP (Szeto *et al.*, 2005). In addition, $MinD_{Ng}$ ATPase activity was also not stimulated in the absence of $MinE_{Ng}$ protein (Fig. 3.11). Changing the ratio of MinE to MinD protein (1:2 to 5:1) did not affect the relative rates of ATPase activity (data not shown). These results suggested that $MinD_{Ng}$ ATPase stimulation was intricately linked to $MinD_{Ng}$ interaction to $MinE_{Ng}$. Studies of the E67L mutant suggested that adequate stimulation of $MinD_{Ng}$ ATPase activity did not occur if the interaction between $MinD_{Ng}$ and $MinE_{Ng}$ was not strong enough even though the weak interaction between the two proteins (2.42 ± 0.28 Miller units, Table 5) was sufficient to induce $MinD_{Ng}$ oscillation. In contrast, if binding was sufficient (e.g. $MinE_{Ng\text{-}K53A}$ interaction with $MinD_{Ng}$, 5.06 ± 0.58 Miller units, Table 5), then ATPase stimulation occurred. The major implication of these findings is that $MinD_{Ng}$ can oscillate regardless of ATPase stimulation by $MinE_{Ng}$.

3.12. $MinD_{Ng}$ dissociation from lipid vesicles is dependent on the concentration of $MinE_{Ng}$

Purified *E. coli* MinD can bind to artificially created phospholipid vesicles *in vitro* using sedimentation assays (Hu *et al.*, 2002;Lackner *et al.*, 2003;Mileykovskaya *et al.*, 2003). Previous studies showed that ATP-bound $MinD_{Ec}$ binds preferentially to anionic

phospholipids such as cardiolipin and phosphatidylglycerol (Mileykovskaya *et al.*, 2003). In addition, $MinD_{Ec}$ can be removed from the lipid vesicle by adding $MinE_{Ec}$ (Hu *et al.*, 2002). This study was conducted to determine if the amount of $MinD_{Ng}$ dissociation from artificial vesicles was specifically dependent on the concentration of $MinE_{Ng}$.

The creation of PG vesicles showed that a typical vesicle can range anywhere from 3-10 μm in diameter (Fig. 2.1). The stability of these vesicles usually lasted four months as determined by phase-contrast microscopy.

When these vesicles were incubated with $MinD_{Ng}$-His and ATP, the $MinD_{Ng}$-His protein was found to remain associated with the vesicles (Fig. 3.12, lanes 1 and 2). Many controls were used to ensure that $MinD_{Ng}$ binding required PG vesicles, ATP, and $MgCl_2$. $MinD_{Ng}$ was detected in the supernatant in reactions without PG vesicles (Fig. 3.12, lane 4). Without ATP, some $MinD_{Ng}$ protein was present in the soluble fractions as well (Fig. 3.12, lane 6). However, in the presence of $MinE_{Ng}$, more $MinD_{Ng}$ dissociated from the vesicles (Fig. 3.12, lanes 7 and 8) and was observed in the soluble fraction. This experiment showed that the gonococcal MinD and MinE proteins were involved with MinD binding and association to phospholipids.

Figure 3.13 showed that increasing concentrations of $MinE_{Ng}$ caused more $MinD_{Ng}$ to dissociate from the phospholipids as determined by spot densitometry (data not shown). However, this effect was only significant using $MinE_{Ng}$ concentrations from 0.1 to 0.5 mg/ml. $MinE_{Ng}$ concentrations higher than 0.5 mg/ml did not promote further $MinD_{Ng}$ disassociation from the PG vesicles (Fig. 3.13). As a control, lysozyme (14 kDa) was included to ensure $MinE_{Ng}$ specificity for $MinD_{Ng}$ release from the vesicles (Fig. 3.13). Thus, the amount of $MinD_{Ng}$ dissociation from lipid vesicles was dependent on the

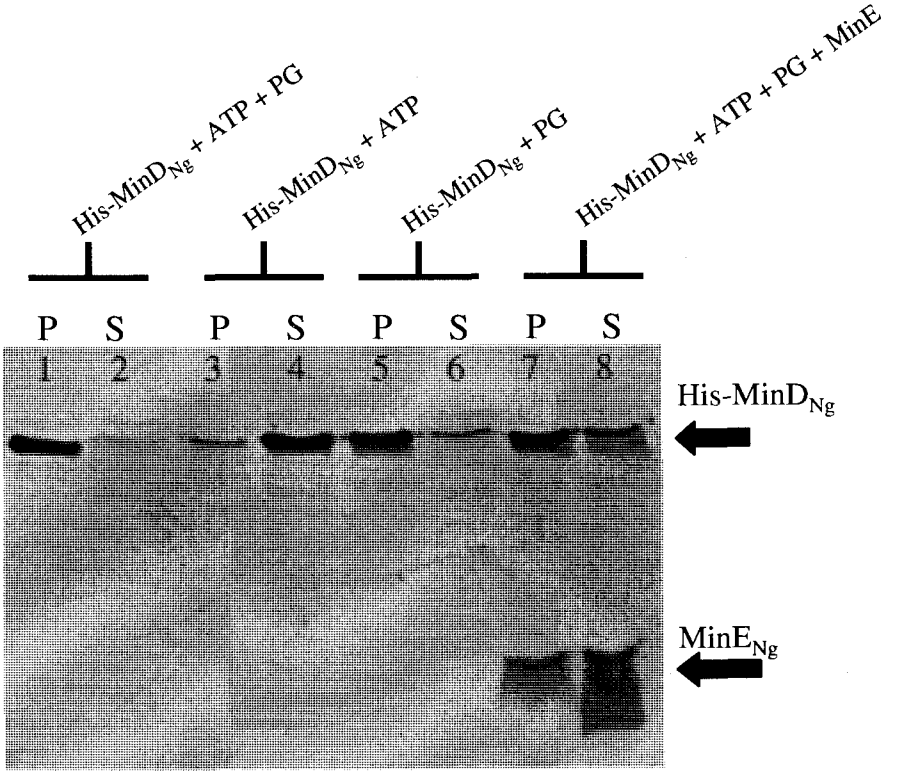

Figure 3.12. Vesicle binding assays. $MinD_{Ng}$ requires ATP and phosphatidylglycerol (PG) to bind to the vesicles when pelleted (P, lane 1), while little is found in the supernatant (S, lane 2). Without the vesicles, $MinD_{Ng}$ is primarily in the supernatant (lane 4), while in the presence of PG only, some $MinD_{Ng}$ did not pellet (lane 6) since ATP is believed to be required as well. With the addition of $MinE_{Ng}$, $MinD_{Ng}$ dissociates from the PG vesicles (lane 8). Assays were performed in duplicate. Image from Szeto, Ph.D. thesis, 2004. Work was done jointly with J. Szeto.

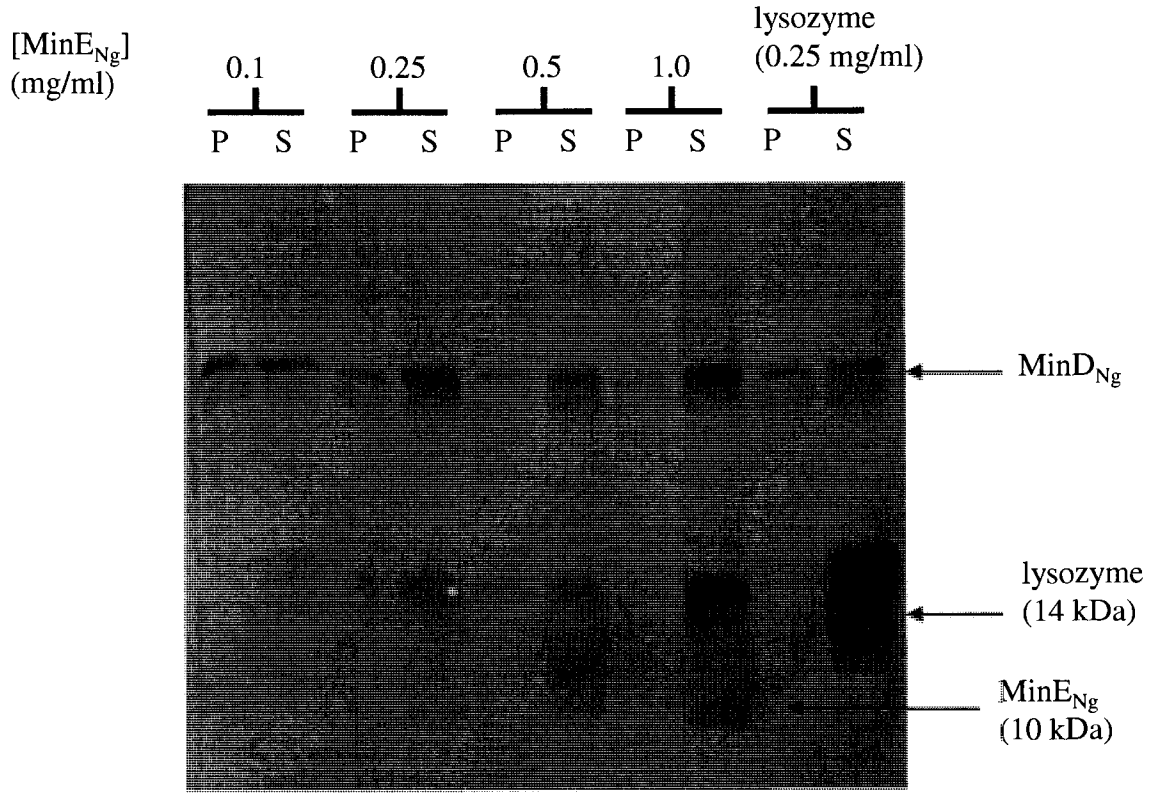

Figure 3.13. MinD$_{Ng}$ displacement from vesicles by increasing concentrations of MinE$_{Ng}$. Progressive increases in the concentration of MinE$_{Ng}$ from 0.1 to 0.5 mg/ml causes more MinD$_{Ng}$ to dissociate from the vesicles. At 1.0 mg/ml, there is no more MinD$_{Ng}$ dissociation. As a control, replacing lysozyme for MinE$_{Ng}$ did not increase the amount of MinD$_{Ng}$ dissociation, showing that the event is MinE$_{Ng}$ specific. Shown are the pelleted (P) and supernatant (S) fractions. This experiment was performed in duplicates.

concentration of $MinE_{Ng}$. This experiment also showed that $MinE_{Ng}$ specifically caused $MinD_{Ng}$ to dissociate from PG vesicles.

3.13. Gonococcal MinE ring/subcellular architecture formation is dependent on protein expression

Previous studies showed that, in the presence of $MinD_{Ec}$, $MinE_{Ec}$-GFP formed rings/zones that oscillate and were recruited to a coiled array (Ramirez-Arcos *et al.*, 2002;Shih *et al.*, 2002;Szeto *et al.*, 2005;Szeto *et al.*, 2004). I was interested to determine if $MinE_{Ng}$-GFP behaved similarly to $MinE_{Ec}$-GFP. From the co-expression of $MinD_{Ec}$ and $MinE_{Ec}$-GFP from pWM1079-H (Table 3) in *E. coli* PB114, I discovered that periods of $MinE_{Ec}$-GFP oscillation may be dependent on protein expression (Fig. 3.14). In the presence of 0.005% arabinose, $MinE_{Ec}$- GFP oscillation was 220 ± 30 s (Fig. 3.14 A, $MinE_{Ec}$ ring shown by arrow, n = 8). However, pole-to-pole movement of $MinE_{Ec}$-GFP appeared to take nearly 480 s (Fig. 3.14 B) in the presence of 0.1% arabinose. These results suggested that protein overexpression may decrease the periodicity of $MinE_{Ec}$-GFP oscillation.

By contrast, the localization of $MinE_{Ng}$-GFP was primarily cytoplasmic in many conditions tested when pSRE-GFP (*$minD_{Ng}$::$minE_{Ng}$-gfp*, Table 3) was transformed into *E. coli* PB114. At 4.5 hours after incubation with arabinose, there was no evidence of $MinE_{Ng}$-GFP ring formation or oscillation, regardless of the concentration of arabinose tested from 0.005 – 0.2% (Fig. 3.15 A). Localization of $MinE_{Ng}$-GFP in these cells was cytoplasmic in all cases. However, from the same samples 2.5 h later (i.e. at 7 h), $MinE_{Ng}$-GFP localization varied depending on the concentration of arabinose. In the presence of 0.005% and 0.01% arabinose, $MinE_{Ng}$-GFP fluorescence remained cytoplasmic (Fig. 3.15 B). However, with 0.05% and 0.1% arabinose, $MinE_{Ng}$-GFP was no longer cytoplasmic; instead, there was

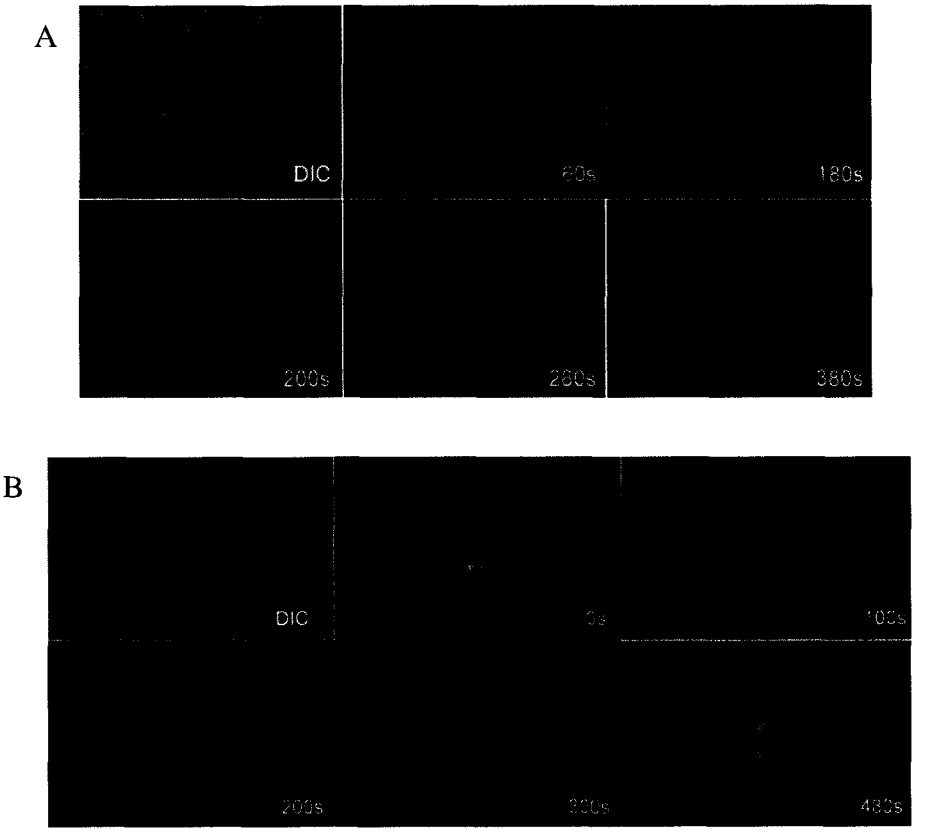

Figure 3.14. Oscillation of $MinE_{Ec}$-GFP is affected by levels of protein expression. In the presence of 0.005% arabinose, $MinE_{Ec}$-GFP oscillation takes approximately 220 ± 30 s for one period (A). This period is nearly doubled to about 480 s (B) in the presence of 0.1 % arabinose. $MinE_{Ec}$ rings are indicated by the arrows.

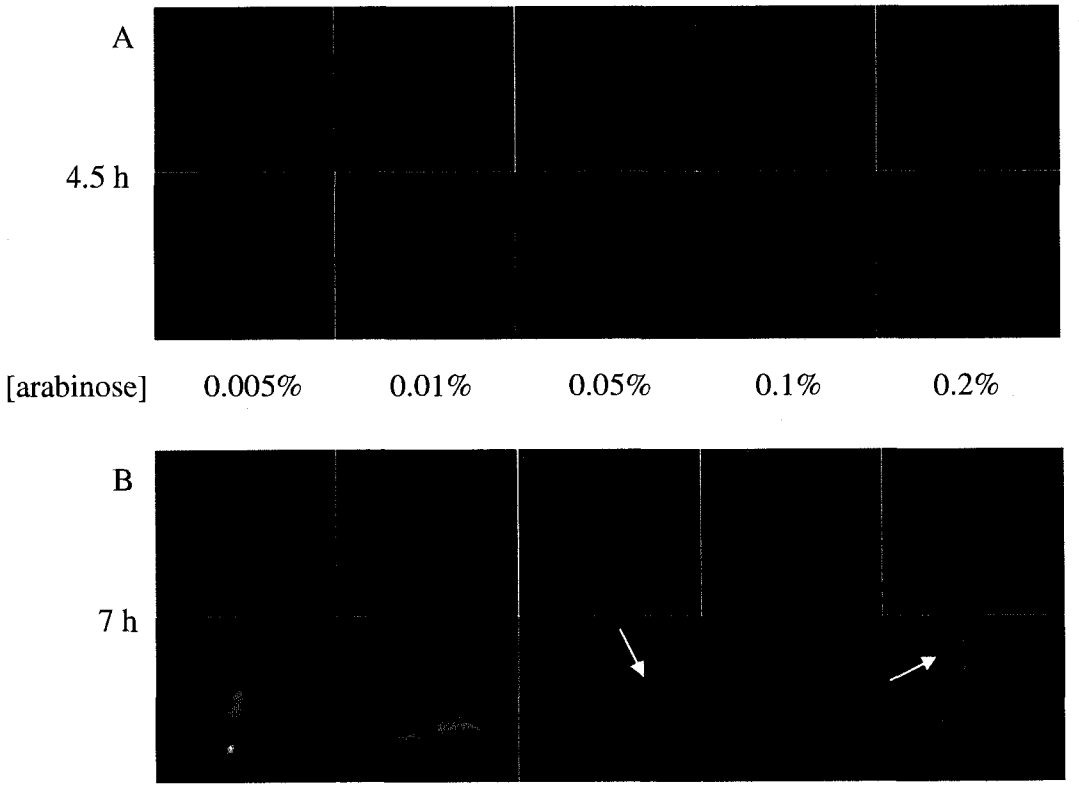

Figure 3.15. Formation of $MinE_{Ng}$-GFP rings and/or subcellular architecture is dependent on levels of arabinose induction and incubation. After 4.5 h of incubation with arabinose, $MinE_{Ng}$-GFP did not form rings. Instead, $MinE_{Ng}$-GFP localization was entirely cytoplasmic at the arabinose concentrations tested (A). However, after 7 h with the same samples, $MinE_{Ng}$-GFP rings and the presence of a helical array were clearly visualized in deconvolved images in the presence of 0.2% arabinose (B). Twenty cells were examined for each sample. Arrows indicate $MinE_{Ng}$-GFP rings.

random localization of the GFP fusion protein with some evidence of $MinE_{Ng}$-GFP rings (Fig. 3.15 B). At 0.2% arabinose, $MinE_{Ng}$-GFP rings were clearly visible in some cells showing $MinE_{Ng}$-GFP localization to a helical subcellular architecture (Fig. 3.15 B). Interestingly, at 7 h, cells induced with 0.05% to 0.2% arabinose, despite the presence of $MinE_{Ng}$ rings, there was no evidence of oscillation (data not shown). As a result, formation of $MinE_{Ng}$-GFP rings and/or subcellular architecture occurred at higher levels of arabinose induction than *E. coli*. The amount of incubation time with arabinose was also a factor in visualizing $MinE_{Ng}$ superstructures.

3.14. Self-interaction is observed in $MinE_{Ng}$

The self-interaction of wild-type $MinE_{Ng}$-His was confirmed by sedimentation equilibrium analysis. The data points from three different loading concentrations (1.53, 1.02 and 0.77 mg/ml) of $MinE_{Ng}$-His, depicted both the concentration and migration of the protein, and matched well with the theoretical fit lines of a dimer (Fig. 3.16 A-C, lower panels). Further analysis showed that these data points had little deviation from their respective theoretical fit lines (Fig. 3.16 A-C, upper panels). The protein was shown to have an average apparent molecular weight of 25,652 Da, supporting a dimer-tetramer-hexamer model. This value represented approximately twice the theoretical molecular weight of a monomer of $MinE_{Ng}$-6XHis: 11 kDa (http://ca.expasy.org/tools/pi_tool.html), indicating that the predominant species of $MinE_{Ng}$ was dimeric. Size-exclusion chromatography also confirmed that $MinE_{Ng}$ was dimeric since a single absorbance peak was seen at 322-323 ml (Fig. 3.17). Another peak was eluted at around 158 ml. When compared to protein standards, this peak corresponded to Blue Dextran, a 2000 kDa carbohydrate. I considered the 158 ml peak as aggregated protein (data not shown). The approximate size of MinE based on a

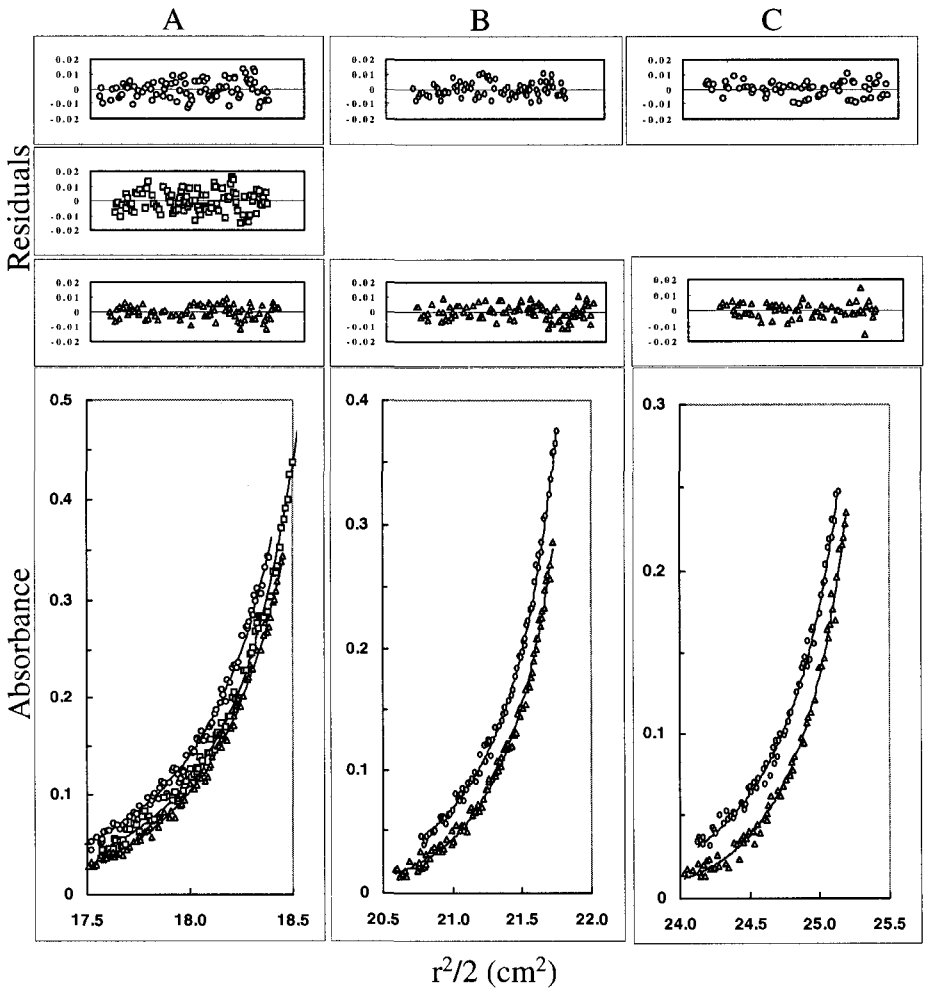

Figure 3.16. Sedimentation equilibrium analysis of wild-type $MinE_{Ng}$. Protein was dissolved in 50 mM Tris, 50 mM NaCl, 1 mM EDTA, pH 7.4 and centrifuged at 26,000 rpm (circles), 28,000 rpm; (squares) and 30,000 rpm (triangles) at 4°C. The protein concentrations used were 1.53, 1.02 and 0.77 mg/ml for Sectors A, B and C, respectively. Lower panels: $r^2/2$ versus absorbance plots. Symbols represent measured data points, and solid lines represent the fit to a dimer-tetramer-hexamer model. Upper panels: Residuals obtained from fitting the measured data points to a two-species model. Two sets of data at 28000 rpm at 1.02 mg/ml were too noisy and thus were not included. The random, nonsystematic distribution of the residuals indicates a good fit of the data to the models.

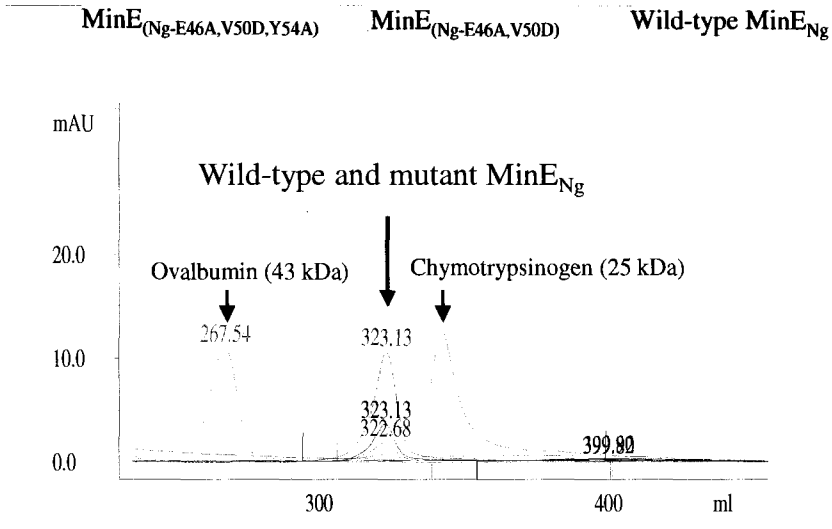

Figure 3.17. Determining the molecular weight of mutant $MinE_{Ng}$ by size-exclusion chromatography. Protein standards, chymotrypsinogen (25 kDa) and ovalbumin (43 kDa) were analyzed by size-exclusion chromatography using the same column and shown relative to the $MinE_{Ng}$ samples. Approximate size of $MinE_{Ng}$ based on a comparison of its elution volume with that of the molecular weight standards is 30 kDa. Experiments were performed in duplicate.

comparison of its elution volume with that of the molecular weight standards was about 30 kDa Although this size is larger than an estimated dimer size (nearly a trimer), the difference reflects the likelihood that differences in shape, in addition to molecular weight, affected the mobility of samples running through a gel filtration column. As such, these physical methods indicated that $MinE_{Ng}$ self-interacts and that a dimer is the predominant molecule.

$MinE_{Ng}$ self-interaction was also demonstrated using bacterial two-hybrid (B2H) assays. The yeast two-hybrid system (Clontech) was initially used to test for $MinE_{Ng}$ self-interaction, but the assay was unable to detect $MinE_{Ng}$-$MinE_{Ng}$ interaction, possibly because of unstable yeast fusion proteins. However, B2H studies, performed in triplicate, revealed low levels of β-galactosidase activity (Fig. 3.18), indicative of interaction; in this system, repressed β-galactosidase activity only occurs if there is an interaction between the two proteins. As such, the above methods showed that gonococcal MinE dimerizes and exhibits self-interaction.

3.15. Elucidating $MinE_{Ng}$ domains of self-interaction

My previous work showed that certain mutations in $MinE_{Ng}$, $MinE_{Ng\text{-}A18D}$, $MinE_{Ng\text{-}L22D}$, $MinE_{Ng\text{-}K53A}$, and $MinE_{Ng\text{-}E67L}$ disrupted $MinD_{Ng}$/$MinE_{Ng}$ interaction (Table 5). In order to determine whether the loss of interaction with $MinD_{Ng}$ resulted from perturbed MinE-MinE interaction, A18D, L22D, R30D, K53A, and E67L $MinE_{Ng}$ mutations were introduced into bacterial two-hybrid plasmids and examined for self-interaction. The negative controls were performed by assaying 1) untransformed *E. coli* R721 and 2) testing interaction between $MinE_{Ng}$ and $FtsZ_{Ec}$. Using the bacterial two-hybrid system, both cases

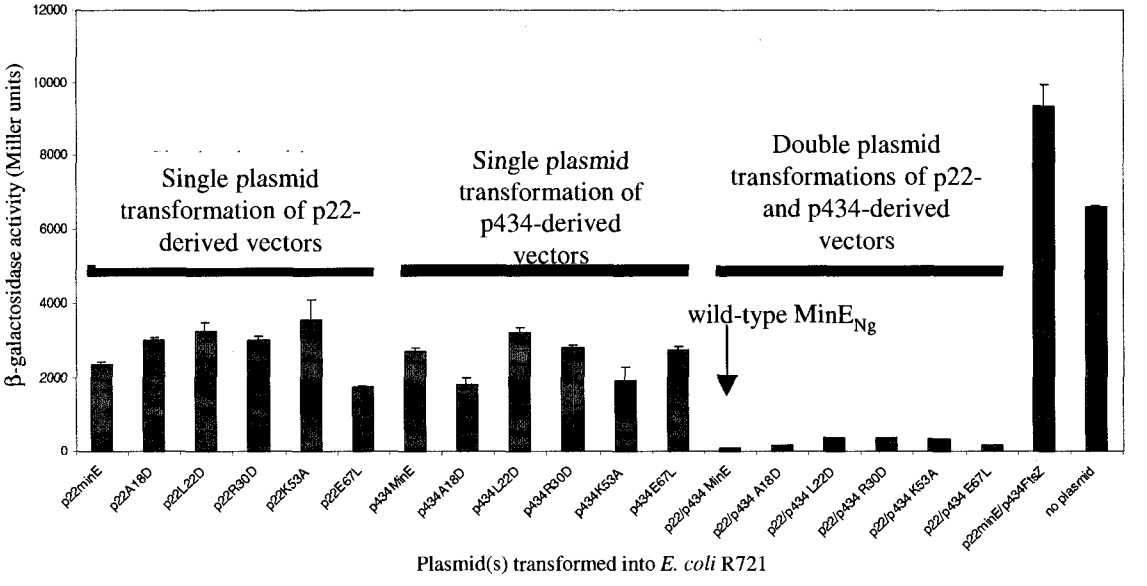

Figure 3.18. Bacterial two-hybrid analyses of mutant MinE$_{Ng}$. The ability of MinE$_{Ng}$ (arrows) to interact with itself, allowed a heterodimeric p22/434 repressor to suppress *lacZ* expression, thus causing low β-galactosidase activities. The A18D, L22D, R30D, K53A, and E67L MinE$_{Ng}$ mutants also displayed low β-galactosidase activity, indicating that the ability of MinE$_{Ng}$ to interact with itself was retained. Single plasmid transformations of *E. coli* R721 were used as controls to show that there were no false positives. Cells expressing MinE$_{Ng}$/FtsZ$_{Ec}$ and no plasmid transformation were also controls. Assays were done in triplicates with error bars indicating ± 1 standard deviation.

resulted in high β-galactosidase activities (~6000 to 10000 Miller units), which indicated that there was no *lacZ* repression; thus, no interaction was observed (Fig. 3.18). Each $MinE_{Ng}$ mutation in each bacterial two-hybrid plasmid was then singly transformed into *E. coli* R721 to determine if the repressor from a single plasmid (either p22 or p434-derivatives) was able to repress *lacZ*. The assay showed similar β-galactosidase activities (approximately 3000 Miller units) relative to the negative controls, indicating that a homodimeric repressor from each plasmid did not prevent *lacZ* expression (Fig. 3.18). However, when wild-type $MinE_{Ng}$ self-interaction was tested by co-transforming p22minE and p434minE into *E. coli* R721, there was only a trace amount of β-galactosidase activity (110 ± 2.2 Miller units, Fig. 3.18), indicating the presence of $MinE_{Ng}$ self-interaction. When each of the five mutations listed above were examined using the same approach, each mutant also exhibited low β-galactosidase activity, indicating that $MinE_{Ng}$ self-association was not disrupted.

Further evidence that the A18D, L22D, R30D, K53A, and E67L $MinE_{Ng}$ mutants self-associated regardless of $MinD_{Ng}$ interaction was obtained by analytical ultracentrifugation experiments. (Fig. 3.19 shows representative K53A mutant). For $MinE_{Ng\text{-}K53A}$, the data points from three different loading concentrations (1.03, 0.68 and 0.51 mg/ml) of the protein, corresponded well to the theoretical fit lines of a dimer (Fig. 3.19 A-C, lower panels). Also, there was little variation from their respective theoretical fit lines (Fig. 3.19 A-C, upper panels). $MinE_{Ng\text{-}K53A}$ was shown to have an average apparent molecular weight of 24,957 Da, supporting a model of a dimer-tetramer-hexamer model, similar to the findings of wild-type $MinE_{Ng}$ (Table 6). The A18D, L22D, R30D, and E67L $MinE_{Ng}$ mutants also

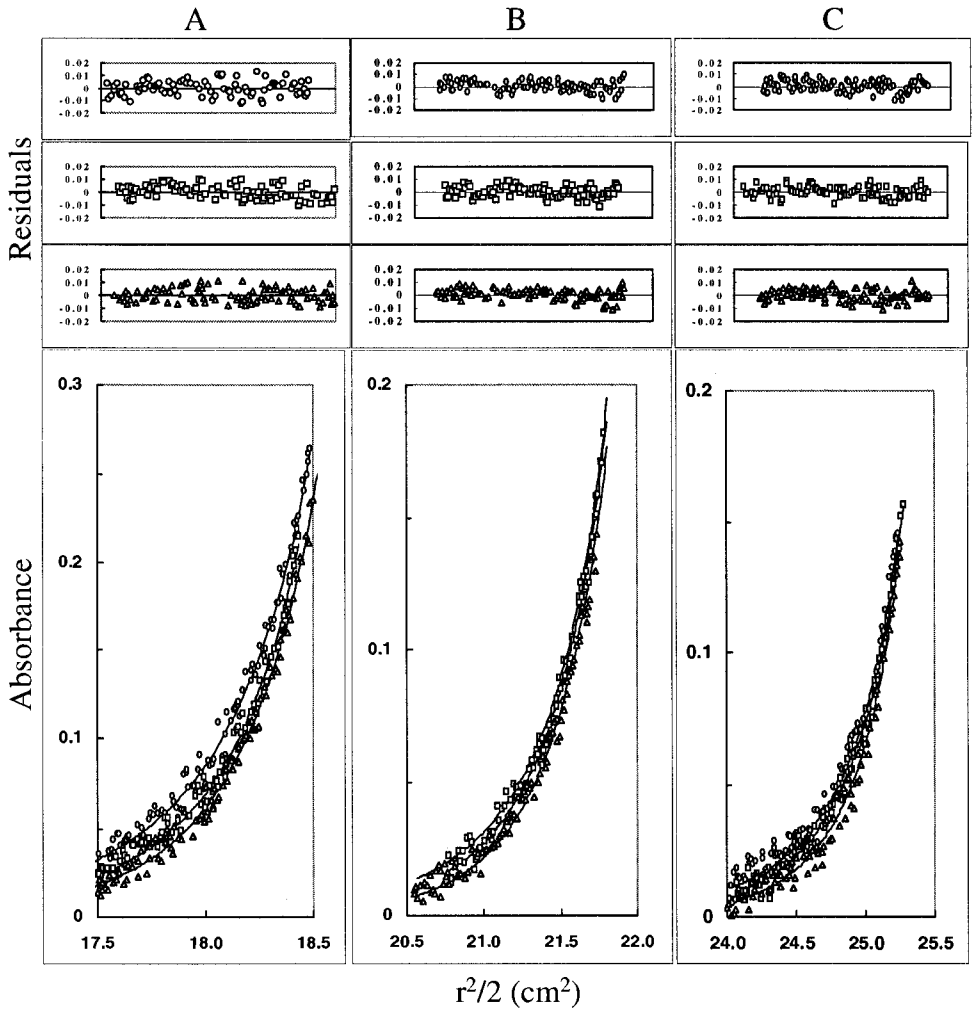

Figure 3.19. Sedimentation equilibrium analysis of $MinE_{Ng\text{-}K53A}$. Protein was dissolved in 50 mM Tris, 50 mM NaCl, 1 mM EDTA, pH 7.4 and centrifuged at 26,000 rpm (circles), 28,000 rpm; (squares) and 30,000 rpm (triangles) at 4°C. The protein concentrations used were 1.03, 0.68 and 0.51 mg/ml for Sectors A, B and C, respectively. Lower panels: $r^2/2$ versus absorbance plots. Symbols represent measured data points, and solid lines represent the fit to a dimer-tetramer-hexamer model. Upper panels: Residuals obtained from fitting the measured data points to a two-species model. The random, nonsystematic distribution of the residuals indicates a good fit of the data to the models.

Table 6. Apparent molecular weights of wild-type and mutant $MinE_{Ng}$ by analytical ultracentrifugation

$MinE_{Ng}$ Protein	**Apparent MW (Da)**	**Best Model Fit**
WT $MinE_{Ng}$	25 652	Dimer-Tetramer-Hexamer
$MinE_{Ng\text{-}A18D}$	21 522	ND
$MinE_{Ng\text{-}L22D}$	24 435	ND
$MinE_{Ng\text{-}R30D}$	23 807	Dimer-Tetramer-Hexamer
$MinE_{Ng\text{-}K53A}$	24 987	Dimer-Tetramer-Hexamer
$MinE_{Ng\text{-}E67L}$	33 470	Dimer-Tetramer-Hexamer

ND – not determined

had similar sedimentation profiles (Table 6). Clearly, $MinE_{Ng}$ self-interaction was not perturbed in these mutants.

NMR studies suggested that domains responsible for $MinE_{Ec}$ self-association (and thus, ring formation) included the C-terminal α-helix (aa 38-53, Fig 3.20 B) and/or β-sheets (aa 72-81, Fig. 3.20 C) (King *et al.*, 2000;King *et al.*, 1999). Two amino acids in $MinE_{Ec}$, D45, and V49, which lie on one face of the alpha helix, were proposed to interact with another MinE molecule (King *et al.*, 2000). D45A and V49A mutants in $MinE_{Ec}$ caused the ability to form MinE rings to be greatly reduced (Shih *et al.*, 2002); in addition, these mutants did not rescue minicell phenotyping in a Δ*min E. coli* background (King *et al.*, 2000). However, both mutants remained dimeric (King *et al.*, 2000). However, such observations do not explain whether a monomer of MinE could remain functional. As a result, using the available *E. coli* MinE model (Fig. 3.20 A), I attempted to abolish $MinE_{Ng}$ self-interaction by individually deleting the α-helix (Fig. 3.20 B) and the β-sheet (Fig. 3.20 C) secondary structures, or by substituting the $MinE_{Ng}$ residues that were equivalent to *E. coli* MinE D45, V49, and Y53 (Fig. 3.20 B, red boxes) with proline, which is known to disrupt α-helical structures. The equivalent gonococcal $MinE_{Ng}$ residues were determined by comparing the $MinE_{Ng}$ amino acid sequence with that of $MinE_{Ec}$ (Fig. 3.20 D). This comparison revealed that the predicted α-helix of $MinE_{Ng}$ resides between aa 39-54, while the β-sheet comprises aa 74-78 (Fig. 3.20 D); the triple proline substitution involved residues E46, V50, and Y54 (Fig. 3.20 D). Using NNPREDICT (http://alexander.compbio.ucsf.edu/~nomi/nnpredict.html) software, the α-helix and β-sheet secondary structures were predicted to be abolished (Fig. 3.21). Compared to wild-type $MinE_{Ng}$ (Fig. 3.21 A), NNPREDICT showed that the deletion of aa 39-54 was predicted to

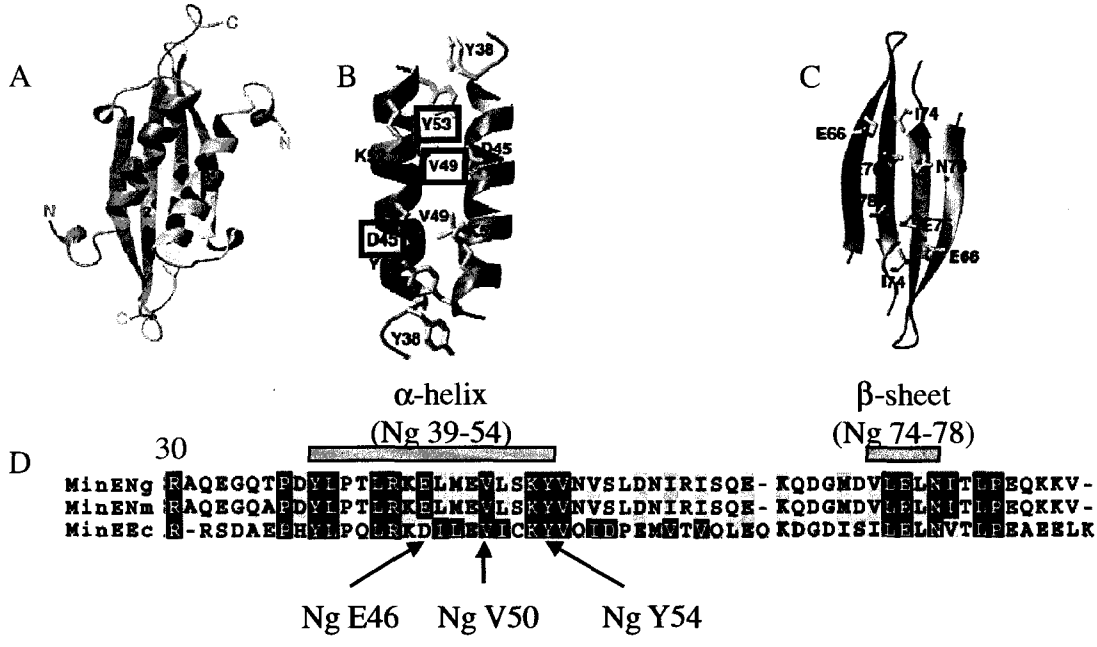

Figure 3.20. NMR structure of the C-terminus of *E. coli* MinE to identify potential domains of gonococcal MinE self-interaction. The structure of the C-terminus (aa 31-88) of *E. coli* MinE (A) (NMR structure from King *et al.*, 2000) provides a visual picture where MinE self-interaction occurs. Since *E. coli* and *N. gonorrhoeae* MinE have similar structures (Ramos *et al.*, 2006), this model can be used to predict domains of gonococcal MinE self-interaction from an amino acid sequence alignment between interacting α-helices (B) and interacting β-sheets (C). As such, mutations to disrupt $MinE_{Ng}$ self-interaction include the deletion of those secondary structures, including a triple proline mutation to the $MinE_{Ng}$ residues that are equivalent to D45, V49, and Y53 (B, red boxes), which were thought to be physically interacting with the α-helix of another $MinE_{Ec}$ molecule. An alignment of $MinE_{Ng}$ and $MinE_{Ec}$ sequences show the corresponding residues in $MinE_{Ng}$ to mutate (D).

A Wild-type $MinE_{Ng}$: * * *

MSLIELLFGRKQKTATVARDRLQIIIAQERAQEGQTPDYLPTLRKELMEVLSKYVNVSLD
NIRISQEKQDGMDVLELNITLPEQKKV

Secondary structure prediction:

--HHHHHHH-------HHH---EEEEHHH--------------HHHHHHHHHHHEE----
------------HHEE----------

B $MinE_{Ng}$: deletion of aa 39-54

MSLIELLFGRKQKTATVARDRLQIIIAQERAQEGQTPD/VNVSLDNIRISQEKQDGMDVLE
LNITLPEQKKV

Secondary structure prediction:

--HHHHHHH-------HHH---EEEEHHH----------------------------HHE
E----------

C $MinE_{Ng}$: deletion of aa 74-78

MSLIELLFGRKQKTATVARDRLQIIIAQERAQEGQTPDYLPTLRKELMEVLSKYVNVSLD
NIRISQEKQDGMD/ITLPEQKKV

Secondary structure prediction:

--HHHHHHH-------HHH---EEEEHHH--------------HHHHHHHHHHHEE----

D $MinE_{Ng}$: E46P, Y50P, Y54P mutation

MSLIELLFGRKQKTATVARDRLQIIIAQERAQEGQTPDYLPTLRKPLMEPLSKPVNVSLD
NIRISQEKQDGMDVLELNITLPEQKKV

Secondary structure prediction:

--HHHHHHH-------HHH---EEEEHHH------------------------------
------------HHEE----------

Figure 3.21. Using NNPREDICT to predict that mutations disrupt secondary structure of $MinE_{Ng}$. Green lettered resides of wild-type $MinE_{Ng}$ sequence (A) belong to α-helix (aa 39-54), while red lettered residues are the β-sheet residues. The asterisk marks the residues that mutated to proline. The slashes in B and C represent the deleted regions when aa 39-54 (B) and 74-78 (C) were removed. The blue residues are the asterisked residues from (A) that were mutated to proline (D). NNPREDICT (prediction below each mutant) revealed that all three $MinE_{Ng}$ mutations (B-D) were predicted to remove the secondary structures. H = predicted helical residues, E = predicted strand residues, hyphen shows no dominant secondary structural predicted.

remove the α-helix (Fig. 3.21 B, slash shows deletion of green residues from Fig. 3.21A), while the deletion of aa 74-78 removed the β- sheet (Fig. 3.21 C, slash shows deletion of red residues from 3.21 A). Finally, introducing proline to E46, V50 and Y54 also abolished the α-helix (Fig. 3.21 D, blue residues).

The $MinE_{Ng}$ mutant proteins that putatively abolished self-interaction were then incorporated into bacterial two-hybrid plasmid vectors to test for mutant $MinE_{Ng}$ self-interaction. When *E. coli* R721 was expressing heterodimeric repressors from both p22 and p434-derived plasmids for each of the three $MinE_{Ng}$ mutations (Δ39-54, Δ74-78, and E46P,V50P,Y54P), bacterial two-hybrid assays showed that the three mutations caused β-galactosidase activities to be similar to values seen when each bacterial two-hybrid plasmid was transformed singly into *E. coli* R721 (Fig. 3.22 A). Since *lacZ* repression did not occur with these $MinE_{Ng}$ mutants, compared to wild-type $MinE_{Ng}$, these results revealed that $MinE_{Ng}$ self-association was disrupted (Fig. 3.22 A), suggesting that both the α-helix and the β-sheet in the C-terminus of $MinE_{Ng}$ were involved with self-interaction. Western blotting showed the presence of wild-type and mutant $MinE_{Ng}$ fusions to the P22 and 434 repressors (Fig. 3.22 B), indicating that the lack of *lacZ* repression was not a result of the repressors themselves being insoluble.

3.16. Confirming the disruption of $MinE_{Ng}$ self-interaction

After $MinE_{Ng}$ domains of self-interaction were identified, I introduced the three $MinE_{Ng}$ mutations (Δ39-54, Δ74-78, and E46P,V50P,Y54P) in pEC1 for protein purification, in order to determine their molecular weights by analytical ultracentrifugation and size-exclusion chromatography. Unfortunately, protein purification using His-tagged nickel

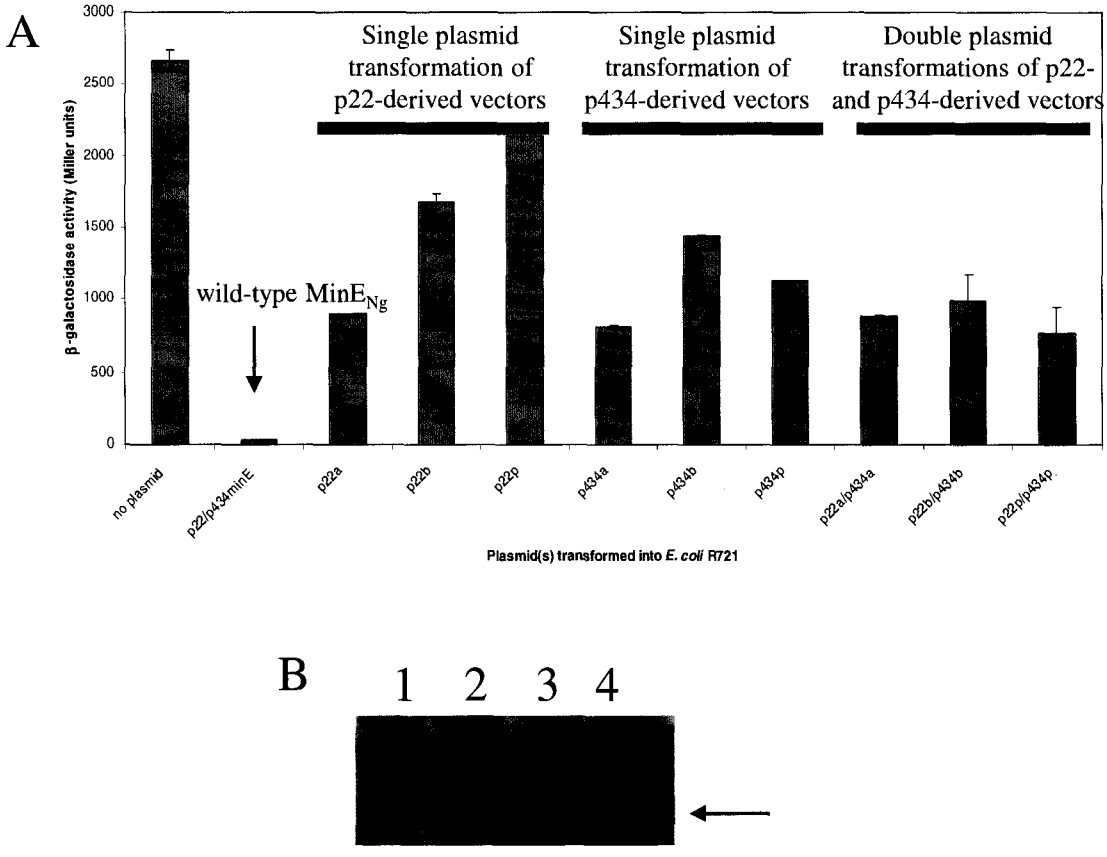

Figure 3.22. Bacterial two-hybrid assays examining how mutations disrupted MinE$_{Ng}$ self interaction. (A) Mutating the α-helix and β-sheet may have disrupted MinE$_{Ng}$ self-interaction. Wild-type MinE$_{Ng}$-MinE$_{Ng}$ self-interaction is indicated by the arrow. (B) Western blot detecting MinE$_{Ng}$ fused to the p22 and 434 repressors. Lane 1: *E. coli* R721 soluble extract. Lane 2: Soluble extract of *E. coli* R721 expressing the P22-MinE$_{Ng}$ and 434-MinE$_{Ng}$ repressors. Lane 3: Soluble extract of *E. coli* R721 expressing the P22-MinE$_{Ng(\Delta 39\text{-}54)}$ and 434-MinE$_{Ng(\Delta 39\text{-}54)}$ repressors. Lane 4: Soluble extract of *E. coli* R721 expressing the P22-MinE$_{Ng(\Delta 74\text{-}78)}$ and 434-MinE$_{Ng(\Delta 74\text{-}78)}$ repressors. Arrow indicates MinE-fusion repressors. Above band is non-specific binding to serve as a loading control. Assays were done in triplicate with average β-galactosidase activity expressed in Miller units ± 1 standard deviation.

column chromatography was not successful in purifying enough soluble protein for analysis (data not shown), despite protein clearly being present in SDS-PAGE gels (Fig. 3.23 shows expression of $MinE_{Ng(\Delta 39\text{-}54)}$). Most likely, introducing three prolines and deleting domains of MinE may also have reduced the solubility of $MinE_{Ng}$. This may lead to the protein being insoluble, as determined by prediction software (http://www.biotech.ou.edu/). This was also shown by protein purification where samples during each purification step showed no visible $MinE_{Ng}$ bands (data not shown). Even the use of 8M urea was not sufficient to solubilize the $MinE_{Ng}$ mutants (data not shown).

As a result, less extreme mutations were generated in an attempt to produce soluble monomeric MinE. Two additional $MinE_{Ng}$ mutants, a double E46A, V50D mutation, and a triple E46A, V50D, Y54A mutation were constructed. Protein purification using nickel column chromatography was successful; however, size-exclusion chromatography revealed that the double and triple $MinE_{Ng}$ mutations did not disrupt self-interaction (Fig. 3.17 A). One peak from both mutants was eluted at 322-323 ml, the same elution peak as wild-type $MinE_{Ng}$. Using chymotrypsinogen (25 kDa) and ovalbumin (43 kDa) as standard controls, the size of $MinE_{Ng}$ based on a comparison of its elution volume to the molecular weight standards was estimated to be about 30 kDa, which most likely represented a dimeric species for both mutants. Another peak was seen at 155-158 ml; however, this peak also corresponded to the 2000 kDa standard as with the other peak seen for wild-type $MinE_{Ng}$ and thus, was likely a peak representing protein aggregation (data not shown). These experiments, performed in duplicate, showed that disrupting $MinE_{Ng}$ self-interaction might have increased the probability of protein insolubility.

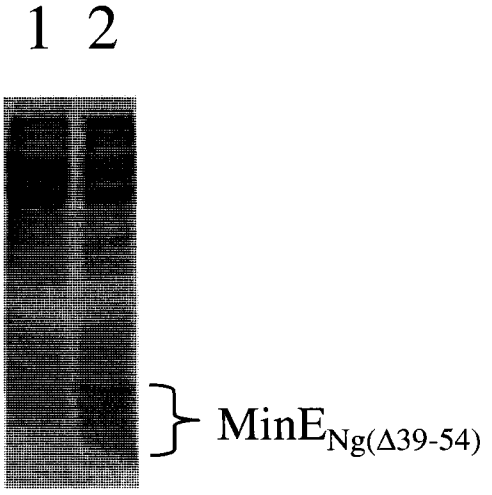

Figure 3.23. Expression of His-tagged MinE$_{Ng(\Delta 39\text{-}54)}$. Despite the inability to purify this mutant, SDS-PAGE of *E. coli* cell lysates show the induction of mutant overexpression with IPTG. Lane 1: *E. coli* C41 cell lysate. Lane 2: *E. coli* C41 transformed with pECa, expressing MinE$_{Ng(\Delta 39\text{-}54)}$.

3.17. Biological implications of disrupted $MinE_{Ng}$-$MinE_{Ng}$ interaction on oscillation of GFP-$MinD_{Ng}$

Bacterial two-hybrid assays suggested that the self-interaction of $MinE_{Ng(\Delta 39\text{-}54)}$, $MinE_{Ng(\Delta 74\text{-}78)}$, and $MinE_{Ng\text{-}E46P,V50P,Y54P}$ was disrupted. Therefore, the effects of these mutants on $MinD_{Ng}$ oscillation were evaluated. Fluorescence microscopy revealed that wild-type GFP-$MinD_{Ng}$ localization in *E. coli* PB114 cells transformed with pSRNE1 ($MinE_{Ng(\Delta 39\text{-}54)}$) was predominantly membrane-localized with slightly more fluorescence at the cell poles (Fig. 3.24 B) in 61.6% of 159 cells counted, contrasting findings with GFP-$MinD_{Ng}$ in the presence of wild-type $MinE_{Ng}$ (pSR15, Table 3, Fig. 3.8). Within this population of cells, there was also no evidence of subcellular architecture, although some cells revealed discontinuous distribution of GFP-$MinD_{Ng}$ localization (Fig. 3.24 B, white arrow). The remainder of the cells examined showed sporadic GFP-$MinD_{Ng}$ fluorescence throughout the cytoplasm. $MinD_{Ng}$ localization to subcellular architecture was observed in this smaller population (Fig. 3.24 B, yellow arrow). Regardless of the presence of subcellular architecture, $MinD_{Ng}$ did not oscillate.

Similar observations were noted in *E. coli* PB114 cells co-expressing GFP-$MinD_{Ng}$ and $MinE_{Ng(\Delta 74\text{-}78)}$. The majority (82-88%) of cells (n = 209) did not demonstrate $MinD_{Ng}$ oscillation. In this population of cells, there were primarily three patterns of $MinD_{Ng}$ localization; about 77% of cells showed $MinD_{Ng}$ membrane localization (Fig. 3.25 B'). 14% of the cells had the GFP-$MinD_{Ng}$ signal dispersed throughout the cytoplasm (Fig. 3.25 C'), and a few cells (~9%) showed possible recruitment of $MinD_{Ng}$ to subcellular architecture (Fig. 3.25 D'). However, unlike $MinE_{Ng(\Delta 39\text{-}54)}$, $MinE_{Ng(\Delta 74\text{-}78)}$ induced very slow pole-to-pole

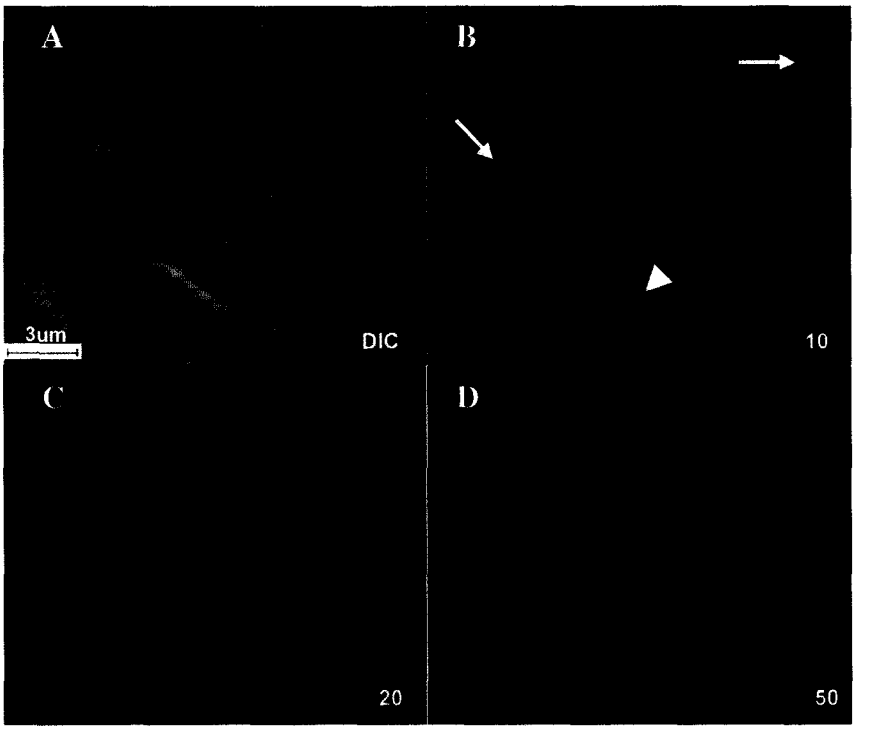

Figure 3.24. Localization of GFP-MinD$_{Ng}$ in the presence of MinE$_{Ng(\Delta 39\text{-}54)}$ in *E. coli* PB114 cells. Co-expression of GFP-MinD$_{Ng}$ and MinE$_{Ng(\Delta 39\text{-}54)}$ showed that the majority of fluorescence is localized to the cell membrane. A few cells show some brighter spots of fluorescence at the cell poles, but this may be contributed to inclusion bodies. Instead of pole-to-pole oscillation, GFP signals were detected throughout the length of the cells. From a sample size of 159 cells, for some cells (arrows in B) (61.6%) GFP was seen highlighted around cell membrane. In contrast, some cells (arrowhead in B) (38.4%) displayed dispersed GFP within the cytoplasm. No typical pole-to-pole oscillation was observed within these cells. Images B, C, D were taken at 10s, 20s and 50s, respectively.

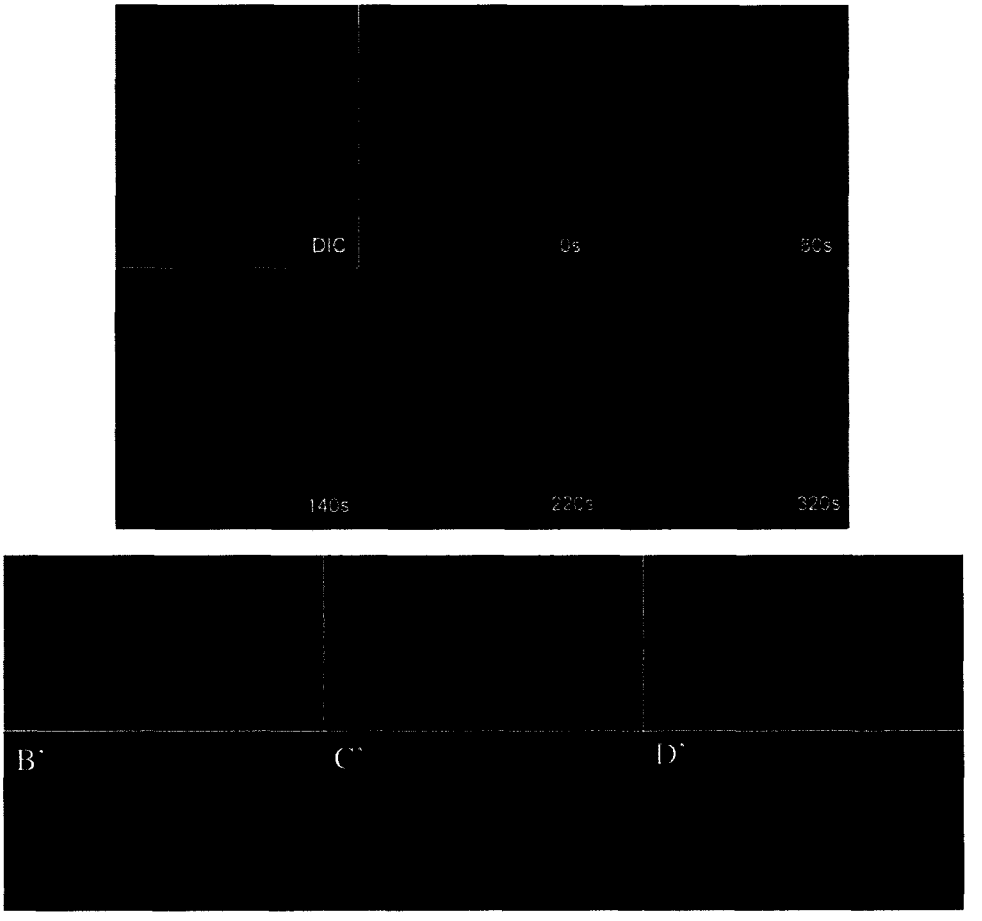

Figure 3.25. Localization of GFP-MinD$_{Ng}$ in the presence of MinE$_{Ng(\Delta 74\text{-}78)}$ in *E. coli* PB114 cells. In these studies, 209 cells were examined. In 12-18% of cells (A), slow pole-to-pole movement was observed, the time for completing one oscillation cycle was much longer than that of GFP-MinD$_{Ng}$ in wild type MinE$_{Ng}$ background. The average time to complete one cycle was increased approximately 10-fold to 300±40s (n = 10). In cells that did not display oscillation, most cells show MinD$_{Ng}$ membrane localization (B') whereas some cells revealed cytoplasmic fluorescence throughout the bacterium (C'). Interestingly, a third pattern was seen in a small population of cells where the fluorescence appeared to possibly localize to subcellular architecture (D'). Image B, C and D are DIC panels of corresponding fluorescence panels B', C' and D'.

movement of GFP-$MinD_{Ng}$ (300 ± 40s) in 10 of the 209 cells examined (Fig. 3.25A shows a cell displaying $MinD_{Ng}$ movement from one end of the cell to other and back in approximately 320 s). Regardless of whether $MinD_{Ng}$ oscillation was observed, the loss of $MinE_{Ng}$ self-interaction clearly altered the ability of $MinD_{Ng}$ to oscillate from pole-to-pole.

Surprisingly, I found that overexpression of $MinE_{Ng(\Delta 74\text{-}78)}$ caused *E. coli* PB114 cells to become more filamentous (Fig. 3.26). More than 100 *E. coli* cells co-expressing GFP-$MinD_{Ng}$ and either wild-type $MinE_{Ng}$, $MinE_{Ng(\Delta 39\text{-}54)}$ or $MinE_{Ng(\Delta 74\text{-}78)}$ were evaluated (n =113, 110, and 114 respectively). *E. coli* cells (except minicells) with a length smaller than 4 μm were considered as being normal, while cells with length from 4-15 μm were grouped as short filaments. Cells longer than 15 μm were grouped as being long filaments. Approximately 80% of *E. coli* cells expressing wild-type $MinE_{Ng}$ and $MinE_{Ng(\Delta 39\text{-}54)}$ were shorter than 4 μm, while the rest of the populations were reported as short filaments under the reported culture conditions. By comparison, 40% of cells expressing $MinE_{Ng(\Delta 74\text{-}78)}$ were of normal length, while 20% of cells were considered long filaments (Fig. 3.26).

3.18. $MinE_{Ng}$ self-interaction is a prerequisite of $MinD_{Ng}$/$MinE_{Ng}$ interaction

The failure of $MinD_{Ng}$ to oscillate in the presence of $MinE_{Ng(\Delta 39\text{-}54)}$ and $MinE_{Ng(\Delta 74\text{-}78)}$ might be attributed to disrupted $MinD_{Ng}$/$MinE_{Ng}$ interaction. Therefore, the interaction between $MinD_{Ng}$ and either $MinE_{Ng(\Delta 39\text{-}54)}$, $MinE_{Ng(\Delta 74\text{-}78)}$, or $MinE_{Ng\text{-}E46P,V50P,Y54P}$ were assayed by the bacterial two-hybrid system (Table 7). Interaction between $MinD_{Ng}$ and wild-type $MinE_{Ng}$ was observed (177.2 ± 3.1 Miller units, Table 7), while no interaction was observed in cells that were singly transformed with p22minD or p434minD (Table 7). However, $MinD_{Ng}$/$MinE_{Ng}$ interaction was clearly altered in the presence of each $MinE_{Ng}$

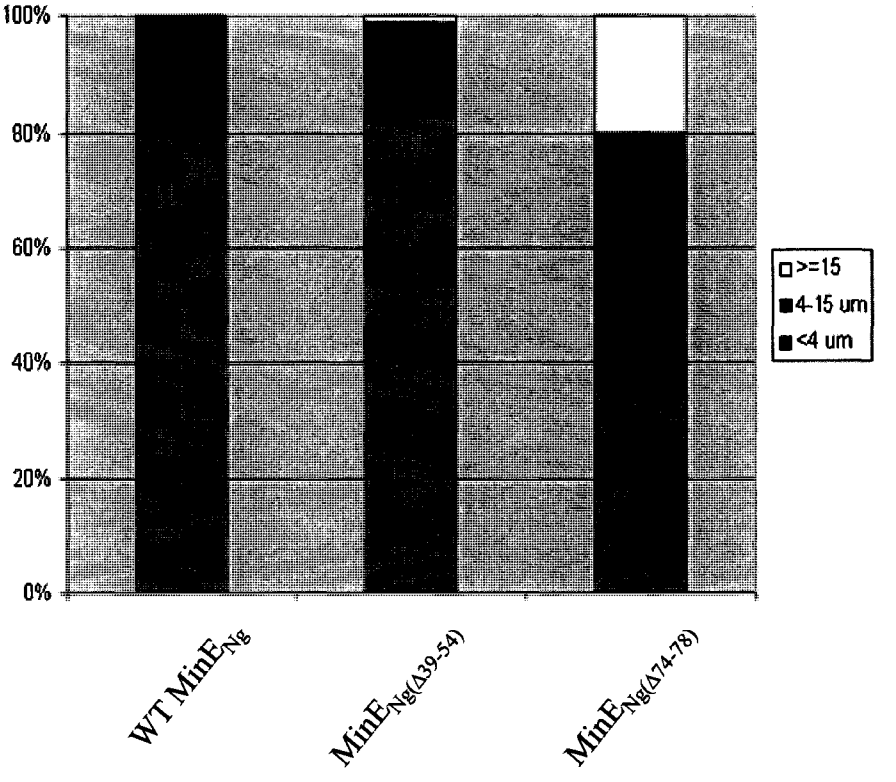

Figure 3.26. MinE$_{Ng}$ self-interaction may be linked to cell elongation. Different truncation mutant had varied impacts on cell phenotype. Blue bar indicates percentage of cells shorter than 4 μm. Purple bar indicates the portion of cells defined as short filaments. Beige bar stands for the portion of cells longer than 15 μm (n = 110 for each sample). The x-axis indicated the wild-type/mutant MinE$_{Ng}$ that was co-expressed with GFP-MinD$_{Ng}$. WT indicates wild-type.

Table 7. Bacterial two-hybrid assays of $MinE_{Ng}$ interaction with $MinD_{Ng}$

Fusion to P22 repressor[a]	Fusion to 434 repressor[b]	β-galactosidase activity[c]
-	-	2663 ± 73
$MinD_{Ng}$	-	979.0 ± 48.5
-	$MinD_{Ng}$	1364 ± 48.8
$MinD_{Ng}$	$MinE_{Ng}$	177.2 ± 3.1
$MinD_{Ng}$	$MinE_{Ng(\Delta 39\text{-}54)}$	538.2 ± 11.8
$MinD_{Ng}$	$MinE_{Ng(\Delta 74\text{-}78)}$	612.8 ± 13.5
$MinD_{Ng}$	$MinE_{Ng\text{-}E46P,V50P,Y54P}$	693.8 ± 8.2

[a] N-terminal repressor of P22 phage protein
[b] N-terminal repressor of 434 phage protein
[c] measured in Miller units

mutant. The bacterial two-hybrid assays indicated that interaction between $MinD_{Ng}$ and $MinE_{Ng(\Delta 39\text{-}54)}$, $MinE_{Ng(\Delta 74\text{-}78)}$, or $MinE_{Ng\text{-}E46P,V50P,Y54P}$ was disrupted (538.2 ± 11.8, 612.8 ± 13.5, and 693.8 ± 8.2, respectively, Table 7), irrespective of which repressor was fused to $MinD_{Ng}$ or $MinE_{Ng}$ (data not shown). As a result, disrupting $MinE_{Ng}$ self-interaction could have impaired the ability of $MinE_{Ng}$ to interact with $MinD_{Ng}$.

CHAPTER 4

Discussion

Portions of this chapter were published in:

[**Eng, N.F.**, Szeto, J., Acharya, S., Tessier, D., and Dillon, J.R. (2006) The C-terminus of MinE from *Neisseria gonorrhoeae* acts as a topological specificity factor by modulating MinD activity in bacterial cell division. Res Microbiol. 157, 333-344.]

[Szeto, J., **Eng, N.F.**, Acharya, S., Rigden, M.D., and Dillon, J.R. (2004) A conserved polar region in the cell division site determinant MinD is required for responding to MinE-induced oscillation, but not for localization within coiled arrays, Res Microbiol. 156, 17-29.]

and

[Ramos, D., Ducat, T., Cheng, J., **Eng, N. F.**, Dillon, J. A. R., and Goto, N. K. (2006) Conformation of the cell division regulator MinE: Evidence for interactions between the topological specificity and anti-minCD domains. Biochem. 45, 4593-4601]

This is the first study of the role of MinE from a coccal microorganism. The study of gonococcal MinE led to many new discoveries: 1) $MinE_{Ng}$ may have a putative role in chromosome condensation, 2) both the N- and C-termini of $MinE_{Ng}$ are involved with $MinD_{Ng}$ interaction, 3) the length of $MinD_{Ng}$ oscillation cycles, in the presence of $MinE_{Ng}$, is dependent on $MinD_{Ng}$ ATPase stimulation (i.e. more ATPase activity, shorter oscillation periods), 4) weak interactions between $MinE_{Ng}$ and $MinD_{Ng}$ do not promote $MinD_{Ng}$ ATPase activity *in vitro*, but may still allow $MinD_{Ng}$ oscillation *in vivo*, 5) $MinE_{Ng}$ self-interaction may be required for proper $MinD_{Ng}$ function, and 6) unlike $MinE_{Ec}$, $MinE_{Ng}$ rings/coils are absent in an *E. coli* background unless $MinE_{Ng}$ is highly expressed. Clearly, these new findings show that cell division site selection, with respect to the $MinE_{Ng}$, is a complicated process.

4.1. $MinE_{Ng}$ may be an essential cell division protein and may possess a novel function

Most of the current knowledge of bacterial cell division originated from the analysis of bacilli like *E. coli* and *B. subtilis*. It was once perceived that the Min proteins could not exist in coccal microorganisms because such bacteria lacked obvious midcells (Weaver, 2000). However, our laboratory refuted this hypothesis by identifying and characterizing *minC*, *minD* and *minE* homologues from the Gram-negative *N. gonorrhoeae* (Ramirez-Arcos *et al.*, 2001b). While $MinC_{Ng}$ and $MinD_{Ng}$ have been well studied (Ramirez-Arcos *et al.*, 2001b;Szeto *et al.*, 2001a), this is the first study that examined the role of MinE from a naturally round bacteria.

Homologues of MinE were found in many prokaryotes (Fig. 3.1). While the majority of MinE homologues were identified from Gram-negative bacteria, some were found in Gram-positive bacteria such as *Clostridium perfringens*, *Moorella thermoacetica*, and

Deinococcus geothermalis. Other than these bacteria, there were no other known MinE homologues in Gram-positive bacteria. Many of the recently-discovered MinE homologues were found primarily in bacteria living in extreme conditions that were anaerobic (*M. thermoacetica*), thermophilic (*D. geothermalis*), methane-oxidizing (*M. capsulatus*), and ammonia-oxidizing (*N. oceani*). Since MinE was found in bacteria that thrive in such extreme conditions, this suggested that MinE could have originated from early life on Earth, where such extreme circumstances were typical. As a result, it is possible that the MinE found in Gram-negative and the few Gram-positive bacteria could have evolved from a common ancestor.

MinD is present in Archael bacteria like *Pyrococcus furiosus* and in the Gram-positive coccus *Deinococcus radiodurans* without the presence of other Min proteins. In these organisms, MinD was the only homologue found, without the presence of MinC or MinE (Szeto, 2004). In contrast, the presence of MinE was always accompanied by the presence of MinD in organisms analyzed to date. Interestingly, while MinD and MinE were found in the Gram-negative round cyanobacterium *Gloeobacter violaceus*, MinC was not present in this organism. It is possible that MinD and MinE may have different functions in this organism, or that another structural homologue of MinC may be employed in *G. violaceus*. In the algae *Chlorella vulgaris* and *Guillardia theta*, only MinD and MinE were found as well (Itoh *et al.*, 2001).

N. gonorrhoeae, *N. meningitidis*, and *M. capsulatus* are currently the few coccal organisms that possess all three *min* genes. As such, these are the few bacteria that allow for the study of all three Min proteins in a naturally occurring coccus. Our laboratory showed that disrupting the *minC* and *minD* genes in *N. gonorrhoeae* caused aberrant cell division along many planes (Ramirez-Arcos *et al.*, 2001b;Szeto *et al.*, 2001a). This observation was

also recorded when *ftsE* and *ftsX* were insertionally inactivated in *N. gonorrhoeae* (Bernatchez *et al.*, 2000). However, despite many attempts, a knockout strain of $minE_{Ng}$ was not achieved. Therefore, $minE_{Ng}$ may be an essential gene as there has yet to be a reported strain of a *minE* knockout in any species. Since there are *E. coli* strains (e.g. PB114, WM1250) where the entire *min* operon was inactivated (de Boer and Crossley, 1989;Ramirez-Arcos *et al.*, 2002), it would be interesting to determine if disruption of the *N. gonorrhoeae min* operon would be lethal.

The creation of the shuttle vector became an essential tool in studying the overexpression of Min proteins in its native organism; the overexpression of $MinC_{Ng}$ and $MinD_{Ng}$ from the pFP25 vector (pFP20 + $minC_{Ng}$, $minD_{Ng}$) revealed significant cell enlargement, as one might expect from cell division inhibition (Szeto *et al.*, 2001a). However, overexpression of MinC or MinD alone in *N. gonorrhoeae* did not result in enlarged gonococci; hence, expression of their endogenous promoters may not be strong enough to induce this phenotype or both may be required (Szeto, 2004). As a result, modifications to pFP20 were required in order to control and increase expression. The inclusion of the *lac* promoter revealed that overexpression of $MinC_{Ng}$ alone was adequate to inhibit cell division in *E. coli*, although it is unknown if overexpression from the shuttle vector pNE11 (pNE2 + $minC_{Ng}$) would cause cell division inhibition in *N. gonorrhoeae*. The minicell phenotype induced by excess $MinE_{Ng}$ from pNE13 (pNE2 + $minE_{Ng}$) in an *E. coli* background showed that *E. coli* was able to overexpress $MinE_{Ng}$ from the shuttle vector.

When pNE13 (pNE2 + $minE_{Ng}$) was transformed into *N. gonorrhoeae* F62, it was surprising to see that the cell size was relatively unchanged based on TEM imaging. I predicted that excess $MinE_{Ng}$ would induce abnormal cell division, as overexpression of $MinE_{Ec}$ (de Boer and Crossley, 1989) and $MinE_{Ng}$ (these studies) induced a minicell

phenotype in *E. coli*. Instead, the most noticeable change caused by $MinE_{Ng}$ overexpression in *N. gonorrhoeae* was the absence of nucleoid condensation in *N. gonorrhoeae* NE1 cells at 12 hours. In contrast, wild-type *N. gonorrhoeae* F62 cells, the isogenic parent strain, at 12 hours clearly displayed the compacting of the nucleoid and concurrent segregation into the daughter cells. Samples taken 4 hours later, showed that wild-type F62 cells were enlarging, and dying, while cells overexpressing $MinE_{Ng}$ finally started to initiate chromosome condensation. These results suggest that excess $MinE_{Ng}$ may delay chromosome condensation. Interestingly, preliminary analysis of conserved motifs using PROSCAN (http://npsa-pbil.ibcp.fr/cgi-bin/npsa_automat.pl?page=npsa_prosite.html) showed that $MinE_{Ng}$ has many motifs that were at least 70% conserved that were linked to the bacterial regulatory AraC family proteins and the MerR family of transcriptional regulators. One of the possible themes emerging from these groups is that AraC and MerR family members contain motifs that can bind DNA. However, physiologically, it is unlikely that DNA-binding is a function of $MinE_{Ng}$. Alternatively, it may be possible that excess $MinE_{Ng}$ may counter chromosome condensation.

The reason behind the increase in the number of *N. gonorrhoeae* NE1 cells ($MinE_{Ng}$ overexpression) after 12 hours of growth is not clear. It is possible that the delay of chromosome condensation could affect the rate at which *N. gonorrhoeae* cells grow and utilize the nutrients in the media. As such, NE1 cells may not exhaust nutrients as rapidly as wild-type cells do, allowing these cells to use the available nutrients in the medium to increase their numbers.

According to my growth studies, wild-type *N. gonorrhoeae* F62 cells entered a relatively slow death phase after 16 hours, while the number of viable NE1 cells sharply fell between 12 and 16 hours. If excess $MinE_{Ng}$ were to delay chromosome condensation, this

result would be predicted if chromosome condensation and divisome formation were not linked in *N. gonorrhoeae*. Both the sister-cohesion and factory-extrusion models of chromosome segregation would then be able to predict this result. In both cases, septation would proceed before the nucleoid could condense and segregate, potentially killing many cells. As such, this explanation could explain why *N. gonorrhoeae* NE1 cells ($MinE_{Ng}$ overexpression) were dying faster than *N. gonorrhoeae* F62 cells (no overexpression) according to the growth curves at 16 hours. However, the TEM data of these strains revealed that at 16 hours, the *N. gonorrhoeae* NE1 cells were not dying, but instead appeared healthier than wild-type *N. gonorrhoeae* F62 cells. Although it is not known why NE1 cells continued to be healthy at 16 hours, while there were more viable, yet sick, wild-type *N. gonorrhoeae* F62 cells, it is possible that NE1 cells that have yet to divide can survive since the replicated nucleoids have yet to segregate.

Western blotting using anti-$MinE_{Ng}$ from section 2.25 was able to detect purified $MinE_{Ng}$ and $MinE_{Ng}$ overexpression in *E. coli*. However, detection of $MinE_{Ng}$ from its native organism was not possible. This dilemma prevented many experiments in the gonococcus from taking place. For example, it is possible that the observations from the growth curves and the TEM data may have been a result from other sequences present on pNE13; however, it has been shown that there were no morphological differences between cells that did/did not possess the pNE2 vector (data not shown), suggesting that the other sequences in the shuttle vector may not play a role. Nonetheless, antibody directed against native $MinE_{Ng}$, denatured $MinE_{Ng}$, peptides of $MinE_{Ng}$ and even anti-$MinE_{Ec}$ was not sensitive and specific enough to detect $MinE_{Ng}$ expression in the host organism. Other approaches like biotinylation and conjugation did not improve sensitivity and specificity either (data not shown). It is unclear why detection of endogenous $MinE_{Ng}$ from its native organism was not

successful. It is possible that $MinE_{Ng}$ protein levels in *N. gonorrhoeae* are extremely low so that sensitivity and specificity of anti-$MinE_{Ng}$ are not adequate to detect $MinE_{Ng}$ using the approaches in this project. Antibodies against $MinC_{Ng}$ and $MinD_{Ng}$ detected their respective proteins in the host organism. This suggested that $MinC_{Ng}$ and $MinD_{Ng}$ are relatively higher in quantity than $MinE_{Ng}$. Radioactive detection is one method that may be able to detect low levels of $MinE_{Ng}$. Real-time quantitative PCR is also a good approach to detect transcript levels of $MinE_{Ng}$ from *N. gonorrhoeae* and should be strongly considered in further studies of $MinE_{Ng}$ in its native organism. Interestingly, since levels of *E. coli* MinD and MinE were relatively the same (Shih *et al.*, 2003), if the possibility of low $MinE_{Ng}$ levels in *N. gonorrhoeae* is true, then this could represent a significant difference in the division patterns of rod- and round-shaped bacteria.

This is the first study of MinE function in a naturally occurring coccus. I showed that gonococcal $minE_{Ng}$ was likely an essential gene, since methods of homologous recombination to knock out $minE_{Ng}$ were not successful. Overexpression of $MinE_{Ng}$ from a shuttle vector induced a minicell phenotype in *E. coli*, suggesting that gonococcal MinE is a cell division protein; in addition, this result showed that the inclusion of the *lac* promoter in the shuttle vector was a useful modification that can used for future studies of other gonococcal proteins. Furthermore, overexpression of $MinE_{Ng}$ in its native organism may cause nucleoid condensation delay, possibly slowing down cell division progression, a previously unrecognized role of $MinE_{Ng}$. Further studies of $MinE_{Ng}$ as a nucleoid factor should be investigated.

4.2. $MinE_{Ng}$ possesses two possible sites that are associated with $MinD_{Ng}$ interaction and is required for $MinD_{Ng}$ to oscillate along subcellular architecture

In *E. coli*, topological specificity is the ability of MinE to ensure that MinC and MinD are localized to the cell poles, thereby allowing FtsZ rings to form at midcell to initiate cell division (King *et al.*, 2000;Zhao *et al.*, 1995). Before my studies, it was unclear how MinE imparted topological specificity to MinD at the molecular level. I initially characterized $MinE_{Ng}$ by generating many truncations to determine domains of $MinE_{Ng}$ that interacted with $MinD_{Ng}$. Two $MinE_{Ng}$ domains that may interact with $MinD_{Ng}$ were identified. Site-specific substitutions to conserved residues of $MinE_{Ng}$ were generated in order to study the two $MinE_{Ng}$ regions more closely. Since gonococcal MinE is from a round bacterium, I selected conserved *N. gonorrhoeae* MinE residues (A18, L22, R30, K53, E67) that have been previously examined in $MinE_{Ec}$ (A18, L22, R30, K52, E66) in order to compare functionality from round and rod-shaped bacteria and to elucidate gonococcal MinD binding sites without relying on previous studies with $MinE_{Ec}$. These investigations produced four major findings: 1) contrary to reports with the *E. coli* protein, I discovered that both N- and C-terminal domains of $MinE_{Ng}$ are important for $MinD_{Ng}$ binding; 2) interaction between $MinD_{Ng}$ and $MinE_{Ng}$ was required for the recruitment of $MinD_{Ng}$ to the coiled array; 3) the oscillation of $MinD_{Ng}$ was observed even when *in vitro* assays showed impaired ability to stimulate $MinD_{Ng}$ ATPase activity; and 4) the extent of $MinD_{Ng}$ ATPase stimulation depended on the binding strength between $MinD_{Ng}$ and the C-terminus of $MinE_{Ng}$.

The N-terminus of *E. coli* MinE (aa 1-30) counteracted the functions of MinC and MinD by serving as a MinD binding site; the ability of MinE to behave as an anti-MinCD factor has been shown in numerous studies (Hu and Lutkenhaus, 2001;Ma *et al.*, 2003;Zhao

et al., 1995) by mutating various amino acids. While the substitution of many residues did not disrupt the ability of $MinE_{Ec}$ to interact with $MinD_{Ec}$, only certain amino acids had a profound effect on $MinE_{Ec}$ function when mutated (Hu and Lutkenhaus, 2001;Ma *et al.*, 2003). For example, two mutants, $MinE_{Ec\text{-}A18E,K19L}$ and $MinE_{Ec\text{-}I17A,A18R}$ caused MinCD-induced filamentation in a Δ*min* background and thus, prevented $MinD_{Ec}$ oscillation, while $MinE_{Ec\text{-}N16S,I17R}$ and $MinE_{Ec\text{-}K19A,E20A}$ retained the ability to confer $MinD_{Ec}$ movement (Hu and Lutkenhaus, 2001), presumably by maintaining $MinD_{Ec}$ interaction. These *E. coli* MinE studies suggest that A18 alone was responsible for $MinD_{Ec}$ interaction. Indeed, a later study showed that $MinE_{Ec\text{-}A18T}$ was unable to interact with $MinD_{Ec}$ and that no oscillation of $MinD_{Ec}$ was observed (Ma *et al.*, 2003). Further investigations showed that mutating L22 and I25 of *E. coli* MinE was also unable to interact with $MinD_{Ec}$. Since the N-terminus of $MinE_{Ec}$ has a propensity to form a nascent α-helix based on NMR studies on a 22-residue fragment from the N-terminus of $MinE_{Ec}$ (King *et al.*, 2000), a helical-wheel projection of the first 35 residues of $MinE_{Ec}$ was constructed (Ma *et al.*, 2003). The A18, L22 and I25 residues of $MinE_{Ec}$ were aligned on one side of the helix, raising the strong possibility that $MinD_{Ec}$ binds to $MinE_{Ec}$ through one side of the helix (Ma *et al.*, 2003). Yeast two-hybrid studies confirmed that A18 and L22 of gonococcal MinE were critical to $MinD_{Ng}$ interaction. Mutating these residues resulted in abolished $MinD_{Ng}$ interaction and as a result, there was no stimulation of $MinD_{Ng}$ ATPase activity or induction of $MinD_{Ng}$ oscillation. With 66% similarity between the N-termini of *N. gonorrhoeae* and *E. coli* MinE, the structure and function of the N-terminus of MinE, as an anti-MinCD domain, is most likely conserved across species.

The C-terminus of *E. coli* MinE (aa 31-88) is mainly responsible for providing self-interaction and topological specificity to prevent MinC and MinD from inhabiting the midcell and blocking cell division (King *et al.*, 2000;Zhao *et al.*, 1995). NMR studies of the C-terminus of $MinE_{Ec}$ revealed that this domain consisted of an α-helix and two β-sheets (King *et al.*, 2000). Studies showed that topological specificity of $MinE_{Ec}$ resided in aa 53-81, while the extreme seven C-terminal amino acids of the 88 aa protein were not essential for $MinE_{Ec}$ function (Zhao *et al.*, 1995). However, how the C-terminus acts as a topological specificity factor, or the possibility that the C-terminus may also be involved with MinD binding has not been previously determined. Yeast two-hybrid data in this study clearly showed that mutation of K53 and E67 of $MinE_{Ng}$ greatly hindered the ability of $MinE_{Ng}$ to interact with $MinD_{Ng}$ (Table 3). Since this finding was not reported before with *E. coli* MinE, this result may reflect on the increased variation among MinE orthologues at the C-terminus (Fig. 3.1) and possibly the differences in how MinE functions in round and rod-shaped bacteria. Western blotting would have been appropriate to demonstrate that the yeast fusion proteins were soluble; however, attempts at detecting Min_{Ng} proteins have not been successful (data not shown). Nonetheless, my studies of the C-terminus of $MinE_{Ng}$ imply that both the N- and C-termini of $MinE_{Ng}$ are important for $MinD_{Ng}$ association.

As only the C-terminus of *E. coli* MinE has been solved by NMR (King *et al.*, 2000), it is unknown how the N-terminus is spatially related. However, since $MinE_{Ng}$ truncations such as $MinE_{Ng\text{-}59aaCT}$ and $MinE_{Ng\text{-}54aaNT}$ were unable to interact with $MinD_{Ng}$ in the yeast two-hybrid assays, it is possible that the N- and C-termini may be in close proximity to each other in associating with $MinD_{Ng}$. Recently, a collaboration with Ramos and co-workers (2006) showed that this may be the case. Circular dichroism analysis of $MinE_{Ng\text{-}A18D}$

revealed that there was no perturbation to its secondary structural content compared to wild-type $MinE_{Ng}$; however, NMR heteronuclear single-quantum coherence (HSQC) studies showed that this mutation caused a change in the local chemical environments of amino acids in the N- and C-termini of $MinE_{Ng}$, possibly implying that the N- and C-termini domains may interact (Ramos *et al.*, 2006), which in turn, accounts for the finding of two $MinD_{Ng}$ binding domains. This finding was complemented by the generation of an E46A mutation in gonococcal MinE; this mutation to the C-terminus of $MinE_{Ng}$ led to noticeable alterations to the peak intensities of N-terminal residues in the HSQC spectrum (Ramos *et al.*, 2006). Interestingly, the N-terminal $MinE_{Ng\text{-}L22D}$ mutant destabilized $MinE_{Ng}$ in both domains, as indicated by a small decrease in helix and an increase of random coil characteristics as determined by circular dichroism, suggesting that N- and C-terminal domains of $MinE_{Ng}$ were not structurally independent (Ramos *et al.*, 2006).

NMR studies of gonococcal MinE showed that residues 20-30 of the anti-MinCD domain were in a β-conformation (Ramos *et al.*, 2006), a stark difference from the apparent α-helical content in the N-terminus of *E. coli* MinE (King *et al.*, 1999;Ma *et al.*, 2003). Since a $MinE_{Ec1\text{-}22}$ fragment retained anti-MinCD properties (Zhao *et al.*, 1995), it is possible that the rest of the N-terminus does not directly interact with MinD, but instead, functions as a structural stabilizer. This hypothesis was supported by studies of the gonococcal L22D mutant, which caused structural instability of $MinE_{Ng}$ (Ramos *et al.*, 2006). In addition, a fragment of $MinE_{Ec}$ (aa 1-31) and L22R and I25R point mutations of wild-type *E. coli* MinE permitted unusual membrane localization of $MinE_{Ec}$ compared to wild-type $MinE_{Ec}$ (Ma *et al.*, 2003). As such, deleting most of MinE or mutating residues 20-

30 could cause structural perturbations that would result in exposing motifs that can favour membrane binding, while wild-type MinE would normally keep these motifs inaccessible.

Further analysis of the N- and C-terminal $MinE_{Ng}$ mutants revealed some of the intricacies of the coiled array and its role in $MinD_{Ng}$ oscillation. GFP-$MinD_{Ng}$ localization experiments showed that C-terminal $MinE_{Ng}$ mutants retained their ability to interact with $MinD_{Ng}$, permitting $MinD_{Ng}$ trafficking to a coiled array (Fig. 3.9 C-D), while the non-$MinD_{Ng}$ binding N-terminal $MinE_{Ng}$ mutants did not facilitate $MinD_{Ng}$ recruitment to the subcellular architecture (Fig. 3.9 B). Previously, our laboratory showed that a $MinD_{Ng\text{-}loop}$ mutant did not respond to $MinE_{Ng}$ stimulation or demonstrate oscillatory behaviour; however, this mutant retained the ability to be recruited to the coiled array while interacting with $MinE_{Ng}$ (Szeto *et al.*, 2005). As a result, $MinD_{Ng}$ localization to the coiled/polymeric array required $MinE_{Ng}$ interaction. Once recruited, the inherent ATPase activity of $MinD_{Ng}$ should be sufficient to induce $MinD_{Ng}$ oscillation. My studies showed that although interaction with $MinD_{Ng}$ was very weak, the C-terminal $MinE_{Ng\text{-}E67L}$ mutant induced $MinD_{Ng}$ oscillation regardless of ATPase stimulation. This suggested that the first role of $MinE_{Ng}$ is to interact with $MinD_{Ng}$ and assist in its recruitment to the coiled array for subsequent oscillation regardless of ATPase stimulation.

The second role of $MinE_{Ng}$ is to regulate $MinD_{Ng}$ activity. Studies of the C-terminal $MinE_{Ng\text{-}K53A}$ and $MinE_{Ng\text{-}E67L}$ mutants suggested that stimulation of ATPase activity and faster oscillatory periods were apparently dependent on increased binding between $MinE_{Ng}$ and $MinD_{Ng}$. Gradient protein activation as a result of stronger protein-protein interactions has been described. For example, the degree of T cell activation depends on how strong different peptide ligands bind to T cell receptors (Krogsgaard *et al.*, 2003). Interestingly, my studies suggested that activation of ATP hydrolysis by $MinD_{Ng}$ required more than mere

interaction with $MinE_{Ng}$. The absence of minicells when overexpressing the $MinE_{Ng\text{-}E67L}$ mutant in an *E. coli* (*+min*) background and its inability to stimulate $MinD_{Ng}$ in hydrolysing ATP implied that this mutant was not functional. This phenomenon was most likely attributed to the very weak interaction of this mutant to $MinD_{Ng}$, since Western blotting showed that mutating E67 did not decrease protein expression. However, if interaction between $MinE_{Ng}$ and $MinD_{Ng}$ was significant (i.e. stronger than interaction between $MinE_{Ng\text{-}E67L}$ and $MinD_{Ng}$), function would be conferred to $MinE_{Ng}$ in stimulating sufficient ATPase activity to counter the presence of $MinC_{Ec}$ and $MinD_{Ec}$ at the cell poles, giving rise to minicell formation. A possible caveat to these results is that the *in vitro* studies (ATPase assays) may be missing a component that may not fully explain what occurs *in vivo* (GFP oscillation). Nonetheless, the N-terminus of $MinE_{Ng}$ is likely the main determinant in inducing $MinD_{Ng}$ oscillation, since interaction with this domain is apparently essential in priming $MinE_{Ng}$ function. I propose that the C-terminus of $MinE_{Ng}$ then imparts topological specificity to $MinD_{Ng}$ through two mechanisms: 1) a threshold of $MinD_{Ng}$ interaction behaves like a switch to "turn on" the stimulation of ATPase activity and 2) increased $MinD_{Ng}$ interaction stimulates more ATPase activity, analogous to the function of an electrical dimmer switch. The threshold of $MinD_{Ng}$ interaction may have been developed to ensure that $MinD_{Ng}$ ATPase stimulation is $MinE_{Ng}$-specific.

Interestingly, Figure 3.12 revealed that $MinD_{Ng}$ can associate with the PG vesicles without the addition of ATP. One possible reason for this is that the inclusion of the C-terminal His-tag to $MinD_{Ng}$ could have increased the affinity of $MinD_{Ng}$ for PG vesicles. This study attempted to include N-terminally His-tagged $MinD_{Ng}$ as well; unfortunately, insufficient purified protein did not allow this possibility to be tested (data not shown). At the concentration of $MinD_{Ng}$ used in the lipid-binding assays (~ 0.4 μM), it is likely that,

regardless of the presence of ATP or ADP, $MinD_{Ng}$ is equally able to bind to PG vesicles. This has been shown in previous studies involving *E. coli* MinD (Mileykovskaya *et al.*, 2003). At higher concentrations of $MinD_{Ec}$, it seems that ATP is more important in retaining the ability of $MinD_{Ec}$ to bind to phospholipid vesicles (Mileykovskaya *et al.*, 2003); as such, ATP is likely needed for higher concentrations of $MinD_{Ng}$ to bind to PG vesicles.

Mutating *E. coli* K52 and E66 (*E. coli* equivalents to gonococcal K53 and E67) did not restore proper *E. coli* phenotype in a Δ*min* background, suggesting that these two residues did not play a role in providing topological specificity (King *et al.*, 2000). However, mutating the equivalent residues in gonococcal MinE (i.e. K53A and E67L $MinE_{Ng}$ mutants) altered normal $MinD_{Ng}$ activity and oscillation, demonstrating that these residues, at least for $MinE_{Ng}$, are important for function. It is possible, however, that these differences indicated that not all MinE have identical function, particularly when comparing MinE from the round *N. gonorrhoeae* and the rod-shaped *E. coli*.

The coiled array seemed to play a critical role in division site selection by acting as a medium through which $MinD_{Ng}$ travels from pole-to-pole in *E. coli*. The composition of the coiled array itself is still unknown; perhaps a complex of MinD-MinE molecules have a formation that is favourable to binding to pre-existing subcellular architecture or that a MinD-MinE complex is the basic unit of the coil itself. In the absence of MinE, MinD can interact and recruit MinC to the cell membrane, and induce cell filamentation, without being localized to the coiled array (Zhou and Lutkenhaus, 2004). However, I showed that the presence of $MinE_{Ng}$ is needed to recruit $MinD_{Ng}$ to the coiled array, therefore suggesting that MinE, but not MinC, plays a role in localizing MinD to helical arrays. It is possible that MinCD first migrates to the cell membrane, mediated by the membrane targeting sequence

(MTS) of MinD (Szeto *et al.*, 2002). Subsequent interaction with MinE causes MinC displacement, followed by favourable recruitment of MinD-MinE to the coiled array. There, ATP hydrolysis by MinD causes ADP-induced conformation changes that release both MinD and MinE from the array.

The discovery of the $MinD_{Ec}$ helical array and the advent of deconvolution and three-dimensional imaging software have made for better resolution of other, previously undetected, helical subcellular architectures. Other proteins that have been found to form similar coiled structures include MreB, a factor responsible for conferring the rod-shape morphology to bacteria like *E. coli* (Shih *et al.*, 2005), CreS, (i.e. crescentin), the protein that provides the curved-shape morphology to *C. crescentus* (Ausmees and Jacobs-Wagner, 2003), FtsZ (Margolin, 2005;Salimnia *et al.*, 2000), and SetB, which is responsible for chromosome segregation (Espeli *et al.*, 2003). Many of the helical structures do not colocalize, such as the *E. coli* MreB and MinD arrays (Shih *et al.*, 2005) and the evolutionary purpose of the subcellular architectures are unknown. The possibility that all of these structures could merely be artifacts induced by protein overexpression cannot be ruled out, as not one study has showed whether these structures exist at physiological protein levels. In my studies, overexpression has been shown to affect $MinE_{Ec}$ oscillation (Fig. 3.14). I also showed that $MinE_{Ng}$ did not form rings or localize to subcellular structures unless $MinE_{Ng}$-GFP was highly overexpressed (Fig. 3.15). Previous work with pSRE-GFP (*minD*$_{Ng}$::*minE*$_{Ng}$-*gfp*) revealed that $MinE_{Ng}$-GFP was diffusely localized throughout the cytoplasm (Ramirez-Arcos *et al.*, 2002). At the time, it was believed that uncontrolled overexpression of the GFP fusion abolished the ability of $MinE_{Ng}$ to form rings like *E. coli* MinE (Ramirez-Arcos *et al.*, 2002). However, my results are the first to suggest that $MinE_{Ng}$ must be highly expressed in order to visualize rings or coils compared to *E. coli* MinE. Most

likely, at physiological levels, $MinE_{Ng}$ does not form rings, since at lower levels of $MinE_{Ng}$-GFP overexpression, fluorescence was distributed homogenously throughout (Fig. 3.15). Since the $MinE_{Ng}$-GFP rings, in the presence of 0.05 to 0.2% arabinose, did not even oscillate, it is also possible that these structures could be inclusion bodies. These results provide further evidence that despite being functionally similar, MinE from *N. gonorrhoeae* behaves differently from *E. coli* MinE.

Ultimately, the localization of Min_{Ng} in *N. gonorrhoeae* would have been ideal in order to study how these proteins behave in a true coccus. The Dillon laboratory has previously attempted to visualize GFP-labelled $MinC_{Ng}$ in *N. gonorrhoeae* using the pFP20 shuttle vector (Table 3); however, GFP fluorescence was observed throughout the small *N. gonorrhoeae* cells, suggesting that more stringent control of protein expression and/or improved microscopic technology are needed in the future with the aim of furthering our current understanding of Min behaviour in round bacteria.

My work demonstrates that $MinE_{Ng}$ seems to satisfy the definition of "topological specificity" by providing at least two critical events. First, the N-terminus of $MinE_{Ng}$ must bind to $MinD_{Ng}$ to facilitate recruitment of the latter to the coiled array. Once there, $MinD_{Ng}$ can oscillate regardless of stimulation of its ATPase activity. The coiled array itself does not induce oscillation, but rather is a topological orientation that $MinD_{Ng}$ needs to assume before oscillation can occur. In terms of evolution, it is not known why a coiled array is needed to facilitate cell division site selection. Second, the C-terminus of $MinE_{Ng}$ modulates $MinD_{Ng}$ activity by controlling the binding strength between the two proteins. This may be possible if the N-terminus of $MinE_{Ng}$ caused $MinD_{Ng}$ to conformationally change to allow the C-terminus to interact. Once interaction surpasses some threshold (i.e. higher binding strength that the interaction between $MinE_{Ng\text{-}E67L}$ and $MinD_{Ng}$), stronger $MinE_{Ng}$-$MinD_{Ng}$ interactions

lead to increasing ATPase activity that facilitates periods of $MinD_{Ng}$ oscillation that favour proper cell division site selection.

4.3. $MinE_{Ng}$ self-interaction is required to function as a cell division protein

It is important to ascertain whether dimerization of a protein is important for function. For example, *E. coli* 3-deoxy-D-arabino-heptulosonate 7-phosphate synthase must be in a dimerized state in order to synthesize aromatic amino acids (Xu *et al.*, 2004). However, there are cases where disrupting self-interaction does not impair function, as *E. coli* biotin carboxylase does not require dimerization to function in fatty acid metabolism (Shen *et al.*, 2006).

The cell division proteins MinC and MinD require self-association in order to function in proper cell division site selection. In *E. coli*, MinC dimerization was isolated to a C-terminal domain encompassing residues 118-231 (Hu and Lutkenhaus, 2000;Szeto *et al.*, 2001b), while similar results were found in MinC from *N. gonorrhoeae* (Ramirez-Arcos *et al.*, 2004) and the Archael *Thermotoga maritima* (Cordell *et al.*, 2001). This self-interaction property has been shown to be required when MinD recruits MinC to the membrane and thus suggests that MinC dimerization may be needed to inhibit FtsZ polymerization (Szeto *et al.*, 2001b). Evidence showing that MinD exhibited self-interaction was reported from *N. gonorrhoeae* (Szeto *et al.*, 2001a), and from *E. coli* (Lutkenhaus and Sundaramoorthy, 2003). It is believed that MinD dimerization is required to bind ATP properly, a conformation needed for subsequent ATP hydrolysis and MinD oscillation (Lutkenhaus and Sundaramoorthy, 2003).

While MinE is known to dimerize as well (Pichoff *et al.*, 1995;Zhao *et al.*, 1995), it is not known if dimerization is important for its biological function. My research focused on

the nature of MinE self-association and its role in cell division site selection. My goal was to generate monomeric MinE in order to test its ability to function as a cell division protein (i.e. can monomeric MinE remain a functional protein in cell division site selection, or can monomeric MinE stimulate MinD ATPase activity and induce MinD oscillation?). $MinE_{Ng}$ self-interaction was determined using a modified bacterial two-hybrid system, analytical ultracentrifugation and size-exclusion chromatography. My studies indicated that disrupting $MinE_{Ng}$ self-interaction caused the protein to become non-functional by preventing MinD oscillation, thus impairing cell division.

To date, there has been no reported information on the effects of disrupting MinE self-interaction on its biological function even though NMR studies of $MinE_{Ec}$ showed that proper function should be linked to a dimeric structure (King *et al.*, 2000). In *E. coli,* studies of $MinE_{Ec\text{-}D45A}$ and $MinE_{Ec\text{-}V49A}$, which have lower propensities to form $MinE_{Ec}$ rings, retained the ability to dimerize (King *et al.*, 2000). These results suggested that $MinE_{Ec}$ self-interaction may not be coupled to $MinE_{Ec}$ ring formation. Furthermore, even though a $MinE_{Ec(1\text{-}31)}$ peptide interacted with $MinD_{Ec}$ (Ma *et al.*, 2003), it was unclear if $MinE_{Ec}$ self-interaction was abolished or if the ability of this peptide to induce $MinD_{Ec}$ oscillation was compromised with the absence of its C-terminus. Thus, I was interested in determining if $MinE_{Ng}$ self-association is linked to its biological function.

I showed through analytical ultracentrifugation (AUC) that His-tagged $MinE_{Ng}$ is predominantly dimeric. Although confirmation of this association could not be established using the yeast two-hybrid system, I was able to validate $MinE_{Ng}$ self-interaction using a bacterial two-hybrid (B2H) system (Di Lallo *et al.*, 2001) and size-exclusion chromatography. B2H assays employed the binding of unique phage hybrid-repressors to unique phage hybrid-DNA operators genetically incorporated into *E. coli* (i.e. *E. coli* R721,

Table 1) to prevent the expression of β-galactosidase. Using B2H, $MinE_{Ng}$ self-interaction was observed not only with wild-type $MinE_{Ng}$, but also in the five $MinE_{Ng}$ point mutations (A18D, L22D, R30D, K53A, and E67L) described in 3.7. This result suggested that $MinE_{Ng}$ self-interaction is not likely perturbed by individual point mutations.

The idea that functional $MinE_{Ng}$ should be dimeric was supported by studies showing the failure of the A18D and the L22D $MinE_{Ng}$ mutants to interact with $MinD_{Ng}$ (Eng *et al.*, 2006) but retaining their ability to self-interact. However, it was still uncertain if disrupting $MinE_{Ng}$ self-interaction (i.e. monomeric $MinE_{Ng}$) affected association with $MinD_{Ng}$ and/or retained biological function. Using B2H assays, I determined that $MinE_{Ng}$ self-interaction may have been disrupted when significant mutations to the C-terminal α-helix ($MinE_{Ng(\Delta 39-54)}$ and $MinE_{Ng\text{-}E46P,V50P,Y54P}$), and the C-terminal β-sheet ($MinE_{Ng(\Delta 74-78)}$) of $MinE_{Ng}$ were introduced.

The lack of GFP-$MinD_{Ng}$ oscillation in cells transformed with pSRNE1 (Δ39-54 $MinE_{Ng}$ mutation) and pSRNE2 (Δ74-78 $MinE_{Ng}$ mutation) suggested that these mutants did not interact with $MinD_{Ng}$, which could be a reason why oscillation was not observed in most cells. Earlier, I showed that $MinE_{Ng\text{-}A18D}$ and $MinE_{Ng\text{-}L22D}$, which did not interact with $MinD_{Ng}$, also caused GFP-$MinD_{Ng}$ to be localized around the cell periphery (Eng *et al.*, 2006). Interestingly, a few *E. coli* PB114 cells expressing $MinE_{Ng(\Delta 74-78)}$ showed traces of possible $MinD_{Ng}$ recruitment to a coiled array, even though little or no oscillation was observed. Since $MinD_{Ng}$-$MinE_{Ng}$ interaction is required to recruit $MinD_{Ng}$ to the coiled array (Eng *et al.*, 2006), the presence of subcellular architecture implied that both $MinE_{Ng(\Delta 39-54)}$ and $MinE_{Ng(\Delta 74-78)}$ could interact with $MinD_{Ng}$. However, the bacterial two-hybrid data showed that the ability of these $MinE_{Ng}$ mutants to interact with $MinD_{Ng}$ was clearly

impaired. It follows that in order for $MinE_{Ng}$ to be biologically active, $MinE_{Ng}$ must first self-associate before it can interact with $MinD_{Ng}$. Thus, proper $MinD_{Ng}$ oscillation would occur in the presence of dimeric $MinE_{Ng}$ interacting with dimeric $MinD_{Ng}$. The presence of the coils may still occur, since interaction was not completely disrupted; it is possible that the putative monomer of $MinE_{Ng}$ still possessed the ability to bind to $MinD_{Ng}$ for recruitment to the coiled array. However, a monomer of $MinE_{Ng}$ interacting with $MinD_{Ng}$ is not likely favourable for physiological $MinD_{Ng}$ oscillation periods.

It should be noted that the loss of self-interaction for $MinE_{Ng(\Delta 39\text{-}54)}$ and $MinE_{Ng(\Delta 74\text{-}78)}$ could not be confirmed using physical methods since they were insoluble. Disrupting MinE dimerization could have possibly prevented proper folding of MinE. Based on the extensive dimeric interface of the NMR structure of *E. coli* MinE (King *et al.*, 2000), disrupting self-interaction could expose many hydrophobic surfaces that would prevent a monomer of $MinE_{Ng}$ from being stable, causing insolubility. As such, this could have been a reason why there was no self-interaction detected with the $MinE_{Ng(\Delta 39\text{-}54)}$ and $MinE_{Ng(\Delta 74\text{-}78)}$ mutants in the bacterial two-hybrid assays. However, Western blotting showed that the mutant P22- and 434-$MinE_{Ng}$ fusion repressors were expressed in the soluble fraction of *E. coli* R721 cells, indicating that the fusion repressors were indeed soluble.

It is unclear why more intense GFP-$MinD_{Ng}$ fluorescence was observed intermittently along the cell membrane or at the cell poles (Fig. 3.24 B) when $MinE_{Ng(\Delta 39\text{-}54)}$ was co-expressed. Although, it is possible that the brighter spots could be $MinD_{Ng}$ inclusion bodies, spots of non-oscillating discontinuous $MinD_{Ng}$ localization along the cell membrane have been previously observed. Our laboratory showed that the $MinD_{Ng\text{-}loop}$ mutant, which is unable to stimulate ATPase activity in the presence of $MinE_{Ng}$, can also display a clear

banding pattern, indicating subcellular architecture (Szeto *et al.*, 2005); however, in some cases, like Fig. 3.24 B, intermittent brighter fluorescence along the cell membrane was also observed. As such, this finding supports the idea that a putative monomer of $MinE_{Ng}$ may be able to recruit $MinD_{Ng}$ to the coiled array, but fails to induce $MinD_{Ng}$ oscillation that would facilitate proper cell division site selection. Therefore, proper $MinD_{Ng}$ oscillation and function is likely dependent on $MinE_{Ng}$ self-interaction. It is noteworthy that these domains (aa 39-54 and 74-78) confirmed that the C-terminus of $MinE_{Ng}$ is involved in $MinD_{Ng}$ interaction, as described earlier (section 3.7).

Interestingly, the localization of $MinD_{Ng}$ to the cell membrane in *E. coli* PB114 cells transformed with pSRNE2 ($MinE_{Ng(\Delta 74\text{-}78)}$) also caused many cells to become unusually long and filamentous (Fig. 3.26). However, since $MinC_{Ec}$ was not present in *E. coli* PB114, it is unclear if, or how, $MinD_{Ng}$ localization to the cell membrane would cause filamentation, such as preventing FtsZ polymerization.

In the pursuit to generate monomeric $MinE_{Ng}$ protein that can be purified, less extreme mutations to the α-helix (aa 39-54) were introduced to $MinE_{Ng}$ since the previous three $MinE_{Ng}$ mutants likely caused $MinE_{Ng}$ to become insoluble. Instead, two mutants were constructed, a double E46A, V50D $MinE_{Ng}$ mutant, and a triple E46A, V50D, Y54A substitution. In these two mutants, the charge on the amino acids was changed instead. While protein purification was successful, size-exclusion chromatography showed that these mutants remained dimeric. This showed that these substitutions were not able to disrupt $MinE_{Ng}$ self-interaction and that dimerized $MinE_{Ng}$ was the predominant oligomer physiologically. This result makes sense; if $MinE_{Ng}$ self-interaction was easily reversible,

monomeric $MinE_{Ng}$ would theoretically be less efficient as a cell division protein inducing $MinD_{Ng}$ oscillation.

NMR studies of the C-terminus of $MinE_{Ec}$ revealed that self-interaction is believed to take place between the C-terminal antiparallel α-helices and/or β-sheets (King *et al.*, 2000). However, studies of $MinE_{Ng}$ have suggested that the topological specificity domain may interact intramolecularly with the anti-MinCD domain (Ramos *et al.*, 2006); however, it may be possible that the topological specificity domain (TSD) of one MinE monomer could intermolecularly interact with the anti-MinCD domain of another monomer, otherwise known as "domain swapping". Analytical ultracentrifugation experiments with *E. coli* MinE showed that tetrameric and octameric species were only prevalent with the whole protein (Zhang *et al.*, 1998); these higher order structures were not observed when examining the TSD alone (King *et al.*, 1999). These results support the possibility that oligomerization of MinE may also involve interdimer interactions between the anti-MinCD and TSD domains. However, further studies are needed to test this hypothesis, with a complete structure of the full length of the MinE protein.

This is the first study to demonstrate that the ability of $MinE_{Ng}$ to interact with itself is an important association that may be linked to its role as a functional cell division protein. Without this interaction, the ability of $MinD_{Ng}$ to oscillate and facilitate cell division site selection is disabled.

4.4. Future considerations and concluding statements

With the discovery of the MinC, MinD, and MinE proteins from *E. coli*, (de Boer and Crossley, 1989), the knowledge about where and how bacteria divide has greatly

advanced in two rod-shaped organisms, *B. subtilis*, and *E. coli*. Once *min* gene homologues were identified from *N. gonorrhoeae* (Ramirez-Arcos *et al.*, 2001b), our laboratory has pioneered investigations of Min proteins originating from a naturally round coccal bacterium. In this project, MinE from *N. gonorrhoeae* was shown to be important in cell division, that multiple $MinE_{Ng}$ domains are important for $MinD_{Ng}$ interaction, that the coiled array, as a result of MinD/MinE interaction, prepared $MinD_{Ng}$ for pole-to-pole movement, and that proper function may require $MinE_{Ng}$ to be dimeric. Also, $MinE_{Ng}$ was found to play a role in nucleoid condensation, a finding that has not been previously reported with other MinE homologues. In *Sinorhizobium meliloti*, MinE carried an additional function of having a role in nitrogen fixation (Cheng *et al.*, 2007)

Recent analysis of the entire $MinE_{Ng}$ protein has already shown that structural differences do, in fact, exist between *E. coli* and *N. gonorrhoeae* MinE. NMR studies of the complete gonococcal MinE protein showed that residues 20-30 of the anti-MinCD domain are in β-conformation (Ramos *et al.*, 2006), which is different from the α-helical content in the N-terminus of *E. coli* MinE (King *et al.*, 1999;Ma *et al.*, 2003). Many studies have shown that α-helices are often involved in protein interaction. For example, the α-7 helix of *E. coli* MalE maltose binding protein is required to interact with the MalFGK2 complex (Szmelcman *et al.*, 1997); it has also been shown that MinC and MinE compete for the same binding site on the α-7 helix of MinD (Ma *et al.*, 2004;Ramirez-Arcos *et al.*, 2004). However, it is currently unknown how the β-sheet characteristics of the N-terminus of $MinE_{Ng}$ would interact with the α-7 helix of MinD, although it is possible (Chou *et al.*, 1985).

I discovered that the C-terminus (aa 31-87) and N-terminus (aa 1 –30) of $MinE_{Ng}$ were both involved with $MinD_{Ng}$ interaction where previous studies of *E. coli* MinE have shown that only the N-terminus participated in MinD interaction. It is possible that this result was not previously discovered in the *E. coli* homologue since there has not been a recorded study examining MinD interaction after mutating K52 and E66 in *E. coli* MinE (King *et al.*, 2000) which reside in the MinE topological specificity domain. While resolving a complete visual representation of MinE has yet to be attained, it is difficult to use structural modeling to determine how MinD and MinE interacts. Since aa 31-36 is highly variable among MinE homologues (Fig. 3.1), this could imply the N- and C-termini of MinE are linked by this short region as a flexible linker that has no structural properties. If this is the case, then it would be extremely important to determine the spatial orientation of the two termini with respect to each other, since it would have a profound effect on the understanding of how MinD and MinE can interact and help explain various unexplained phenomenon such as the ability of $MinE_{Ec(1-31)}$ to localize to the cell membrane (Ma *et al.*, 2003). Even though the C-terminus of *E. coli* MinE has been resolved by NMR, the possibility of "domain swapping" as a means of intermolecular dimerization as discussed is another reason why the full structure of MinE is required to further the current knowledge of MinE function. Thus, determining the complete structure of MinE will be critical and beneficial in furthering the current knowledge of cell division site selection.

In my studies, there were other noticeable differences between *E. coli* and gonococcal MinE. My analysis of $MinE_{Ng\text{-}K53A}$ and $MinE_{Ng\text{-}E67L}$ revealed that the K53 and E67 residues are important for $MinD_{Ng}$ interaction and are needed for $MinE_{Ng}$ to function properly. In contrast, the equivalent K52 and E66 residues in $MinE_{Ec}$ suggests that they are not (King *et al.*, 2000). It is unknown why these differences exist, particularly, since the C-

termini of both proteins have similar secondary structural content as determined by solution NMR (Ramos *et al.*, 2006). Further studies should be done to investigate the possibility that this result could be a subtle difference of the function of MinE from rod- and round-shaped microorganisms. In addition, while *E. coli* MinE can form rings and coils (Lackner *et al.*, 2003;Shih *et al.*, 2003), I did not observe such structures with $MinE_{Ng}$-GFP using pSRE-GFP (*minD*$_{Ng}$::*minE*$_{Ng}$-*gfp*) (Ramirez-Arcos *et al.*, 2002). Despite controlling expression by titering arabinose, fluorescence was consistently cytoplasmic (Fig. 3.15 A), unless the fusion protein was highly expressed (Fig. 3.15 B). The reason why $MinE_{Ng}$ rings have not been observed at lower expression levels is not clear; although it is possible that the GFP moiety (27 kDa) could mask the smaller $MinE_{Ng}$ (10 kDa) protein, *E. coli* MinE rings were still observed. This raises the possibility that gonococcal MinE activates $MinD_{Ng}$ in a different manner than *E. coli* MinE. More studies will have to be performed to investigate this anomaly.

MinE from different organisms may not have identical functions, even though they may be similar. These subtle differences may reflect on the possibility that MinE functions differently between rod- and round-shaped organisms. Studies have showed that *E. coli* MinE in a round *E. coli* strain (Δ*min*, Δ*rodA*) does not follow a pole-to-pole oscillation pattern; instead $MinE_{Ec}$ oscillates in a circular path (Corbin *et al.*, 2002). Min oscillation along one axis was only apparent once invagination occurred and the cells started to elongate due to replication (Corbin *et al.*, 2002). It may be possible that $MinE_{Ng}$ would cause MinD to oscillate along one axis in a single cell if $MinE_{Ng}$ were expressed in its own native background. Since mutant round *E. coli* cells (~ 3 μm) are much larger than *N. gonorrhoeae* (0.5-1.0 μm), the size of cells could also affect Min protein behaviour. Unfortunately, the

current genetic tools and fluorescence microscopy technology do not allow for live *in vivo* visualization of Min protein oscillation in small *N. gonorrhoeae* cells; as such, the lack of resolution necessary to observe the coiled subcellular architecture in *N. gonorrhoeae* has hampered research of possible Min_{Ng} oscillation in the gonococcus. Clearly, even though the general function of MinE in cell division seems to be conserved, how this function is carried out in different bacterial morphologies may vary.

Nonetheless, my research shows that $MinE_{Ng}$ is a very small protein (~ 10 kDa) that has a key role in ensuring proper cell division site selection. Although MinC and MinD are needed to prevent cell division from occurring throughout bacteria, MinE drives MinC and MinD oscillation so that the midcell of bacteria are clear of any of MinCD complexes, allowing for FtsZ polymerization and eventual divisome formation to take place. By mapping all of the results of this study and others (King *et al.*, 2000;Shih *et al.*, 2002;Zhao *et al.*, 1995) onto the solved NMR structure of the C-terminus of *E. coli* MinE (aa 31-88), a comparison of MinE findings can be made (Fig. 4.1 shows a dimer of $MinE_{Ec}$) (King *et al.*, 2000). Since a structure of the N-terminus of MinE has yet to be elucidated, it is not included in this figure; however, it is accepted that the N-terminus is responsible for MinD interaction (Ma *et al.*, 2003; this study). Despite many residues of $MinE_{Ng}$ being previously studied in their equivalents in *E. coli*, it is important to fully examine these residues by exposing mutants to a battery of protein-protein interaction assays, ATPase assays and microscopy. Even though K52 and E66 have been previously studied in *E. coli*, (equivalent to K53 and E67 of $MinE_{Ng}$), as being unimportant for $MinE_{Ec}$ function (King *et al.*, 2000), my analysis of these residues in $MinE_{Ng}$ revealed that $MinD_{Ng}$ can oscillate regardless of ATPase stimulation as long as interaction with $MinE_{Ng}$ is maintained. In addition, albeit the dimerization interface of MinE is most likely in the aa 38-53 domain of *E. coli* MinE

Figure 4.1. Comparison of MinE studies from *N. gonorrhoeae* and *E. coli* mapped onto the NMR structure of the C-terminus of *E. coli* MinE (aa 31-88). (A) Residues and domains identified from previous studies of $MinE_{Ec}$ (King *et al.*, 2000; Shih *et al.*, 2002; Zhao *et al.*, 1995) and this study. To highlight the studies of $MinE_{Ng}$ self-interaction, the dimer of this C-terminus is shown. The blue α-helix displays the domain believed to be important in $MinE_{Ec}$ self-interaction (King *et al.*, 2000). Its removal within gonococcal MinE disrupted self-interaction. The purple residues were mutated in $MinE_{Ng}$ (E46, V50, Y54) to proline which also disrupted self-interaction, while less extreme mutations to D45 and V49 to *E. coli* MinE did not disrupt $MinE_{Ec}$ dimerization, even though the propensity to form $MinE_{Ec}$ rings decreased (Shih *et al.*, 2002). The red residue was mutated (K53A) in $MinE_{Ng}$, showing that the mutant was less able to interact with $MinD_{Ng}$, causing a corresponding decrease in hydrolytic activity of the latter, while the mutation in $MinE_{Ec}$ (K52A) did not show any significant importance (King *et al.*, 2000). It is postulated that the cyan residues is a variable linker to the N-terminus of MinE due to the lack of conservation, while the orange residues are believed to be not important for $MinE_{Ec}$ function (Zhao *et al.*, 1995) (B) represents a 180° rotation of (A), showing studies of E66 of $MinE_{Ec}$ and E67 of $MinE_{Ng}$ (green), and the β-sheet (yellow) that is responsible for $MinE_{Ng}$ self-interaction (aa 74-78 of $MinE_{Ng}$). The N-terminus of MinE (aa 1-30) has yet to resolved as a visual structure and is therefore, not included in this figure.

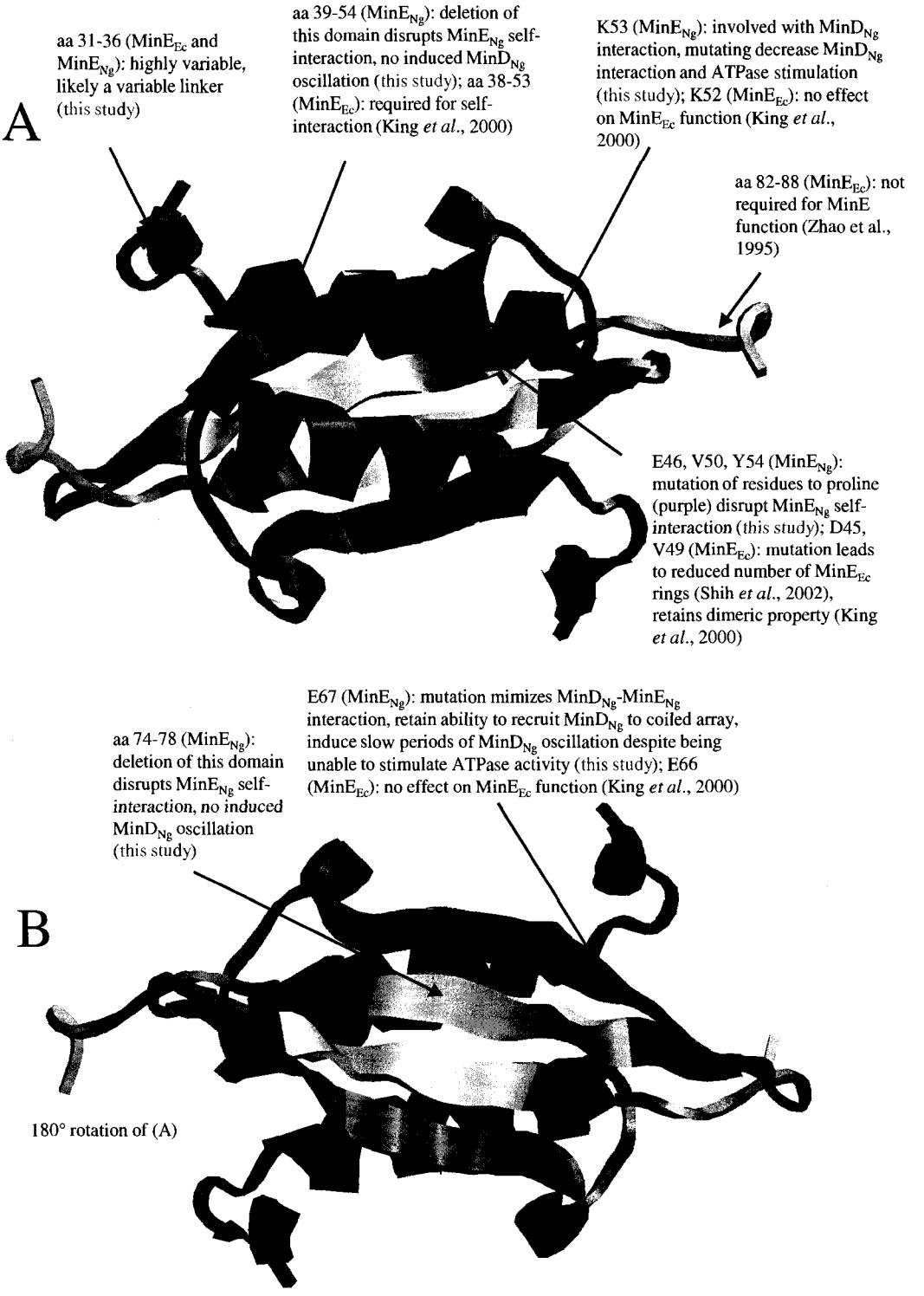
A
aa 31-36 ($MinE_{Ec}$ and $MinE_{Ng}$): highly variable, likely a variable linker (this study)
aa 39-54 ($MinE_{Ng}$): deletion of this domain disrupts $MinE_{Ng}$ self-interaction, no induced $MinD_{Ng}$ oscillation (this study); aa 38-53 ($MinE_{Ec}$): required for self-interaction (King *et al.*, 2000)
K53 ($MinE_{Ng}$): involved with $MinD_{Ng}$ interaction, mutating decrease $MinD_{Ng}$ interaction and ATPase stimulation (this study); K52 ($MinE_{Ec}$): no effect on $MinE_{Ec}$ function (King *et al.*, 2000)
aa 82-88 ($MinE_{Ec}$): not required for MinE function (Zhao et al., 1995)
E46, V50, Y54 ($MinE_{Ng}$): mutation of residues to proline (purple) disrupt $MinE_{Ng}$ self-interaction (this study); D45, V49 ($MinE_{Ec}$): mutation leads to reduced number of $MinE_{Ec}$ rings (Shih *et al.*, 2002), retains dimeric property (King *et al.*, 2000)
E67 ($MinE_{Ng}$): mutation mimizes $MinD_{Ng}$-$MinE_{Ng}$ interaction, retain ability to recruit $MinD_{Ng}$ to coiled array, induce slow periods of $MinD_{Ng}$ oscillation despite being unable to stimulate ATPase activity (this study); E66 ($MinE_{Ec}$): no effect on $MinE_{Ec}$ function (King *et al.*, 2000)
aa 74-78 ($MinE_{Ng}$): deletion of this domain disrupts $MinE_{Ng}$ self-interaction, no induced $MinD_{Ng}$ oscillation (this study)
B
180° rotation of (A)

(King *et al.*, 2000), it was not known if disrupting self-interaction caused MinE dysfunction, which this study has suggested.

Preliminary studies in our laboratory showed that the presence of the gonococcal MinC and MinD may be determined by which growth phase *N. gonorrhoeae* cells are in (unpublished data). This aspect of the study of Min proteins has never been conducted before; it will be interesting to determine if $MinE_{Ng}$ is regulated by growth phases as well. In addition, the laboratory is currently studying if $OxyR_{Ng}$ regulates the expression of gonococcal Min proteins. Unlike in *E. coli*, $oxyR_{Ng}$ is immediately located downstream of $minE_{Ng}$ (Fig. 1.13); studies have shown that $oxyR_{Ng}$ is indeed co-transcribed with the three min_{Ng} genes (data not shown). $OxyR_{Ng}$ encodes for a transcriptional regulator that represses catalase expression; hydrogen peroxide counters this repression, allowing for catalase production (Tseng *et al.*, 2003). Thus, it is possible that environmental conditions that include peroxides can affect the regulation of gonococcal Min proteins through $OxyR_{Ng}$. Previous research on other environmental factors such as anaerobiosis and urea have shown to influence the activity of the promoter regions upstream of each min_{Ng} gene (Ramirez-Arcos *et al.*, 2001a). Thus, there are many new exciting directions in studying gonococcal Min proteins.

Since other bacteria do not possess Min homologues, our laboratory is currently studying how cell division site selection occurs in the Gram-positive coccus *E. faecalis*, one such organism that does not encode for Min proteins. Thus, it is not surprising that another mechanism must have evolved that permits this organism, and others, in deciding the future site of cytokinesis. The Min system is an elegant mechanism of cell division site selection in bacteria that possess them; it will be even more interesting to see what other systems have evolved in other bacteria to deal with this important life process.

REFERENCES

Aarsman, M. E. G., Piette, A., Fraipont, C., Vinkenvleugel, T. M. F., Nguyen-Disteche, M., and Den Blaauwen, T. (2005) Maturation of the *Escherichia coli* divisome occurs in two steps. *Mol Microbiol* **55:** 1631-1645.

Addinall, S., Bi, E., and Lutkenhaus, J. (1996) FtsZ ring formation in fts mutants. *J Bacteriol* **178:** 3877-3884.

Addinall, S., Cao, C., and Lutkenhaus, J. (1997) FtsN, a late recruit to the septum in *Escherichia coli*. *Mol Microbiol* **25:** 303-309.

Addinall, S. G. and Holland, B. (2002) The tubulin ancestor, FtsZ, draughtsman, designer and driving force for bacterial cytokinesis. *J Mol Biol* **318:** 219-236.

Adler, H. I., Fisher, W. D., Cohen, A., and Hardigree, A. A. (1967) Miniature *Escherichia coli* cells deficient in DNA. *Proc Natl Acad Sci USA* **57:** 321-326.

Aldridge, C., Maple, J., and Moller, S. G. (2005) The molecular biology of plastid division in higher plants. *J Exp Bot* **56:** 1061-1077.

Anderson, D. E., Gueiros-Filho, F. J., and Erickson, H. P. (2004) Assembly dynamics of FtsZ rings in *Bacillus subtilis* and *Escherichia coli* and effects of FtsZ-regulating proteins. *J Bacteriol* **186:** 5775-5781.

Apicella, M. A., Ketterer, M., Lee, F. K. N., Zhou, D. G., Rice, P. A., and Blake, M. S. (1996) The pathogenesis of gonococcal urethritis in men: Confocal and immunoelectron microscopic analysis of urethral exudates from men infected with *Neisseria gonorrhoeae*. *J Infect Dis* **173:** 636-646.

Ausmees, N. and Jacobs-Wagner, C. (2003) Spatial and temporal control of differentiation and cell cycle progression in *Caulobacter crescentus*. *Annu Rev Microbiol* **57:** 225-247.

Aussel, L., Barre, F. X., Aroyo, M., Stasiak, A., Stasiak, A. Z., and Sherratt, D. (2002) FtsK is a DNA motor protein that activates chromosome dimer resolution by switching the catalytic state of the XerC and XerD recombinases. *Cell* **108:** 195-205.

Ayala, J. A., Garrido, T., de Pedro, M. A., and Vicente, M. (1994) Molecular biology of bacterial septation. In *Bacterial cell wall*. Ghuysen, J. M. and Hakenbeck, R. (ed.) Amsterdam: Elsevier, pp. 73-102.

Bartosik, A. A. and Jagura-Burdzy, G. (2005) Bacterial chromosome segregation. *Acta Biochim Polon* **52:** 1-34.

Begg, K., Dewar, S., and Donachie, W. (1995) A new *Escherichia coli* cell division gene, *ftsK*. *J Bacteriol* **177:** 6211-6222.

Ben Yehuda, S., Rudner, D. Z., and Losick, R. (2002) RacA, a bacterial protein that anchors chromosomes to the cell poles. *Science* **299:** 532-536.

Bernatchez, S., Francis, F., Salimnia, H., Beveridge, T., Li, H., and Dillon, J. R. (2000) Genomic, transcriptional and phenotypic analysis of *ftsE* and *ftsX* of *Neisseria gonorrhoeae*. *DNA Research* **7:** 75-81.

Bernhardt, T. G. and de Boer, P. A. J. (2003) The *Escherichia coli* amidase AmiC is a periplasmic septal ring component exported via the twin-arginine transport pathway. *Mol Microbiol* **48:** 1171-1182.

Bernhardt, T. G. and de Boer, P. A. J. (2004) Screening for synthetic lethal mutants in *Escherichia coli* and identification of EnvC (YibP) as a periplasmic septal ring factor with murein hydrolase activity. *Mol Microbiol* **52:** 1255-1269.

Bernhardt, T. G. and de Boer, P. A. J. (2005) SlmA, a nucleoid-associated, FtsZ binding protein required for blocking septal ring assembly over chromosomes in *E. coli*. *Mol Cell* **18:** 555-564.

Bi, E. and Lutkenhaus, J. (1993) Cell division inhibitors SulA and MinCD prevent formation of the FtsZ ring. *J Bacteriol* **175:** 1118-1125.

Bi, E. and Lutkenhaus, J. (1991) FtsZ ring structure associated with division in *Escherichia coli*. *Nature* **354:** 161-164.

Bigot, S., Corre, J., Louarn, J. M., Cornet, F., and Barre, F. X. (2004) FtsK activities in Xer recombination, DNA mobilization and cell division involve overlapping and separate domains of the protein. *Mol Microbiol* **54:** 876-886.

Brun, Y. V., Marczynski, G., and Shapiro, L. (1994) The expression of asymmetry during *Caulobacter* cell differentiation. *Annu Rev Biochem* **63:** 419-450.

Buddelmeijer, N. and Beckwith, J. (2002) Assembly of cell division proteins at the *E. coli* cell center. *Curr Opin Microbiol* **5:** 553-557.

Buddelmeijer, N. and Beckwith, J. (2004) A complex of the *Escherichia coli* cell division proteins FtsL, FtsB and FtsQ forms independently of its localization to the septal region. *Mol Microbiol* **52:** 1315-1327.

Cha, J. and Stewart, G. (1997) The *divIVA* minicell locus of *B. subtilis*. *J Bacteriol* **179:** 1671-1683.

Chen, A., Boulton, I. C., Pongoski, J., Cochrane, A., and Gray-Owen, S. D. (2003) Induction of HIV-1 long terminal repeat-mediated transcription by *Neisseria gonorrhoeae*. *Aids* **17:** 625-628.

Chen, J. C. and Beckwith, J. (2001) FtsQ, FtsL and FtsI require FtsK, but not FtsN, for co-localization with FtsZ during *Escherichia coli* cell division. *Mol Microbiol* **42:** 395-413.

Chen, J. C., Weiss, D. S., Ghigo, J., and Beckwith, J. (1999) Septal localization of FtsQ, an essential cell division protein in *Escherichia coli*. *J Bacteriol* **181:** 521-530.

Cheng, J., Sibley, C. D., Zaheer, R., and Finan, T. M. (2007) A *Sinorhizobium meliloti minE* mutant has an altered morphology and exhibits defects in legume symbiosis. *Microbiol* **153:** 375-387.

Chou, K. C., Nemethy, G., Rumsey, S., Tuttle, R. W., and Scheraga, H. A. (1985) Interactions between an alpha-helix and a beta sheet. Energetics of alpha/beta packing in proteins. *J Mol Biol* **186:** 591-609.

Corbin, B. D., Yu, X.-C., and Margolin, W. (2002) Exploring intracelluar space: function of the Min system in round-shaped *Escherichia coli*. *EMBO J* **21:** 1-11.

Cordell, S. C., Anderson, R. E., and Lowe, J. (2001) Crystal structure of the bacterial cell division inhibitor MinC. *EMBO J* **20:** 2454-2461.

Cordell, S. C. and Lowe, J. (2001) Crystal structure of the bacterial cell division regulator MinD. *FEBS Lett* **492:** 160-165.

Cordell, S. C., Robinson, E. J. H., and Lowe, J. (2003) Crystal structure of the SOS cell division inhibitor SulA and in complex with FtsZ. *Proc Natl Acad Sci USA* **100:** 7889-7894.

Daniel, R. A., Williams, A. M., and Errington, J. (1996) A complex four-gene operon containing essential cell division gene *pbpB* in *Bacillus subtilis*. *J Bacteriol* **178:** 2343-2350.

Datta, P., Dasgupta, A., Singh, A. K., Mukherjee, P., Kundu, M., and Basu, J. (2006) Interaction between FtsW and penicillin-binding protein 3 (PBP3) directs PBP3 to mid-cell, controls cell septation and mediates the formation of a trimeric complex involving FtsZ, FtsW and PBP3 in mycobacteria. *Mol Microbiol* **62:** 1655-1673.

Davie, E., Sydnor, K., and Rothfield, L. I. (1984) Genetic basis of minicell formation in *Escherichia coli* K-12. *J Bacteriol* **158:** 1202-1203.

de Boer, P. and Crossley, R. (1989) A division inhibitor and a topological specificity factor coded for by the minicell locus determine proper placement of the division septum in *Escherichia coli*. *Cell* **56:** 641-649.

de Boer, P., Crossley, R., and Rothfield, L. (1992) Roles of MinC and MinD in the site-specific septation block mediated by the MinCDE system of *Escherichia coli*. *J Bacteriol* **174:** 63-70.

de Boer, P., Crossley, R., and Rothfield, L. (1988) Isolation and properties of *minB*, a complex genetic locus involved in correct placement of the division site in *Escherichia coli*. *J Bacteriol* **170:** 2106-2112.

de Boer, P., Crossley, R. E., Hand, A. R., and Rothfield, L. (1991) The MinD protein is a membrane ATPase required for the correct placement of the *Escherichia coli* division site. *EMBO J* **10:** 4371-4380.

Den Blaauwen, T., Buddelmeijer, N., Aarsman, M. E. G., Hameete, C. M., and Nanninga, N. (1999) Timing of FtsZ assembly in *Escherichia coli. J Bacteriol* **181:** 5167-5175.

Di Lallo, G., Castagnoli, L., Ghelardini, P., and Paolozzi, L. (2001) A two-hybrid system based on chimeric operator recognition for studying protein homo/heterodimerization in *Escherichia coli. Microbiol* **147:** 1651-1656.

Di Lallo, G., Fagioli, M., Barionovi, D., Ghelardini, P., and Paolozzi, L. (2003) Use of a two-hybrid assay to study the assembly of a complex multicomponent protein machinery: bacterial septosome differentiation. *Microbiol* **149:** 3353-3359.

Donachie, W. (1993) The cell cycle of *Escherichia coli. Annu Rev Microbiol* 199-230.

Donachie, W. D. (2001) Co-ordinate regulation of the *Escherichia coli* cell cycle or The cloud of unknowing. *Mol Microbiol* **40:** 779-785.

Draper, G. C. and Gober, J. W. (2002) Bacterial chromosome segregation. *Annu Rev Microbiol* **56:** 567-597.

Drew, D. A., Osborn, M. J., and Rothfield, L. I. (2005) A polymerization-depolymerization model that accurately generates the self-sustained oscillatory system involved in bacterial division site placement. *Proc Natl Acad Sci USA* **102:** 6114-6118.

Edwards, D. and Errington, J. (1997) The *Bacillus subtilis* DivIVA protein targets to the division septum and controls the site specificity of cell division. *Mol Microbiol* **25:** 905-915.

Elkins, C., Carbonetti, N. H., Varela, V. A., Stirewalt, D., Klapper, D. G., and Sparling, P. F. (1992) Antibodies to N-terminal peptides of gonococcal porin are bactericidal when gonococcal lipopolysaccharide is not sialylated. *Mol Microbiol* **6:** 2617-2628.

Eng, N. F., Szeto, J., Acharya, S., Tessier, D., and Dillon, J. A. R. (2006) The C-terminus of MinE from *Neisseria gonorrhoeae* acts as a topological specificity factor by modulating MinD activity in bacterial cell division. *Res Microbiol* **157:** 333-344.

Errington, J., Daniel, R. A., and Scheffers, D. J. (2003) Cytokinesis in bacteria. *Microbiol Mol Biol Rev* **67:** 52-65.

Espeli, O., Nurse, P., Levine, C., Lee, C., and Marians, K. J. (2003) SetB: an integral membrane protein that affects chromosome segregation in *Escherichia coli. Mol Microbiol* **50:** 495-509.

Fadda, D., Santona, A., D'Ulisse, V., Ghelardini, P., Ennas, MG., Whalen, MB. *et al.* (2007) *Streptococcus pneumoniae* DivIVA: localization and interactions in a MinCD free context. *J Bacteriol* **189:** 1288-1298.

Feucht, A., Lucet, I., Yudkin, M. D., and Errington, J. (2001) Cytological and biochemical characterization of the FtsA cell division protein of *Bacillus subtilis*. *Mol Microbiol* **40:** 115-125.

Figge, R. M., Easter, J., and Gober, J. W. (2003) Productive interaction between the chromosome partitioning proteins, ParA and ParB, is required for the progression of the cell cycle in *Caulobacter crescentus*. *Mol Microbiol* **47:** 1225-1237.

Fitz-James, P. (1964) Thin sections of dividing *Neisseria gonorrhoeae*. *J Bacteriol* **87:** 1477-1482.

Fleischmann, R. D., Adams, M. D., White, O., Clayton, R. A., Kirkness, E. F., Kerlavage, A. R. *et al.* (1995) Whole-Genome Random Sequencing and Assembly of Haemophilus-Influenzae Rd. *Science* **269:** 496-512.

Francis, F., Ramirez-Arcos, S., Salimnia, H., Victor, C., and Dillon, J. A. R. (2000) Organization and transcription of the division cell wall (*dcw*) cluster in *Neisseria gonorrhoeae*. *Gene* **251:** 141-151.

Fu, X., Shih, Y.-L., Zhang, Y., and Rothfield, L. I. (2001) The MinE ring required for proper placement of the division site is a mobile structure that changes its cellular location during the *Escherichia coli* division cycle. *Proc Natl Acad Sci USA* **98:** 980-985.

Fussenegger, M., Kahrs, A. F., Facius, D., and Meyer, T. F. (1996) Tetrapac (*tpc*), a novel genotype of *Neisseria gonorrhoeae* affecting epithelial cell invasion, natural transformation competence and cell separation. *Mol Microbiol* **19:** 1357-1372.

Geissler, B., Elraheb, D., and Margolin, W. (2003) A gain-of-function mutation in *ftsA* bypasses the requirement for the essential cell division gene *zipA* in *Escherichia coli*. *Proc Natl Acad Sci USA* **100:** 4197-4202.

Gerbase, A. C., Rowley, J. T., Heymann, D. H. L., Berkley, S. F. B., and Piot, P. (1998) Global prevalence and incidence estimates of selected curable STDs. *Sex Trans Infect* **74:** S12-S16.

Goehring, N. W., Gonzalez, M. D., and Beckwith, J. (2006) Premature targeting of cell division proteins to midcell reveals hierarchies of protein interactions involved in divisome assembly. *Mol Microbiol* **61:** 33-45.

Goodman, S. D. and Scocca, J. J. (1988) Identification and arrangement of the DNA sequences recognized in specific transformation of *Neisseria gonorrhoeae*. *Proc Natl Acad Sci USA* **85:** 6982-6986.

Gordon, G. S., Sitnikov, D., Webb, C. D., Teleman, A., Straight, A., Losick, R. *et al.* (1997) Chromosome and low copy plasmid segregation in *E. coli*: Visual evidence for distinct mechanisms. *Cell* **90:** 1113-1121.

Greco, V. (2004) *Functional analysis of the role of conserved glycine residues and N-terminal motifs in the cell division inhibitor MinC from Neisseria gonorrhoeae.* Ottawa, Ontario: University of Ottawa, M.Sc. thesis.

Greco-Stewart, V., Ramirez-Arcos, S., Liao, M., and Dillon, J. R. (2007) N terminus determinants of MinC from *Neisseria gonorrhoeae* mediate interaction with FtsZ but do not affect interaction with MinD or homodimerization. *Arch Microb* **in print**.

Gueiros, F. J. and Losick, R. (2002) A widely conserved bacterial cell division protein that promotes assembly of the tubulin-like protein FtsZ. *Genes Dev* **16:** 2544-2556.

Haeusser, D. P., Schwartz, R. L., Smith, A. M., Oates, M. E., and Levin, P. A. (2004) EzrA prevents aberrant cell division by modulating assembly of the cytoskeletal protein FtsZ. *Mol Microbiol* **52:** 801-814.

Hale, C. and de Boer, P. (1997) Direct binding of FtsZ to ZipA, an essential component of the septal ring structure that mediates cell division in *E. coli. Cell* **88:** 175-185.

Hale, C. and de Boer, P. (1999) Recruitment of ZipA to the septal ring of *Escherichia coli* is dependent on FtsZ and independent of FtsA. *J Bacteriol* **181:** 167-176.

Hale, C. A., Meinhardt, H., and de Boer, P. A. (2001) Dynamic localization cycle of the cell division regulator MinE in *Escherichia coli. EMBO J* **20:** 1563-1572.

Harder, K. W., Owen, P., Wong, L. K., Aebersold, R., Clark-Lewis, I., and Jirik, F. R. (1994) Characterization and kinetic analysis of the intracellular domain of human protein tyrosine phosphatase beta (HPTP beta) using synthetic phosphopeptides. *Biochem J* **298:** 395-401.

Harry, E. J. and Lewis, P. J. (2003) Early targeting of Min proteins to the cell poles in germinated spores of *Bacillus subtilis*: evidence for division apparatus-independent recruitment of Min proteins to the division site. *Mol Microbiol* **47:** 37-48.

Hayashi, I., Oyama, T., and Morikawa, K. (2001) Structural and functional studies of MinD ATPase: implications for the molecular recognition of the bacterial cell division apparatus. *EMBO J* **20:** 1819-1828.

Henriques, A. O., Delencastre, H., and Piggot, P. J. (1992) A *Bacillus subtilis* morphogene cluster that includes *spoVE* is homologous to the *mra* region of *Escherichia coli. Biochimie* **74:** 735-748.

Henriques, A. O., Glaser, P., and Piggot, P. J. M. C. P. Jr. (1998) Control of cell shape and elongation by the *rodA* gene in *Bacillus subtilis. Mol Microbiol* **28:** 235-247.

Hiraga, S., Ichinose, C., Onogi, T., Niki, H., and Yamazoe, M. (2000) Bidirectional migration of SeqA-bound hemimethylated DNA clusters and pairing of *oriC* copies in *Escherichia coli. Genes Cells* **5:** 327-341.

Holtje, J. (1998) Growth of the stress-bearing and shape-maintaining murein sacculus of *Escherichia coli*. *Microbiol Mol Biol Rev* **62:** 181-203.

Howard, M., Rutenberg, A. D., and de Vet, S. (2001) Dynamic compartmentalization of bacteria: accurate division in *E. coli*. *Phys Rev Lett* **87:** 278102.

Hu, Z., Gogol, E. P., and Lutkenhaus, J. (2002) Dynamic assembly of MinD on phospholipid vesicles regulated by ATP and MinE. *Proc Natl Acad Sci U S A*.

Hu, Z. and Lutkenhaus, J. (2003) A conserved sequence at the C-terminus of MinD is required for binding to the membrane and targeting MinC to the septum. *Mol Microbiol* **47:** 345-355.

Hu, Z. and Lutkenhaus, J. (2000) Analysis of MinC reveals two independent domains involved in interaction with MinD and FtsZ. *J Bacteriol* **182:** 3965-3971.

Hu, Z. and Lutkenhaus, J. (1999) Topological regulation of cell division in *Escherichia coli* involves rapid pole to pole oscillation of the division inhibitor MinC under the control of MinD and MinE. *Mol Microbiol* **34:** 82-90.

Hu, Z. and Lutkenhaus, J. (2001) Topological regulation of cell division in *E. coli*: spatiotemporal oscillation of MinD requires stimulation of its ATPase by MinE and phospholipid. *Mol Cell* **7:** 1337-1343.

Hu, Z., Mukherjee, A., Pichoff, S., and Lutkenhaus, J. (1999) The MinC component of the division site selection system in *Escherichia coli* interacts with FtsZ to prevent polymerization. *Proc Natl Acad Sci USA* **96:** 14819-14824.

Hu, Z., Saez, C., and Lutkenhaus, J. (2003) Recruitment of MinC, an inhibitor of Z-ring formation, to the membrane in *Escherichia coli*: Role of MinD and MinE. *J Bacteriol* **185:** 196-203.

Huang, J., Cao, C., and Lutkenhaus, J. (1996) Interaction between FtsZ and inhibitors of cell division. *J Bacteriol* **178:** 5080-5085.

Ikeda, M., Sato, T., Wachi, M., Jung, H. K., Ishino, F., Kobayashi, Y. *et al.* (1989) Structural similarity among *Escherichia coli* FtsW and RodA proteins and *Bacillus subtilis* SpoVE protein, which function in cell division, cell elongation, and spore formation, respectively. *J Bacteriol* **171:** 6375-6378.

Itoh, R., Fujiwara, M., Nagata, N., and Yoshida, S. (2001) A chloroplast protein homologous to the eubacterial topological specificity factor MinE plays a role in chloroplast division. *Plant Physiol* **127:** 1644-1655.

Jensen, R. B. (2006) Coordination between chromosome replication, segregation, and cell division in *Caulobacter crescentus*. *J Bacteriol* **188:** 2244-2253.

Jensen, R. B. and Shapiro, L. (1999) Chromosome segregation during the prokaryotic cell division cycle. *Curr Opin Cell Biol* **11:** 726-731.

Jensen, R. B., Wang, S. C., and Shapiro, L. (2002) Dynamic localization of proteins and DNA during a bacterial cell cycle. *Nat Rev Mol Cell Biol* **3:** 167-176.

Johnson, J. E., Lackner, L. L., Hale, C. A., and de Boer, P. A. J. (2004) ZipA is required for targeting of (D)MinC/DicB, but not (D)MinC/MinD, complexes to septal ring assemblies in *Escherichia coli. J Bacteriol* **186:** 2418-2429.

Johnson, M. L., Correia, J. J., Yphantis, D. A., and Halvorson, H. R. (1981) Analysis of data from the analytical ultracentrifuge by non-linear least-squares techniques. *Biophys J* **36:** 575-588.

Juni, E. and Heym, G. (1977) Simple method for distinguishing gonococcal colony types. *J Clin Microbiol* **6:** 511-517.

Karimova, G., Dautin, N., and Ladant, D. (2005) Interaction network among *Escherichia coli* membrane proteins involved in cell division as revealed by bacterial two-hybrid analysis. *J Bacteriol* **187:** 2233-2243.

Kellogg, Jr. D. S., Peacock, Jr., Deacon, W. F., Brown, L., and Pirkle, C. I. (1963) *Neisseria gonorrhoeae* I. Virulence genetically linked to clonal variation. *J Bacteriol* **85:** 1274-1279.

King, G. F., Rowland, S. L., Pan, B., Mackay, J. P., Mullen, G. P., and Rothfield, L. I. (1999) The dimerization and topological specificity functions of MinE reside in a structurally autonomous C-terminal domain. *Mol Microbiol* **31:** 1161-1169.

King, G. F., Shih, Y. L., Maciejewski, M. W., Bains, N. P., Pan, B., Rowland, S. L. *et al.* (2000) Structural basis for the topological specificity function of MinE. *Nat Struct Biol* **7:** 1013-1017.

Kini, R. M. and Evans, H. J. (1995) A hypothetical structural role for proline residues in the flanking segments of protein-protein interaction sites. *Biochem Biophys Res Comm* **212:** 1115-1124.

Koonin, E. V. (1993) A superfamily of ATPases with diverse functions containing either classical or deviant ATP-binding motif. *J Mol Biol* **229:** 1165-1174.

Krogsgaard, M., Prado, N., Adams, E. J., He, X. L., Chow, D. C., Wilson, D. B. *et al.* (2003) Evidence that structural rearrangements and/or flexibility during TCR binding can contribute to T cell activation. *Mol Cell* **12:** 1367-1378.

Kruse, K. (2002) A dynamic model for detemining the middle of *Escherichia coli. Biophys J* **82:** 618-627.

Kupsch, E. M., Aubel, D., Gibbs, C. P., Kahrs, A. F., Rudel, T., and Meyer, T. F. (1996) Construction of Hermes shuttle vectors: A versatile system useful for genetic

complementation of transformable and non-transformable *Neisseria* mutants. *Mol Gen Genet* **250:** 558-569.

Lackner, L. L., Raskin, D. M., and de Boer, P. A. (2003) ATP-dependent interactions between *Escherichia coli* Min proteins and the phospholipid membrane *in vitro*. *J Bacteriol* **185:** 735-749.

Lara, B., Rico, A. I., Petruzzelli, S., Santona, A., Dumas, J., Biton, J. *et al.* (2005) Cell division in cocci: localization and properties of the *Streptococcus pneumoniae* FtsA protein. *Mol Microbiol* **55:** 699-711.

Laue, T. M., Shah, B. D., Ridgeway, T. M., and Pelletier, S. L. (1991) Computer-aided interpretation of analytical sedimentation data for proteins. In *Analytical Ultracentrifugation in Biochemistry and Polymer Science*. Harding, S. E., Rowe, A. J., and Horton, J. C. (ed.) Cambridge, UK: R. Soc. Chem., pp. 90-125.

Laue, T. M. and Stafford, W. F. (1999) Modern applications of analytical ultracentrifugation. *Annu Rev Biophys Biomol Struct* **28:** 75-100.

Lemon, K. P. and Grossman, A. D. (1998) Localization of bacterial DNA polymerase: evidence for a factory model of replication. *Science* **282:** 1516-1519.

Lemon, K. P. and Grossman, A. D. (2001) The extrusion-capture model for chromosome partitioning in bacteria. *Genes Dev* **15:** 2031-2041.

Levin, P. A., Kurtser, I. G., and Grossman, A. D. (1999) Identification and characterization of a negative regulator of FtsZ ring formation in *Bacillus subtilis*. *Proc Natl Acad Sci USA* **96:** 9642-9647.

Lin, D. C. H. and Grossman, A. D. (1998) Identification and characterization of a bacterial chromosome partitioning site. *Cell* **92:** 675-685.

Lin, Z. and Mallavia, L. P. (1998) Membrane association of active plasmid partitioning protein A in *Escherichia coli*. *J Biol Chem* **273:** 11302-11312.

Lowe, J. and Amos, L. (1998) Crystal structure of the bacterial cell-division protein FtsZ. *Nature* **391:** 203-206.

Lutkenhaus, J. and Sundaramoorthy, M. (2003) MinD and role of the deviant Walker A motif, dimerization and membrane binding in oscillation. *Mol Microbiol* **48:** 295-303.

Ma, L. Y., King, G., and Rothfield, L. (2003) Mapping the MinE site involved in interaction with the MinD division site selection protein of *Escherichia coli*. *J Bacteriol* **185:** 4948-4955.

Ma, L. Y., King, G. F., and Rothfield, L. (2004) Positioning of the MinE binding site on the MinD surface suggests a plausible mechanism for activation of the *Escherichia coli* MinD ATPase during division site selection. *Mol Microbiol* **54:** 99-108.

Ma, X., Ehrhardt, D., and Margolin, W. (1996) Colocalization of cell division proteins FtsZ and FtsA to cytoskeletal structures in living *Escherichia coli* cells by using green fluorescent protein. *Proc Natl Acad Sci USA* **93:** 12998-13003.

Margolin, W. (2001) Spatial regulation of cytokinesis in bacteria. *Curr Opin Microbiol* **4:** 647-652.

Margolin, W. (2005) FtsZ and the division of prokaryotic cells and organelles. *Nat Rev Mol Cell Biol* **6:** 862-871.

Marston, A., Thomaides, H., Edwards, D., Sharpe, M., and Errington, J. (1998) Polar localization of the MinD protein of *Bacillus subtilis* and its role in selection of the mid-cell division site. *Genes Dev* **12:** 3419-3430.

Marston, A. L. and Errington, J. (1999) Selection of the midcell division site in *Bacillus subtilis* through MinD-dependent polar localization and activation of MinC. *Mol Microbiol* **33:** 84-96.

Massidda, O., Anderluzzi, D., Friedli, L., and Feger, G. (1998) Unconventional organization of the division and cell wall gene cluster of *Stretococcus pneumoniae*. *Microbiol* **144:** 3069-3078.

Mazouni, K., Domain, F., Cassier-Chauvat, C., and Chauvat, F. (2004) Molecular analysis of the key cytokinetic components of cyanobacteria: FtsZ, ZipN and MinCDE. *Mol Microbiol* **52:** 1145-1158.

Meinhardt, H. and de Boer, P. A. (2001) Pattern formation in *Escherichia coli*: a model for the pole-to-pole oscillations of Min proteins and the localization of the division site. *Proc Natl Acad Sci USA* **98:** 14202-14207.

Mengin-Lecreulx, D., Ayala, J., Bouhss, A., van Heijenoort, J., Parquet, C., and Hara, H. (1998) Contribution of the Pmra promoter to expression of genes in the *Escherichia coli mra* cluster of cell envelope biosynthesis and cell division genes. *J Bacteriol* **180:** 4406-4412.

Merz, A. J. and So, M. (2000) Interactions of pathogenic Neisseriae with epithelial cell membranes. *Annu Rev Cell Dev Biol* **16:** 423-457.

Messer, W. (2002) The bacterial replication initiator DnaA. DnaA and oriC, the bacterial mode to initiate DNA replication. *FEMS Microbiol Rev* **26:** 355-374.

Mileykovskaya, E., Fishov, I., Fu, X., Corbin, B. D., Margolin, W., and Dowhan, W. (2003) Effects of phospholipid composition on MinD-membrane interactions *in vitro* and *in vivo*. *J Biol Chem* **278:** 22193-22198.

Miller, J. H. (1972) Assay of β-galactosidase. In *Experiments in Molecular Genetics*. Miller, J. H. (ed.) New York: Cold Spring Harbor Laboratory, Cold Spring Harbor, pp. 352-355.

Mingorance, J., Tamames, J., and Vicente, M. (2004) Genomic channeling in bacterial cell division. *J Mol Recognit* **17:** 481-487.

Miroux, B. and Walker, J. E. (1996) Over-production of proteins in *Escherichia coli*: mutant hosts that allow synthesis of some membrane proteins and globular proteins at high levels. *J Mol Biol* **260:** 289-298.

Miyagishima, S. Y., Nozaki, H., Nishida, K., Nishida, K., Matsuzaki, M., and Kuroiwa, T. (2004) Two types of FtsZ proteins in mitochondria and red-lineage chloroplasts: The duplication of FtsZ is implicated in endosymbiosis. *J Mol Evol* **58:** 291-303.

Moller-Jensen, J., Jensen, R. B., Lowe, J., and Gerdes, K. (2002) Prokaryotic DNA segregation by an actin-like filament. *EMBO J* **21:** 3119-3127.

Mukherjee, A., Dai, K., and Lutkenhaus, J. (1993) *Escherichia coli* cell division protein FtsZ is a guanine nucleotide binding protein. *Proc Natl Acad Sci USA* **90:** 1053-1057.

Nanninga, N. (1998) Morphogenesis of *Escherichia coli*. *Microbiol Mol Biol Rev* **62:** 110-129.

Niki, H., Jaffe, A., Imamura, R., Ogura, T., and Hiraga, S. (1991) The new gene mukB codes for a 177 kd protein with coiled-coil domains involved in chromosome partioning of *E. coli*. *EMBO J* **10:** 183-193.

Oliva, M. A., Cordell, S. C., and Lowe, J. (2004) Structural insights into FtsZ protofilament formation. *Nat Struct Mol Biol* **11:** 1243-1250.

Osteryoung, K. W. and Nunnari, J. (2003) The division of endosymbiotic organelles. *Science* **302:** 1698-1704.

Pagotto, F., Salimnia, H., Totten, P. A., and Dillon, J. R. (2000) Development of a stable shuttle vector for *Neisseria gonorrhoeae, Haemophilus sp.* and other bacteria. *Gene* **244:** 13-19.

Perry, S. E. and Edwards, D. H. (2004) Identification of a polar targeting determinant for *Bacillus subtilis* DivIVA. *Mol Microbiol* **54:** 1237-1249.

Picard, F. J. and Dillon, J. R. (1989) Biochemical and genetic studies with arginine and proline auxotypes of *Neisseria gonorrhoeae*. *Can J Microbiol* **35:** 1069-1075.

Pichoff, S. and Lutkenhaus, J. (2002) Unique and overlapping roles for ZipA and FtsA in septal ring assembly in *Escherichia coli*. *EMBO J* **21:** 685-693.

Pichoff, S. and Lutkenhaus, J. (2005) Tethering the Z ring to the membrane through a conserved membrane targeting sequence in FtsA. *Mol Microbiol* **55:** 1722-1734.

Pichoff, S., Vollrath, B., Touriol, C., and Bouche, J. (1995) Deletion analysis of gene *minE* which encodes the topological specificity factor of cell division in *Escherichia coli. Mol Microbiol* **18:** 321-329.

Pinho, M. G. and Errington, J. (2004) A divIVA null mutant of *Staphylococcus aureus* undergoes normal cell division. *FEMS Microbiol Lett* **240:** 145-149.

Pringle, R., Adams, A. E., Drubin, D. G., and Haarer, B. K. (1991) Immunofluorescence methods for yeast. *Methods Enzymol* **194:** 565-602.

Pucci, M., Thanassi, J., Discotto, L., Kessler, R., and Dougherty, T. (1997) Identification and characterization of cell wall-cell division gene clusters in pathogenic gram-positive cocci. *J Bacteriol* **179:** 5632-5635.

Ramirez-Arcos, S., Greco, V., Douglas, H., Tessier, D., Fan, D., Szeto, J. *et al.* (2004) Conserved glycines in the C terminus of MinC proteins are implicated in their functionality as cell division inhibitors. *J Bacteriol* **186:** 2841-2855.

Ramirez-Arcos, S., Liao, M., Marthaler, S., Rigden, M., and Dillon, J. A. R. (2005) *Enterococcus faecalis divIVA*: an essential gene involved in cell division, cell growth and chromosome segregation. *Microbiol* **151:** 1381-1393.

Ramirez-Arcos, S., Salimnia, H., Bergevin, I., Paradisa, M., and Dillon, J. A. (2001a) Expression of *Neisseria gonorrhoeae* cell division genes *ftsZ, ftsE* and *minD* is influenced by environmental conditions. *Res Microbiol* **152:** 781-791.

Ramirez-Arcos, S., Szeto, J., Beveridge, T. J., Victor, C., Francis, F., and Dillon, J. R. (2001b) Deletion of the cell division inhibitor MinC results in lysis of *Neisseria gonorrhoeae. Microbiol* **147:** 225-237.

Ramirez-Arcos, S., Szeto, J., Dillon, J. R., and Margolin, W. (2002) Conservation of dynamic localization among MinD and MinE orthologs: oscillation of *Neisseria gonorrhoeae* proteins in *Esherichia coli. Mol Microbiol* **46:** 493-504.

Ramos, A., Adham, S. A. I., and Gil, J. A. (2003) Cloning and expression of the inorganic pyrophosphatase gene from the amino acid producer *Brevibacterium lactofermentum* ATCC 13869. *FEMS Microbiol Lett* **225:** 85-92.

Ramos, D., Ducat, T., Cheng, J., Eng, N. F., Dillon, J. A. R., and Goto, N. K. (2006) Conformation of the cell division regulator MinE: Evidence for interactions between the topological specificity and anti-minCD domains. *Biochem* **45:** 4593-4601.

Raskin, D. M. and de Boer, P. A. J. (1999b) Rapid pole-to-pole oscillation of a protein required for directing division to the middle of *Escherichia coli. Proc Natl Acad Sci USA* **96:** 4971-4976.

Raskin, D. M. and de Boer, P. A. J. (1999a) MinDE-dependent pole-to-pole oscillation of division inhibitor MinC in *Escherichia coli. J Bacteriol* **181:** 6419-6424.

Raskin, D. M. and de Boer, P. A. J. (1997) The MinE ring: an FtsZ-independent cell structure required for selection of the correct division site in *E. coli*. *Cell* **91:** 685-694.

RayChaudhuri, C. and Park, J. (1992) *Escherichia coli* cell-division gene *ftsZ* encodes a novel GTP-binding protein. *Nature* **359:** 251-256.

RayChaudhuri, D. (1999) ZipA is a MAP-Tau homolog and is essential for structural integrity of the cytokinetic FtsZ ring during bacterial cell division. *EMBO J* **18:** 2372-2383.

Reddy, M. (2007) Role of FtsEX in cell division of *Escherichia coli*: viability of *ftsEX* mutants is dependent on functional SufI or high osmotic strength. *J Bacteriol* **189:** 98-108.

Redick, S. D., Stricker, J., Briscoe, G., and Erickson, H. P. (2005) Mutants of FtsZ targeting the protofilament interface: Effects on cell division and GTPase activity. *J Bacteriol* **187:** 2727-2736.

Rico, A. I., Garcia-Ovalle, M., Mingorance, J., and Vicente, M. (2004) Role of two essential domains of *Escherichia coli* FtsA in localization and progression of the division ring. *Mol Microbiol* **53:** 1359-1371.

Roberts, M., Piot, P., and Falkow, S. (1979) Ecology of Gonococcal Plasmids. *J Gen Microbiol* **114:** 491-494.

Roe, B. A., Lin, S. P., Song, L., Yuan, X., Clifton, S., Ducey, T. *et al.* (2000) Gonococcal Genome Sequencing Project (Funded by USPHS/ NIH grant # AI 38399). *University of Oklahoma.*

Rowland, S. L., Fu, X., Sayed, M. A., Zhang, Y., Cook, W. R., and Rothfield, L. I. (2000) Membrane redistribution of the *Escherichia coli* MinD protein induced by MinE. *J Bacteriol* **182:** 613-619.

Sakai, N., Yao, M., Itou, H., Watanabe, N., Yumoto, F., Tanokura, M. *et al.* (2001) The three-dimensional structure of septum site-determining protein MinD from *Pyrococcus horikoshii* OT3 in complex with Mg-ADP. *Structure* **9:** 817-826.

Salimnia, H., Radia, A., Bernatchez, S., and Dillon, J. R. (2000) Characterization of the *ftsZ* cell division gene of *Neisseria gonorrhoeae*: expression and localization in *E. coli* and *N. gonorrhoeae*. *Arch Microbiol* **173:** 10-20.

Sambrook, J., Fritsch, E. F., and Maniatis, T. (1989) *Molecular Cloning, 2nd edition. A Laboratory Manual.* Cold Spring Harbour, New York: Cold Spring Harbour Press.

Sambrook, J. and Russell D.W. (2001) *Molecular cloning: a laboratory manual.* Cold Spring Harbour, New York: Cold Spring Harbour Laboratory Press.

Sanchez, M., Valencia, A., Ferrandiz, M., Sander, C., and Vicente, M. (1994) Correlation between the structure and biochemical activities of FtsA, an essential cell division protein of the actin family. *EMBO J* **13:** 4919-4925.

Sanchez-Pulido, L., Devos, D., Genevrois, S., Vicente, M., and Valencia, A. (2003) POTRA: a conserved domain in the FtsQ family and a class of beta-barrel outer membrane proteins. *Trends Biochem Sciences* **28:** 523-526.

Sawitzke, J. and Austin, S. (2001) An analysis of the factory model for chromosome replication and segregation in bacteria. *Mol Microbiol* **40:** 786-794.

Schindelin, N., Kisker, C., Sehlessman, J. L., Howard, J. B., and Rees, D. C. (1997) Structure of ADP center dot AIF(4)(-)-stabilized nitrogenase complex and its implications for signal transduction. *Nature* **387:** 370-376.

Schmidt, K. L., Peterson, N. D., Kustusch, R. J., Wissel, M. C., Graham, B., Phillips, G. J. *et al.* (2004) A predicted ABC transporter, FtsEX, is needed for cell division in *Escherichia coli*. *J Bacteriol* **186:** 785-793.

Selinger, D. W., Saxena, R. M., Cheung, K. J., Church, G. M., and Rosenow, C. (2003) Global RNA half-life analysis in *Escherichia coli* reveals positional patterns of transcript degradation. *Genome Res* **13:** 216-223.

Shen, Y., Chou, C. Y., Chang, G. G., and Tong, L. (2006) Is dimerization required for the catalytic activity of bacterial biotin carboxylase? *Mol Cell* **22:** 807-818.

Shih, Y. L., Fu, X., King, G. F., Le, T., and Rothfield, L. (2002) Division site placement in *E.coli*: mutations that prevent formation of the MinE ring lead to loss of the normal midcell arrest of growth of polar MinD membrane domains. *EMBO J* **21:** 3347-3357.

Shih, Y. L., Kawagishi, I., and Rothfield, L. (2005) The MreB and Min cytoskeletal-like systems play independent roles in prokaryotic polar differentiation. *Mol Microbiol* **58:** 917-928.

Shih, Y. L., Le, T., and Rothfield, L. (2003) Division site selection in *Escherichia coli* involves dynamic redistribution of Min proteins within coiled structures that extend between the two cell poles. *Proc Natl Acad Sci USA* **100:** 7865-7870.

Shiomi, D. and Margolin, W. (2007) The C-terminal domain of MinC inhibits assembly of the Z ring in *Escherichia coli*. *J Bacteriol* **189:** 236-243.

Small, E., Marrington, R., Rodger, A., Scott, D. J., Sloan, K., Roper, D. *et al.* (2007) FtsZ polymer-bundling by the *Escherichia coli* ZapA orthologue, YgfE, involves a conformational change in bound GTP. *J Mol Biol* **369:** 210-221.

Snapper, C. M., Rosas, F. R., Kehry, M. R., Mond, J. J., and Wetzler, L. M. (1997) Neisserial porins may provide critical second signals to polysaccharide-activated murine B cells for induction of immunoglobulin secretion. *Infect Immun* **65:** 3203-3208.

Snyder, L. A. S., Saunders, N. J., and Shafer, W. M. (2001) A putatively phase variable gene (*dca*) required for natural competence in *Neisseria gonorrhoeae* but not *Neisseria*

meningitidis is located within the division cell wall (*dcw*) gene cluster. *J Bacteriol* **183:** 1233-1241.

Snyder, L. A. S., Shafer, W. M., and Saunders, N. J. (2003) Divergence and transcriptional analysis of the division cell wall (*dcw*) gene cluster in *Neisseria* spp. *Mol Microbiol* **47:** 431-441.

Sparling, P. F. (1999) Biology of *Neisseria gonorrhoeae*. In *Sexually transmitted diseases*. Holmes, K. K., Mardh, P. A., Sparling, P. F., Lemon, S. M., Stamm, W. E., Piot, P. *et al.* (ed.) New York: McGraw-Hill, pp. 433-449.

Stein, D. C. (1991) Transformation of *Neisseria gonorrhoeae*: physical requirements of the transforming DNA. *Can J Microbiol* **37:** 345-349.

Stricker, J., Maddox, P., Salmon, E. D., and Erickson, H. P. (2002) Rapid assembly dynamics of the *Escherichia coli* FtsZ-ring demonstrated by fluorescence recovery after photobleaching. *Proc Natl Acad Sci USA* **99:** 3171-3175.

Suefuji, K., Valluzzi, R., and RayChaudhuri, D. (2002) Dynamic assembly of MinD into filament bundles modulated by ATP, phospholipids, and MinE. *Proc Natl Acad Sci U S A* **99:** 16776-16781.

Sun, Q. and Margolin, W. (2001) Influence of the nucleoid on placement of FtsZ and MinE rings in *Escherichia coli*. *J Bacteriol* **183:** 1413-1422.

Sun, Q. and Margolin, W. (2004) Effects of perturbing nucleoid structure on nucleoid occlusion-mediated toporegulation of FtsZ ring assembly. *J Bacteriol* **186:** 3951-3959.

Sunako, Y., Onogi, T., and Hiraga, S. (2001) Sister chromosome cohesion of *Escherichia coli*. *Mol Microbiol* **42:** 1233-1241.

Szeto, J. (2004) *Splitting heirs: A study of the cell division site determinant MinD from the coccus Neisseria gonorrhoeae*. Ottawa, Ontario: University of Ottawa, Ph.D. thesis.

Szeto, J., Acharya, S., Eng, N. F., and Dillon, J. A. R. (2004) The N terminus of MinD contains determinants which affect its dynamic localization and enzymatic activity. *J Bacteriol* **186:** 7175-7185.

Szeto, J., Eng, N. F., Acharya, S., Rigden, M. D., and Dillon, J. A. R. (2005) A conserved polar region in the cell division site determinant MinD is required for responding to MinE-induced oscillation but not for localization within coiled arrays. *Res Microbiol* **156:** 17-29.

Szeto, J., Ramirez-Arcos, S., Raymond, C., Hicks, L. D., Kay, C. M., and Dillon, J. A. (2001a) Gonococcal MinD affects cell division in *Neisseria gonorrhoeae* and *Escherichia coli* and exhibits a novel self-interaction. *J Bacteriol* **183:** 6253-6264.

Szeto, T. H., Rowland, S. L., Habrukowich, C. L., and King, G. F. (2003) The MinD membrane targeting sequence is a transplantable lipid-binding helix. *J Biol Chem* **278:** 40050-40056.

Szeto, T. H., Rowland, S. L., and King, G. F. (2001b) The dimerization function of MinC resides in a structurally autonomous C-terminal domain. *J Bacteriol* **183:** 6684-6687.

Szeto, T. H., Rowland, S. L., Rothfield, L. I., and King, G. F. (2002) Membrane localization of MinD is mediated by a C-terminal motif that is conserved across eubacteria, archaea, and chloroplasts. *Proc Natl Acad Sci USA* **99:** 15693-15698.

Szmelcman, S., Sassoon, N., and Hofnung, M. (1997) Residues in the alpha helix 7 of the bacterial maltose binding protein which are important in interactions with the Mal FGK2 complex. *Protein Sci* **6:** 628-636.

Tamames, J., Gonzalez-Moreno, M., Mingorance, J., Valencia, A., and Vicente, M. (2001) Bringing gene order into bacterial shape. *Trends Genet* **17:** 124-126.

Thanbichler, M. and Shapiro, L. (2006) MipZ, a spatial regulator coordinating chromosome segregation with cell division in *Caulobacter. Cell* **126:** 147-162.

Thanedar, S. and Margolin, W. (2004) FtsZ exhibits rapid movement and oscillation waves in helix-like patterns in *Escherichia coli. Curr Biol* **14:** 1167-1173.

Thomaides, H. B., Freeman, M., El Karoui, M., and Errington, J. (2001) Division site selection protein DivIVA of *Bacillus subtilis* has a second distinct function in chromosome segregation during sporulation. *Genes Dev* **15:** 1662-1673.

Tostevin, F. and Howard, M. (2006) A stochastic model of Min oscillations in *Escherichia coli* and Min protein segregation during cell division. *Phys Biol* **3:** 1-12.

Tseng, H. J., Mcewan, A. G., Apicella, M. A., and Jennings, M. P. (2003) OxyR acts as a repressor of catalase expression in *Neisseria gonorrhoeae. Infect Immun* **71:** 550-556.

Vale, R. D. (1996) Switches, latches, and amplifiers: Common themes of G proteins and molecular motors. *J Cell Biol* **135:** 291-302.

Varley, A. and Stewart, G. (1992) The *divIVB* region of the *Bacillus subtilis* chromosome encoded homologs of *E.coli* septum placement (MinCD) and Cell shape (MreBCD) determinants. *J Bacteriol* **174:** 6729-6742.

Varma, A. and Young, K. D. (2004) FtsZ collaborates with penicillin binding proteins to generate bacterial cell shape in *Escherichia coli. J Bacteriol* **186:** 6768-6774.

Vicente, M., Gomez, M., and Ayala, J. (1998) Regulation of transcription of cell division genes in the *Escherichia coli dcw* cluster. *Cell Mol Life Sci* 317-324.

Vicente, M. and Rico, A. I. (2006) The order of the ring: assembly of *Escherichia coli* cell division components. *Mol Microbiol* **61:** 5-8.

Vicente, M., Rico, A. I., Martinez-Arteaga, R., and Mingorance, J. (2006) Septum enlightenment: Assembly of bacterial division proteins. *J Bacteriol* **188:** 19-27.

Weart, R. B., Nakano, S., Lane, B. E., Zuber, P., and Levin, P. A. (2005) The ClpX chaperone modulates assembly of the tubulin-like protein FtsZ. *Mol Microbiol* **57:** 238-249.

Weaver, K. E. (2000) Enterococcal Genetics. In *Gram-Positive Pathogens*. Fischetti, V. A., Novick, R. P., Ferretti, J. J., Portnoy, D. A., and Rood, J. I. (ed.) Washinton, D.C.: ASM Press, pp. 259-271.

Weiss, D., Pogliano, K., Carson, M., Guzman, L., Fraipont, C., Nguyen-Disteche, M. *et al.* (1997) Localization of the *Escherichia coli* cell division protein FtsI (PBP3) to the division site and cell pole. *Mol Microbiol* **25:** 671-681.

West, S. E. and Clark, V. L. (1989) Genetic loci and linkage associations in *Neisseria gonorrhoeae* and *Neisseria meningitidis*. *Clin Microbiol Rev* **2:** S92-S103.

Westling-Haggstrom, B., Elmros, T., Normark, S., and Winblad, B. (1977) Growth pattern and cell division in *Neisseria gonorrhoeae*. *J Bacteriol* **29:** 333-342.

Woldringh, C. L. (2002) The role of co-transcriptional translation and protein translocation (transertion) in bacterial chromosome segregation. *Mol Microbiol* **45:** 17-29.

Woldringh, C. L., Mulder, E., Huls, P. G., and Vischer, N. (1991) Toporegulation of bacterial division according to the nucleoid occlusion model. *Res Microbiol* **142:** 309-320.

Woldringh, C. L., Mulder, E., Valkenburg, J. A., Wientjes, F. B., Zaritsky, A., and Nanninga, N. (1990) Role of the nucleoid in the toporegulation of division. *Res Microbiol* **141:** 39-49.

Wu, L. J. and Errington, J. (2003) RacA and the Soj-Spo0J system combine to effect polar chromosome segregation in sporulating *Bacillus subtilis*. *Mol Microbiol* **49:** 1463-1475.

Wu, L. J. and Errington, J. (2004) Coordination of cell division and chromosome segregation by a nucleoid occlusion protein in *Bacillus subtillis*. *Cell* **117:** 915-925.

Xu, J. F., Hu, C. Y., Shen, S. Y., Wang, W. R., Jiang, P. H., and Huang, W. D. (2004) Requirement of the N-terminus for dimer formation of phenylalanine-sensitive 3-deoxy-D-arabino-heptulosonate synthase AroG of *Escherichia coli*. *J Basic Microbiol* **44:** 400-406.

Yu, X. and Margolin, W. (1999) FtsZ ring clusters in *min* and partition mutants: role of both the Min system and the nucleoid in regulating FtsZ ring localization. *Mol Microbiol* **32:** 315-326.

Yu, X. and Margolin, W. (1997) Ca^{2+} -mediated GTP-dependent dynamic assembly of bacterial cell division protein FtsZ into asters and polymer networks in vitro. *EMBO J* **16:** 5455-5463.

Zhang, Y., Rowland, S., King, G., Braswell, E., and Rothfield, L. (1998) The relationship between hetero-oligomer formation and function of the topological specificity domain of the *Escherichia coli* MinE protein. *Mol Microbiol* **30:** 265-273.

Zhao, C., de Boer, P., and Rothfield, L. (1995) Proper placement of the *Escherichia coli* division site requires two functions that are associated with different domains of the MinE protein. *Proc Natl Acad Sci USA* **92:** 4313-4317.

Zhou, H. J. and Lutkenhaus, J. (2005) MinC mutants deficient in MinD- and DicB-mediated cell division inhibition due to loss of interaction with MinD, DicB, or a septal component. *J Bacteriol* **187:** 2846-2857.

Zhou, H. J. and Lutkenhaus, J. (2004) The switch I and II regions of MinD are required for binding and activating MinC. *J Bacteriol* **186:** 1546-1555.

Zhou, H. J., Schulze, R., Cox, S., Saez, C., Hu, Z. L., and Lutkenhaus, J. (2005) Analysis of MinD mutations reveals residues required for MinE stimulation of the MinD ATPase and residues required for MinC interaction. *J Bacteriol* **187:** 629-638.

CONTRIBUTION OF COLLABORATORS

The author would like to thank the many past and current members of the Dillon laboratory for technical assistance in many aspects of these studies. Dr. Sandra Ramirez-Arcos constructed pSRBDR30D and pSR15 and provided insight in the beginning of this project. Dr. Jason Szeto provided appropriate controls for the ATPase assays and assisted in the development of phosphatidylglycerol vesicles. Dr. Szeto also initiated studies of $MinE_{Ng}$-$MinD_{Ng}$ interactions by generating the $MinE_{Ng}$ truncations, and helped standardize the Olympus BX61 microscopy for studies of GFP-$MinD_{Ng}$. Dr. Mingmin Liao helped standardize the operating procedures to perform the growth studies of *N. gonorrhoeae*. Dan Tessier assisted in the construction of pSRDT18, pSRDT22, pSRDT30, pSRDT53 and pSRDT67. Sudeep Acharya assisted with the ATPase assays. Cherise Baier and Lauren Lapointe-Shaw, as summer students under my supervision, assisted in the bacterial two-hybrid assays. Luc Tessier, Institute of Biological Sciences, National Research Council of Canada (NRC-IBS) provided Q-TOF mass spectrometry analysis of $MinE_{Ng}$-His. Dennis Ramos and Dr. Natalie Goto studied $MinE_{Ng}$ using NMR. The author would also like to thank Emmanuel Guigard and Dr. Cyril Kay, University of Alberta, for performing the analytical ultracentrifugation analysis of wild-type and mutant $MinE_{Ng}$. Peter Rippstein, Laboratory Pathology facilities, Ottawa Hospital, Civic Campus completed the transmission electron microscopy experiments. Will Deck of the Vaccine and Infectious Disease Organization (VIDO) at the University of Saskatchewan performed size-exclusion chromatography on $MinE_{Ng}$-His.

APPENDICES

This chapter describes other experiments that were performed in addition to my main project. The purpose, results and discussion of each study are described, along with the reasons why they were not completed or included in the body of thesis. Table A.1 details all the plasmids used in this Appendix. Primers are described in Table A.2.

A. USING GST PULLDOWN EXPERIMENTS TO TEST FOR $MinE_{Ng}$ SELF-INTERACTION

These studies were done in parallel in the examining the ability of $MinE_{Ng}$ to interact with itself. However, since $MinE_{Ng}$ self-interaction was observed using analytical ultracentrifugation, size-exclusion chromatography, and bacterial two-hybrid assays, examining this interaction using glutathione-S-transferase (GST) fused to $MinE_{Ng}$ to "pulldown" $MinE_{Ng}$ protein was not necessary, but is described here for future investigations.

MATERIALS AND METHODS

Construction of GST-tagged $MinE_{Ng}$

The wild-type and mutant *minE*$_{Ng}$ gene was amplified from wild-type and mutant *minE*$_{Ng}$ encoded on pEC1, pEA18D, pEL22D, pER30D, pEK53A, and pEE67L (Table 3), using GEX2TminE1 and GEX2TminE2 (Table A.2). Amplicons were purified and digested with BamHI and EcoRI. Digested amplicons were then cloned into plasmid pGEX2T (Amersham, Table A.1) that was previously digested at the unique BamHI and EcoRI sites. This approach led to the fusion of the GST tag at the N-terminus end of $MinE_{Ng}$. The generated plasmids were named pGEXminE (wild-type), pGSTEA18D (A18D mutation), pGSTEL22D (L22D mutation), pGSTER30D (R30D mutation, pGSTEK53A (K53A

Table A.1. Plasmids used in this study.

Plasmids	Relevant Genotype	Source/Reference
GST pulldowns		
pGEX2T	$Amp^R P_{tac}$::*gst*::*lacI*^{q}	Amersham
pGEXminE	$Amp^R P_{tac}$::*gst-minE*$_{Ng}$::*lacI*^{q}	This study
pGEXEA18D	$Amp^R P_{tac}$::*gst-minE*$_{Ng\text{-}A18D}$::*lacI*^{q}	This study
pGEXEL22D	$Amp^R P_{tac}$::*gst-minE*$_{Ng\text{-}L22D}$::*lacI*^{q}	This study
pGEXER30D	$Amp^R P_{tac}$::*gst-minE*$_{Ng\text{-}R30D}$::*lacI*^{q}	This study
pGEXEK53A	$Amp^R P_{tac}$::*gst-minE*$_{Ng\text{-}K53A}$::*lacI*^{q}	This study
pGEXEE67L	$Amp^R P_{tac}$::*gst-minE*$_{Ng\text{-}E67L}$::*lacI*^{q}	This study
FRET plasmids		
pDH22	$Amp^R Kan^R P_{MET}$::N-terminal tag of *yfp*	Yeast Resource Center
pBS5	$Amp^R Kan^R P_{MET}$::N-terminal tag of *cfp*[1]	Yeast Resource Center
pDH3	$Amp^R Kan^R P_{MET}$::C-terminal tag of *cfp*[2]	Yeast Resource Center
pYDEC1	$Amp^R P_{lac}$::*yfp-minD*$_{Ng}$::*minE*$_{Ng}$-*cfp*[1]	This study
pYDEC2	$Amp^R P_{lac}$::*yfp-minD*$_{Ng}$::*minE*$_{Ng}$-*cfp*[2]	This study

[1] – the *cfp* originally coded for N-terminal fusions was used as a C-terminal tag in pYDEC1

[2] – this *cfp* contains an alternate nucleotide sequence. See website (http://depts.washington.edu/yeastrc/index.html)

Table A.2. Primer sequences used for PCR and inverse PCR.

Primer	Sequence (5'- 3'; restriction sites underlined)	Restriction Site
GEX2TminE1	GCGCGGATCCATGTCATTGATCGAACTTT	BamHI
GEX2TminE2	GCGCGAATTCCTATACCTTTTTCTGTTCC[a]	EcoRI
YFP2	GCGCGGATCCTTTGTACAATTCATCCAT[a]	BamHI
minDBam	GCGCGGATCCGTGGCAAAAATTATTGTA	BamHI
minESal	GCGCGTCGACTACCTTTTTCTGTTCCGG[a]	SalI
YFP3	GCGCGTCGACATGTCTAAAGGTGAAGAA	SalI
YFP4	GCGCCTGCAGCTATTTGTACAATTCATC[a]	PstI
YFP5	GCGCGTCGACAGTAAAGGAGAAGAACTT	SalI
YFP6	GCGCGCATGCCTATTTGTATAGTTCATC[a]	SphI
NgMinDSphI	GCGCGCATGCGTGGCAAAAATTATTGTA	SphI
JSD2	GCGCCTGCAGACCTTATCCTCCGAACAGA[a]	PstI

[a] Denotes primer annealing to complementary strand.

mutation), and pGSTEE67L (E67L mutation) (Table A.1). These plasmids were then transformed into *E. coli* C41 to overexpress the GST-fusion proteins.

Growth conditions, purification of GST-tagged $MinE_{Ng}$ and western blotting

Overnight cultures of transformed *E. coli* C41 with pGEX-derived plasmids and pET30a-derived plasmids were added to 100 ml of fresh LB medium with 100 μg/ml ampicillin (for pGEX derivations) or 50 μg/ml kanamycin (pET30a derivations) in a 3:1000 dilution. Cultures were then allowed to grow for 2.5-3 hours. At that time, 0.1 mM IPTG was added to *E. coli* cells transformed with pGEX-derived plasmids and 0.4 mM IPTG was added to cells transformed with pET30a plasmid derivatives. Cells were then pelleted at 6000 rpm for 10 minutes at 4 °C.

GST-tagged $MinE_{Ng}$ fusions were purified by a GST-purification kit from Novagen. Briefly, pelleted cells were resuspended in 5 ml of 1X GST/bind/wash buffer (GBW) (+ 2% Triton X-100). Cells were sonicated in 10 second bursts three times, followed by centrifugation at 10000 rpm at 4 °C. The supernatant was then added to GST-resin, which had previously been washed with 1X GBW buffer. The mixture was allowed to incubate at 4 °C for an hour. The GST-embedded beads were then rinsed with the GBW buffer.

Cells transformed with pET30a derivations were similarly sonicated and centrifuged in 5 ml of extraction buffer (50 mM Tris/HCl, pH 8.0, 100 mM NaCl, and 2% Triton X-100). The supernatant was then added to the GST-embedded beads at 4 °C for one hour. Resin was then rinsed with extraction buffer and samples were run on 15% SDS-PAGE. Western blotting to detect $MinE_{Ng}$-His was performed (see 2.25) using mouse anti-His antibody (Biorad).

RESULTS AND DISCUSSION

Even though $MinE_{Ng}$ self-interaction was demonstrated using size-exclusion chromatography and analytical ultracentrifugation experiments, the possibility that self-interaction occurring through the His-tag cannot be discounted since $MinE_{Ng}$-His was used in these experiments. However, the bacterial two-hybrid assays, which did not involve His-tagged fusion proteins, dismissed this notion. In addition, glutathione-S-transferase (GST) pulldown assays verified this for wild-type $MinE_{Ng}$ and $MinE_{Ng\text{-}L22D}$ as well. Western blotting showed that GST beads alone did not interact with $MinE_{Ng}$-His, while GST-$MinE_{Ng}$ "pulled down" $MinE_{Ng}$-His, demonstrating the specificity of $MinE_{Ng}$ self-interaction (Fig. A.1). A similar experiment was performed with the L22D $MinE_{Ng}$ mutant. There was much more non-specific binding of GST to the $MinE_{Ng\text{-}L22D}$ protein; only by spot densitometry was I able to determine that GST-$MinE_{Ng\text{-}L22D}$ pulled down slightly more $MinE_{Ng\text{-}L22D}$ (Fig. A.1).

One of the drawbacks of GST-pulldown experiments was that many optimizations were required. One aspect, in particular, was the amount of Triton X-100 detergent required. When 0.2% Triton X-100 was used, it was sufficient to ensure specific binding between GST-$MinE_{Ng}$ and $MinE_{Ng}$-His, but not between GST-$MinE_{Ng}$ and $MinE_{Ng\text{-}L22D}$-His (Fig. A.1). Thus, optimizing each $MinE_{Ng}$ mutant was difficult; since the three experiments (analytical ultracentrifugation, size-exclusion chromatography, and bacterial two-hybrid assays) to test for $MinE_{Ng}$ self-interaction were able to clearly show whether or not the ability of mutant $MinE_{Ng}$ to interact with itself was maintained, I did not pursue the GST pulldown assays further.

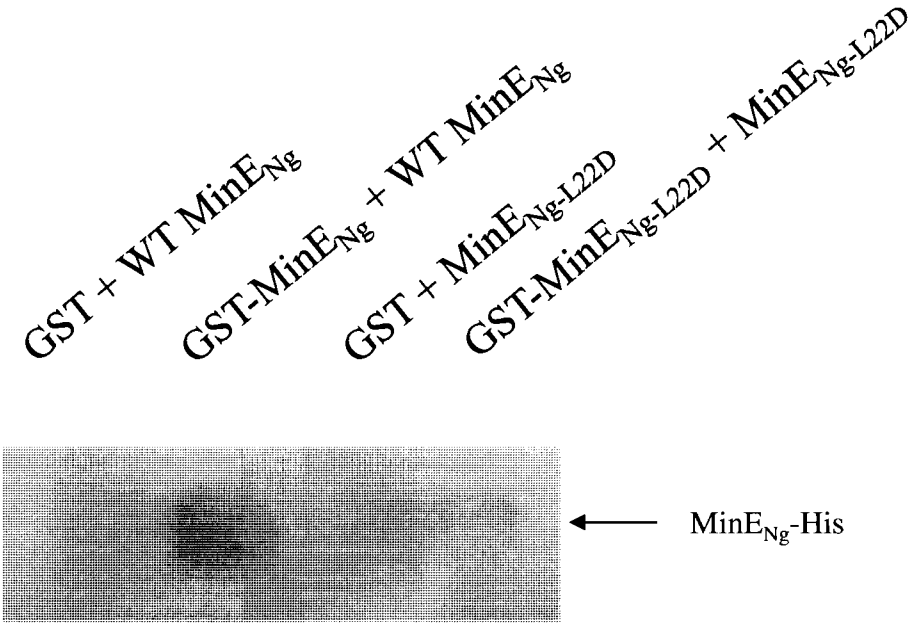

Figure A.1. GST pulldown of MinE$_{Ng}$-His shows that self-interaction is not disrupted. Western blotting of samples that contained GST resin, wild-type/mutant GST-MinE$_{Ng}$ and wild-type/mutant MinE$_{Ng}$-His were separated on 15% SDS-PAGE gel where the "pulldown" of MinE$_{Ng}$-His was detected using mouse anti-His. GST beads alone did not interact with MinE$_{Ng}$-His, while GST-MinE$_{Ng}$ could, which shows that the specificity of MinE$_{Ng}$ self-interaction. Here, a similar experiment was performed with the L22D MinE$_{Ng}$ mutant. There was a little non-specific binding of GST to the MinE$_{Ng-L22D}$ protein, but more was pulled down with resin bound to GST-MinE$_{Ng-L22D}$.

B. CONSTRUCTION OF FRET PLASMIDS FOR *IN VIVO* OBSERVATIONS OF Min_{Ng} PROTEIN INTERACTIONS

The nature of the coiled array found in *E. coli* (Shih *et al.*, 2003) is currently not known. To investigate these coils, as it relates to the Min proteins, our laboratory is attempting to understand the function of the coiled array by using fluorescence resonance energy transfer (FRET) technology to monitor the *in vivo* interactions of Min_{Ng} in real-time. These studies will enable us to determine if, in fact, $MinD_{Ng}$ AND $MinE_{Ng}$ are both required to form the coiled array, or provide insight into the formation of this subcellular architecture. However, only the plasmid construction has been completed (Table A.1). These plasmids will be needed to perform FRET analysis in the future.

MATERIALS AND METHODS

Construction of FRET plasmids.

Plasmids encoding fluorophores that will be used for FRET were obtained from the Yeast Resource Center (University of Washington). The *yfp* gene was amplified from pDH22 (Table A.1) using YFP1 and YFP2 primers (Table A.2). The $minD_{Ng}$ and $minE_{Ng}$ genes were amplified from pSR15 (Table 3) using primers minDBam and minESal (Table A.2). Two *cfp* genes were amplified, one (*cfp1*) was similar in nucleotide sequence to *yfp*, while the other (*cfp2*) was different in sequence. The *cfp1* gene was amplified from pBS5 (Table A.1) using YFP3 and YFP4 primers (Table A.2). The YFP5 and YFP6 primers (Table A.2) were used to amplify *cfp2* from pDH3 (Table A.1). The three amplicons, *yfp*, $minD_{Ng}$*::*$minE_{Ng}$, and *cfp1/cfp2* were cloned into pUC18 (Table 3) to generate pYDEC1 (with *cfp1*) and pYDEC2 (with *cfp2*, Table A.1), for FRET analysis in *E. coli* PB114.

RESULTS AND DISCUSSION

Figure A.2 depicted the successful cloning of *yfp*, $minD_{Ng}$, $minE_{Ng}$ and *cfp* into pUC18. First, *yfp* was cloned into pUC18 (Fig. A.2 A). $minD_{Ng}$ and $minE_{Ng}$ were then cloned into the pUC18-*yfp* construct so that $minD_{Ng}$ was expressed in fusion at the 3' end of *yfp* (Fig. A.2 B). Finally, *cfp1* and *cfp2* amplified from pBS5 and pDH3, respectively, were cloned in fusion with the 3' end of $minE_{Ng}$ to give rise to pYDEC1 and pYDEC2 (Fig. A.2 C).

With the discovery of the recruitment of $MinD_{Ec}$ to the coiled array in *E. coli* (Shih *et al.*, 2003), and with additional proteins like MreB (Shih *et al.*, 2005), CreS (Ausmees and Jacobs-Wagner, 2003), FtsZ (Margolin, 2005), and SetB (Espeli *et al.*, 2003) also forming helical-like structures, it was unclear whether these arrays were the same one, or if there are several different helical arrays. Previous studies have shown that $MinD_{Ec}$ and $MreB_{Ec}$ in fact, do not colocalize to the same coiled array (Shih *et al.*, 2005). As a result, the nature of the coiled array, as it relates to MinD, is unknown, and is of great interest. As discussed previously, it is not clear if there is a pre-exisiting helical structure that MinD binds to, or if oligomerized MinD molecules make up the coil itself. The construction of pYDEC1 and pYDEC2 should provide some insight into the nature of the $MinD_{Ng}$ coiled array. It is hoped that future graduate students can use these plasmids to investigate this fascinating phenomenon.

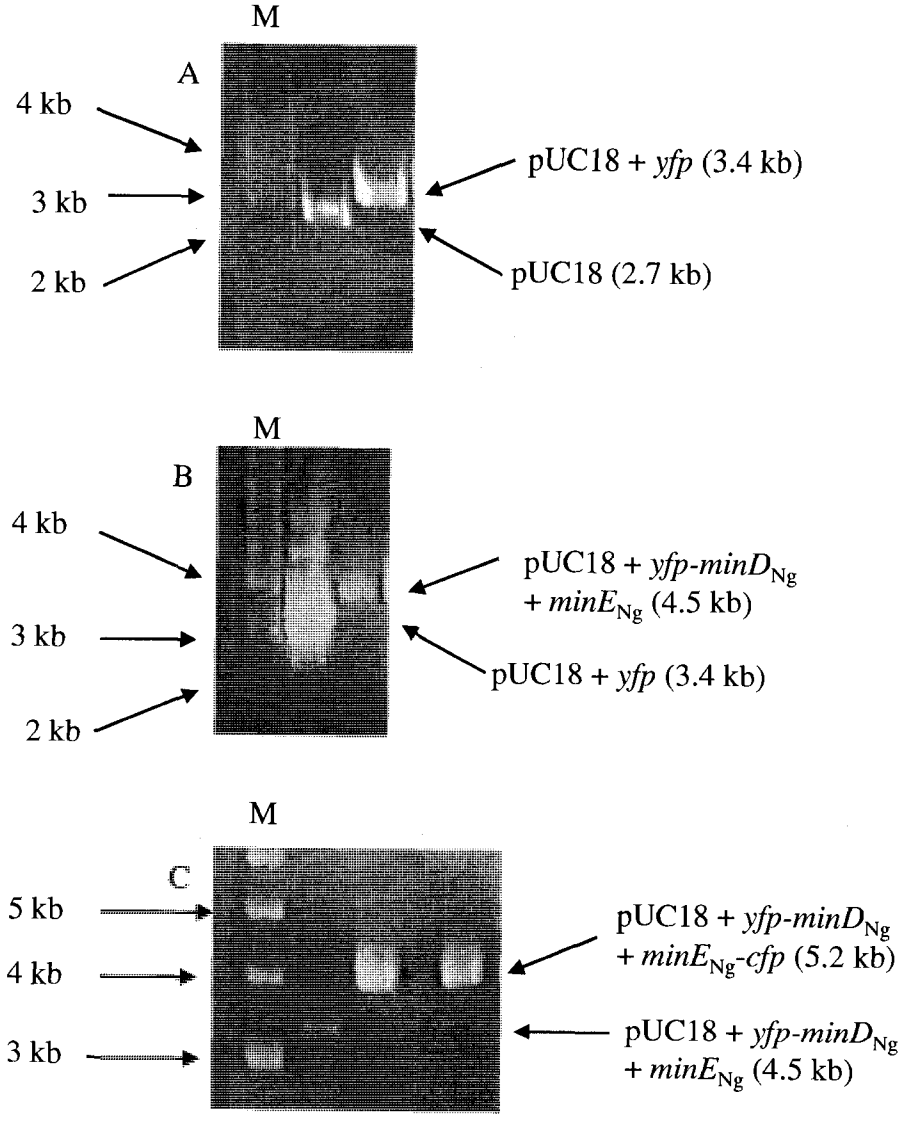

Figure A.2. Construction of pYDEC1 and pYDEC2. (A) shows the cloning of *yfp* into pUC18, while (B) shows the cloning of $minD_{Ng}$ and $minE_{Ng}$ into the pUC18 + *yfp* plasmid with the constructs being resolved on 1% agarose gel electrophoresis with ethidium bromide staining. (C) shows the pYDEC1 (lane 1) and pYDEC2 (lane 2) plasmids that have *yfp*, $minD_{Ng}$, $minE_{Ng}$, and *cfp* cloned into pUC18. (M) indicates supercoiled marker, parentheses show the size of the plasmids as genes were cloned.

C. IMPROVING GENETIC TOOLS TO STUDY EXPRESSION OF CELL DIVISION GENES IN *NEISSERIA GONORRHOEAE*

Introducing genetic changes into *N. gonorrhoeae* has traditionally been limited to transformation, due to the natural competence of this microorganism (Stein, 1991). The transformation of *N. gonorrhoeae* requires the presence of a specific gonococcal uptake sequence on the DNA to be introduced (Pagotto *et al.*, 2000). Disrupting chromosomal genes via insertional inactivation by homologous recombination is a limited technique since it cannot be used to study genes essential for viability (Pagotto *et al.*, 2000). As a result, a few genetic tools have been developed in an attempt to acquire more methods to manipulate gonococcal genes. For example, suicide vectors allow the introduction and subsequent allelic exchange of gonococcal genes (Pagotto *et al.*, 2000). The Hermes shuttle vectors can also be introduced into *N. gonorrhoeae* to permit genetic complementation with cloned genes (Kupsch *et al.*, 1996). Unfortunately, this is a multi-step process involving conjugation into another host first.

Our lab used pFP20 (Table 3) to express gonococcal cell division proteins $MinC_{Ng}$, $MinD_{Ng}$, and $MinE_{Ng}$ in *N. gonorrhoeae* (Ramirez-Arcos *et al.*, 2001b;Szeto *et al.*, 2001a). $MinC_{Ng}$ and $MinD_{Ng}$ are functional across species and can inhibit cell division when either are expressed in wild-type *E. coli* indicator strains. Overexpression of $MinC_{Ng}$ and $MinD_{Ng}$ together from endogenous promoters, can inhibit cell division in its native organism, as evidenced by enlarged cells. However, overexpression of MinC or MinD alone in *N. gonorrhoeae* did not result in enlarged gonococci; hence, expression of their endogenous promoters may not be strong enough to cause this phenotype. As a result, modifications to pFP20 were necessary to control and increase expression.

MATERIALS AND METHODS

Modifying pFP20 to increase Min_{Ng} expression

Previously, P_{lac}, *minDE*$_{Ng}$ and *gfp* were cloned into pFP20 at the EcoRI and KpnI sites to generate pVG14 (Greco, 2004, Fig. A.3). Digestion of pVG14 at the two PstI sites allowed the removal of *minDE*$_{Ng}$ and *gfp*. The vector was religated to give rise to pNE2. The availability of the SphI and PstI sites allowed for the proper orientation and cloning of *minCDE*$_{Ng}$, *minC*$_{Ng}$, *minD*$_{Ng}$, *minE*$_{Ng}$, *minCD*$_{Ng}$, and *minDE*$_{Ng}$ to generate pNE10, pNE11, pNE12, pNE13, pNE14, and pNE15, respectively. Respectively, each gene was amplified from *N. gonorrhoeae* CH811 DNA using primer pairs NgMinCSphI/JSE2, NgMinCSphI/JSC2, NgMinDSphI/JSD2, NgMinESphI/JSE2, NgMinCSphI/JSD2, and NgMinDSphI/JSE2 (Tables A.2 and 2)

RESULTS AND DISCUSSION

To ensure P_{lac} functionality in our new constructs, pNE11 and pNE12 were transformed into *E. coli* PB103 and effects of overexpression of $MinC_{Ng}$ and $MinD_{Ng}$ in the rod-shaped cells were studied. Microscopic analysis revealed filamentation, indicating that $MinC_{Ng}$ overexpression from pNE11 (Fig. 3.2 B) inhibited *E. coli* cell division. $MinC_{Ng}$ and $MinD_{Ng}$ overexpression was also confirmed by Western blots (Fig. A.4). *E. coli* cells overexpressing $MinE_{Ng}$ was discussed earlier. Thus, the pNE2 construct provides a new tool required to control expression of the Min_{Ng} or any other proteins in its native organism and thus allow better characterization of gonococcal protein function which was previously not possible to perform. The other constructs have not been examined due to my focus on

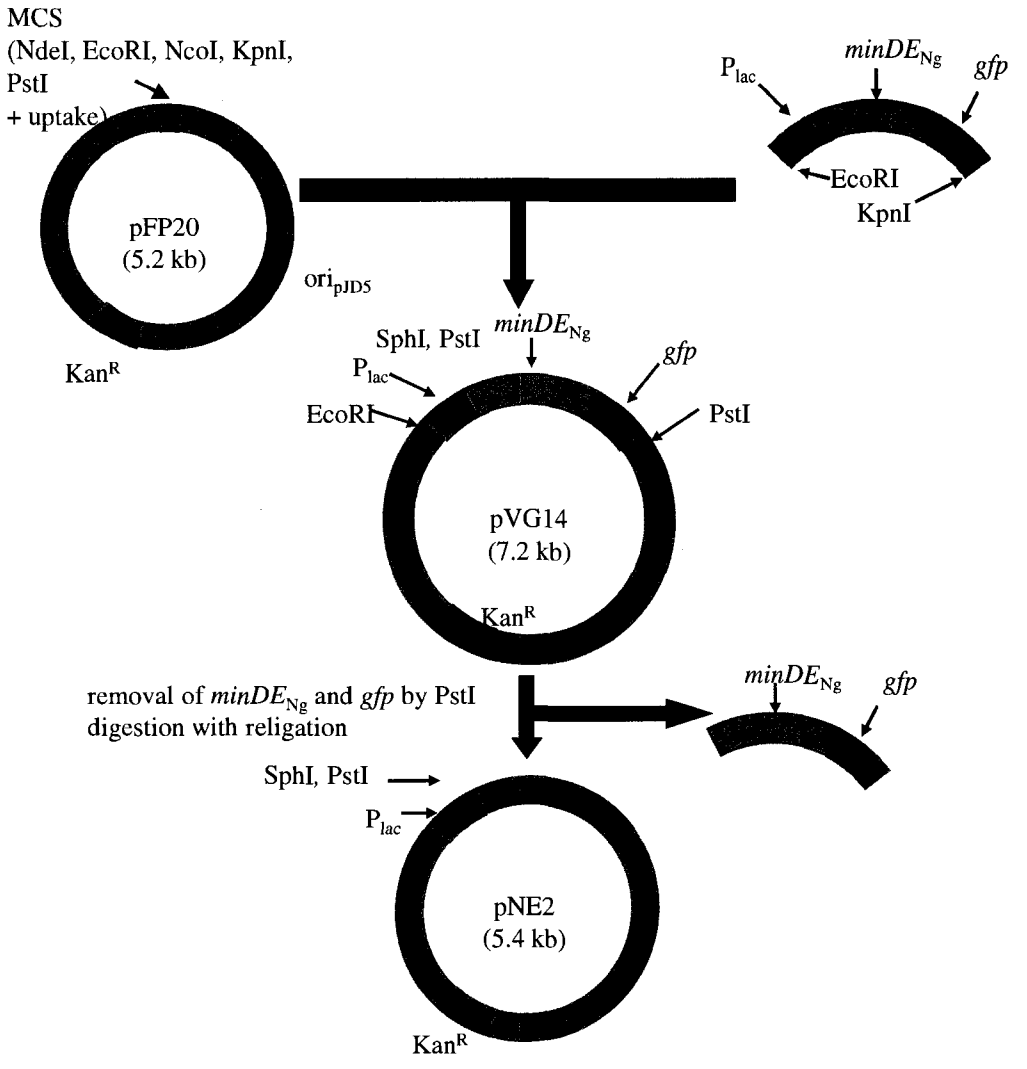

Figure A.3. Construction of pNE2. Large dark green arrowheads indicate newly introduced restriction sites from primers used in PCR. All the *min* genes were cloned into the SphI and PstI sites of pNE2. Initially, *minDE* PCR product from pSR1 with primers that included BamHI and NcoI sites was cloned into pEGFP from Clontech that already has P_{lac}. Following, there was PCR with primers that included EcoRI and KpnI sites which were used to clone all of P_{lac}, *minDE* and *gfp* from the modified pEGFP into the unique sites of pFP20.

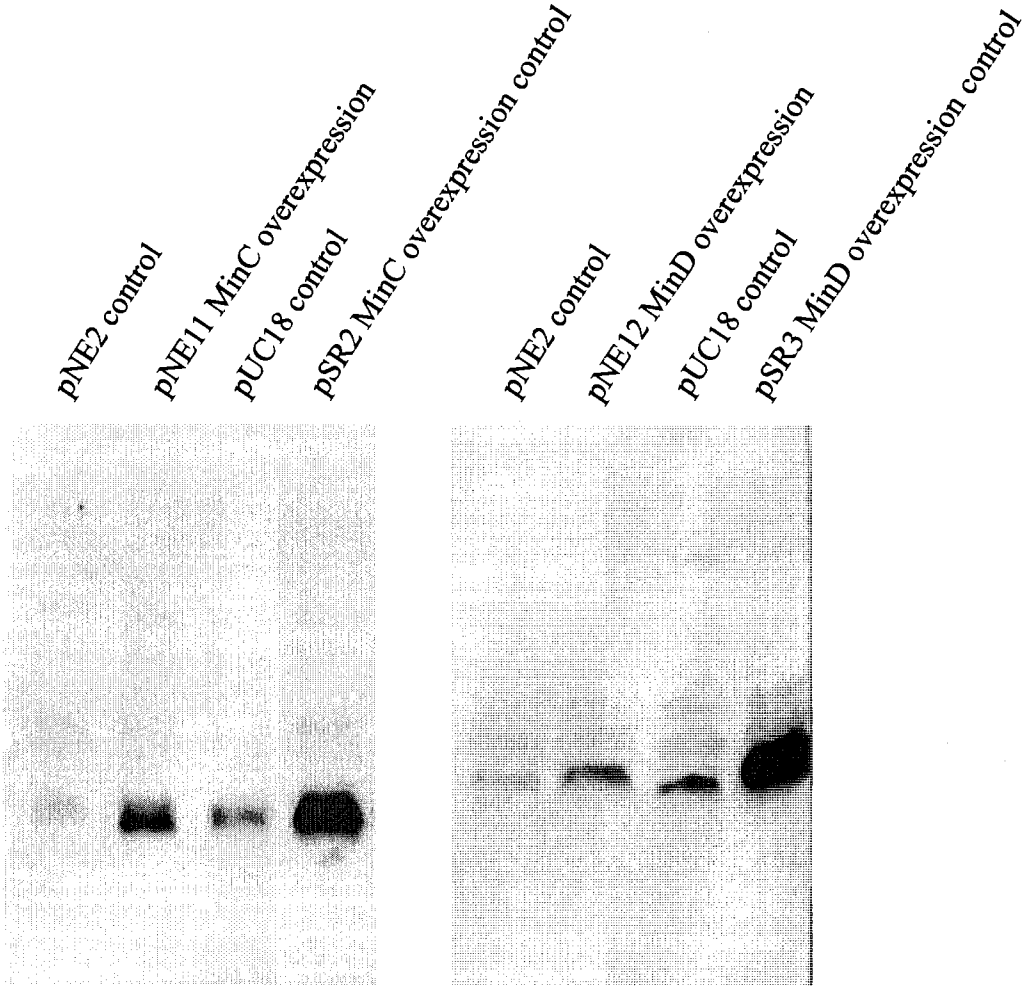

Figure A.4. Expression of $MinC_{Ng}$ and $MinD_{Ng}$ from shuttle vectors. These Western blots indicate that MinC from pNE11 is overexpressed when compared to pNE2 and pUC18 controls. Overexpression of MinD from pNE12 still occurs, although not to the same extent. These proteins were from cell lysates recovered from overnight cultures at 37°C. pSR2 and pSR3 serves as controls for MinC and MinD overexpression respectively. The pNE2 and pUC18 controls show endogenous MinC and MinD expression from *E. coli*.

$MinE_{Ng}$. Nonetheless, future graduate students can use these improved plasmids as effective tools to study proteins from *N. gonorrhoeae.*

D. COPYRIGHT PERMISSION NOTICES

Permission to use some figures in this thesis follows this page.

From: "Millerd, Tiffany"
Subject: RE: permission to use figure
Date: Thu, 7 June, 2007 12:18 pm
To: "Nelson Eng"

Dear Dr. Eng,

Permission is granted for your use of the figure as described in your message below. Please cite the full journal references and "Copyright (Copyright year) National Academy of Sciences, U.S.A."

Best regards,
Tiffany Millerd for
Diane Sullenberger
Executive Editor
PNAS

-----Original Message-----
From: Nelson Eng [mailto:
Sent: Wednesday, May 23, 2007 2:59 PM
To: PNAS Permissions
Subject: permission to use figure

To whom this may concern,

My name is Nelson Eng, a PhD student at the University of Ottawa, under the supervision of Dr. Jo-Anne Dillon. I am currently writing my thesis and would like to include a figure from PNAS and incorporate it into my thesis. The figure will not be altered:

Article:

Shih, YL., Le, T., and Rothfield, L. (2003) Division site selection in Escherichia coli involves dynamic redistribution of Min proteins within coiled structures that extend between the two poles. Proc. Natl. Acad. Sci. USA. Volume 100, Issue 13 pp. 7865-7870.

I would like to use Figure 2E on page 7867.

I look forward to your response if I could use this figure in my thesis.

Thank you.

Nelson Eng

--
Nelson Eng, B.Sc., Ph.D. candidate
Department of Biochemistry, Microbiology and Immunology
Faculty of Medicine
University of Ottawa
451 Smyth Road
Ottawa, Ontario
K1H 8M5

--
Nelson Eng, B.Sc., Ph.D. candidate
Department of Biochemistry, Microbiology and Immunology
Faculty of Medicine

University of Ottawa
451 Smyth Road
Ottawa, Ontario
K1H 8M5

--
Nelson Eng, B.Sc., Ph.D. candidate
Department of Biochemistry, Microbiology and Immunology
Faculty of Medicine
University of Ottawa
451 Smyth Road
Ottawa, Ontario
K1H 8M5

Download this as a file

From: "Downing, Hannah (ELS-OXF)"
Subject: RE: Obtain Permission
Date: Wed, 6 June, 2007 9:31 am
To:

Dear Nelson Eng

We hereby grant you permission to reprint the material detailed below at no charge in your thesis subject to the following conditions:

1. If any part of the material to be used (for example, figures) has appeared in our publication with credit or acknowledgement to another source, permission must also be sought from that source. If such permission is not obtained then that material may not be included in your publication/copies.

2. Suitable acknowledgment to the source must be made, either as a footnote or in a reference list at the end of your publication, as follows:

"This article was published in Publication title, Vol number, Author(s), Title of article, Page Nos, Copyright Elsevier (or appropriate Society name) (Year)."

3. Your thesis may be submitted to your institution in either print or electronic form.

4. Reproduction of this material is confined to the purpose for which permission is hereby given.

5. This permission is granted for non-exclusive world English rights only. For other languages please reapply separately for each one required. Permission excludes use in an electronic form other than submission. Should you have a specific electronic project in mind please reapply for permission.

6. This includes permission for the Library and Archives of Canada to supply single copies, on demand, of the complete thesis. Should your thesis be published commercially, please reapply for permission.

Yours sincerely

Clare Truter

Rights Manager, S&T

-----Original Message-----
From: David, Natalie (ELS-OXF)
Sent: 24 May 2007 16:19
To: Rights and Permissions (ELS)
Subject: FW: Obtain Permission

-----Original Message-----
From: [redacted]
Sent: 23 May 2007 20:04
To: Health Permissions (ELS)
Subject: Obtain Permission

This Email was sent from the Elsevier Corporate Web Site and is related to Obtain Permission form:

Product: Customer Support
Component: Obtain Permission
Web server: [redacted]
IP address: 10.10.24.149
Client: Mozilla/4.0 (compatible; MSIE 7.0; Windows NT 5.1; .NET CLR 1.1.4322; InfoPath.1; .NET CLR 2.0.50727)
Invoked from:
http://www.elsevier.com/wps/find/obtainpermissionform.cws_home?isSubmitted=yes&navigateXmlFileName=/store/prod_webcache_act/framework_support/obtainpermission.xml

Request From:
Nelson Eng
University of Ottawa
451 Smyth Road
K1H8M5
Ottawa
Canada

Contact Details:
Telephone:
Fax:
Email Address:

To use the following material:
ISSN/ISBN:
Title: Cell
Author(s): Thanbichler, M., and Shapiro, L.
Volume: 126
Issue: 1
Year: 2006
Pages: 147 - 162
Article title: MipZ, a spatial regulator coordinating...

How much of the requested material is to be used:
Only Figure 8 on page 160.

Are you the author: No
Author at institute: No

How/where will the requested material be used: In a thesis or dissertation

Details:

I hope to use this figure in my introduction of my PhD thesis. Also, I plan to slightly modify to image to include a bit more detail on the representative bacteria.

Additional Info: The entire title is: MipZ, a spatial regulator coordinating chromosome segregation with cell division in Caulobacter. This whole title did not fit on the article title field (limit 50).

- end -

For further info regarding this automatic email, please contact:
WEB APPLICATIONS TEAM (

Download this as a file

From: "Downing, Hannah (ELS-OXF)"
Subject: RE: Obtain Permission
Date: Wed, 6 June, 2007 9:30 am
To:

Dear Nelson Eng

We hereby grant you permission to reprint the material detailed below at no charge in your thesis subject to the following conditions:

1. If any part of the material to be used (for example, figures) has appeared in our publication with credit or acknowledgement to another source, permission must also be sought from that source. If such permission is not obtained then that material may not be included in your publication/copies.

2. Suitable acknowledgment to the source must be made, either as a footnote or in a reference list at the end of your publication, as follows:

"This article was published in Publication title, Vol number, Author(s), Title of article, Page Nos, Copyright Elsevier (or appropriate Society name) (Year)."

3. Your thesis may be submitted to your institution in either print or electronic form.

4. Reproduction of this material is confined to the purpose for which permission is hereby given.

5. This permission is granted for non-exclusive world English rights only. For other languages please reapply separately for each one required. Permission excludes use in an electronic form other than submission. Should you have a specific electronic project in mind please reapply for permission.

6. This includes permission for the Library and Archives of Canada to supply single copies, on demand, of the complete thesis. Should your thesis be published commercially, please reapply for permission.

Yours sincerely

Clare Truter

Rights Manager, S&T

-----Original Message-----
From: David, Natalie (ELS-OXF)
Sent: 24 May 2007 16:08
To: Rights and Permissions (ELS)
Subject: FW: Obtain Permission

-----Original Message-----
From:
Sent: 23 May 2007 18:07
To: Health Permissions (ELS)
Subject: Obtain Permission

This Email was sent from the Elsevier Corporate Web Site and is related to Obtain Permission form:

Product: Customer Support
Component: Obtain Permission
Web server:
IP address: 10.10.24.148
Client: Mozilla/4.0 (compatible; MSIE 7.0; Windows NT 5.1; .NET CLR 1.1.4322; InfoPath.1; .NET CLR 2.0.50727)
Invoked from:
http://www.elsevier.com/wps/find/obtainpermissionform.cws_home?isSubmitted=yes&navigateXmlFileName=/store/prod_webcache_act/framework_support/obtainpermission.xml

Request From:
Nelson Eng
University of Ottawa
451 Smyth Road
K1H8M5
Ottawa
Canada

Contact Details:
Telephone:
Fax:
Email Address:

To use the following material:
ISSN/ISBN:
Title: Journal of Molecular Biology
Author(s): Addinall, S.G., and Holland, B.
Volume: 318
Issue: 2
Year: 2002
Pages: 219 - 236
Article title: The tubulin ancestor, FtsZ, draughtsman,...

How much of the requested material is to be used:
Figure 1a

Are you the author: No

Author at institute: No

How/where will the requested material be used: In a thesis or dissertation

Details:

I would like to use a small portion of Figure 1a to include in the introduction of my thesis to emphasize a point.

Additional Info: The full title of article is: The tubulin ancestor, FtsZ, draughtsman, designer and driving force for bacterial cytokinesis. The field above prevents me from using the entire length of the title.

- end -

For further info regarding this automatic email, please contact:
WEB APPLICATIONS TEAM (

Download this as a file

From: "Journals Rights"
Subject: RE: permission to use figure
Date: Thu, 24 May, 2007 10:06 am
To: "Nelson Eng"

Dear Nelson,

Thank you for your e-mail request. Permission is granted for you to use the material below for your thesis, subject to the usual acknowledgements and on the understanding that you will reapply for permission if you wish to distribute or publish your thesis commercially.

With best wishes,
Sally

Sally Byers
Permissions Assistant
Wiley-Blackwell Publishing Ltd.

From: Nelson Eng
Sent: 23 May 2007 17:42
To: Journals Rights
Subject: permission to use figure

To whom this may concern,

My name is Nelson Eng, a PhD student at the University of Ottawa, under the supervision of Dr. Jo-Anne Dillon. I am currently writing my thesis and would like to include a figure from Molecular Microbiology and incorporate it into my thesis. The figure will not be altered:

Article:

Goehring, N.W., Gonzalez, M.D., and Beckwith, J. (2006) Premature targeting of cell division proteins to midcell reveals hierarchies of protein interactions involved in divisome assembly. Molecular Microbiology. Volume 61, Issue 1, pp. 33-45.

I would like to use Figure 5 on page 40.

I look forward to your response if I could use these figures in my thesis.

Thank you.

Nelson Eng

--
Nelson Eng, B.Sc., Ph.D. candidate
Department of Biochemistry, Microbiology and Immunology
Faculty of Medicine
University of Ottawa
451 Smyth Road
Ottawa, Ontario

K1H 8M5
(306) 966-1553

Download this as a file

From: "Downing, Hannah (ELS-OXF)" <H.Downing@elsevier.com>
Subject: RE: permission to use figure
Date: Thu, 24 May, 2007 8:28 am
To: "Nelson Eng"

Dear Nelson Eng

We hereby grant you permission to reprint the material detailed below at no charge in your thesis subject to the following conditions:

1. If any part of the material to be used (for example, figures) has appeared in our publication with credit or acknowledgement to another source, permission must also be sought from that source. If such permission is not obtained then that material may not be included in your publication/copies.

2. Suitable acknowledgment to the source must be made, either as a footnote or in a reference list at the end of your publication, as follows:

"This article was published in Publication title, Vol number, Author(s), Title of article, Page Nos, Copyright Elsevier (or appropriate Society name) (Year)."

3. Your thesis may be submitted to your institution in either print or electronic form.

4. Reproduction of this material is confined to the purpose for which permission is hereby given.

5. This permission is granted for non-exclusive world English rights only. For other languages please reapply separately for each one required. Permission excludes use in an electronic form other than submission. Should you have a specific electronic project in mind please reapply for permission.

6. This includes permission for UMI to supply single copies, on demand, of the complete thesis. Should your thesis be published commercially, please reapply for permission.

Yours sincerely

Clare Truter

Rights Manager, S&T

-----Original Message-----
From: Nelson Eng [mailto:]
Sent: 23 May 2007 18:28
To: Rights and Permissions (ELS)
Subject: permission to use figure

To whom this may concern,

My name is Nelson Eng, a PhD student at the University of Ottawa, under the supervision of Dr. Jo-Anne Dillon. I am currently writing my thesis and would like to include a figure from Molecular Microbiology and incorporate it into my thesis. The figure will not be altered:

Article:

Goehring, N.W., and Beckwith, J. (2005) Diverse Paths to Midcell: Assembly of the Bacterial Cell Division Machinery. Current Biology. Volume 15 Issue 13, pp. R514-R526

I would like to use Figure 2 on page R517.

I look forward to your response if I could use this figure in my thesis.

Thank you.

Nelson Eng

--
Nelson Eng, B.Sc., Ph.D. candidate
Department of Biochemistry, Microbiology and Immunology Faculty of Medicine University of Ottawa

--
Nelson Eng, B.Sc., Ph.D. candidate
Department of Biochemistry, Microbiology and Immunology
Faculty of Medicine
University of Ottawa

Download this as a file

From: "Kendra Waite" <
Subject: RE: permission to use figure (MIC Feedback Form)
Date: Thu, 24 May, 2007 3:44 am
To: "Nelson Eng"

Dear Nelson Eng

On behalf of SGM as copyright holder I am happy to grant permission for Figure 2c-e from Deletion of the cell division inhibitor MinC results in lysis of Neisseria gonorrhoeae by S. Ramirez-Arcos, J. Szeto, T.J. Beveridge, C. Victor, F. Francis and J.R. Dillon which was published in Microbiology (2001), Volume 147 pp. 225-237, to be reproduced, provided that the source is acknowledged.

Yours sincerely

Kendra Waite
Editorial Assistant
Society for General Microbiology

Web: http://www.sgm.ac.ukOn-line journals: http://www.sgmjournals.org

Marlborough House
Basingstoke Road
Spencers Wood
Reading RG7 1AG, UK

-----Original Message-----
From: Nelson Eng [mailto:
Posted At: 23 May 2007 18:43
Posted To: micro.permission
Conversation: permission to use figure (MIC Feedback Form)
Subject: permission to use figure (MIC Feedback Form)

Comments sent via MICROBIOLOGY Feedback Page

NAME: Nelson Eng
EMAIL:
IP ADDRESS: 128.233.43.31
HOSTNAME: VIDOMINGMIN.usask.ca
PREVIOUS PAGE: http://mic.sgmjournals.org/
BROWSER: Mozilla/4.0 (compatible; MSIE 7.0; Windows NT 5.1; .NET CLR 1.1.4322; InfoPath.1; .NET CLR 2.0.50727)
PROMOTIONAL USE: Not granted

COMMENTS:
To whom this may concern,

My name is Nelson Eng, a PhD student at the University of Ottawa, under the supervision of Dr. Jo-Anne Dillon. I am currently writing my thesis and would like to include a figure from Microbiology and incorporate it into my thesis. The figure will not be altered:

Article:

Ramirez-Arcos, S., Szeto. J., Beveridge, T.J., Victor, C., Francis, F., and Dillon, J.R. (2001) Deletion of the cell division inhibitor MinC

From: "Downing, Hannah (ELS-OXF)" <H.Downing@elsevier.com>
Subject: RE: permission to use figure
Date: Thu, 24 May, 2007 8:28 am
To: "Nelson Eng" <neng048@uottawa.ca>

Dear Nelson Eng

We hereby grant you permission to reprint the material detailed below at no charge in your thesis subject to the following conditions:

1. If any part of the material to be used (for example, figures) has appeared in our publication with credit or acknowledgement to another source, permission must also be sought from that source. If such permission is not obtained then that material may not be included in your publication/copies.

2. Suitable acknowledgment to the source must be made, either as a footnote or in a reference list at the end of your publication, as follows:

"This article was published in Publication title, Vol number, Author(s), Title of article, Page Nos, Copyright Elsevier (or appropriate Society name) (Year)."

3. Your thesis may be submitted to your institution in either print or electronic form.

4. Reproduction of this material is confined to the purpose for which permission is hereby given.

5. This permission is granted for non-exclusive world English rights only. For other languages please reapply separately for each one required. Permission excludes use in an electronic form other than submission. Should you have a specific electronic project in mind please reapply for permission.

6. This includes permission for UMI to supply single copies, on demand, of the complete thesis. Should your thesis be published commercially, please reapply for permission.

Yours sincerely

results in lysis of Neisseria gonorrhoeae. Microbiology.
Volume 147 pp. 225-237.

I would like to use Figure 2c-e on page 230.

I look forward to your response if I could use this figure in my thesis.
Please note that the my supervisor is also the corresponding author.

Thank you.

Nelson Eng

From: "Jason Szeto" <
Subject: Re: permission
Date: Wed, 23 May, 2007 7:54 pm
To: "Nelson Eng" >

Hi Nelson,
You can certainly use the figures in question for your thesis.

Best regards,
Jason

On 5/23/07, Nelson Eng <; > wrote:
> Dear Dr. Szeto,
>
> My name is Nelson Eng, a PhD student at the University of Ottawa, under
> the supervision of Dr. Jo-Anne Dillon. I am currently writing my thesis
> and would like to include a figure from your thesis (2004) published by
> the University of Ottawa and incorporate it into my thesis. The figures
> will not be altered:
>
> I would like to use
> Figure 1.2 (with slight modifications)
> Figure 1.5
> Figure 4.6A and B
> Figure A.2D
>
> I look forward to your response if I could use these figures in my thesis.
>
> Thank you.
>
> Nelson Eng
>
>
>
> --
> Nelson Eng, B.Sc., Ph.D. candidate
> Department of Biochemistry, Microbiology and Immunology
> Faculty of Medicine
> University of Ottawa
> 451 Smyth Road
> Ottawa, Ontario
> K1H 8M5
> (306) 966-1553
>

--
Jason Szeto, PhD.
Program in Cell Biology
The Hospital for Sick Children
555 University Avenue
Toronto, Ontario
M5G 1X8

Download this as a file

CURRICULUM VITAE

Nelson Francis Eng

Education

2001-2007 **Ph.D. - Microbiology and Immunology**
Department of Biochemistry, Microbiology, and Immunology
University of Ottawa, Ottawa, Ontario
Thesis title – **Functional characterization of the cell division protein MinE from the Gram-negative coccus *Neisseria gonorrhoeae***

1997-2001 **B.Sc. Honours – Biochemistry**
Department of Chemistry and Biochemistry
Laurentian University, Sudbury, Ontario
Thesis title – **Defining human CDC7 functional domains**

Honours and Distinctions

2007-2009 Saskatchewan Health Research Foundation (SHRF) Postdoctoral Fellowship Award

2005-2006 Canadian Institutes of Health Research (CIHR) Doctoral Research Award

2004 Winner at University of Ottawa 2004 Graduate Student Poster Competition

2003-2005 National Science and Engineering Research Council of Canada (NSERC) Doctoral Canada Graduate Scholarship (CGS D)

2001-2006 University of Ottawa National Excellence Scholarship

2001-2005 University of Ottawa Strategic Areas of Development Award in Molecular Sciences

2001-2003 National Science and Engineering Research Council of Canada (NSERC) Postgraduate Scholarship – Master's (PGS A)

2001, 2003 Ontario Graduate Scholarship (declined)

2001	Recipient of Governor General's Silver Academic Medal as Top Undergraduate Student
2000	National Science and Engineering Research Council of Canada (NSERC) Undergraduate Student Research Award (USRA)
1997-2001	Dean's Entrance Scholarship for Excellence in Sciences Scholarship
1997	Recipient of Governor General's Bronze Academic Medal as Top High School Student

Professional associations

2005-present American Society of Microbiology

University activities

09/2002-12/2002	Teaching assistant for General Microbiology course for Dr. Jo-Anne Dillon Department of Biology, University of Ottawa
05/2001-08/2001	Research assistant for Dr. Hoyun Lee Department of Biochemistry, Microbiology, and Immunology, University of Ottawa
05/1999-08/1999	Teaching assistant for Organic Chemistry Laboratory for Dr. Ken Westaway Department of Chemistry and Biochemistry, Laurentian University

Supervision of students

05/2006-08/2006	Cherise Baier, undergraduate summer student Department of Microbiology, University of Saskatchewan
09/2005-04/2006	Shanna Banman, 4th year undergraduate Honours student Department of Biochemistry, University of Saskatchewan
10/2004-05/2006	Kelli Bell, research technician Vaccine and Infectious Disease Organization, University of Saskatchewan
05/2004-08/2004 05/2003-08/2003	Lauren Lapointe-Shaw, undergraduate summer student Department of Biology, McGill University
09/2003-06/2004	Dr. Tatiana Morozova, postdoctoral fellow Department of Biochemistry, Microbiology, and Immunology, University of Ottawa

01/2002-04/2002	Julia Romero, Master's student Department of Biochemistry, Microbiology and Immunology, University of Ottawa
05/2001-08/2001	Jean-Pierre Martel, M.D. student Department of Medicine, University of Ottawa
05/2001-08/2001	Melanie Squarzolo, undergraduate summer student Department of Chemistry and Biochemistry, Laurentian University
05/2000-08/2000	Jason Chung, undergraduate summer student Department of Biology, McMaster University

Publications in refereed journals

Yang, Y., Liao, M., Gu, W-M., Bell, K., Wu, L., **Eng, N.F.**, Zhang, C-G., Chen, Y.,Jolly, A.M., and Dillon, J.R. (2006) Antimicrobial susceptibility and molecular determinants of quinolone resistance in *Neisseria gonorrhoeae* isolates from Shanghai. Journal of Antimicrobial Chemotherapy. 58, 868–872.

Eng, N.F., Szeto, J., Acharya, S., Tessier, D., and Dillon, J.R. (2006) The C-terminus of MinE from *Neisseria gonorrhoeae* acts as a topological specificity factor by modulating MinD activity in bacterial cell division. Research in Microbiology. 157, 333-344.

Ramos, D., Ducat, T., Cheng, J., **Eng, N.F.**, Dillon, J.R., and Goto, N.K. (2006) Conformation of the cell division regulator MinE: Evidence for interactions between the topological specificity and anti-MinCD domains. Biochemistry. 45, 4593-4601.

Szeto, J., **Eng, N.F.**, Acharya, S., Rigden, M.D., and Dillon, J.R. (2005) A conserved polar region in the cell division site-determinant MinD is required for responding to MinE-induced oscillation but not for localization within coiled arrays. Research in Microbiology. 156, 17-29.

Szeto, J., Acharya, S., **Eng, N.F.**, and Dillon, J.R. (2004) The N-terminus of MinD contains determinants which affect its dynamic localization and enzymatic activity. Journal of Bacteriology. 186, 7175-7185.

Publications in preparation

Eng, N.F., Wang, M., Baier, C.E., Guigard, E., Kay, C.M. and Dillon, J.R. (2007) Self-interaction of MinE from *Neisseria gonorrhoeae* is required for MinD functionality. To be submitted to Research in Microbiology.

Published conference abstracts

Eng, N.F., and Dillon, J.R. (2006) Analysis of mutants reveal importance of MinE self-interaction in bacterial cell division site selection. Department of Biochemistry, Microbiology and Immunology Graduate Students 2006 Poster Competition, University of Ottawa, Ottawa.

Yang, Y., Liao, M., Gu, W-M., Bell, K., Wu, L., **Eng, N.F.**, Zhang, C-G., Chen, Y., Jolly, A.M., and Dillon, J.R. (2006) Antimicrobial Susceptibility and Molecular Determinants of Quinolone Resistance in *Neisseria gonorrhoeae* Isolates from Shanghai. 15th International Pathogenic Neisseria Conference. Cairns Convention Center, Cairns, North Queensland, Australia. September 10-15, 2006.

Liao, M., Bell, K., Gu, W-M., Yang, Y., **Eng, N.F.**, Fu, W., Wu, L., Zhang, C-G., Chen, Y., Jolly, A.M., and Dillon, J.R. (2006) Genetic Diversity of *porB* for 174 *Neisseria gonorrhoeae* Isolates from Shanghai: Impact on Molecular Epidemiology and Antimicrobial Resistance. 15th International Pathogenic Neisseria Conference. Cairns Convention Center, Cairns, North Queensland, Australia. September 10-15, 2006.

Szeto, J., **Eng, N.F.**, and Dillon, J.R. (2005) FtsZ, the nucleoid, and MinD localize in patterns that accommodate perpendicular and alternating cell division patterns in Gram negative cocci. 2nd ASM Conference on Prokaryotic Development, University of British Columbia, Vancouver, British Columbia, Canada, July 13-16, 2005.

Rigden, M.D., Ramirez-Arcos, S., **Eng, N.F.** and Dillon, J.R. (2005) Role of coiled-coil domains in the oligomerization of DivIVA. 2nd ASM Conference on Prokaryotic Development, University of British Columbia, Vancouver, British Columbia, Canada, July 13-16, 2005.

Liao, M., Li, H., Bell, K., **Eng, N.F.**, and Dillon, J.R. (2005) Comparison of Ribotyping, Pulsed Field Gel Electrophoresis and Genetic Typing to Discriminate Gonococcal Strains Associated with Either Outbreak Clusters or Random Isolates with IB-5 and IB-7. ISSTDR, Amsterdam, The Netherlands, July 10-13, 2005.

Liao, M., Bell, K., Yang, Y., **Eng, N.F.**, Gu, W.M., Chen, Y., Jolly, A.M., and Dillon, J.R. (2005) Strain Differentiation of *Neisseria gonorrhoeae* Isolates from Identified Sex Networks in Shanghai by Genetic Typing. ISSTDR, Amsterdam, The Netherlands, July 10-13, 2005.

Ramos, D., **Eng, N.F.**, Dillon, J.R., and Goto, N. (2004) Structural Studies of the Gonococcal Cell Division Protein MinE Using Liquid-State NMR. MOOT XVII NMR Symposium, Queen's University, Kingston. September 25-26, 2004.

Acharya, S., Szeto, J., **Eng, N.F.**, Goto, N., and Dillon, J.R. (2004) Structural Studies of $MinD_{Ng}$ for the Identification of Motifs Responsible for Oscillation, Dimerization and Enzymatic Activity. MOOT XVII NMR Symposium, Queen's University, Kingston. September 25-26, 2004.

Eng, N.F., Tessier, D., Szeto, J., Acharya, S., and Dillon, J.R. (2004) Characterization of Gonococcal MinE Reveals Two Critical Functions for Proper Bacterial Cell Division Site Selection. 14th International Pathogenic Neisseria Confererence, University of Wisconsin, Milwaukee. September 5-10, 2004.

Eng, N.F., Tessier, D., Szeto, J., Acharya, S., and Dillon J.R. (2004) Oscillation and Localization of MinD at the Polymeric Array are Influenced by MinD/MinE Binding Affinities. Gordon Research Conference, New London, New Hampshire. June 27 – July 2, 2004.

Eng, N.F., Tessier, D., Szeto, J., Acharya, S., and Dillon, J.R. (2004) MinE from *Neisseria gonorrhoeae* Comprises Two Distinct Domains Critical for Bacterial Cell Division Site Selection. 2004 Canadian Student Health Research Forum, University of Manitoba, Winnipeg. June 7-9, 2004.

Eng, N.F., Tessier, D., Szeto, J., Acharya, S., and Dillon, J.R. (2004) Mapping Functional Domains of MinE: A Protein Critical for Proper Bacterial Division Site Selection. Department of Biochemistry, Microbiology, and Immunology Graduate Students 2004 Poster Competition, University of Ottawa, Ottawa.

Acharya, S., Szeto, J., **Eng, N.F.**, Rigden, M.D., Goto, N., and Dillon, J.R. (2004) Structural and Functional Analysis of the *Neisseria gonorrhoeae* Cell Division Site Determinant MinD. Department of Biochemistry, Microbiology, and Immunology Graduate Students 2004 Poster Competition, University of Ottawa, Ottawa.

Eng, N.F. and Dillon, J.R. (2002) Improving Genetic Tools to Study Expression of Cell Division Genes in *Neisseria gonorrhoeae*. Department of Biochemistry, Microbiology, and Immunology Graduate Students 2002 Poster Presentations, University of Ottawa, Ottawa.